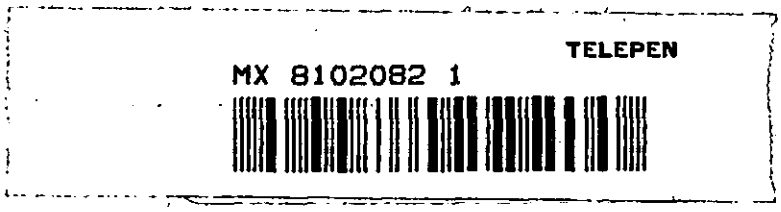
TELEPEN
MX 8102082 1

HIGH TEMPERATURE CORROSION BY COMBUSTION GASES PRODUCED BY BURNING LIQUID FUELS CONTAINING SULPHUR, SODIUM AND VANADIUM

By

Fazlur Rahman KHAN, B.Sc.(Eng.),M.Sc.

DECEMBER 1980

HIGH TEMPERATURE CORROSION BY COMBUSTION GASES PRODUCED BY BURNING LIQUID FUELS CONTAINING SULPHUR, SODIUM AND VANADIUM.

By

Fazlur Rahman KHAN, B.Sc.(Eng.), M.Sc.

A thesis submitted to CNAA in partial fulfilment of the requirements for the degree of Doctor of Philosophy.

Supervisors: Dr. S.H. AHMED, Ph.D., C.Eng., MIMechE, MInstE.

Dr. John GOLDEN, Ph.D.

Mr. D.F. ROSBOROUGH, B.Sc., C.Eng., FInstE.
(President, Institute of Energy).

Fuel and Combustion Technology
Engineering, Science and Mathematics
Middlesex Polytechnic,
Enfield, EN3 4SF.

Collaborating Establishment : Esso Research Station.

DECEMBER 1980

CONTENTS

ABSTRACT.

HIGH TEMPERATURE CORROSION BY COMBUSTION GASES PRODUCED BY BURNING LIQUID FUELS CONTAINING SULPHUR, SODIUM AND VANADIUM - By F.R. KHAN.

High temperature corrosion, at 730° C, by combustion gases produced by burning liquid fuels in a laboratory combustor has been investigated. A selected range of steels and alloys (mild steel, stainless steel type 347, Nimonic N90, N105, and IN657) have been tested in the combustion gases using fuels containing varying amounts of impurities in the range of 0 - 6% sulphur, 0 - 60 ppm sodium, and 0 - 300 ppm vanadium. On the basis of the comprehensive results a computer programme was written to predict corrosion rates of mild steel by combustion gases produced by burning fuels containing impurities such as sulphur, sodium and vanadium. The programme was tested, and the predictions which included the change of fuel were experimentally verified. Oil soluble additives have been used to show the effect on corrosion rates of the materials tested. By using X-ray diffraction analysis of the oxide layers, and with the help of electron microscopy, an attempt was made to investigate the mechanism of corrosion in the individual and collective presence of sulphur, sodium and vanadium supplied by the test fuels. It is shown, for example, that the presence of sulphur in the fuel helps in the formation of FeO in the surface oxide layers.

The ignition delay time or simply the ignition delay, which is the time lapse between the introduction of a fuel droplet into a heated atmosphere and its eventual ignition, was measured for all the test fuels. It is shown that the addition of elemental impurities such as sulphur sodium and vanadium have no significant effect on the ignition delay of the fuel but the addition of oil soluble additive makes the, ignition delay - temperature, curve steeper at the operating temperature and also reduces corrosion of materials. Light hydrocarbon fuels having lower ignition delay than Kerosene at the operating temperature can be used as an additive to reduce the formation of sulphur trioxide in the combustion gases.

CHAPTER 'ONE'

GENERAL INTRODUCTION.

Corrosion generally implies the deterioration or destruction of a material, usually a metal, by reaction with its environment (193)* . Corrosion in the normal sense involves loss of electrons from the metal to the environment and the formation of corrosion products such as oxides.

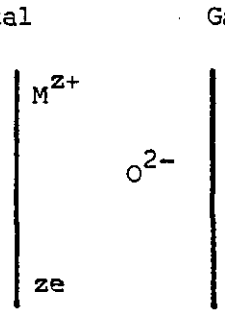

Oxidation : $M \rightarrow M^{z+} + ze$

Reduction : $O_2 \rightarrow ze + \frac{z}{2} O^{2-}$

Combined : $M + O_2 \longrightarrow MO_{z/2}$

where z is the number of electrons in the oxygen transfer process.

Corrosion of metals is influenced by their environment. The degree of this influence is relative to the physical state of the environment, its temperature, concentration and working condition (e.g. time of exposure, effect of cycling). Figure 1(1) shows different corrosive environments. Corrosion of metals is also influenced by their metallurgical composition and microstructure (193).

Corrosion of oil-fired boilers can conveniently be divided into two temperature regions as shown in figure 1(2). Corrosion of surfaces operating above temperatures where ash components tend to become liquid (at approximately 600° C and above) are referred to as High Temperature Corrosion; and corrosion of surfaces operating at or below temperatures where, aqueous condensate are produced i.e. below the acid dew point of the gases (approximately 150° C) is called Low Temperature Corrosion (3,52). For practical purposes corrosion is not a serious threat to surfaces operating between the two limiting

* The numbers in brackets refer to selected entries from the references of literature survey.

temperatures given above (52).

In boilers and gas turbines, the corrosive atmosphere often may be quite complex depending on the fuel burned, the impurities present and the combustion conditions. Alkalies, chlorides, sulphur oxides and vanadium compounds, resulting from combustion of the fuel will cause severely corrosive conditions, particularly at temperatures above about 650° C. The intergranular penetration of metals by ferrous oxide - ferrous sulphide complexes, and the accelerated attack by vanadium-containing compounds such as $NaVO_3$ and $Na_2O.V_2O_4.5V_2O_5$ are examples of corrosion by molten salts, but SO_3 and nascent oxygen also are suggested as being potentially severe corrodents (88, 164).

Research workers using various test procedures including crucible tests, rig tests, oxygen consumption tests, have found that most of the ordinary alloys are corroded at a rapid rate, particularly at temperatures above 700° C. Specific effects have been reported for V_2O_5 and Na_2SO_4. High-nickel alloys suffer severe attack if the oil-ash contains sulphur (164). Iron and nickel alloys containing over 50 per cent chromium have shown better resistance to ash attack. Also, aluminium or beryllium alloying additions seem to give improved performance, perhaps because of the formation of more resistant oxide films (88).

A great deal of effort has been directed to the study of oil additives which will combine with the corrosive components to form high melting point compounds. Magnesium oxides, dolomite, calcium, aluminium and silicon compounds seem to have the desired effect, but the selection of one or another of these appears to depend on the temperature of operation, the composition of the oil and the resulting formation of deposits (186).

The present trend towards the construction of very large generating units in new power stations places increasingly stringent demands on their availability. This in turn requires a continuous improvement in the reliability of the various boiler components, and thus in the

performance of their constructional materials under operational conditions. The ability of these materials to withstand corrosion is of particular importance in this context. The rate at which corrosion occurs in a plant influences the maximum superheater metal temperature, and hence the maximum steam temperature and thermal efficiency (99).

The importance of understanding the mechanisms whereby corrosion takes place, so that it may be combated and plant performance improved, has long been recognised. The associated problems have been the subject of intensive research for many years. Industrial research engineers like Rosborough (90, 92, 172), Baker (24), Hart (105), Cutler (41), Jackson (127), and Mortimer (224) have carried out plant trials and research to improve the performances of boiler tubes and turbine blade materials in presence of impurities generated by the fuel. Such work is necessarily restricted by every day demands of the plant.

Alongside these industrial efforts, academic research has been carried out, e.g. by Coates (32), Elliot (60), Hills (11) and Penfold (179), on the attack on steel specimens by specific corrodents such as fused vanadates and sulphates.

My main consideration was to set up a simulation of the combustion conditions of the industrial plant in the laboratory, and to examine the individual and collective corrossive effects of the impurities present in the fuel upon a selected range of steels and alloys in actual use in the industry.

It has long been known that the presence of sulphur, sodium and vanadium in residual fuel oil is mainly responsible for the corrosion of heat exchange surfaces in boilers, and for the rapid deterioration of gas turbine blades (60). A review of the work done in this field (99) gives a general outline of the present understanding of the corrosion process, but the individual and collective effects of corrosion due to the presence of the three major impurities has not been studied in detail. The range of impurity contents studied was dictated by the type of fuels and their impurity levels that an industrial combustion engineer might expect to meet (185).

A fully detailed exposition of the present state of work in this area and the relationship of my work to it is given in the comprehensive literature survey which follows.

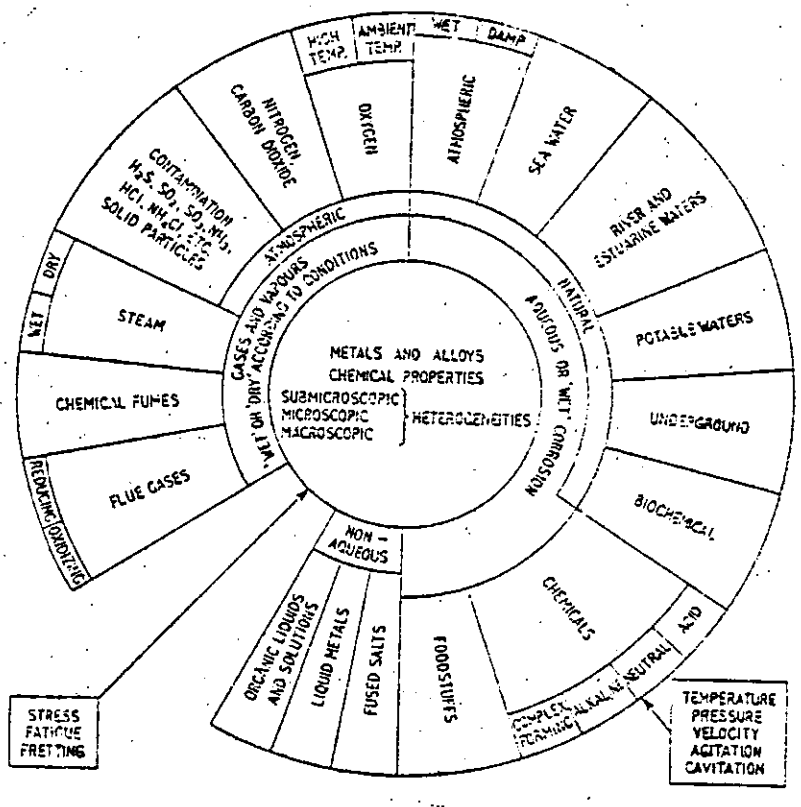

Fig. 1(1) Environments in Corrosion. (193).

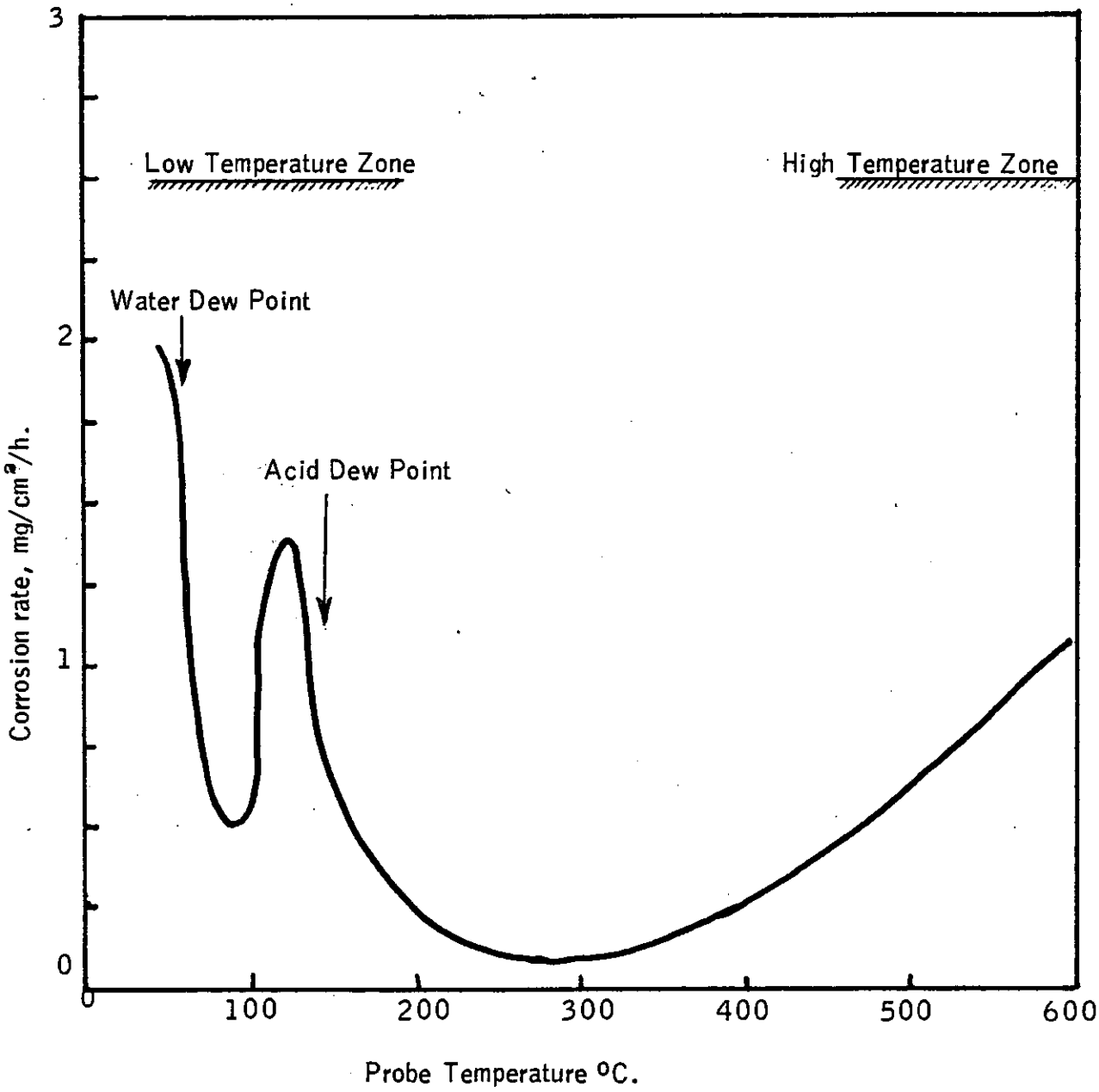

Fig.1(2). Relationship between corrosion rate and probe temperature (2).

CHAPTER TWO

LITERATURE SURVEY - a guide

2.1 Introduction

Corrosion, such as deposits on the fireside surfaces of boilers or gas turbines, presents enormous problems in industry, as evidenced by the vast amount of technical literature on this important subject.

Interest in the corrosion of high temperature alloys by petroleum fuel oil ash deposits really dates from Amgwerd's classic investigation in the late 1940's, originally published as a University thesis, and later in the open literature[1]. This type of corrosion is essentially a reaction involving molten fuel ash. Boiler tube surface temperatures were at that time too low for the boiler to be seriously troubled with the problem. The research activity which occured in the period 1950-1975 in a number of countries, in Government research establishments, oil companies' laboratories, research associations and in industries has been extensively reviewed (3,7,25,40,50,62,65,66,88,92,101,126, 142,156,164,172,210,212). These works have resulted in a fair understanding of the problem of corrosion by fuel ash in the presence of a large excess of oxygen, and have attempted to give an empirical description of the nature of the problem, means of combating it, and also a reasonable working hypothesis to describe the underlying mechanism. In spite of this, the fuel-burning gas turbine has found only a token application, using selected fuels of restricted ash content and composition. Boiler users still face the same problems with boiler tube surfaces, in trying to raise the maximum steam temperature (156).

The study of the causes of deposits, of their composition, and of their corrosive effect is not simple. The impurities in the fuel, the temperatures reached owing to the combustion system employed, and the aerodynamic behaviours of the gases fixed by boiler or turbine design are the imposed variables subject to varying degrees of control. Additional knowledge should be

useful regarding the interactions between these variables which cause deposits, (164).

2.2 Mechanism and Kinetics of Oxidation at High Temperatures.

The mechanism of oxidation of various metals and alloys has been studied extensively, and excellent reviews by Kubashewski and Hopkins (136), Hauffe (117) and Evans (64) are available. Wagner (219) has pointed out that the reaction between a solid metal and an oxidising gas seems to be one of the simplest chemical reactions, but that actually the mechanism is highly complex. Generally, the first result of a metal-gas reaction is the formation of a solid reaction product, or film, on the metal surface. At elevated temperatures, this film does not prevent the continued oxidation of metal because both the metal and gas can diffuse through the layer of reaction product. However, the rate of reaction will decrease in most cases. Lewis (150) has demonstrated that "the rate of oxidation of materials which are oxidation resistant is generally governed by the rate of diffusion of ions through the partially protective oxide film formed. As the thickness of the film increases, the rate of diffusion becomes slower, and the familiar parabolic law is followed (Fig. 2(1)). The phase equilibrium diagram of the binary system Fe–O_2 is shown in figure 2(2).

The mechanism by which metal diffuses through oxides has been studied by many investigators. A simple, brief summary of some of these studies was given by Corey (33). Metal ions can diffuse through oxide in two ways: (i) they can go into solution at the metal-oxide interface moving interstitally between the atoms comprising the oxides, or (ii) they can move into vacant positions in the oxide lattice. The second mechanism can occur because some oxides and sulphides contain less metal than corresponds to the stoichiometric formula. This results in vacancies in the lattice and the metal ions at the metal scale interface can move into them (87).

Kubashewski and Hopkins (136) have reviewed the progress of various investigators in developing a theory that will explain the oxidation of alloys. The broad picture appears to be that alloys based on the high melting point metals such as niobium, tantalum, tungsten and molybdennum, have satisfactory strength at high temperatures. They are, however, unsuitable for high service in oxidising atmospheres due to excessive oxidation, and appear feasible only with protective coatings. On the other hand, satisfactory alloys based on nickel and iron have been developed for stress carrying applications under oxidising conditions. Generally these alloys rely on additions of chromium and sometimes aluminium, for their oxidation resistance. Leslie and Fontana (151) found 'catastrophic oxidation' in a molybdenum-containing stainless steel because of the formation of volatile molybdic oxide (M_0O_3) which disrupted the protective scale. Bradbury, Hancock and Lewis (28) found that vanadium aditions to a carbide hardened alloys based on the nickel-chrome-cobalt system also caused serious attack. The results of the vanadium additions are shown in Table 2(1), where it can be seen that the effect of the vanadium additions is to cause highly localised attack, probably associated with pockets of liquid phase. This means that the actual loss in some areas is much greater than the overall weight gain measurements would indicate, thus illustrating the danger of using gravimetric results without microscopical examination or other supporting techniques (88).

The effect of stresses in the oxide scale during growth is important in determining the service life of components operating in oxidising atmospheres because these stresses influence scale adherence and resistance to cracking (115). Hancock and Fletcher (118) have shown that, when nickel is oxidised, the mechanism of oxidation is by cationic diffusion through the oxide scale, and the effect of this mechanism is to supersaturate the underlying metal with vacancies which seriously modify the subsequent creep behaviour. The effect is demonstrated by Figure 2(3) which shows the difference between creep testing specimens which have been previously: (a) oxidised at 1,000° C and (b) vacuum annealed for the same time at the same temperature. The amount of surface

oxidation is negligible (below 0.001") on a quarter inch diameter specimen, but the oxidised specimen has a high vacancy supersaturation and this is reflected in the creep behaviour. The effect becomes more pronounced if thin specimens are used and indicates that when using sheet material at high temperatures, oxidation is important even if it appears to be superficial and of "negligible" thickness (88).

The complexity of high-temperature corrosion mechanism, whether by gases or salts, is clearly evident from the results of these few fundamental studies. For practical reasons, the objective of many other investigations has been to observe the behaviour of materials in actual or synthetic products of combustion, to guide in the solution of pressing corrosion problems.

2.2.1. Corrosion in oil-fired boilers and turbines.

Corrosion by fuel-oil ash was not considered a pressing problem in steam power plants until the advent of the mercury boiler. Fuller (73) refers to the corrosion of steel in an oil fired mercury boiler having been observed some 35 years ago. However, it is only within the last 20 years that the problem has received much attention. Collins (47) discussed the problems connected with oil-fired boiler operation, pointing out the marked effect of temperature on corrosion. Metal loss is increased tenfold by increasing the metal temperature from 500° C to 600° C. At the higher temperature, measurable corrosion occurred quickly, even at low vanadium concentrations.

Most of the published literature on oil-ash corrosion is concerned with the problem as related to gas turbines. The obvious reasons are that operating temperatures are in the high range where corrosion by molten ash becomes severe. Several good general reviews have been written dealing with the problem as a whole, including a discussion of corrosion effects, behaviour of commercial and experimental materials,

and the use of additives to overcome corrosion difficulties (88, 164). Most of the research has been concerned with a comparison of the resistance to corrosion of the various known alloys which might be used as materials of constructions. Some investigators, having concluded that the prospects for a metallurgical solution to corrosion problems are not good, have therefore investigated methods of alleviating the harmful effects.

A series of corrosion - rig tests using an oil-fired burner and plant trials using operation boilers, have demonstrated the acceptability of the decision to apply the limit to steam outlet temperature to 540° C. Typical characteristics of oil-fired boilers are shown in Table 2(2). The plant trials were carried out at Marchwood and Bankside Power Stations, and rig tests were carried out at Marchwood Engineering Laboratories and at the Central Electricity Research Laboratories. The primary objective of the tests was to establish the corrosion rates of ferritic and austinitic steels over the typical operating temperature range of superheater and reheater tubes, for different flue gas temperatures.

Concerning the corosion problems in superheaters and reheaters, Mortimer (224) discussed that the courses open are:

1. Reduced metal temperatures
2. Reduced gas temperatures
3. Shield tubes from aggressive atmosphere
4. Use thicker tubes
5. Better selection or blending of fuel
6. Use improved alloys for example as co-extruded tubes.

For a given steam temperature of 570° C the metal surface temperature is 650° C (224).

steam 570° C nominal max.	outer wall of tube	Fe/Cr/Ni spinel containing lamellae of sulphide 650°C. 680°C.	molten sulphate Na/K	Fe_2O_3 780°C	Ash >1000°C

The formation of the oxides is influenced by dissolution in the sulphate and precipitation at the hot end of the gradient. The molten sulphate has a significant partial pressure of SO_3 which dissolves the oxide to form complex sulphates which decompose at the higher temperatures (780° C). This produces a corrosion rate dependant upon the temperature gradient. Above a temperature of about 680° C the sulphate is no longer capable of dissolving the oxide and the corrosion rate returns to the level of normal oxidation reaction (224).

2.2.2. Reaction of Metals and Alloys with products of combustion.

Much of the early experimental work was designed to obtain an indication of the effect of individual components of combustion atmospheres on various alloys used in steam power plants. It is obvious that the presence of free oxygen in a gas mixture will result in oxidation of metals. Laboratory oxidation tests by Marson and Cobb (163) on mild steel specimens exposed for 3 hours at 650° C showed that the relative scaling effect decreased in the order dry air, 80 N_2 - 20 H_2O, CO_2. The weight of oxides formed in the dry air was approximately twenty times that in CO_2. The CO_2 and H_2O in the products of combustion not in equilibrium with CO and H_2 over iron and iron oxides are also oxidising in effects. The proportion of CO_2 and H_2O in the combustion gases is dependent on the carbon and hydrogen content of the original fuel.

2.3 Fuel Contaminants.

Residual fuel oil contains the residues of crude oil refinery processes diluted with distillate hydro-carbons, and therefore, contains most of the harmful impurities present in the initial crude oil (164).

The high temperature corrosion problems with residual fuel oil are generally worse than with solid fuel combustion for, although the ash contents rarely exceeds 0.1%, it contains considerable quantities of vanadium and it is the presence of this vanadium that produces the principal differences between corrosion in coal and oil fired boilers (164). The corrosion behaviour is complex, depending upon the analysis of the fuel used and also upon the location of the installation, for example, high temperature corrosion is invariably worse in marine environments. Table 2(3) shows the typical impurities in oil used in power stations and Table 2(4) shows the ash elements in crude oil.

2.3.1. Ash Constituents in Residual Fuel Oil.

The combustion of a single atomised droplet of oil begins with the evaporation and ignition of the lighter hydrocarbons. This is followed by decomposition of the heavier hydrocarbons and, finally, the combustion of the residual carbon matrix. Because the temperatures reached during the decomposition stage are relatively high, a portion of the inorganic compounds which have high vapour pressures at these temperatures are vaporised. Sodium chloride in particular, is vaporised in this manner. Its vapour pressure is about 10 mm Hg at 800° C, and that of vanadium pentoxide (V_2O_5) is slightly less than 0.3 mm Hg. at the same temperature. Most of the ash-forming compounds other than NaCl become concentrated in the carbon residue of the burning particle. During combustion, ash particles of the metallic oxides are formed. The organic vanadium complexes in the oil are decomposed, and the vanadium is oxidised first to the stable and nonvolatile forms V_2O_3 and V_2O_4, and finally to V_2O_5. With other metal ash constituents present such as iron, nickel, sodium and calcium, various reactions take place with vanadium oxides to form a series of vanadates. The vapour pressures of all these compounds are lower than that of V_2O_5 (88). Table 2(5) shows possible constituents formed during combustion and their melting points.

2.3.1.1. Removal of Ash forming constitutents.

As problems involving corrosion and deposits developed in boiler and gas-turbine units fired with residual oils, one of the first steps taken was to investigate possible ways to reduce the concentration of ash-forming constituents to a lower and perhaps to a tolerable level. Some possible ways of separating and removing the ash-forming constituents are filtration, centrifuging, treatment by solvents distillation, treatment by ion-exchange and other-processes.

2.3.2. Sulphur in Heavy Fuel Oil.

The presence of sulphur in crude oil introduces problems in connection with its handling and processing as well as in utilization of the refinery products. For the lighter refined products, the problems are associated with odour, corrosion, and the adverse effect of sulphur on the octane number and lead susceptibility. For the heavy fuel oils, the presence of the sulphur is a significant factor in problems of combustion involving: (i) air pollution, (ii) contamination of furnace and kiln charges; (iii) low-temperature corrosion of metal components in boiler systems, such as economisers and air preheaters; and (iv) the formation, in combination with metallic constituents of the ash, of deposits and corrosive slags in high temperature sections of the boiler.

The sulphur content of residual fuel oils varies with the type and origin of the crude oil and the type of refining process. During refining, the sulphur as well as the ash is concentrated in the high-boiling residual fraction. Table 2(6) shows the distribution of sulphur in the various fractions resulting from distillation of crude oil. The sulphur content of the several petroleum fractions increase with the boiling range, from which it can be concluded that sulphur compounds of high molecular weight predominate in crude oil.

2.4 Occurence of oxides of sulphur.

Residual oils which may have an ash content from 0.01 to 0.1 per cent, usually contain from 1 to 4 per cent sulphur, and during combustion most of this sulphur is oxidised to SO_2 which appears in the gas stream. A relatively small amount of SO_3 is formed during combustion or is converted from SO_2. Consequently, both oxides appear in the flue gases in amount which depend on the fuel composition, ash characteristics, the condition of the heating surfaces, and the design of the system.

2.4.1. Mechanism of formation of Sulphur Trioxide.

Four mechanisms have been proposed to explain the formation of sulphur trioxide in boilers (137) :

(i) The reaction of SO_2 with atomic oxygen in the high temperature flame zone (2,97,110,210, etc.).

(ii) The heterogeneous catalysis of the SO_2/SO_3 reaction on boiler surfaces (99,100,101).

(iii) The homogeneous gas phase reaction between SO_2 and O_2 (97,99,110).

(iv) Low temperature oxidation on surfaces below the acid dew point (6,180).

All four theories are valid but their relative importance varies from one plant to another.

(a) Atomic oxygen theory.

The flame or atomic oxygen theory was first proposed by Dooley and Whittingham (53) and Gaydon (77), see figure 2(4). Whittingham using small diffusion flames of carbon monoxide, hydrogen and methane, containing SO_2 showed that there was a marked difference in the degree of oxidation of sulphur dioxide with different flames (Figure 2(5)). He observed that the increasing order of conversion of SO_2 into SO_3 was in the methane, hydrogen and then carbon monoxide flame - which is in the same order as that of increasing atomic oxygen concentration in these flames, as observed by Gaydon (77).

Dooley & Whittingham (53) argued that if atomic oxygen is involved in the formation of SO_3 in the flame, then the introduction to the flame of substance known to react with atomic oxygen will suppress the formation of SO_3. On the above assumption they introduced different percentages of NO to the flame and confirmed experimentally the suppressed formation of SO_3, figure 2(6). More evidence of SO_3 formation in flames was offered by Crumbley and Fletcher (37) as shown in figure 2(7) and by Hedley (97,110). Hedley used an oil fired laboratory furnace where the temperature and mixing history of the gas were known, and carried out a quantitative investigation of the oxidation of SO_2 and SO_3. The results showed that the concentrations of SO_3 were in excess of those that one might expect from normal-thermodynamic considerations involving molecular oxygen (Figure 2(8)).

Levy and Merrymem (140) working with H_2S-O_2-Air flat flames showed that (a) SO_3 was formed about one flame length thickness past the visible flame zone, and (b) the formation of SO_3 in the flame was directly related to the oxygen concentration through the reaction zone (Figure 2(9)).

Barrett, Hummel and Reid (12) investigated formation of SO_3 in a Stainless Steel Combustor while burning natural gas hydrogen sulphide mixture and operating at a maximum wall temperature of 260° C. The concentration of SO_3 was measured at distance of 3 to 24 inches from burner plate with excess air levels of 1 to 12 per cent. No significant variation of SO_3 concentration was observed along the combustor at any excess air level. It was concluded that all of the SO_3 was formed in the first 3 inches of the combustor or approximately within the visible flame.

Halstead (99) reviewing the progress made on the subject states that on leaving the flame, the concentration of atomic oxygen decreases rapidly and the formation of additional SO_3 downstream of the flame becomes dependent on intermolecular reactions. He added that molecular re-oxidation of SO_2 ($SO_2 + \frac{1}{2}O_2 \rightarrow SO_3$) as the temperature falls is considered to be very slow though its rate can be increased by catalysts, both gaseous and condensed phase.

Ahmed and Zaczek (2) investigated formation of SO_3 using a liquid-fuel firing combustor with a laminar, pre-mixed flames. They found that SO_3 was only formed when there was excess oxygen in the combustion gases and under sub-stoichiometric conditions no SO_3 could be detected. An increase in the quantity of combustion air in excess of stoichiometric requirement led to an increase in the concentration of SO_3 in combustion gases. The level of SO_3 content in the flue gases reached its maximum at about 4% excess oxygen concentration in the flue gases, (figures 2(10) and 2(11)). The effect of residence time of the combustion gases in the high-temperature zone showed that in the first instance the amount of SO_3 formed was in excess of that, which could be predicted from thermodynamic considerations involving molecular oxygen. Sulphur trioxide thus formed, began to dissociate back into sulphur dioxide and oxygen as gases continued to pass along the combustion chamber, figure 2(12).

(b) <u>The heterogeneous catalysis of SO_2/SO_3 reaction at boiler surfaces</u>.

The formation of sulphur trioxide in boilers by heterogeneous catalysis was probably first proposed by Harlow (100,101). The use of ferric oxide (Fe_2O_3) to promote the oxidation of SO_2 to SO_3 is well known and Harlow suggested that the presence of SO_3 in the boiler

flue gases was due to the catalytic oxidation of SO_2 over hot boiler surfaces. This cannot, however, explain the existance of SO_3 found by other workers (12,97) within the combustion chamber before the gases come into contact with catalytic surfaces. Work done by Baerrett (12) does show that Fe_2O_3 - covered surfaces catalyse oxidation of SO_2 to SO_3 at temperatures near 650° C, figures 2(13) and 2(14). The indications are that some SO_3 is formed during the passage of flue gases through the boiler, especially at high temperatures, and when excess oxygen is available.

(c) The homogeneous gas phase reaction between SO_2 and O_2.

Oxides of nitrogen have been used as catalysts in the manufacture of sulphuric acid in the lead chamber process. This is essentially a low-temperature operation and gases are cooled to nearly 93° C before entering the reaction chamber. It has been suggested (53,97) that the presence of nitrogen oxides in the flame gases is more likely to reduce the amount of SO_3 formed because of the removal of oxygen atoms from the system.

(d) The low temperature oxidation of Sulphur dioxide on metal Surfaces below acid dew-point.

Low temperature oxidation of sulphur dioxide is a very commonly encountered phenomenon. Ryland and Jenkinson (188) proposed that economiser deposits especially ferric sulphates, can catalyse the oxidation of sulphur dioxide. During trials at a Power Station, Alexander et.al. (6) confirmed an increase in the conversion of SO_2 to SO_3 during the passage of flue gases through the economiser and reported this as evidence for the hypothesis suggested by Rylands and Jenkinson (188).

2.4.2. Measurement of the extent of formation of SO_3.

To assess the extent to which the SO_2 in the combustion gases has been oxidised to SO_3, an experimental method

is required. Two methods are available, the analysis of a sample of the gases for SO_2 and SO_3 and the determination of the dew point of the gases. Both are fraught with certain difficulties but both have been developed to workable methods.

Corbett (47) has presented a satisfactory method for the analytical determination of SO_2 and SO_3.

Fielder et.al.(72) developed a method for the determination of SO_3 and SO_2 and on the basis of this CERL in collaboration with Gallenkamp developed a laboratory apparatus for the determination of SO_3 and SO_2.

Goksoyr and Ross (79) developed a simplified method of analytical determination of SO_3. Salooja (196) pointed out the serious errors in the methods for the determination of SO_2 and SO_3.

Recently CEGB has developed an instrument for the automatic monitor of SO_3 in the flue gases.

2.4.3. Effects of various factors on the formation of SO_3.

The following list gives some conditions which are known to have an effect on the oxidation of sulphur:

(a) The sulphur content in the fuel.
(b) The excess of combustion air used.
(c) The method of introducing air into the combustion zone.
(d) The nature of the fuel.
(e) The flame temperature.
(f) The method of atomisation.

2.5 Ignition delay property of fuel.

The ignition delay time or simply the ignition delay is termed as the time lapse between the introduction of a fuel droplet into a heated atmosphere and its eventual ignition (189).

In most oil-fired appliances the fuel is suitably atomized, before combustion, into a spray of fine droplets. The subsequent processes occuring in the chamber are numerous and complex and are influenced by several factors - (e.g. droplet size, mixing, heat transfer, evaporation, ignition, combustion). Photographic studies have shown that in compression ignition engines, particularly those with small combustion chambers, a large proportion of the injected fuel strikes the combustion chamber walls even if this is not intended. In gas turbines employing vapourising tubes, the fuel comes into contact with a heated surface. The significant aspects of the problem are evaporation, ignition and the combustion of the droplets (189). Over the past 50 years or more, a considerable amount of work has been carried out on the spontaneous ignition of liquid fuels. Most of these work has been confined to the determination of the minimum temperatures (spontaneous ignition temperature) at which a droplet of the liquid fuel under consideration would undergo spontaneous ignition when allowed to fall into a heated crucible or vessel. Satcunanathan and Zaczek (189) investigated the spontaneous ignition and ignition delays of some liquid fuel droplets impinging on a hot surface. They showed that ignition delays of some commercially important fuels such as Kerosene and Diesel fuel, have a minimum value of some particular temperature.

Ahmed and Zaczek (2) suggested that there is a relationship between the ignition delay and the formation of SO_3 in the combustion gases.

There is, therefore, a need for the measurement of ignition delays of individual liquid fuels.

2.6 Corrosion by Deposits.

2.6.1. Mechanism of deposition.

The most serious deposition problem occurs when fuel oil is used for firing boilers and turbines. There are essential differences on behaviour between boiler and turbine practice which radically effect the type of corrosion that occurs.

When impure fuels are burnt the combustion atmosphere will consist of a mixture of solid, liquid and gaseous products the nature and composition of which will depend upon the impurities present in the fuel. The deposition of these impurities will depend upon the melting points and vapour pressure of the impurities, the temperature of the gas stream; the temperature of the target area and the flow of combustion products around it. Figures 2(15) and 2(16) show the structure of scale and deposits and temperature gradient within them.

In gas turbines there is little temperature difference between the gas stream and the turbine blades. The concave side of the blade will be struck by all the nongaseous particles in the gas stream and, if the temperature is such that some of these are highly viscous liquids or plastic, solids then they will probably stick and form deposits. This will not happen to the same extent on the convex side of the blade where deposition from the vapour phase would be more likely to occur (88).

In boilers the main deposition problems are in the super heater banks. The deposition behaviour on the superheater tubes in boilers differs from that of the blades in turbines because the rates of gas flow are very much lower and also there is a difference between the gas temperature (1100° C - 540° C) and the surface temperature of the superheater tubes (590° C - 400° C). The temperature drop

between gas and tube is sufficient to cause deposition from the Vapour phase and impact deposition would not be as selective due to the lower gas velocities. Thus major deposits build up on the half of the tube facing the gas stream. The deposits will act as a heat insulator and the surface temperature of the deposits will rise and may become liquid and this would mean that larger solid particles may now stick to the surface. Deposit Corrosion will depend upon the gas flow around the component, the position of the component, the temperature of the gas stream and the temperature of the component in addition to the melting points and vapour pressures of the impurities present.

2.6.2. Sulphate Deposits.

It has been suggested that corrosion by sulphates in boilers occurs by means of the formation of pyrosulphates $Na_2S_2O_7$, and $K_2S_2O_7$. The reaction suggested is that sulphur trioxide forms catalytically on the scale and the following reactions take place.

$$SO_2 + \tfrac{1}{2}O_2 \xrightarrow{Fe_2O_3} SO_3$$

$$SO_3 + (Na,K)_2SO_4 \longrightarrow (Na,K)_2S_2O_7 \text{ (liquid)}$$

$$3(Na,K)_2S_2O_7\text{(liquid)} + Fe_2O_3 \longrightarrow 2(Na,K)_3Fe(SO_4)_3.$$

The conversion of sodium and potassium sulphates to pyrosulphates has been studied by Wickert (212). Maximum conversion occurs in the temperature range 370 - 480° C. The maximum temperature for this type of attack will depend upon the maximum temperature of the stability of the phases. This will depend upon the SO_3 concentration but values of about 590° C and 800° C appear to be reasonable for the potassium and sodium pyrosulphates. Wickert has also shown that attack by SO_3 in the presence of sodium sulphate has a maximum value between temperatures of 600 and 750° C and which seem to agree with pyrosulphate mechanism.

The formation of complex alkali iron trisulphates $Na_3Fe(SO_4)_3$ and $K_3Fe(SO_4)_3$ in boiler deposits is studied by Jackson (123). The reactions are considered to be as follows:

$$SO_2 + \tfrac{1}{2}O_2 \xrightarrow[\text{Catalyst}]{Fe_2O_3} SO_3$$

$$2MCl + SO_3 + H_2O \longrightarrow M_2SO_4 + 2HCl$$

$$3M_2SO_4 + Fe_2O_3 + 3SO_3 + 1\tfrac{1}{2}O_2 \longrightarrow 2M_3Fe(SO_4)_3.$$
(scale)

where M = Na and/or K.

As the maximum generation of SO_3 is between 600 and 700° C it is claimed that, at the oxide/deposit interface in boiler deposits, where this order of temperature could be observed, the complex sulphates decompose to give SO_3 which diffuses and attacks the metal.

2.6.3. Vanadate Deposits.

It has been mentioned that in residual fuel oil deposits Vanadium oxides can be a major constituent. Wickert (212) has shown that oxidation under such a fuel oil deposit increases with increasing temperatures, whereas corrosion under sulphates goes through a maximum.

The type of attack has been suggested to occur by various mechanisms and according to a review of the subject (88) three mechanisms appear to be possible:-

1. The Vanadium compounds acts as a carrier for oxygen.
2. The Vanadium compounds dissolve the oxide scale.
3. Vanadium enters the oxide scale on the metal, increasing the defect mechanisms and allowing accelerated attack.

In practice 1.1.5. sodium vanadyl vanadate ($Na_2O.V_2O_4.5\ V_2O_5$) is frequently found in boiler deposits as reported by Small, Strawson and Lewis (199) and they consider that this is the most aggresive of the sodium/vanadium oxide mixtures.

The oxygen carrier mechanism is postulated as:-

$$SO_2 + Air \longrightarrow SO_3$$

$$SO_3 + Na_2O.\ V_2O_4.5V_2O_5 \longrightarrow Na_2O.\ 6V_2O_5 + SO_2$$

$$Na_2O.6V_2O_5 + \text{metal} \longrightarrow \text{metal oxide} + Na_2O.V_2O_4.5V_2O_5$$

From the literature it is known that a great deal of work has been done on the resistance of conventional alloys to vanadium pentoxide slags. It is also known that the slags are only particularly aggressive when molten and that the reaction seems to be determined by the rate of oxygen arrival at the metal surface diffusion through the slag. More work is obviously needed on the mechanism of vanadium slag attack (88).

2.7 Methods of Reducing Corrosion.

It is impossible to prevent some degree of interaction between a metallic component and high temperature gases but a reduction of the interaction to a low value may be possible. There are many ways by which this could be attempted in a contaminated combustion atmosphere and the approaches used depend upon either (a) changing the environmental conditions or (b) changing the material.

There are three basic ways in which the environmental conditions can be modified to reduce the corrosion problems and these are:-

(i) Removal of harmful impurities present in the environment.

(ii) Addition of a compound to counteract the harmful inpurities.

(iii) Changing the combustion conditions to minimise attack.

The selection of materials to withstand corrosive attack is the ultimate problem which is never going to be completely solved and it is considered together with the possibilities of protecting existing alloys by coatings of corrosion resistant materials.

2.7.1. Changes in Environmental conditions.

2.7.1.1. Removal of harmful impurities.

The corrosion problems in atmospheres arising from the combustion of fuel oil would undoubtedly be reduced if contaminants such as chlorine, sulphur and the ash-forming elements could be removed. The possibility of removal has been reviewed by Edwards (65), Williams and Crawly (219) and Samms and Smith (188). The conclusions reached are that the removal of harmful constituents, particularly sulphur, from fuel oil is not economically possible. Water washing of fuel oil however can reduce the sodium concentration appreciably. Water washing and centrifuging of fuel oil used in marine boilers has been found to reduce the sodium concentration by about 75-

80% with consequent reduction in Supherheater deposition (188, 201).

Water washing however does not remove vanadium and a 20% Na_2O/V_2O_5 mixture was found to be most corrosive (171).

2.7.1.2. The use of fuel additives.

The effect of additives on combustion conditions has been extensively reviewed (6,52,69,88,120,121, 122,158,212). Fuel additives had been developed mainly to resist the vanadium pentoxide type of attack that occurs with residual fuel oil (24,39, 49,56,62,89,133,168,182,186,203,211).

According to Jenkinson and Zaczek (120) the ideal additive should:-

(a) Contain no metal radical to increase deposit bulk.

(b) Be soluble in fuel oil.

(c) Improve combustion conditions, especially atomisation.

(d) Reduce the ignition time lag.

(e) Reduce sulphur trioxide in the gas stream to less than 5 ppm in spite of excess air present.

(f) Prevent the formation of as much vanadium pentoxide as possible.

But non of the common inhibitors obey these conditions.

One type of additive works by forming stable vanadate of higher melting point than the vanadium compounds originally present, thus preventing formation of a liquid phase at the operating

temperature. MacFarlane (156) has reviewed the effect of such additives and particularly calcium, magnesium and zinc compounds are discussed. These elements can all form stable vanadates of the form 3 MO. V_2O_5. However, sulphur trioxide will also be present in combustion systems and this may sulphate the addition elements and destroy their effectiveness. It was found that calcium additions were fully sulphated in deposits up to 750° C and 90% sulphated at 800° C and corrosion rates were little better than in untreated fuel. Under similar conditions magnesium was only 30% sulphated in deposits at temperatures above 700° C but fully sulphated at 600° C. Ash deposits from fuel containing zinc were completely unsulphated. With either zinc or magnesium additive it was shown possible to reduce the corrosion rate at 700° C to similar proportion to that observed using distillate fuels. However, when zinc was added below the stoichiometric quantity required to form $3ZnO.V_2O_5$ little benefit was observed as the melting point of the vanadium compounds formed did not increase significantly until enough zinc is present to form $2ZnO.V_2O_5$. Magnesium addition, however, raised the melting point of the deposit appreciably from 680° for $\frac{1}{2}MgO.V_2O_5$ and $3MgO.V_2O_5$ to 1100° C and has been found to be effective. The magnesium can be added to fine dispersions of oxide or carbonate as the oil-soluble naphthenate and acetate or as aquous solutions of sulphate and chloride. The oxide addition appears to be least successful whilst all others are equally effective, but the effectiveness decreases with increasing sulphur content of the fuel due to sulphation (65).

The successful use of solid MgO addition has been reported (49) for a boiler operating at 565° C. It is claimed that the additive cuts down the corrosion experienced by 65–70% and that deposits, instead of being hard, tenacious and insoluble, as in the case with untreated fuel, are soft, powdery and easily removed. One problem with magnesium addition is that they usually cause increased fouling by deposits and as the melting points of the compounds formed are far in excess of the operating temperatures used, it is not obvious why this should be so.

The addition of calcium and barium salts have shown (168) that both are highly sulphated and not recommended.

Dolomite ($CaCO_3$, $MgCO_3$) has been widely used as an additive with mixed success (188). It is claimed that the dolomite additions give less corrosion on high chromium alloys but cause increased attack of low chromium alloys. One disadvantage with dolomite, as with all solid additives, is that it is difficult to disperse uniformly in the combustion system and that streaming can occur, giving uneven corrosive conditions through the installation.

The inert additives such as Kaolin ($Al_2O_3.2Si\ O_2.2H_2O$) to swamp the effect of vanadium pentoxide has been discussed (156, 202). The idea was to add sufficient high melting point inert material to the fuel to swamp the low melting point ash characteristic so that any deposits which do form are easily blown off. This type of additive is primarily of use for turbine practice where the high gas flows would tend to remove such deposits.

The possibility of using a dual inhibitor which contain both magnesium and an inert additive appears to be feasible but the limitations of this type of approach become more economical than metallurgical.

2.7.1.3. Operating procedures (controlled combustion).

Detailed design in boilers and trubines can do a great deal to minimise corrosion problems (214). The points such as avoiding direct impingement of the flame on super heater tubes and design of burners to give uniform conditions throughout the installation can overcome localised problems.

Oil droplets burn by stages and droplet size can affect the corrosive products produced, e.g. coarse atomisation has been shown to be advantageous in reducing deposition from high vanadium fuels (19,50). It is claimed that the increased carbonaceous matter in the larger droplet reduces the oxides of vanadium so that they pass through the turbine rig as the high melting point V_2O_3 and V_2O_4 and this causes reduction in deposition and corrosion. This approach may not be quite so effective in boilers where the gas flow is much slower.

Eisenklam (66) suggested that in boilers a two-stage process might be advantageous. In the first stage combustion is made with a 30% deficiency of oxygen. The temperature may reach about 2000° C and half the energy is removed in the superheater tube bank. The gas leaves the tube bank at about 900° C and further air is added to bring the oxygen level to stoichiometric. The temperature rises during combustion to about 1400° C and the rest of

the heat is removed in another part of the boiler. The advantage of this method is that it limits maximum temperatures and delays the formation of the aggressive oxides of vanadium.

It has been shown (6,37,155,156) that nearly stoichiometric quantities of oxygen reduce the amount of sulphur trioxide formation and, from free energy considerations, they should also restrict vanadium pentoxide formation.

Glaubitz (83) reported that burner developments have made it possible to burn oil under conditions of less than 1% excess air. A boiler with such a burner has been operating for 40,000 hours with reduced fouling and corrosion problems.

2.7.2. Surface Coatings and New Materials.

The use of corrosion resistant coatings for existing alloys has found widest application in the gas turbine field. Metallic coatings have been applied by electrodeposition, high temperature diffusion and plasma arc spraying. The effect of ceramic coatings has also been investigated. The metallic coatings applied have been principally those of silicon, chromium, aluminium, zirconium and beryllium (88, 116).

In the late 1950's, the U.S. Navy boiler turbines laboratory and the U.S. National Bureau of standards, following studies of a large number of alloys in oil ash environments, suggested 50/50 and 60/40 chromium-nickel cast alloys as being potentially suitable for super-heater supports in marine boilers fired by heavy residual fuel and extensive shipboard trials showed these alloys to be vastly superior to the 25Cr/12Ni and 25Cr/2Ni alloys in standard use. The 50/50 chromium-nickel alloys was incorporated in ASTM A560 and in the 1960's was extensively used in refinery heaters,

marine and land based boilers; experience from the corrosion point of view was generally good, showing a marked improvement compared with the usual tube support alloys. In its earliest application of oil refinery heaters, the 50Cr/50Ni alloy showed quite satisfactory in replacing 25Cr/12Ni and 25Cr/20Ni and its relatively low, high temperature strength did not cause any particular problems; at that time, tube supports tended to be designed by 'rule of thumb' methods and were excessively thick, which masked the significantly lower strength of 50Cr/50Ni alloy relative to the alloys it was replacing. In the late 1960's, furnace designers generally started designing the tube supports rather more critically to minimise costs, and subsequently, direct 50Cr/50Ni alloy replacements for standard 25Cr/12Ni and 25Cr/20Ni tube supports with unchanged section thickness frequently failed by creep distortion, cracking and rupture, rather than by corrosion, emphasising the need for a strengthened 50Cr/50Ni alloy (185).

Extensive research resulted in the development in 1971 of a niobium coating 50Cr/50Ni alloy designated IN657 with considerably improved high temperature strength and somewhat better retained ductility, after prolonged high temperature exposure, than the standard 50Cr/50Ni alloy (185).

2.8 Corrosion monitoring techniques.

Corrosion monitoring may be defined as the systematic measurement of the corrosion or degradation of an item of equipment, with the objective of assisting understanding of the corrosion process and/or obtaining information for use in controlling corrosion and its consequences (113,160,193).

The concept of corrosion monitoring has developed from two distinct areas, plant inspection techniques and laboratory corrosion-testing techniques, with the original aim of assessing or predicting the corrosion behaviour of plant and equipment between shutdowns. There are, equally, two sets of objectives which are essentially distinct although related, and to an extent overlapping. The first is to obtain information on the stage of operational equipment - to permit the better scheduling of maintainance work to ease the inspection load during shutdowns and to avoid unplanned shutdown occuring because of unforseen deterioration of plant. The second objective is to obtain information on the interrelation between corrosion processes and operating variables, - to help diagnosis of the problem and to allow improved control of corrosion and more efficient driving of the plant. Figure 2(17) summarises the use of corrosion monitoring.

Many techniques can be used for corrosion monitoring, and it is clearly possible to develop others. Any monitoring technique can provide only a limited amount of information and the techniques should be regarded as complementary rather than competitive. Table 2(7) shows the characteristics of the different monitoring techniques available.

The most obvious method of assessing the corrosivity of an environment to a specific material is to expose a specimen for a given time, and to measure the resultant effects. This is the basis of coupon testing which is the oldest form of corrosion monitoring. It can be adapted to meet the requirements and capabilities of both staff and plant. The tests are usually long term, they are very specific with respect to specimen location, and the corrosion

rate is a composite value for the total exposure time.

The major measurement is weight-loss, and to improve accuracy a large surface area to mass ratio is desirable. The coupons can be in the form of discs, rods, plates or any convenient shape, but the edges should be machined and polished to avoid preferential attack due to residual stresses from the cropping operation. All traces of grease, oxide and other contaminants must be removed prior to installation, and to improve reproducibility, the surface finish should approach that of the proposed plant material, usually polishing on a grade of metallographic paper, or light sand blasting, is preferred but a pickled surface can be more representative. Specimen identification marks are essential and should be positioned where they will be protected by the coupon holder or insulations.

In general, the corrosion rate of freshly exposed material decreases rapidly with exposure time, and the test must be long enough to ensure that the determined corrosion rate is not solely representative of the initial high corrosion rate unless this is specifically required. A useful guide to the duration of a test is given by the relationship:

$$T = \frac{50}{CR}$$

where T = time in hours, and
CR = corrosion rate (mm per year).

After exposure the coupons should be carefully examined and a complete record made of the appearance of corrosion products before cleaning and weighing. All accumulated corrosion products and fouling should be removed either mechanically by scrubbing, scraping, sand-blasting etc. or chemically by washing in solvents, or pickling in inhibited acids or alkalis. Errors may be introduced during this stage due to the loss of "sound metal" or the incomplete removal of corrosion products. This error will be magnified on short corrosion tests when it will represent a reasonable percentage of the total weight loss. From the weight loss results and knowledge of the original dimensions and density of the

metal under test the corrosion rate can be readily determined from the following equation:

$$\text{Corrosion rate (mm per year)} = \frac{\text{Weight loss (mg)} \times 87.6}{\text{area (cm}^2\text{)} \times \text{time (hours)}} \times \text{metal density (g per cm}^3\text{)}$$

The conversion of corrosion rates is shown in Appendix 2(1).

The establishment of the corrosion rate using the simple weighing technique assumes that the metal loss has occurred uniformly, and a visual examination aided by the use of metallurgical microscopes will be required to detect the presence of localised corrosion in the form of pitting, intergranular corrosion, stress corrosion cracking etc, (193).

The coupon testing techniques is still widely used despite the advent of rapid response instruments its main advantage being that many different materials can be exposed at one site and unambiguous data on the form of corrosion on the specimen can be obtained. The main limitations on the technique are its inability to detect short range changes in process variables, and that the behaviour of the specimens may not be truly representative of the plant. If these limitations are unimportant in the circumstances it can be used as the only monitoring technique, (193).

Coupon testing proved to be very suitable for the work described here (see section 6).

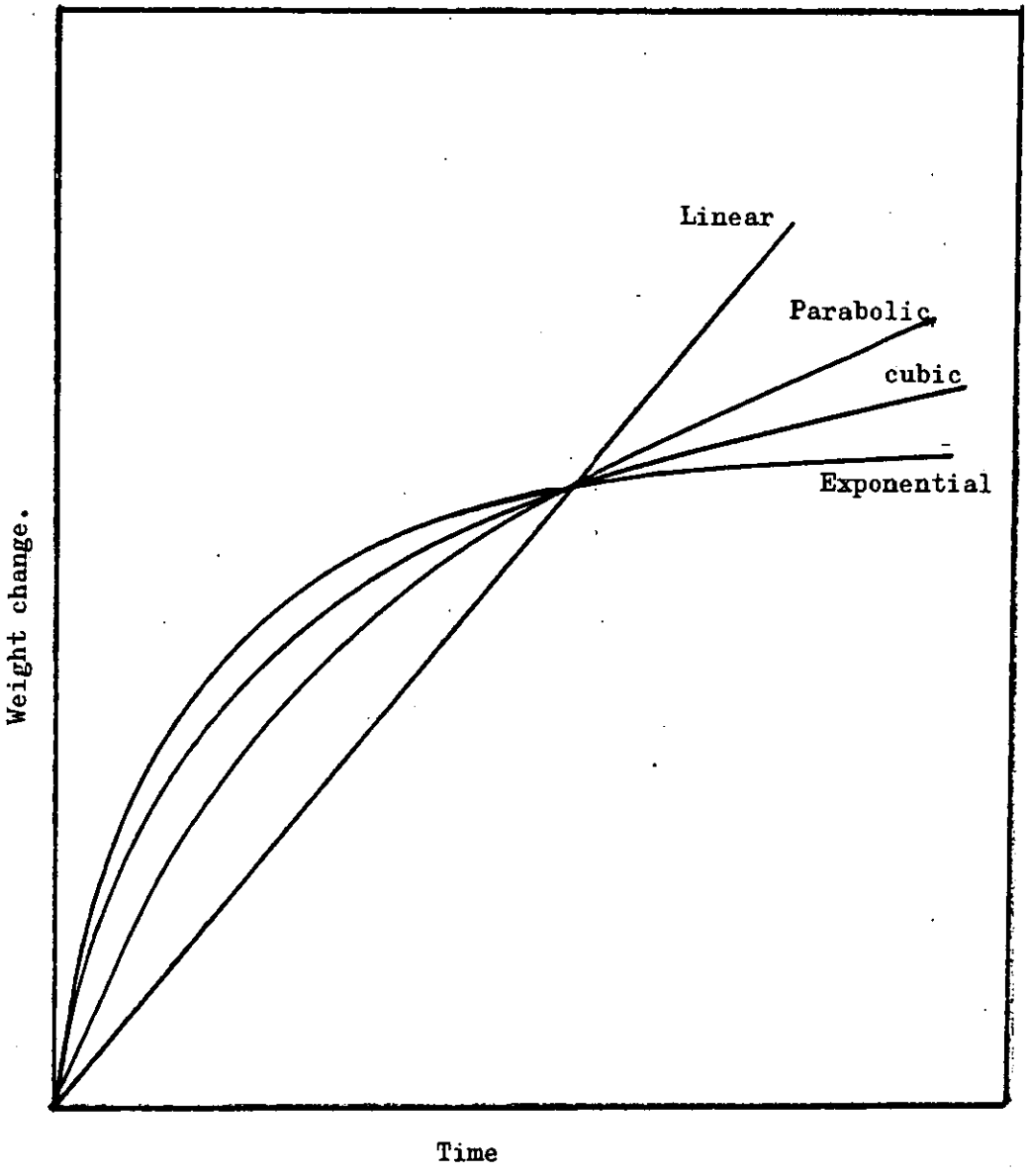

Figure 2(1). Oxidation rate laws (193).

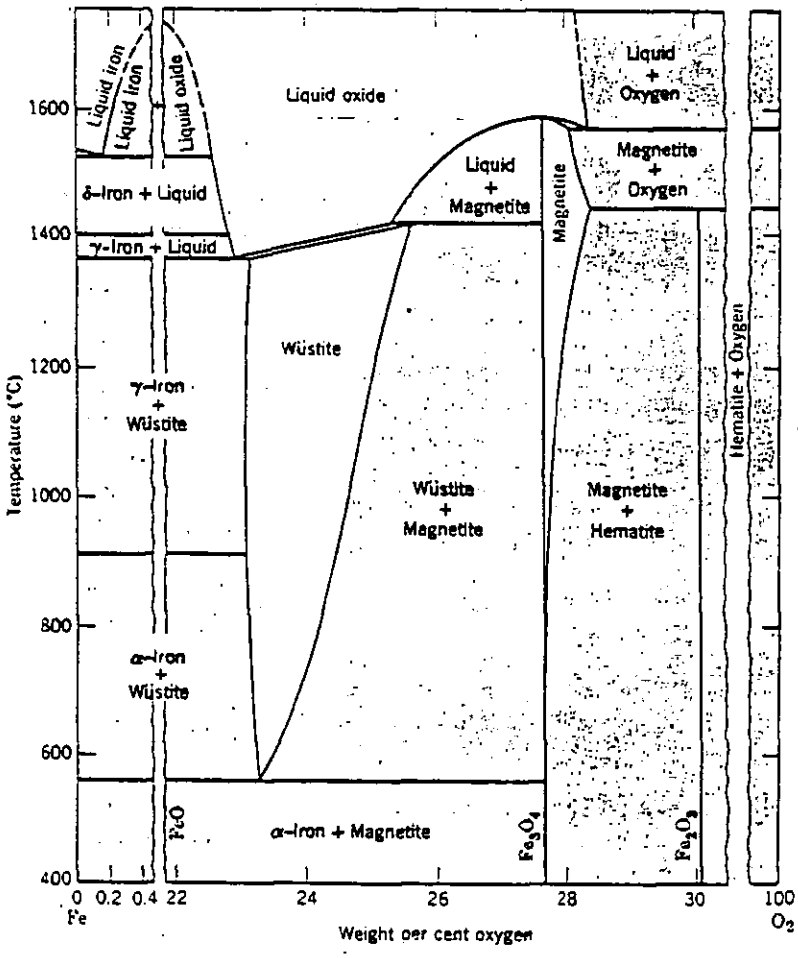

Figure 2(2) Phase equilibrium diagram of the binary system Fe-O_2 at one atm. (after Darken, L.S. and Gurry, R.W., J. Am. Chem. Soc., 68 , 799, 1946).

Table 2(1). Oxidation Resistance of a carbide hardened alloy based on the Nickel-Chromium-Cobalt system (88).

Vanadium Addition %	Weight gain after 100 Hour oxidation at 900° C. mg/cm^2.
0	0.35
.53	1.8
1.06	3.3
2.03	5.75
2.97	3.1
3.82	6.3

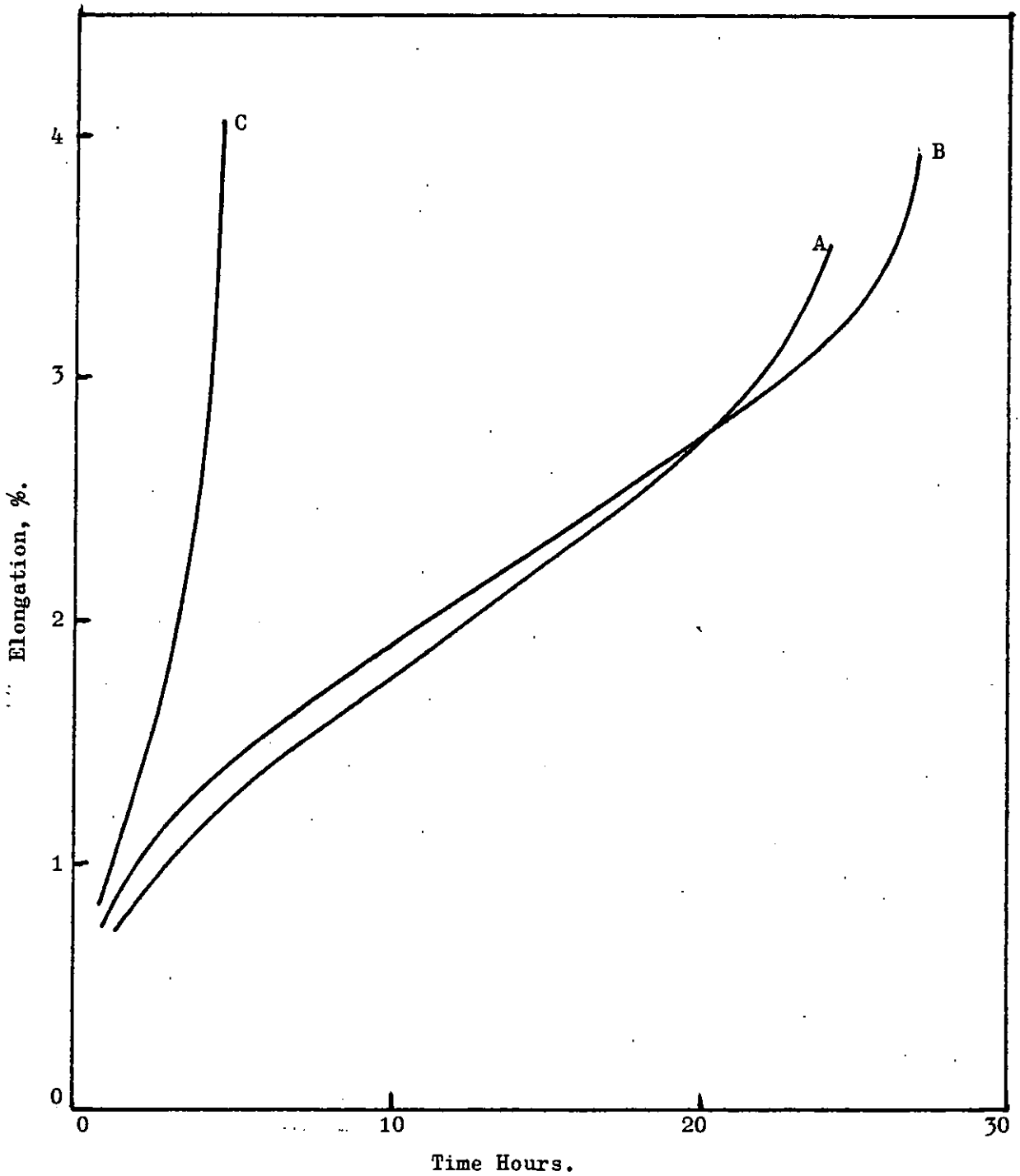

Fig. 2(3). Influence of oxidation on creep tests at 725° C at 1.5 tons/m^2. (88).

A. As received condition

B. Vacuum annealed 24 hours at 100° C

C. Pre-oxidised 24 hours at 1000° C.

TABLE 2(2) TYPICAL CHARACTERISTICS OF OIL-FIRED BOILER (52).

Country	Operating stations	Capacity mw	Pressure Kg/cm²	Steam Condition Temp	
				Superheater °C	Reheater °C
U.K.	Kingsworth Fawley and Pembroke	500	160	540	540
France	Porchville	600	160	565	565
	Nante Chevire	250	163	565	565
Holland	Amer	184	570	540	540
Italy	Lo Spezia	600	250	565	565
Japan	Owase-Mita	375	177	570	540

TABLE 2(3) TYPICAL "IMPURITIES IN OIL" USED IN POWER STATIONS (105).

"Impurities in Oil" (Parts per million by weight)			
Sulphur	20,000	Zinc	4
Nitrogen	1,500	Phosphorus	4
Silicon	300	Chromium	3
Vanadium	150	Cobalt	3
Iron	100	Manganese	2.5
Nickel	50	Copper	2.5
Calcium	100	Lead	2
Potosium	50	Selenium	1
Aluminium	75	Cadmium	0.2
Sodium	50	Antimony	0.02
Chlorine	25	Arsenic	0.01
Magnesium	12	Mercury	0.01

TABLE 2(4) ASH ELEMENTS IN CRUDE OIL (218).

In Parts Per Millian

Element	U.S.A.	Venezuela	Columbia	East Indies	Middle East
Al	.3	1.0	.3	6.0	7
Ca	1.2	1.4	nil	.2	.1
Cr	.1	1.4	nil	.2	.1
Ca	1.6	nil	nil	1.9	nil
Cu	.5	7.3	7	1.0	5
Fe	4.6	30.0	.4	61.0	5
Pb	.7	2.1	nil	.7	.1
Mg	2.0	1.7	1.2	1.7	7
Mn	nil	nil	nil	trace	trace
Mo	.1	.3	nil	.6	.2
Ni	1.2	6.0	10	1.0	30
K	2.9	2.1	nil	nil	.7
Si	.5	1.7	.8	6.9	1
Na	38.0	33.0	9.4	15	.5
Sn	.1	.5	.3	.9	nil
Ti	.2	.3	nil	.3	4
V	1.9	30.0	72	nil	100
Zn	2.1	3.0	nil	.6	2

TABLE 2(5) MELTING POINTS OF MATERIALS THAT POSSIBLY OCCUR IN COMBUSTION DEPOSITS. (88).

Compound		Melting Point °C	Occurrence
Alumina	Al_2O_3	2050	
Amuminium Sulphate	$Al_2(SO_4)_3$	770	
Calcium Oxide	CaO	2572	
Calcium Sulphate	$CaSO_4$	1450	Possible in both
Ferric Oxide	Fe_2O_3	1565	coal and oil
Magnetite	Fe_3O_4	1538	fired installations
Ferric Sulphate	$Fe_2(SO_4)_3$	480	
Magnesium Oxide	MgO	2500	
Magnesium Sulphate	$MgSO_4$	1124	
Nickel Oxide	NiO	2090	
Nickel Sulphate	$NiSO_4$	840	
Silica	SiO_2	1710	
Potasium Sulphate	K_2SO_4	1069	
Sodium Sulphate	Na_2SO_4	884	
Sodium Bisulphate	$NaHSO_4$	250	
Sodium Pyrosulphate	$Na_2S_2O_7$	400	
Potassium Pyrosulphate	$K_2S_2O_7$	300	
Vanadium Trioxide	V_2O_3	1970	
Vanadium Tetraoxide	V_2O_4	1970	
Vanadium Pentoxide	V_2O_5	690	
Sod. meta Vanadate	$Na_2O.V_2O_5$	630	Most important
Sod. Pyrovanadate	$2Na_2O.V_2O_5$	640	in oil fired
Sod. Orthovanadate	$3Na_2O.V_2O_5$	850	installations.
Sod. Vanadyl Vanadates	$Na_2O.V_2O_4.5V_2O_5$	625	
Sod. Vanadyl Vanadates	$5Na_2O.V_2O_4.11V_2O_5$	535	
Nickel Pyrovanadate	$2NiO.V_2O_5$	900	
Nickel Orthoranadate	$3NiO.V_2O_5$	900	
Ferric Metavanadate	$Fe_2O_3.V_2O_5$	860	
Ferric Vanadate	$Fe_3O_4.2V_2O_5$	855	

Table 2(6). SULPHUR CONTENT IN FRACTIONS OF KUWAIT CRUDE OIL (164).

Fraction	Distillation Range, °C.	Total Sulphur weight Per cent.
Crude oil	--	2.55
Gasoline	51 - 123	0.05
Light naphtha	125 - 149	0.05
Heavy naphtha	153 - 197	0.11
Kerosene	207 - 238	0.45
Light gas oil	247 - 269	0.85
Heavy gas oil	281 - 306	1.15
Residual oil	309 - 498	3.70

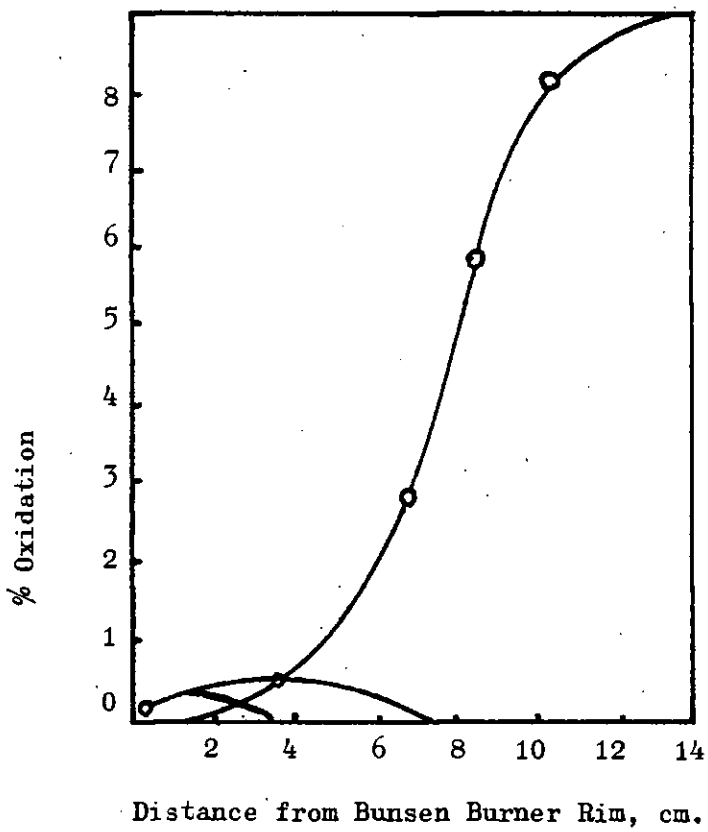

Figure 2(4). Variation of % oxidation of SO_2 with distance from Bunsen burner rim. (after Dooley and Whittingham 53).

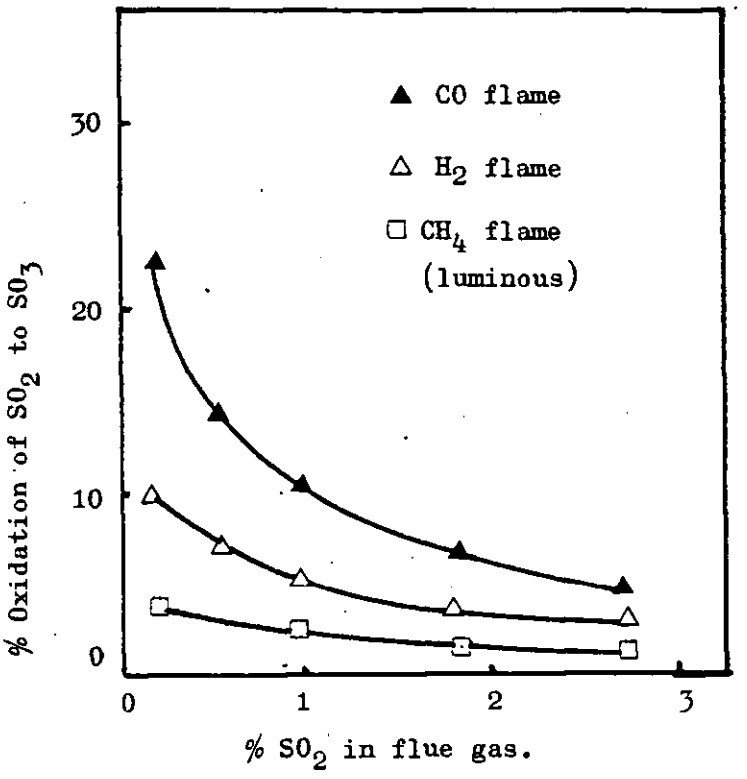

Figure 2(5) Oxidation of SO_2 in flames from different flue gases (after Dooley and Whittingham (53)).

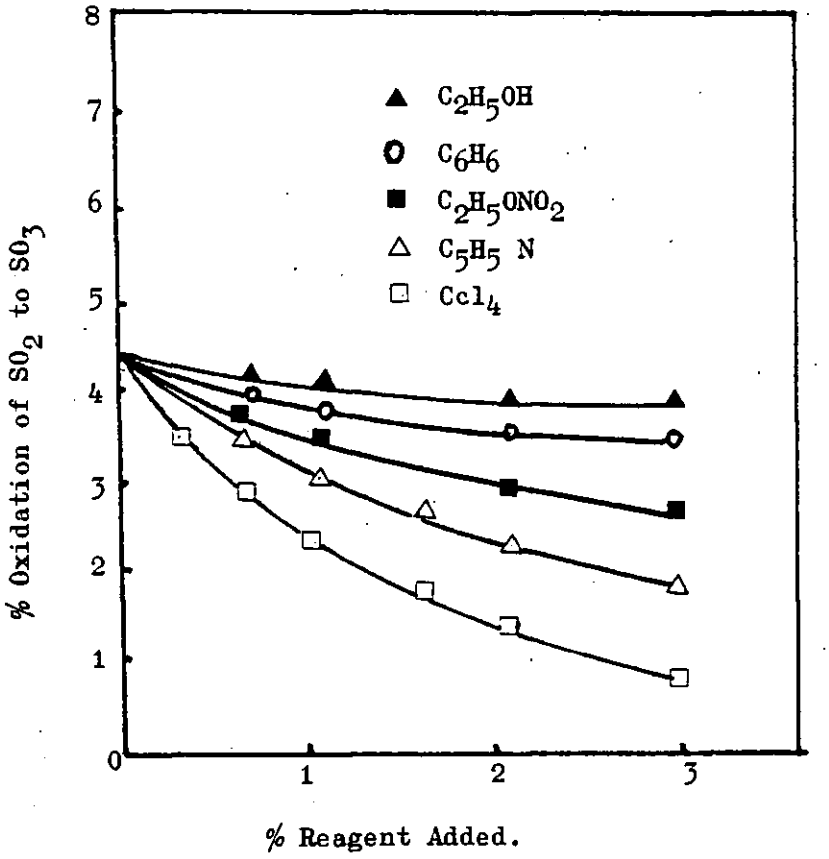

Figure 2(6). Effect of various substances on oxidation of SO_2 in a Bunsen flame. After Dooley & Whittingham (53).

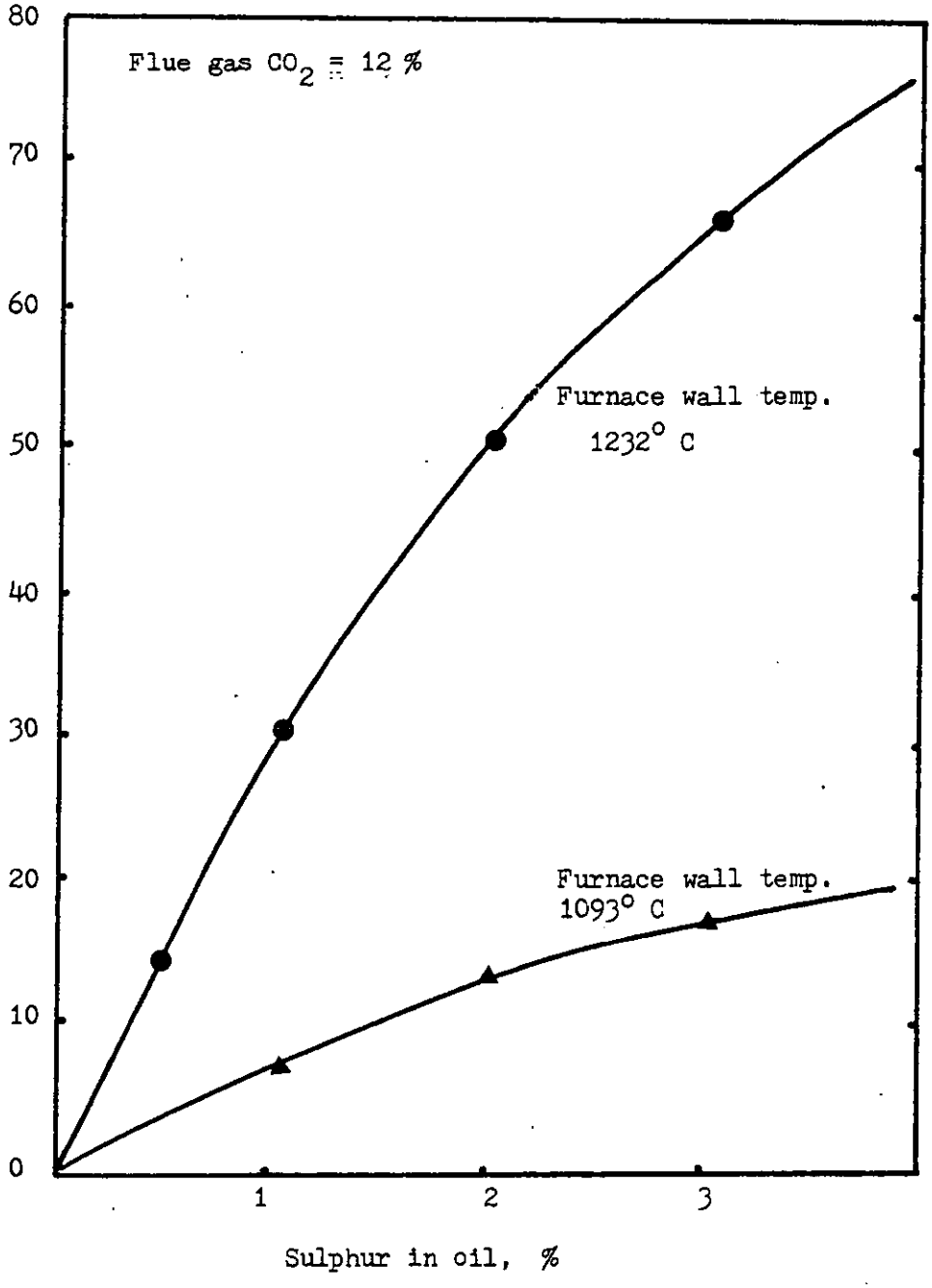

Figure 2(7) Variation of flue gas SO_3 with sulphur content of the oil (after Crumley and Fletcher' 37).

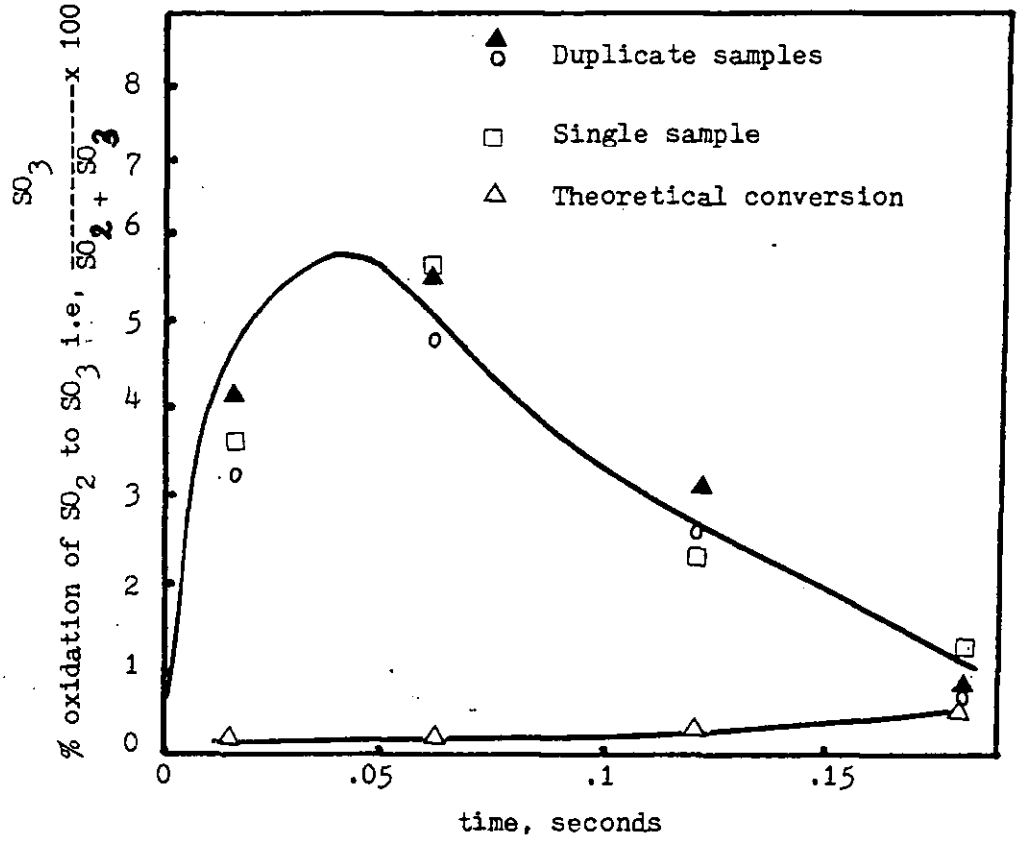

Figure 2(8) Variation of % oxidation of SO_2 with time in a homogeneous plug flow reactor (Hedley, 97).

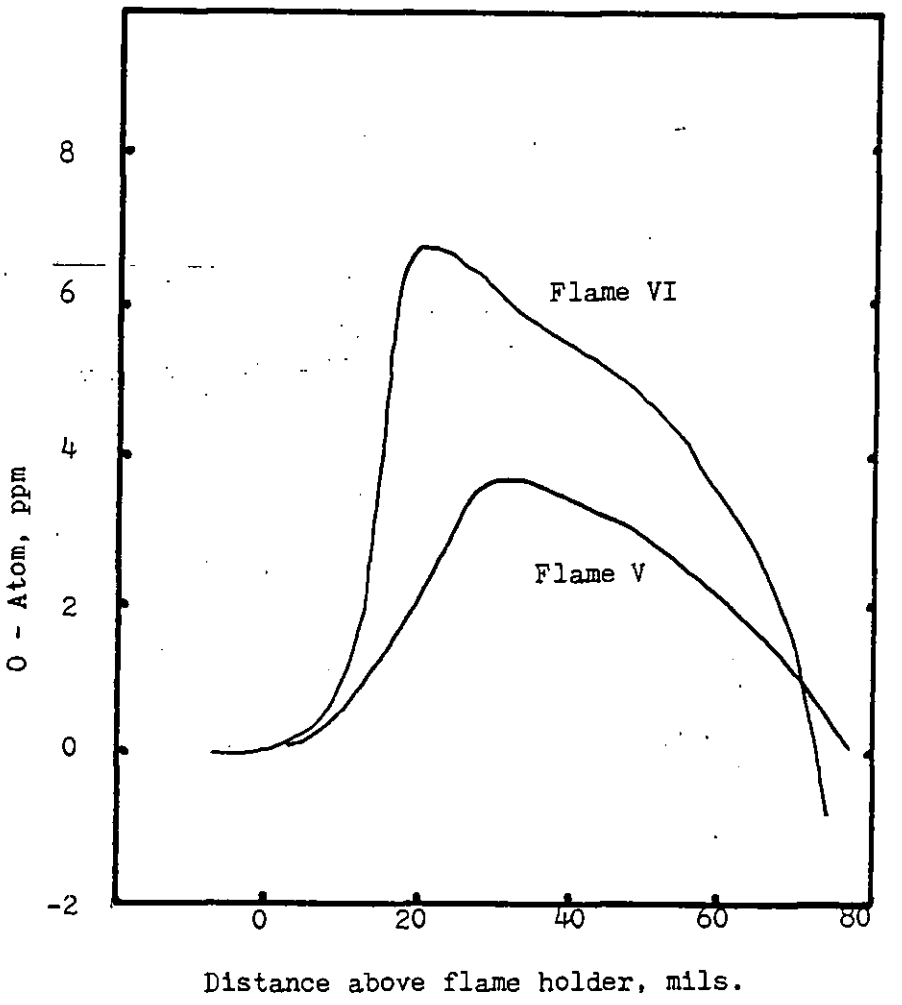

Figure 2(9) O - atom profiles (140).

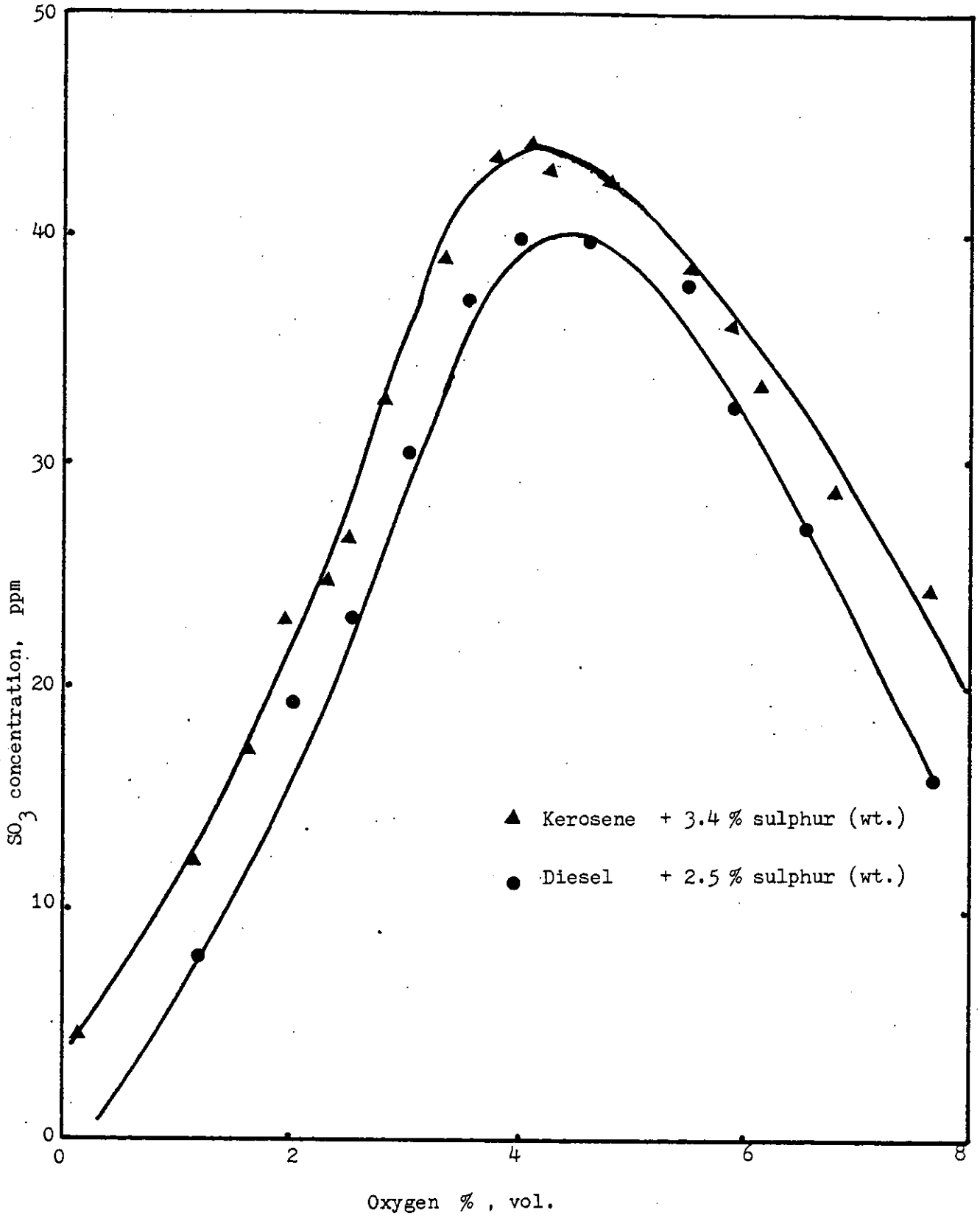

Figure 2(10) Effect of excess oxygen on the formation of SO_3 for Kerosene and Diesel fuels (2).

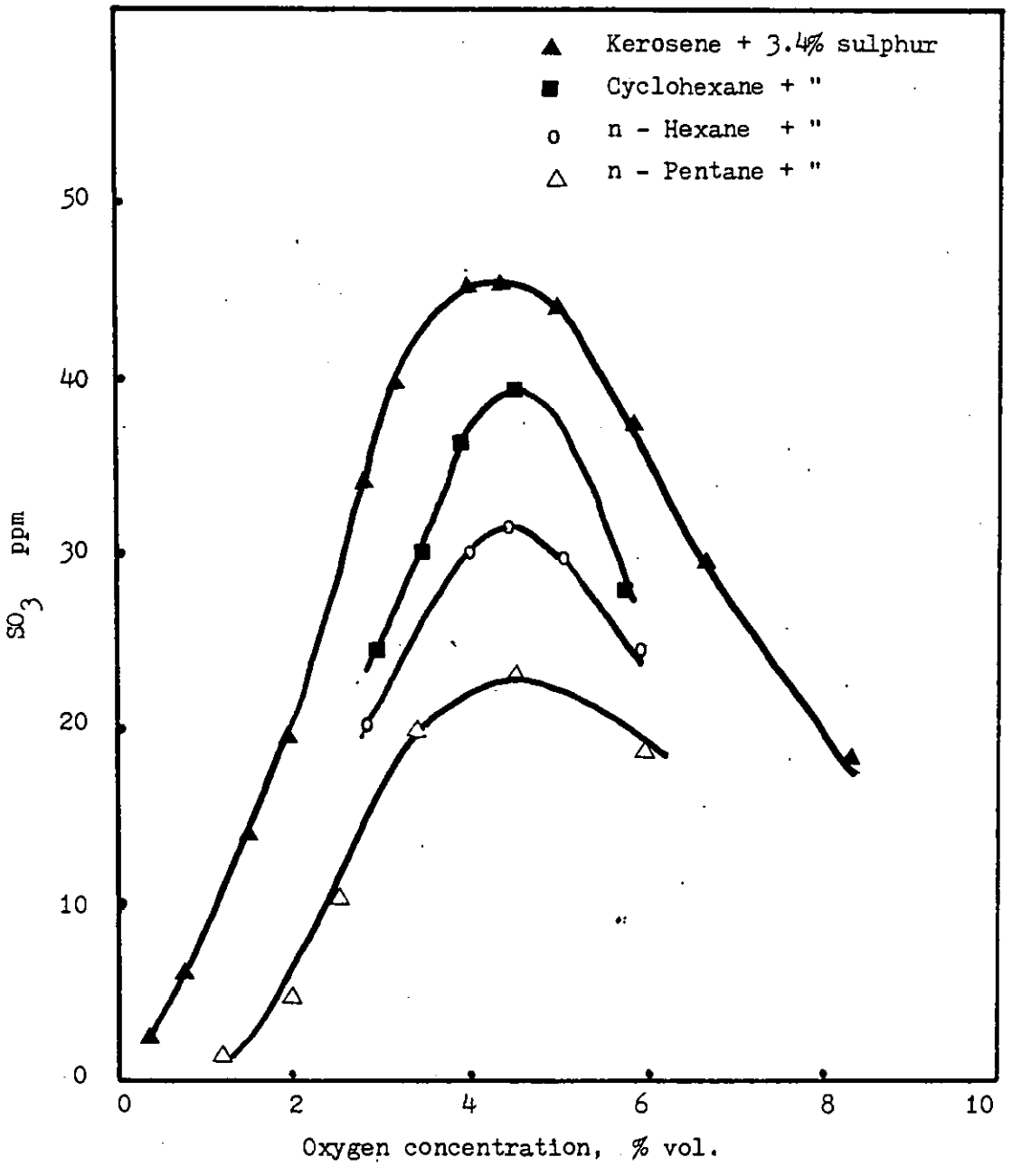

Figure 2(11) Variation of SO_3 content with excess oxygen in the combustion gases for various hydrocarbons doped with same amount of sulphur (3).

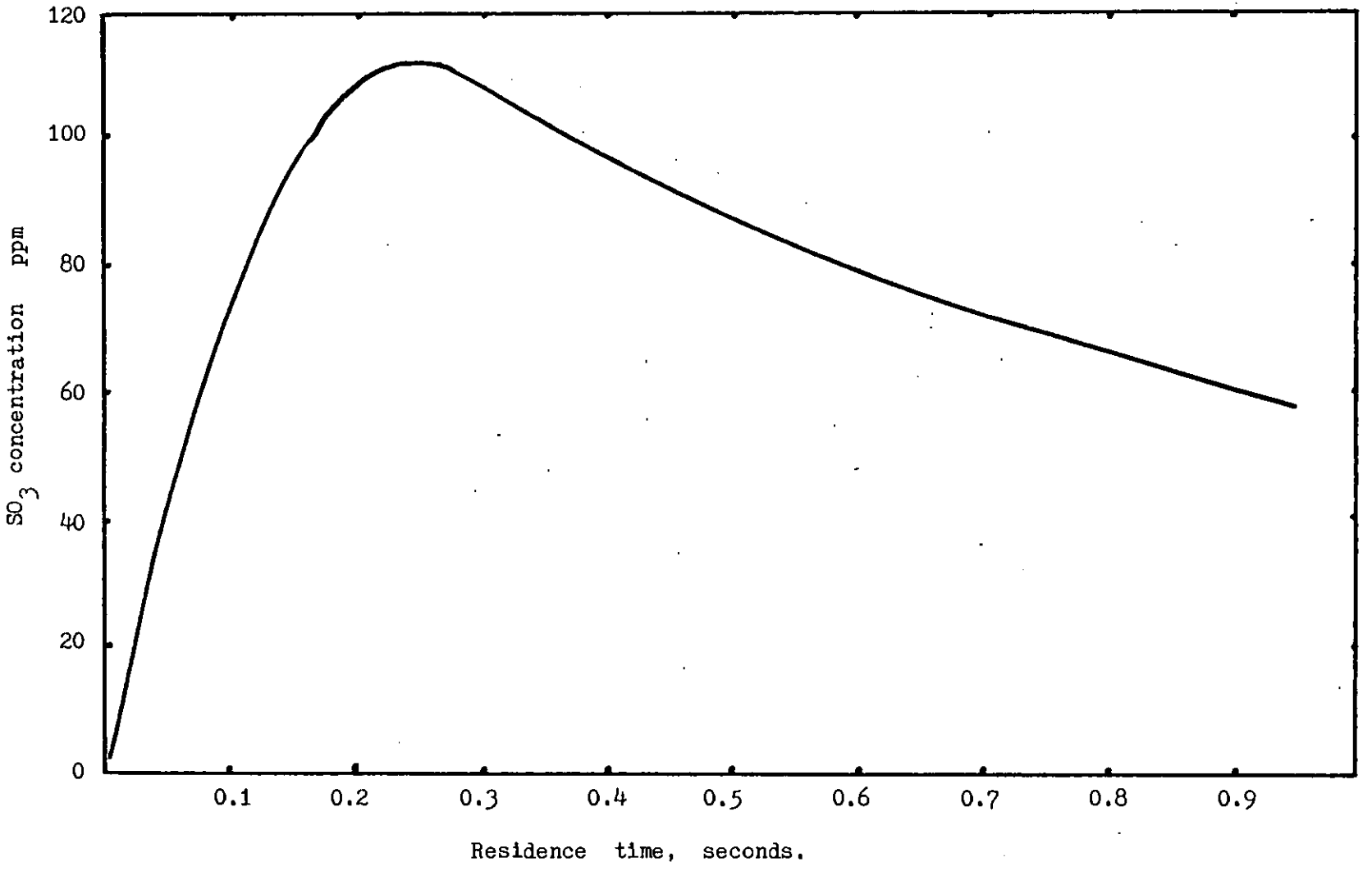

Figure 2(12). Variation of SO_3 concentration with time (2).

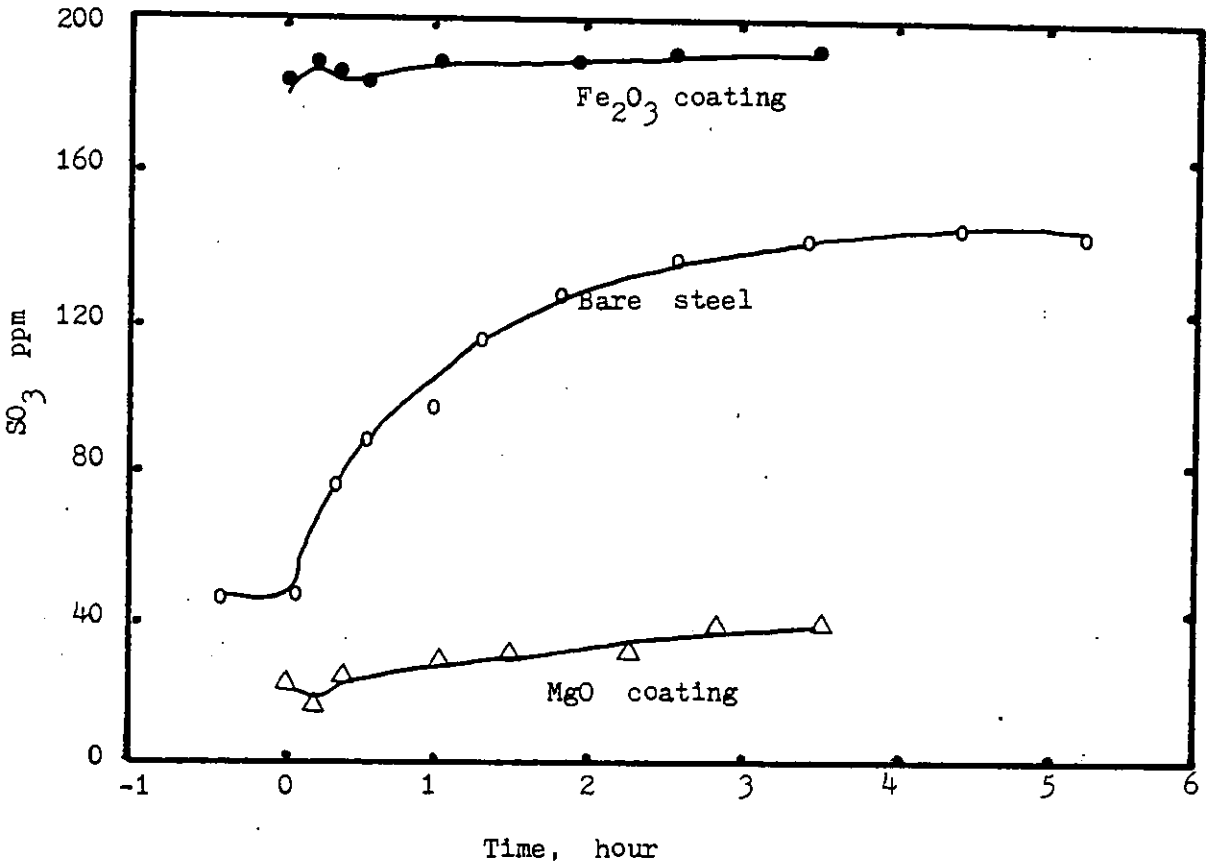

Figure 2(13) SO_3 concentration downstream of bare and coated mild steel specimens (12).

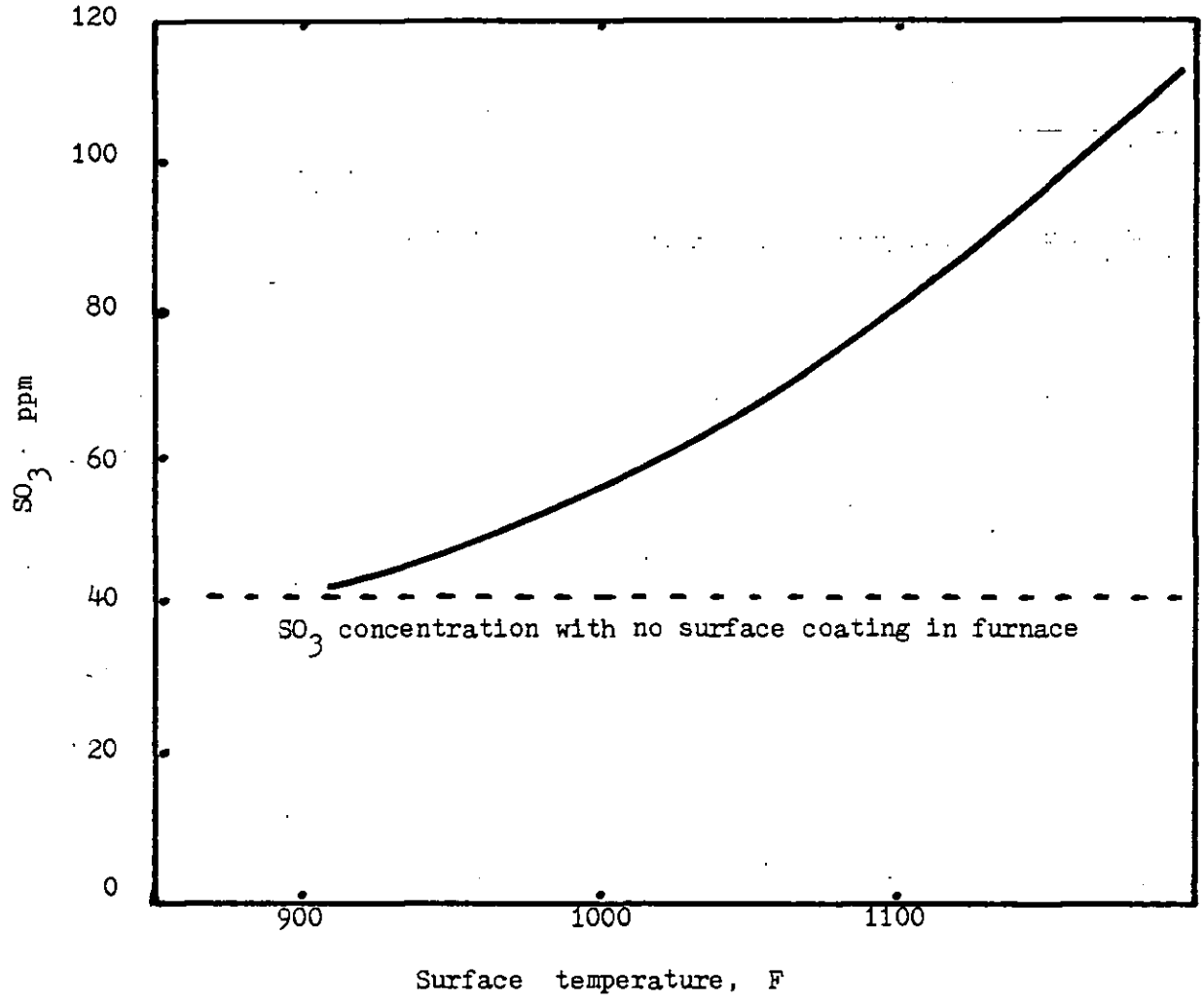

Figure 2(14) SO_3 concentration downstream of an Fe_2O_3 coated surface at several temperatures (Barrett ' 12).

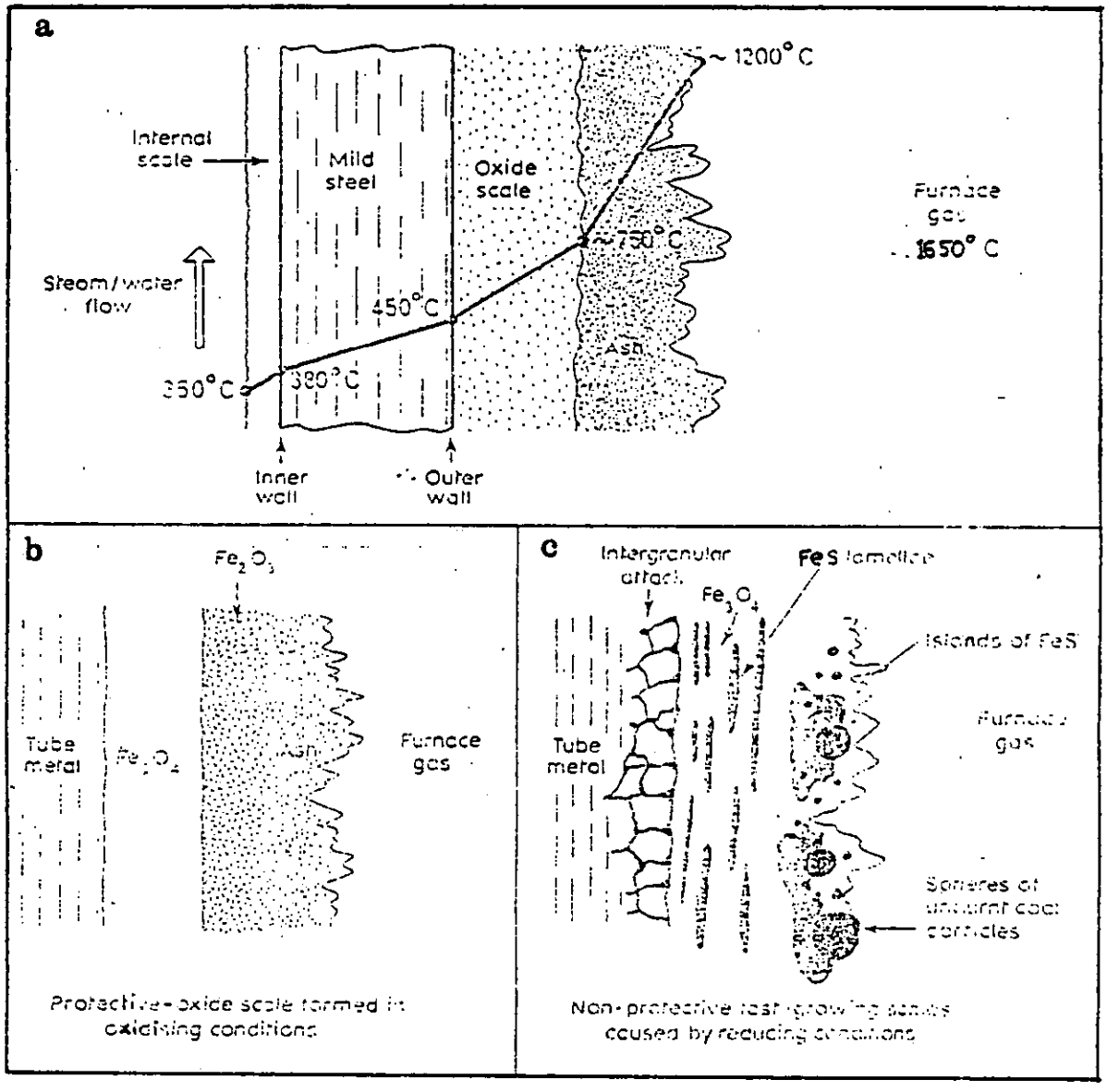

Figure 2 (15) (a) Temperature gradient through the oxide scale and deposited ash.

(b) Protective - oxide scale formed in oxidising conditions.

(c) Non-protective fast growing scales caused by reducing conditions (41).

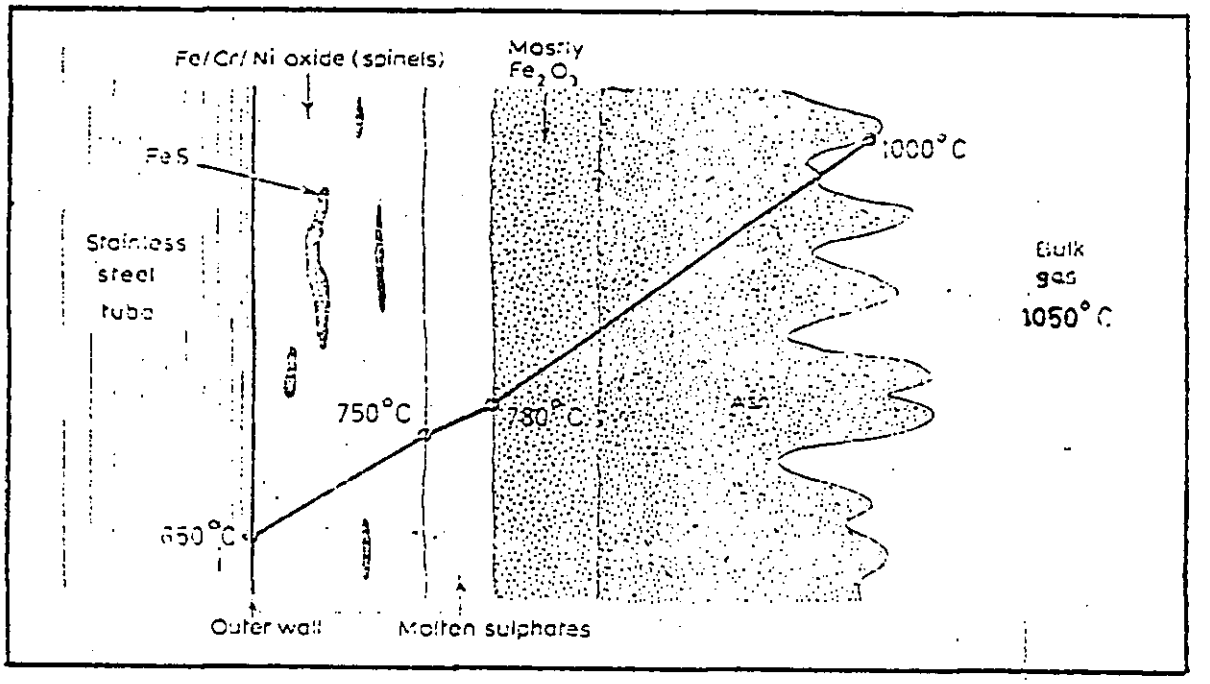

Figure 2 (16). The structure of scale and deposits on superheater tubing and the temperature gradient within them. (41).

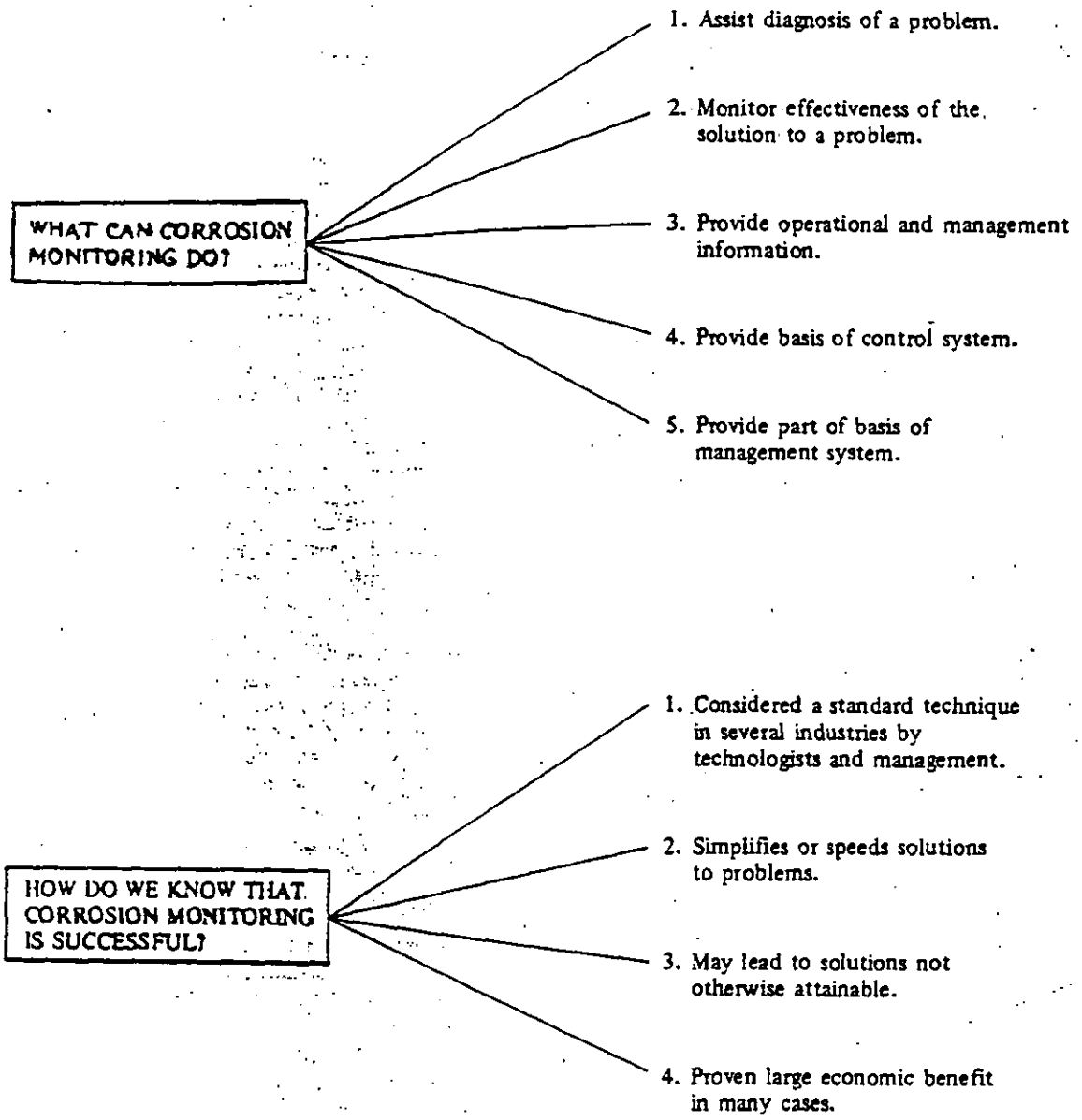

Figure 2(17). Summary of the use of Corrosion Monitoring.(193).

TABLE 2(7). Characteristics of Corrosion Monitoring Techniques (193)

Technique	Time for individual measurement	Type of information	Speed of response to change	Relation to plant	Possible environments	Type of corrosion	Ease of interpretation	Technological culture needed
Electrical resistance	Instantaneous	Integrated corrosion	Moderate	Probe	Any	General	Normally easy	Relatively simple
Polarisation resistance	Instantaneous	Rate	Fast	Probe	Electrolyte	General	Normally easy	Relatively simple
Potential measurement	Instantaneous	Corrosion state and indirect indication of rate	Fast	Probe or plant in general	Electrolyte	General or localised	Normally relatively easy but needs knowledge of corrosion. May need expert	Relatively simple
Galvanic measurements (zero-resistance ammeter)	Instantaneous	Corrosion state and indication of galvanic effects	Fast	Probe or occasionally plant in general	Electrolyte	General or unfavourable conditions localised	Normally relatively easy but needs knowledge of corrosion	Relatively simple
Analytical methods	Normally fairly fast	Corrosion state, total corrosion in system, item corroding	Normally fairly fast	Plant in general	Any	General	Relatively easy but needs knowledge of plant	Moderate to demanding
Acoustic emission	Instantaneous	Crack propagation, cavitation and leak detection	Fast	Plant in general	Any cavitation	Cracking, cavitation and leak detection	Normally easy	Crack propagation specialised, otherwise relatively simple
Thermography	Relatively fast	Distribution of attack	Poor	Localised on plant	Any. Must be warm or sub-ambient	Localised	Easy	Specialised and difficult
Optical aids (closed circuit TV, light tubes, etc)	Fast when access available, otherwise slow	Distribution of attack	Poor	Localised on plant	Any	Localised	Easy	Relatively simple
Visual, with aid of gauges	Slow. Requires entry on shut down	Distribution of attack, indication of rate	Poor	Accessible surfaces	Any	General or localised	Easy	Relatively simple but experience needed
Corrosion coupons	Long duration of exposure	Average corrosion rate and form	Poor	Probe	Any	General or localised	Easy	Simple
Ultrasonics	Fairly fast	Remaining thickness or presence of cracks and pits	Fairly poor	Localised on plant	Any	General or localised	Easy	Simple
Hydrogen probe	Fast or instantaneous	Total corrosion	Fairly poor	Localised on plant or probe	Non-oxidising electrolyte or hot gases	General	Easy	Simple
Sentinel holes	Slow	Go/no go on remaining thickness	Poor	Localised on plant	Any, gas or vapour preferred	General	Easy	Relatively simple
Radiography	Relatively slow	Distribution of corrosion	Poor	Localised on plant	Any	Pitting, possibly cracking	Easy	Simple but specialised radiation hazard

CHAPTER THREE.

OBJECTIVES OF INVESTIGATION.

With modern methods of refining of crude petroleum, high grade petrol is obtained leaving behind a high content of impurities in the residual fuel. The impurities contain substances such as sulphur, sodium and vanadium etc., and it is basically these substances which are mostly responsible for fouling and corrosion in oil-fired installations.

In order to increase thermal cycle efficiency of power generation the trend in modern plant is towards higher metal temperatures. The use of heavy/residual fuel oil for this purpose offers the boiler operators the possibility of reduced investment and operating costs as well as simpler storage and handling of the fuel and fewer problems with flue-gas solid burden. However, there are several problems which may be severe in oil-fired boilers. Among them are air pre-heater corrosion by SO_3 in flue gas and Superheater slagging and corrosion by vanadium and sodium ash in the fuel.

High temperature corrosion problems by combustion cases in an oil-fired laboratory combustor and the individual and collective effects at different ratios of sulphur, sodium and vanadium present in the fuel were proposed for study.

From an assessment of the literature, the present knowledge on the subject may be related to the objectives of the investigation by the following triangular diagram.

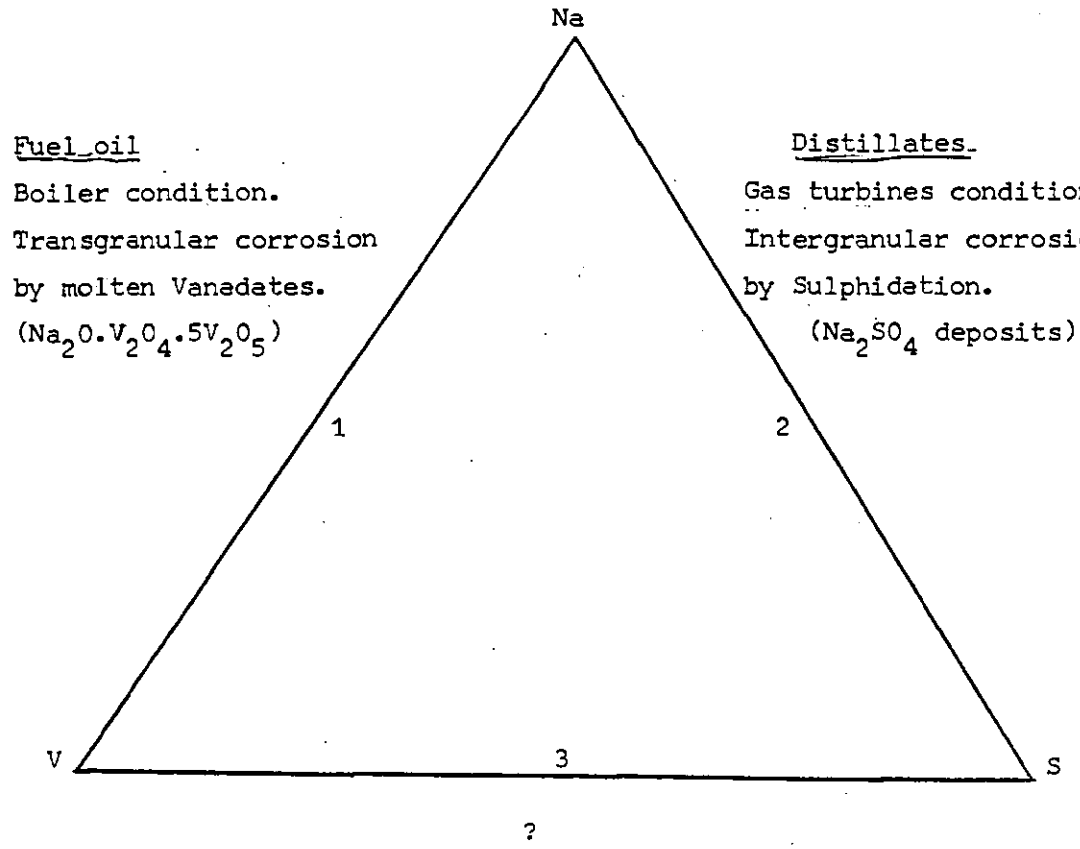

1 : Sodium and vanadium are present in the fuel oils used in the power station boilers. The corrosion mechanism reported is by the formation of 1.1.5 Sodium Vanadyl Vanadates ($Na_2O.V_2O_4.5V_2O_5$) according to the following reactions:

$$SO_2 + Air \longrightarrow SO_3$$

$$SO_3 + Na_2O.V_2O_4.5V_2O_5 \longrightarrow Na_2O.6V_2O_5 + SO_2$$

$$Na_2 + 6V_2O_5 + metal \longrightarrow metal\ oxide + Na_2O.V_2O_4.5V_2O_5$$

Transgranular corrosion occurs by the interaction of the vanadates and the metals.

2 : In practice the second axis (Na - S) situation is observed in gas turbines conditions where distillates containing sodium and sulphur are used.

Metals exposed to this kind of environment suffers intergranular corrosion by sulphidation.

3 : Sulphur (1 - 5%)and Vanadium (up to 250 ppm) are present in the residual fuels depending on the origin of the Crude oil.

The nature and mechanism of corrosion by these two major impurities are still not clear.

It was therefore, intended to carry out an experimental programme which would give some specific information on the high temperature corrosive properties of the flue gases produced during burning of the liquid fuels containing various impurities like sulphur, sodium and vanadium and study their individual and collective relationships at different ratios viz. S:Na:V on a selected range of alloys. The objective of the investigation was to provide relative corrosion data at high temperature (730° C) from which a theory of nature and mechanism of corrosion and/or an empirical practical prediction method be presented. The relationship of ignition delay of liquid fuel with the formation of sulphur trioxide and hence the corrosion rate were also proposed for investigation.

The purpose of the entire investigation was to discover methods of controlling corrosive properties of combustion gases due to the presence of impurities.

CHAPTER FOUR.

PROGRAMME OF EXPERIMENTAL WORK.

1. Literature survey of the Work done on the Subject.

2. Design and construction of the burner and laboratory combustor.

3. Design and construction of specimen holders for corrosion rate measurements.

4. Preparation of apparatus for temperature measurements.

5. Servicing and installation of SO_2, SO_3 gas analysis apparatus.

6. Servicing and installation of CO, CO_2 gas analysis instruments.

7. Servicing of oxygen measurement apparatus.

8. Preparation of metal specimens in the form of 2 cm diameter and 4 mm thick discs of the following materials:

   a) Mild Steel.
   b) Stainless steel type 347.
   c) Nimonic 90.
   d) Nimonic 105.
   e) IN657.
   f) G19 Steel (proposed but not obtainable).

9. Testing the laboratory combustor, measurement of corrosion rate of different metals using Kerosene and Diesel B to perfect the methods of measurement of corrosion rate and gas analysis.

10. Experiments to measure corrosion rate over different time to establish relationship between time and corrosion rate.

11. Introduction of sulphur, vanadium and sodium (added in the fuel in the form of chemicals soluble in oil) in different concentrations in the following order and study corrosion rates by combustion gases.

    a) Sulphur alone.
    b) Vanadium alone.
    c) Sodium alone.
    d) S:V
    e) S:Na
    f) V:Na
    g) S:V:Na

12. Identification of oxide layers produced on different metal surface by the combustion gases, while using above fuels, by X-ray diffraction and scanning electron microscopy. Hence try to establish the mechanism of the formation of oxides and their relationship/ dependence on the impurities present in the fuel.

13. On the basis of the results obtained from (11), write a computer programme to predict expected corrosion rate when using any other fuel, e.g. Light fuel oil containing different concentrations of impurities.

    a) Test the programme practically by using Light fuel oil.

14. Measurement of corrosion rate at different excess air condition.

15. Study the effect of thermal cycling and continuous exposure of metals in combustion gases.

16. Introduction of fuel additives (primarily oil soluble chemicals) and study their effects on corrosion rate.

17. Measure ignition delay property of all the individual oil samples used and study any relationship between the corrosion rate and ignition delay time.

CHAPTER FIVE

Page

DESCRIPTION OF APPARATUS USED

5.0 DESCRIPTION OF APPARATUS : in detail.

5.1. The Laboratory Combustor.

The laboratory combustor designed and constructed for the investigation is shown in figure 5(1) which consists of four main parts:

(i) the fuel tank,
(ii) the burner,
(iii) the combustion chamber, and
(iv) the combustion products exhausts pipes.

The fuel tank is of 8 litre capacity metal cylindrical type, which is fitted with a thermostatically controlled heater. The heater will allow the heavy residual fuel oil to be heated to a suitable temperature for better flow.

The burner consists of two concentric tubes and is arranged in such a way that commercially available stainless steel hypodermic needles can be used and replaced if necessary. The inner tube carries oil and the other tube introduces compressed air to produce atomisation.

The combustion chamber consists of two stainless steel concentric pipes. The inner one is of 7.5 cm diameter and the outer pipe is of 11 cm diameter. The atomised fuel is burnt inside the inner pipe and secondary air is introduced from the outside pipe into the inner pipe at 4 different calculated points so that good combustion is achieved.

The combustion products pass through a long pipe of 7.5 cm diameter to the exhaust. The sampling points for gas analysis, temperature measurements and probes for corrosion rate measurement are located at different points of the pipe.

5.1.1. Starting procedure.

a) Ensure all the valves are shut.
b) Warm up the combustion chamber by bunsen burner.

c) Open the valve for compressed air for atomisation.

d) Purge the combustion chamber with secondary air.

e) Pressurise the fuel tank with nitrogen, setting pressure of the tank to 3 psig.

f) Switch on the Switch of Sparking plugs.

g) Open the valve for oil and set the flow rate according to the oil used (20 cc/min for kerosene, 40 cc/min for Diesel B).

h) Open the secondary air valve and increase slowly until the combustion starts.

i) When the combustion starts adjust, secondary air and oil flow rate very slowly to required condition by looking at the flame through the mirror.

j) If combustion stops and excessive unburnt atomised fuel is seen, stop fuel flow and purge the combustion chamber with air.

k) To stop; stop the fuel flow, stop spark plug switch, let the air flow for about 10 minutes to cool the apparatus, then stop all valves. close all the other valves.

5.1.2. Specimen preparation.

The metals received in the form of 20 mm diameter road. Mild steel and stainless steels were cut to 4 mm thick discs using the electric saw in the workshop. Harder metals like N90 and N105 were cut on the wheel in the metallurgy laboratory. All specimens were marked for identification and polished in the surface grinder in the project workshop.

After making the specimens a seven step specimen preparation was used to ensure constant initial surface conditions.

1. Polishing : surface grinding and polishing on emery papers.
2. Degreasing : 5 minutes in boiling alkaline solution.
3. Rinsing : 5 minutes in cold tap water.
4. Drying : Dipping in alcohol/acetone, (this removed water and dried the specimen quickly).
5. De-oxidising: 1 min in 10% HCl.
6. Rinsing : 1 min in distilled water.
7. Drying : dipping in alcohol/acetone.

Steps 1 through 4 were usually performed several days before the tests, while steps 5 through 7 were performed just prior to tests to ensure an oxide free surface. The specimens were stored in dessicators at all times to prevent access of water.

5.1.3. Specimen holder.

Several designs of specimen holders were considered and constructed. For practical difficulties most of them had to be abandoned. The specimen holder used for the experiments is shown in Figure 5(2). The sepcimen holder for low temperature corrosion measurement is shown in Figure 5(3). Figure 5(4) shows the general arrangement of the laboratory combustor.

5.1.4. Air supply.

The atomising air was supplied from the main compressor through a pressure controlled valve to keep pressure constant at 80 psi (5.6 kg/cm^2).

Secondary air was supplied by a blower through a U-tube manometer.

The manometer reading was calibrated to give air flow rate in litres/min by disconnecting the air inlet pipe to the combustion chamber and measuring air flow for known time by a flowmeter. The calibration results are shown in Table 6(4).

5.1.5. Fuel supply.

The fuel was supplied from the tank as described before. The fuel tank was pressurised by nitrogen gas from a cylinder for easy fuel flow. The pressure of the tank was kept constant at 3 psig.

A secondary tank was connected above the main fuel tank to refil while the combustor was on. Otherwise it was necessary to stop the combustion to fill the tank. This way the

combustor could be run continuously for longer periods.

Fuel flow rate was measured and controlled by a rotameter manufactured by G.E.C. Elliot's, model 1100, range 0 - 100 cc. The rotameter was calibrated for every fuel used by cutting off the oil supply and collecting it in a measuring cylinder for a known time and flow rate was calculated.

5.2 Temperature measurement.

The temperature was measured by using Atkinsons Suction Pyrometer Type M 1100 of the Gas Council, Midland Research Station and the electronic thermocouples were calibrated to measure flue gas temperatures at different points.

5.3 Oxygen Measurement.

The excess oxygen of the flue gas was measured by using the Servomex Portable oxygen analyser type OA.101. Mk.11. The principle of operation of this equipment is that oxygen is unique amongst common gases in being relatively strongly paramagenic. Apart from nitric oxide the nitrogen peroxide, most gases are weakly diamagnetic, and consequently measurement of the susceptibility provides a specific indication of the oxygen content of a gas mixture.

In all servomex oxygen analysers, a light dumb-bell shaped test body is suspended on a platinum-iridium wire in a non-uniform magnetic field. It experiences a torque proportional to the magnetic susceptibility of the gas surrounding the test body. This torque is balanced against a restoring torque due to current flow in a coil wound on the dumb-bell the balance condition being achieved by manual adjustment of a calibrated source to attain the "Zero" position of a beam of light reflected from the dumb-bell. The zero position is initially determined by passing pure nitrogen into the measuring cell. Before introducing the test gas the output dial

is set to 21% oxygen by drawing air into the cell and the span is adjusted to give balance. Since the device is linear, this single adjustment is sufficient to set up the instrument.

5.4 CO and CO_2 gas-measurement.

CO and CO_2 concentrations were measured by Hilger and Watts Infra-red mobile Gas Analyser, G.A.T.8.

The equipment is designed to sample continuously and analyse the concentration of carbon monoxide and carbon dioxide in a gas stream within the ranges 0 - 0.5% and 0.03 - 0.25% Carbon monoxide and 0 - 3% and 2 - 15% Carbon dioxide. The equipment consists of two Infra-red Gas Analysers, Type SC/F2 coupled to a sampling unit, the complete unit is being mounted on a four wheel trolly. Figures 5(5) and 5(6) shows the view of the CO and CO_2 analyser.

5.5 Sulphur Oxide Measurements.

The concentrations of both sulphur dioxide and sulphur trioxide is measured by the Gallenkamp, CERL sulphur oxide analyser GAS.850.G. Figure 5(7) shows the general arrangement of the sulphur oxide analyser.

The flue gas is sampled through a stainless steel probe suitable for flue gas tempteratures of about 500 - 600° C which is so arranged that the temperature of the flue gas does not drop below 250° C before it enters the analyser. In the analyser the solids are removed from the hot gas by a silica wool filter and then the gas is saturated with cold 80 per cent isopropanol (aqueous). This promotes the formation of sulphuric acid mist and at the same time, inhibits the oxidation of the sulphur dioxide present in the gas. The sulphuric acid mist is collected by passage through a sintered glass absorber and is retained together with excess isopropanol, in a collecting vessel. Some sulphur dioxide is also dissolved at this stage and is retained in the collecting vessel but most of it

passes on with the gas stream and is absorbed in standard iodine solution.

The residual gases then pass through an empty wash bottle to trap any water carried over from the iodine solution, through a tube of 'SOXAZORB' absorbent and then are propelled by a diaphragm pump into a reservoir serving as a pulsation damper. The rates of flow of isopropanol and flue gas are indicated by flow meters and controlled by needle valves.

Flue gas is passed through the analyser until the iodine solution becomes decolorised. Immediately this occurs the flows of the flue gas and isoporpanol are stopped. The concentration of sulphur dioxide is determined from the time taken, for the iodine to become decolorised (the rate of flow of flue gas is known) and to this is added the small quantity of sulphur dioxide retained in the isoproponol. The latter is determined by idiometric titration of an aliquot of the isopropanol solution from the collecting vessel.

The sulphuric acid in the isopropanol solution is determined by titration of an aliquot with barium perchlorate to the change point of thoron indicator; the concentration of sulphur trioxide in the flue gas can then be calculated. Appendix 5.1 gives the calculation of sulphur dioxide and sulphur trioxide.

5.6 Measurement of Ignition Delay.

The apparatus to measure the ignition delay is shown in Figure 5(8). This consists of a small electric furnace heating a quartz disc on to which was allowed to fall droplets of fuel under test. The time interval between the droplet entering the apparatus through the central hole in the cover and the ignition was measured by a Cintel microsecond counter triggered by two phototransistor circuits.

The temperature of the disc was raised at a fairly rapid rate initially and droplets of the liquid fuel under test were allowed

to fall on to the hot surface, until ignition was obtained. Having located this temperature approximately, the current supply to the heater was raised very gradually and a droplet was admitted. After each droplet, whether ignition was obtained or not, the ignition space was scavenged by means of the hand bellows shown in Figure 5(8). When ignition occured the surface temperature was recorded against the reading of the microsecond counter. The procedure was repeated at frequent intervals both for increasing temperature and decreasing temperature of the disc.

5.7 Electron Micrographs.

The International Scientific Instruments Super 3 Model Scanning Electron Microscope with a magnification of 200,000 times is used to obtain the micrographs of mounted section of the specimens. The instrument has the facility for X-ray energy spectrum investigation. This is supplied by a link system 2010 pulse processor which can be programmed for element detection. The sample under detection can also be scanned on the Cathode Ray Tube of the microscope and there are facilities for taking photographs.

5.8 X-Ray Diffraction.

X-Ray diffraction is a very powerful and versatile technique for identifying solids and giving information about their structure (119, 170).

The structure of a material is determined by the types of atoms present and their arrangement. The diffraction pattern produced when that material is bombarded with a beam of X-rays is unique. Thus the X-ray diffraction patterns can be used to fingerprint materials.

X-ray diffraction tells us the compounds present in a sample. For example, it is possible to distinguish between the corrosion products of iron, haematite ($-Fe_2O_3$) which gives a very

different pattern from magnetite (Fe_3O_4).

The detailed analysis of a Powder Photograph using X-ray Diffraction is given in Appendix 5.2.

Figures 5(9) and 5(10) show the X-ray generator for powder photograph analysis and X-ray diffractometer respectively.

5.9. Measurement of Sulphur in fuel.

The concentration of Sulphur in the fuel was determined by Flask Combustion method IP242/69T. In this method, the sample absorbed on a pellet wrapped in a piece of filter paper, is rapidly and completely burnt in a closed flask filled with oxygen at atmospheric pressure. The combustion products are absorbed in a hydrogen peroxide solution and the amount of sulphuric acid formed is determined by titration with standard barium perchlorate solution, using Thoron as an indicator. The assembly of the combustion flask is shown in figure 5(11).

The concentration of sulphur is calculated by means of the following equation:

$$\text{Sulphur, \% } W = \frac{(V - \ ) \times N \times 1603}{w}$$

where V is the volume of barium perchlorate solution used for the sample titration.

is the volume of barium perchlorate solution used for the blank titration.

N is the normality of barium perchlorate solution.

w is the weight of sample in milligrams.

5.10 Measurement of Sodium by Flame Photometer.

A corning EEL Scientific Instruments Flame photometer made by Evans Electroselenium Ltd. Pat.No. 712700, Reg.No. DES 8 66150 was used to measure sodium concentration in oil.

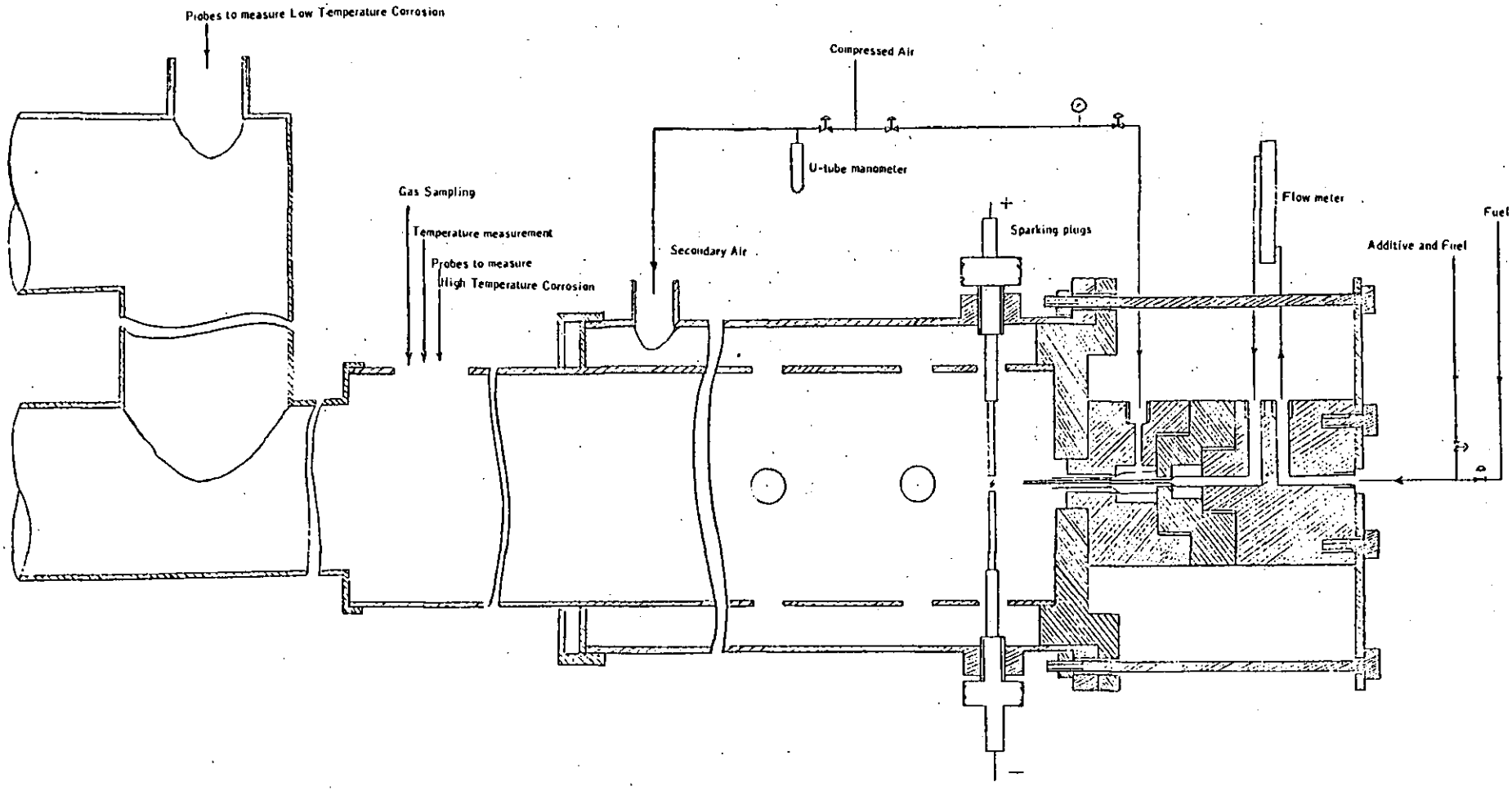

Figure 5(1). Section of the overall assembly of the Laboratory Combustor.

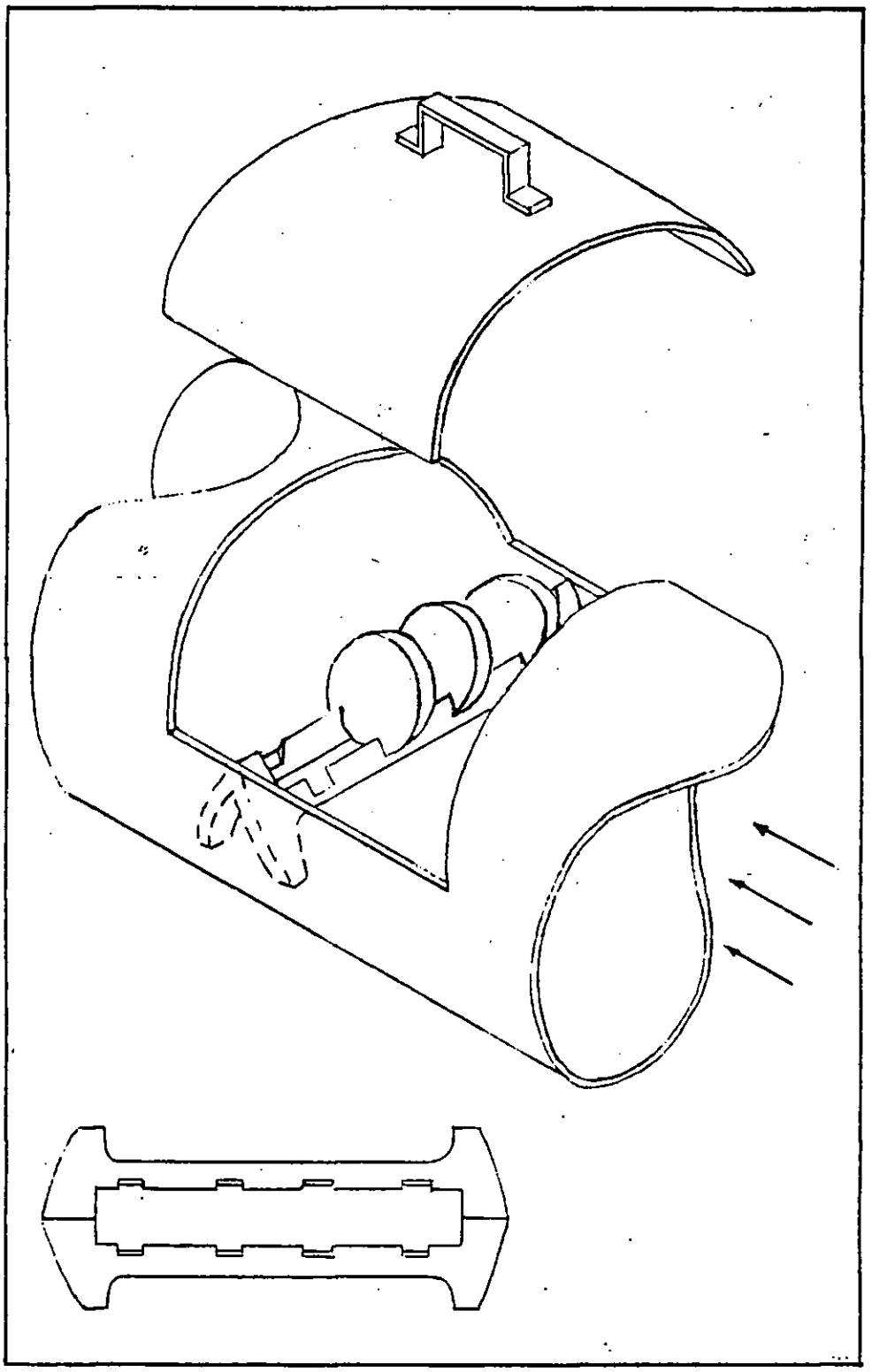

Figure 5(2) View of specimen holder ond three specimens in position for corrosion rote meosurement.

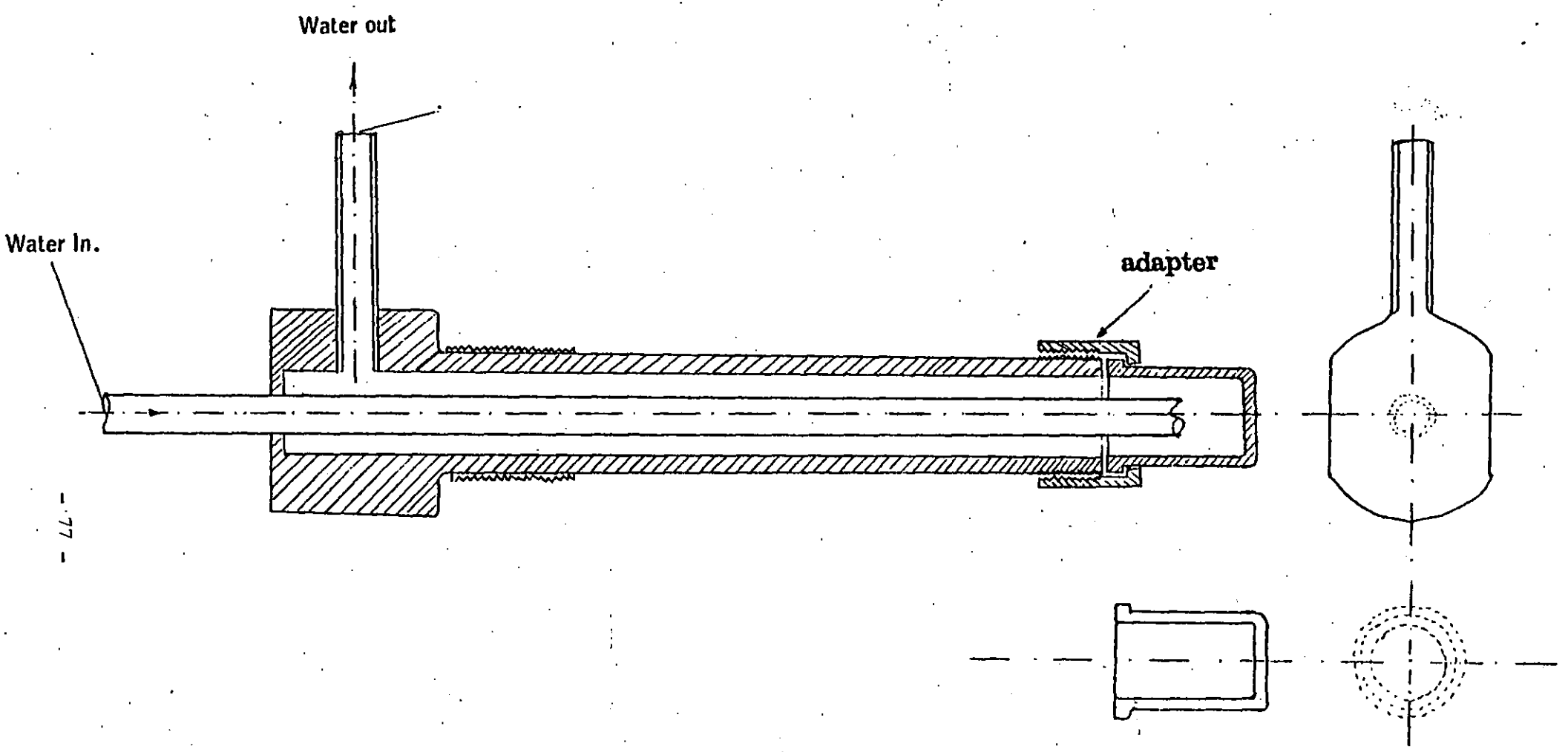

Fig. 5(3) Assy of Probe and Holder for Low Temperature Corrosion measurement (3).

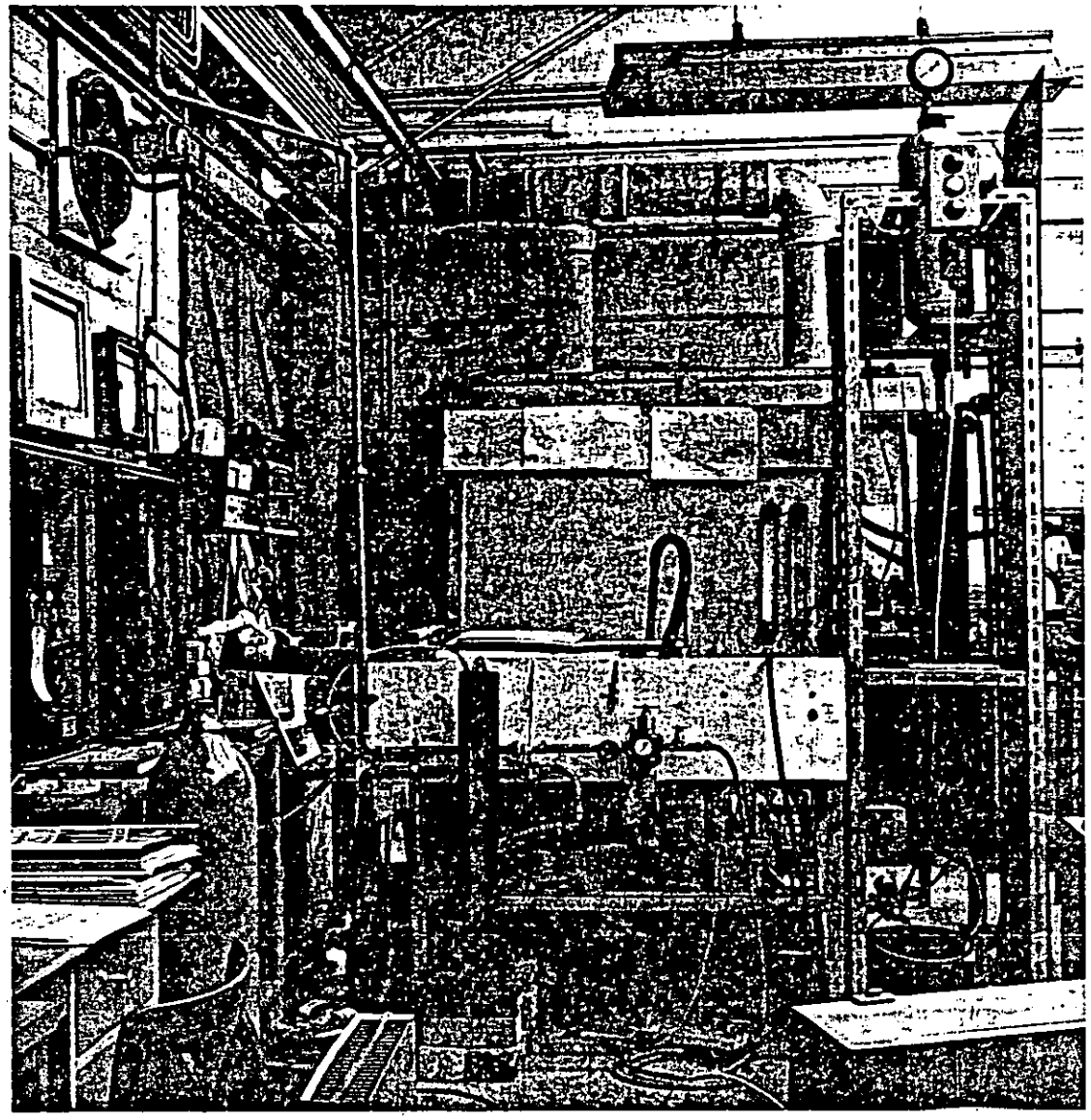

Figure 5(4) General arrangement of the experimental rig.

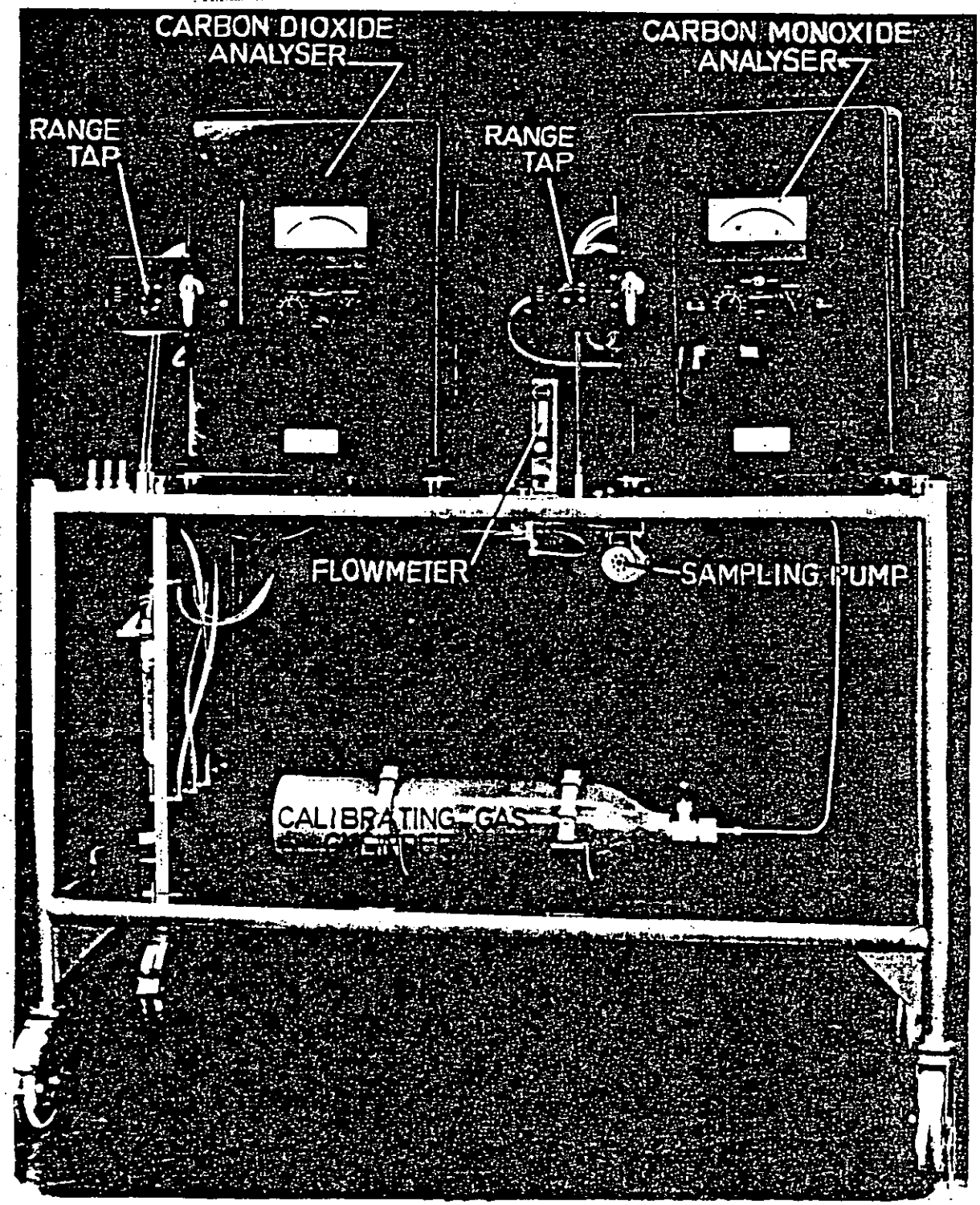

Figure 5(5). Front view of the CO, CO_2 gas analyser.

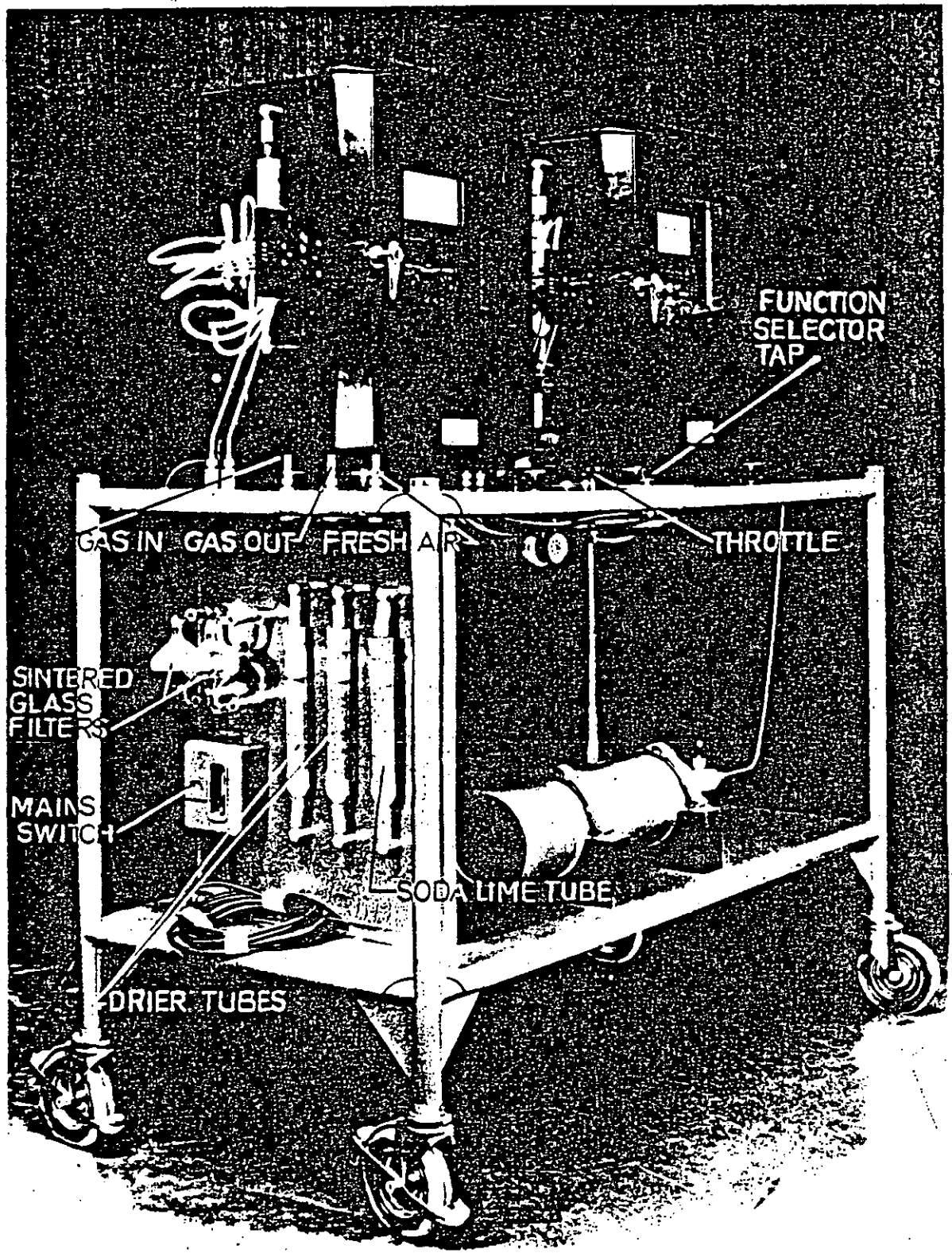

Figure 5(6). General arrangement of the CO, CO_2 gas analyser.

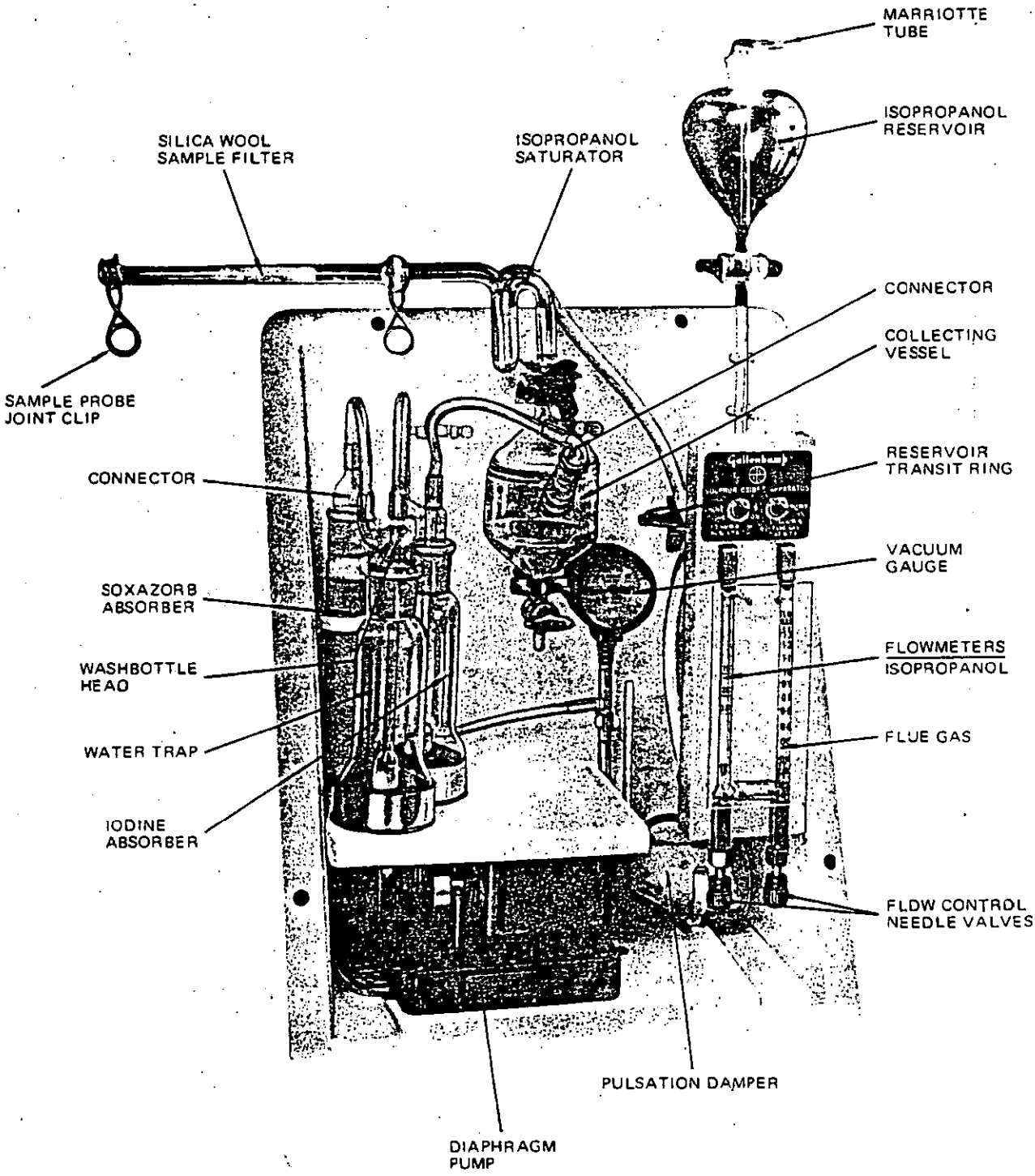

Figure 5(7). General view of the GallenKamp - CERL sulphur oxide analyser GAS.850.G.

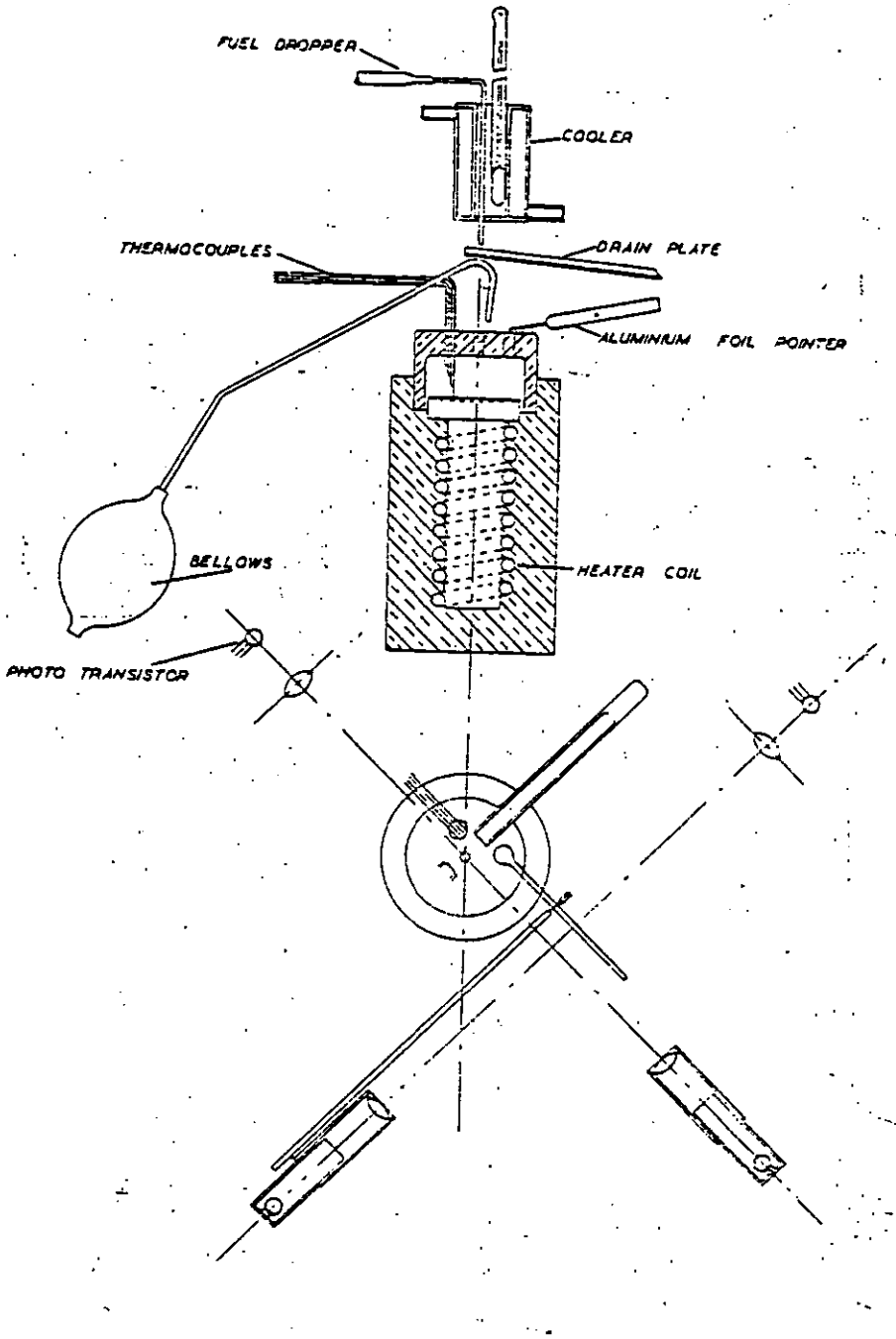

Figure 5(8). Diagramatic view of the Ignition Delay measurement apparatus.

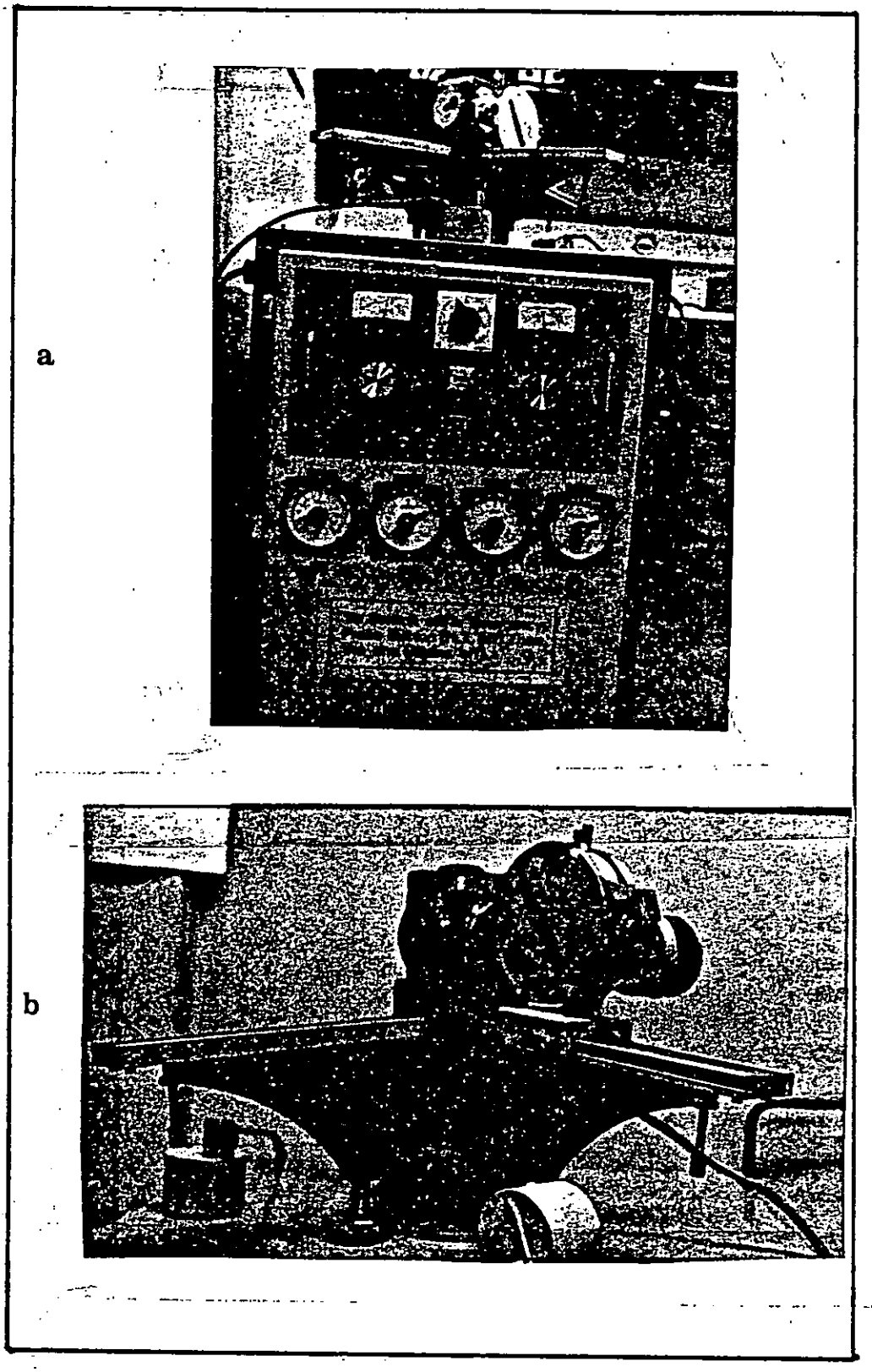

Figure 5(9) a) X-Ray generator for powder photograph analysis.

b) One camera in position.

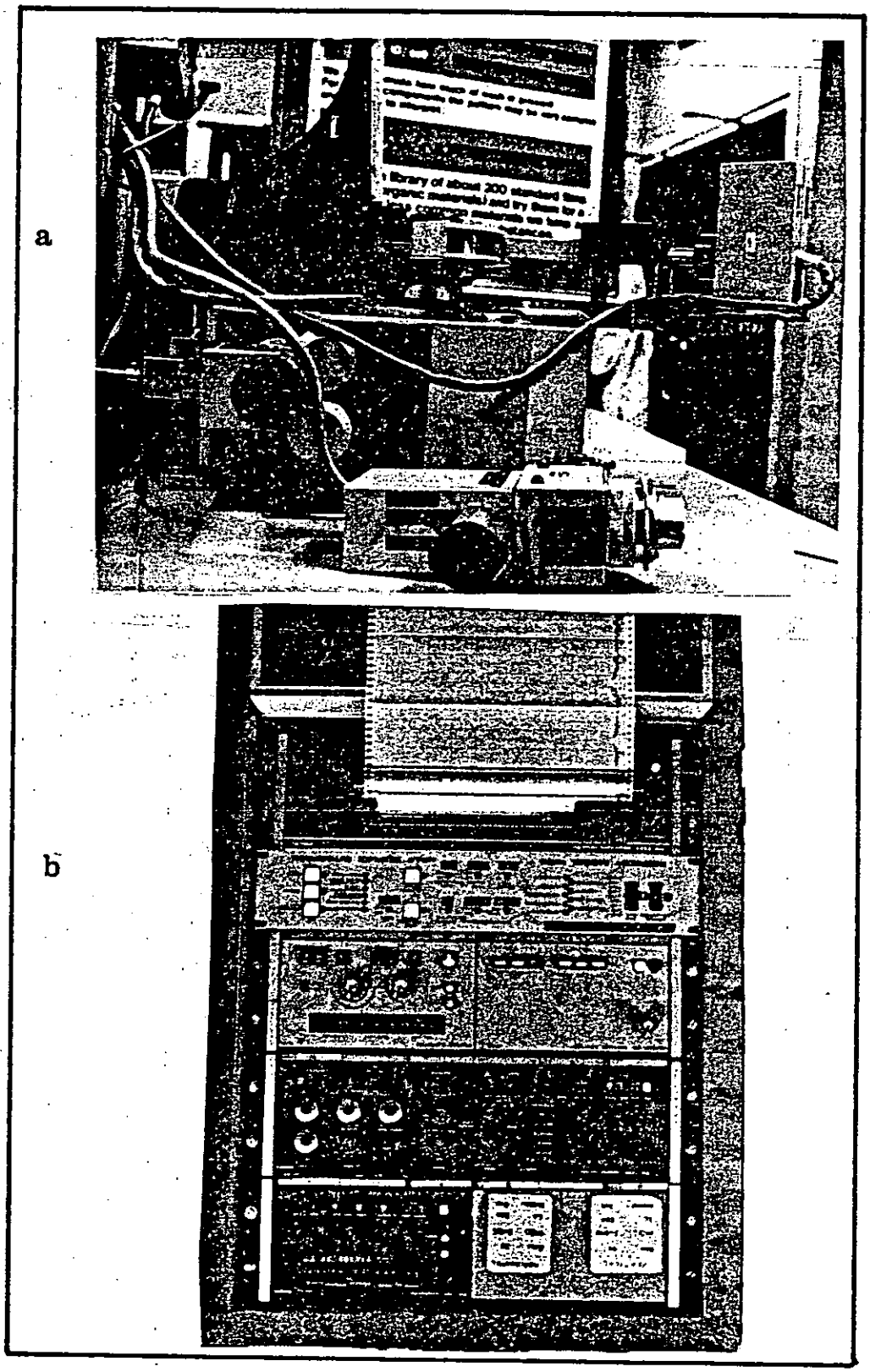

Figure 5(10) X- Ray diffractometer

a) Camera

b) Controls and chart recorder.

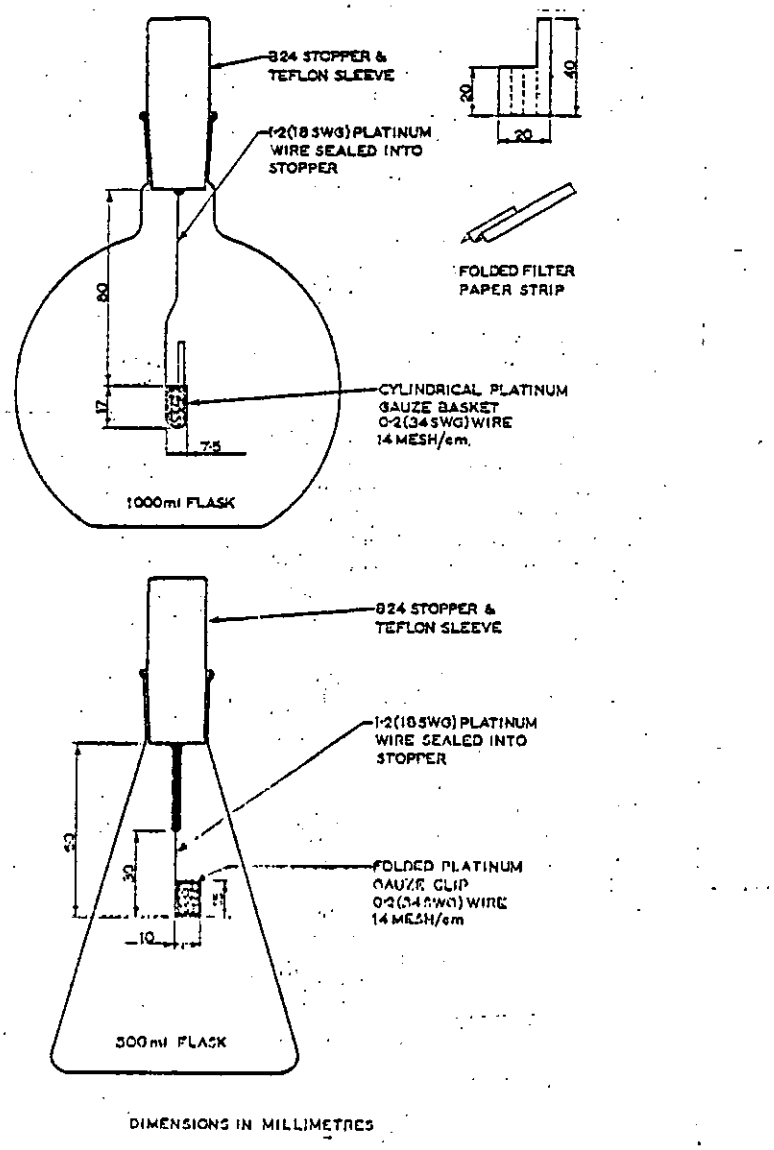

Figure 5(11) Combustion flask assembly to measure sulphur in fuel.

CHAPTER SIX.

EXPERIMENTS AND RESULTS - a guide.

6.0. EXPERIMENTS AND RESULTS - in detail.

6.1. Analysis of Fuels used.

Test fuels used for the investigation contained the following impurities:

Sodium	0	-	60 ppm.
Sulphur	0	-	6%
Vanadium	0	-	300 ppm.

It is recognised that in practice crude oil and residual fuel oil obtained from different parts of the world contains impurities of wide range and variety. Table 2(3) shows typical impurities found in fuel used in power stations.

The experiments were carried out by using Kerosene, Diesel B (received from Shell UK Ltd.) and Light fuel oil (received from Esso Research Laboratory). The reports for chemical analysis and physical constants were given by the suppliers and shown in Table 6(1). For different experiments sodium, sulphur and vanadium were added to the fuels to make upto the required concentration. The samples were then analysed in the chemistry laboratory to check the actual sodium and sulphur in the test fuels.

6.1.1. Measurement of Sulphur in fuel.

The sulphur concentration of Kerosene and Diesel B received from the supplier were analysed following the method described in Section 5.9. Then Known concentration of sulphur as carbon disulphide (CS_2) was added and sulphur concentration measured. The results of these tests are summarised in table 6(2).

6.1.2. Measurement of Sodium by Flame Photometer.

Sodium was added in the test fuels as Nuosyn Sodium (received from Durham Chemicals Ltd.) which is an oil soluble compound containing 5% sodium as metal. The

actual sodium concentrations were analysed by EEL flame photometer with the help of Dr.J.R. Penney. In this particular flame photo-meter, sodium concentrations of up to 5 ppm could be detected. Therefore fuels with higher sodium contents were diluted accordingly. A Known volume of oil sample was washed thoroughly with an equal volume of distilled water. The extracted sodium-water mixture was introduced in the flame photometer and sodium concentration read off. The oil sample was washed several times until no sodium was detected in the extracted water. The commulative results are shown in table 6(3).

6.2. Measurement of combustion gas composition.

Concentrations of O_2, CO, CO_2 and SO_3 in the combustion gases were measured at sampling point at different air flow rates. The fuel flow rate was kept constant throughout the run. The results and operation conditions are given in Table 6(4).

Sulphur trioxide was measured using Kerosene containing different sulphur concentration and keeping all other combustion conditions constant. The results are shown in figure 6(1). The method of measuring sulphur trioxide was calibrated to give an indication of sulphur trioxide just by noting the time to decolorise iodine solution as shown in figure 6(2).

6.3. Temperature measurement.

The temperature of the combustion gas at sampling points was measured by means of Ni-Cr/Ni-Al thermocouples. This was checked and calibrated by a Suction Pyrometer.

6.3.1. Rate of temperature rise of a Specimen.

The rate of temperature rise of a mild steel specimen was measured by drilling a hole in the specimen and putting

the thermocouple tip inside it and introducing the assembly in hot combustion gas. Time and temperature rise was noted and shown in figure 6(3).

6.3.2. Thermal cycling and continuous exposure.

An attempt was made to show the effect of thermal cycling of mild steel specimens. For this experiment four specimens were introduced in hot combustion gas at 730° C for successive one hour exposures. Specimen number one was exposed for one hour, specimen number 2 for three hours, specimen number 3 for six hours and specimen number 4 for twenty hours. All the specimens were observed mounted in plastic, cut a section, polished and photograph taken in the electron microscope. Figure 6(4) shows the metallographic section of metal/scale interface.

6.4 Corrosion rate measurement.

The major measurement was weight loss. The establishment of the corrosion rate using simple weighing technique assumes that the metal loss has occured uniformly. To minimise error in obtaining similar surface finish a proper sample preparation technique was followed as described in section 5.1.2. After the exposure the coupons were carefully examined and all accumulated corrosion products and fouling were removed by mechanically scrubbing, polishing in fine emery papers and chemically by washing in solvents. To minimise error due to loss of 'Sound metal' or incomplete removal of corrosion products the specimens were weighed a number of times during progressive treatment in the abrasive techniques and in pickling solutions. When the change in the weight was a minimum and visual appearance seemed to be perfect, that weight was taken into consideration. For example a typical mild steel specimen weighed about 8 gms; after scrubbing the hard oxide layer the weight loss was around 90 mg. First polishing took about 40 mg., second polishing took about 25 mg. and 5 seconds in pickling solution took about 20 mg. Therefore, the

cummulative weight loss was about 175 mg. This of course, varied with time of exposure and fuel impurity contents. In the case of some mild steel specimens, small pits were observed and polishing and pickling had to be stopped at a stage which depended upon the experience gained from previous experiments. For example pickling times of 10 sec. to 60 secs. gave clear evidence that underlying metal was being removed as well. For Nickel alloys scrubbing and pickling were not necessary. Just polishing in fine wet emery paper gave a weight loss of about 30 mg. and the surface finish appeared to be free of oxide without removal of underlying metal.

6.4.1. Personal accuracy in weighing.

To determine the personal error/accuracy of weighing individual test coupons, a number of selected specimens were weighed on a chemical balance up to four decimal figures. The samples were put in the combustion apparatus and only cold air was passed through. After a few minutes the specimens were weighed again. The results are shown in table 6(5) and figure 6(5). Theoretically there should not be any change in weight. The change observed is considered to be the personal error in weighing in the particular chemical balance.

6.4.2. Relation of corrosion rate to thickness of specimen.

Although it is mentioned earlier that the specimens were 20 mm diameter and 4 mm thick discs, in practice, while preparing the specimens, all of them could not be made exactly of same thickness. Therefore, it was considered that the dependence on corrosion rate on the thickness of specimen should be measured. Specimens of four different thicknesses were introduced in the combustion gas and corrosion rate measured. The results are plotted and shown in figure 6(6). From the results it appeared that there is no significant difference in corrosion rate due to small change in thickness.

6.4.3. Dependence of Corrosion rate along tube diameter.

The specimen holder for high temperature corrosion measurement could take four coupons at one time as shown in figure 5(2). Mild steel specimens were placed in each slot of the holder and corrosion rate measured to see the effect of position along the pipe diameter. The results are shown in figure 6(7).

6.4.4. Relation of corrosion rate to time of exposure.

Mild steel specimens were exposed in combustion gases and corrosion rate was measured at one hour intervals up to six hours. The results are shown in figure 6(8). It can be seen that after about two hours the rate of increase of corrosion rate decreases. Therefore, it was considered that for mild steel three hours exposure time would be sufficient to get appreciable amount of deposits.

6.4.5. Corrosion rate at different excess oxygen.

Corrosion rate of mild steel were measured at different excess oxygen concentration of combustion gases. The results are shown in figure 6(9).

6.5 Measurement of corrosion rate of mild steel using Kerosene at different concentrations of Sulphur, Sodium and Vanadium over three hours exposure time.

Mild steel specimens were exposed for 3 hours in combustion gases produced by burning Kerosene and corrosion rates were measured. To the Kerosene, sulphur as carbon disulphide was added to make sulphur concentrations of 1, 2, 3, 4 and 5 per-cent. Corrosion rates were measured for each concentration. Vanadium as Nuodex Vanadium (received from Durham Chemicals Ltd) was added to each of the above concentrations to make vanadium concentrations of 50, 100, 150, 200, 250 and 300 ppm and corrosion rates were measured. Sodium as Nuosyn Sodium (received from Durham Chemicals Ltd) was added to each of the above solutions to make sodium

concentrations of 20, 40 and 60 ppm and corrosion rate of mild steel were measured. The results are shown in figures 6(10),6(11), 6(12), 6(13), 6(14) and 6(15).

6.6 Computer programme to predict corrosion rate at any concentration of sulphur, sodium and vanadium within the range under the defined conditions.

A computer programme is written based on the results obtained from section 6.5.0, assuming that all the combustion conditions remain constant and the corrosion rate due to addition of impurities follows the pattern obtained by the experimental results. The programme is written in basic conversational language. Corrosion rate by combustion gases produced by burning fuel containing any combination of sodium up to 60 ppm, sulphur up to 5% and Vanadium up to 300 ppm would be predicted. On running the programme the computer will ask the question - "what is the concentration of Sulphur, Sodium and Vanadium"? On feeding the information, the computer gives the corrosion rate for those particular conditions. If the data supplied are out of range the computer will print which concentration is not valid. The example is shown at the end of the programme. The programme is shown in Appendix 6(1).

6.6.1. Prediction of corrosion rates and actual/experimental corrosion rates with Light fuel oil.

The analysis of light fuel oil is given in table 6(1). The concentration of sulphur is 3.2%, sodium 10.5 ppm and vanadium 100 ppm. These figures were fed to the computer to give a corrosion rate at the specific conditions. The corrosion rate as given by the computer is 12.6 $mg/cm^2/h$ (Appendix 6(1), page **226**). To the light fuel oil 1% sulphur, 10 ppm sodium and 100 ppm vanadium were added to make final concentrion of 4.2% sulphur, 20.5 ppm sodium and 200 ppm vanadium. These figures were also fed to the computer and the corrosion rate was shown to be 14.58 $mg/cm^2/h$. (These predicted results are of course for mild steel only).

The actual corrosion rate was measured for both of the light fuel oils described above. The results are shown below.

Fuel	Impurities present			Corrosion rate mg/cm^2/h			
	S	N	V	Mild steel	*SS347	*N105	*IN657
Light fuel oil 1	3.2	10.5	10.0	15.0	1.0	0.6	1.5
Light fuel oil 2	4.2	20.5	20.0	17.5	1.1	0.7	2.0

* These samples were included only to complete the spaces in the specimen holders. They are of general interest.

6.7 Measurement of corrosion rate using Diesel B.

For this set of experiments Diesel B was used with different combinations of sulphur, sodium and vanadium concentrations and corrosion rates were measured over three hours exposure time. Figures 6(16), 6(17) and 6(18) compares the results of corrosion rate obtained by using Kerosene and Diesel B at different concentrations of sulphur, sodium and vanadium. Along with mild steel, corrosion rate of stainless steel type 347, Nimonic N90 and N105 were also measured for some sodium, sulphur and vanadium combinations in Diesel B. Figures 6(19), 6(20) and 6(21) compare the results of different alloys at different sulphur, sodium and vanadium concentrations. Figures 6(23) and 6(25) show the comparison of corrosion rates of different alloys at 5% sulphur with varying sodium and vanadium concentrations and figure 6(27) compares the results at 25 ppm vanadium with varying vanadium concentrations. Figures 6(22), 6(24) and 6(26) show the corrosion rate of mild steel at different vanadium concentrations with increasing sulphur and sodium concentrations.

6.8. Corrosion rate of different materials after exposing for 20 hours in combustion gases by using Kerosene with different concentrations of Sodium, Sulphur and Vanadium.

It was considered to expose Nickel alloys for a longer period to obtain a reasonable amount of deposit. For comparison mild steel specimens were also used. Eight specimens, two each of mild steel, stainless steel type 347,N105 and IN657 were exposed in the combustion gases produced by using Kerosene. The samples were exposed for two 7 hour and one 6 hour period, making the total exposure time to be 20 hours. In between the exposures the samples were carefully taken out of the combustion chamber and kept in the dessicator. Corrosion rate was measured using one set of the specimens and the second set was stored in the dessicator for X-ray analysis. The experiment was repeated for different combinations of sulphur, sodium and vanadium concentrations selected by using the triangular diagram. The composition and results are shown in Table 6(6).

6.9. Corrosion rates using additives.

One iron-based additive (ferrocene) was added with Diesel B to see the effect on corrosion rate of mild steel. The results are shown in figure 6(28).

Econsol D was added to Kerosene with 6 percent sulphur and 300 ppm vanadium to see the effect on corrosion rate of mild steel. The result is shown in figure 6(29).

The corrosion effect of emulsification of oil with small amount of water was briefly investigated. Water was added to Kerosene and Diesel B and corrosion rate of mild steel was measured. The results are shown in figure 6(30).

6·10. Metallurgical.

The composition of the materials tested are shown in Table 6(7). Vickers Hardness Numbers (VHN) were measured before and after exposure in hot combustion gas. The results are shown in table 6(8). Selected specimens reserved from corrosion experiments were mounted in plastic, a section was cut, polished properly in up to one micron diamond wheels, etched and photograph taken in electron microscope. The metallographs of all the materials before and after exposure in hot gas are shwon in figures 6(31), 6(32), 6(33), 6(34), 6(35) and 6(36).

6.11. Identification of oxide layers by X-Ray diffraction.

X-ray analysis of the oxide layers were carried out in the London Research Station of the British Gas Corporation. Samples from selected experiments were taken to the London Research Station and analysed by X-rays in two batches and results interpreted. Firstly all mild steel specimens exposed for 3 hours using Diesel B with different concentrations of sulphur, sodium and vanadium were taken for analysis. In the second batch steels and alloys exposed for 20 hours using Kerosene with different concentrations of sulphur, sodium and vanadium were analysed. In the case of mild steel specimens outside layers were scraped off and analysed by Debye-Scherrer powder photograph method. The inside layer was analysed by putting the whole sample in the diffractometer and the results interpreted from the traces. Appendix 5(2) gives the detailed method of X-ray analysis by powder photograph. The experiment number, experimental conditions samples, method of X-ray analysis and results are shown in Tables 6(9) and 6(10).

The Powder photographs of the various samples are shown in figures 6(37), 6(38), 6(39), 6(40), 6(41) and 6(42).

The diffractometer traces are shown in figures 6(43), 6(44), 6(45), 6(46), 6(47), 6(48), 6(49), 6(50), 6(51), 6(52), 6(53), 6(54), 6(55) and 6(56).

6.12. Ignition Delay experiments.

The ignition delay experiments were carried out in three sections:

1) To see if the fuels used for corrosion experiments had the similar ignition delay property after the addition of the impurities and additives.

2) To check the ignition delay of hydrocarbons as an additive with Kerosene.

3) To see the relationship between ignition delay and formation of sulphur trioxide.

For the first section the ignition delay of Kerosene alone and Kerosene with different concentrations of sulphur, sodium, vanadium and ferrocene were measured up to 750° C. The results are shown in Table 6(11) and plotted in figures 6(57), 6(58), 6(59) and 6(60).

For the second section the ignition delay of hydrocarbons; cyclohexane, n-Hexane, n-pentane and benzene were measured and compared with Kerosene in figure 6(61). Then 20% of the hydrocarbons were mixed with Kerosene separately and ignition delay measured. The results are compared separately in figures 6(62), 6(63), 6(64) and 6(65). All the ignition delay results of the hydrocarbons and Kerosene - hydrocarbon mixtures are shown in Table 6(12). Table 6(13) shows the properties of different fuels used for ignition delay. Figure 6(66) shows the variation of ignition delay of hydrocarbons with time in a log-linear graph.

For the third section the concentrations of sulphur trioxide in the combustion gases produced by burning the different Kerosene-hydrocarbon mixtures were measured. The results are shown in Table 6(14).

Table : 6(1)

ANALYSIS OF OIL USED IN EXPERIMENTS. (Data given by Supplier).

	KEROSENE	DIESEL B	LIGHT FUEL OIL
Viscosity, Kinematic	28 sec.	33 sec.	220 sec.
Sulphur Content. %.	0.2%	1.0	3.2
Water Content % vol.	-	0.02	0.50
Sediment. %.	-	0.01	0.10
Ash %.	-	0.01 min^{m}.	0.05
Cetane Number	-	35 minimum	-
Smoke Pt.	25 mm, min^{m}	-	-
Gross calorific value,			
Mj/l	36.7	38.4	40.1
Mj/Kg	-	46.5	43.3
Pour Point. ^{o}C.	-	-	-
Flash Point ^{o}C.	38 minimum	66 close 150 open	66 minimum
Density at 15^{o} C Kg/l	0.820	0.825	0.96
Char value mg/Kg	15	-	-
Boiling Point ^{o}C..	300	-	-
Distillation @ 200^{o} C	15% min^{m}.	-	-
Vanadium. ppm.	-	39 ppm.	100 ppm.
Sodium.	-	-	10.5 ppm.

TABLE 6 (2) MEASUREMENT OF SULPHUR IN FUEL.

Sample, fuels	$S\% = \frac{(V-v) \times N \times 1603}{W}$	Average S%
Kerosene	0.14 0.15 0.10	0.13
Diesel B	1.1 0.9 1.6	1.2
Kerosene + 1%S	1.2 0.9 1.1	1.1
Kerosene + 2%S	1.9 2.2 2.2	2.06
Kerosene + 3%S	3.3 2.9 3.1	3.1
Kerosene + 4%S	3.9 4.1 4.2	4.05
Kerosene + 5%S	5.1 4.9 5.1	5.03
Kerosene + 6%S	6.0 5.9 6.1	6.0
Diesel B + 5%S	6.5 6.1 6.3	6.3

TABLE 6 (3) MEASUREMENT OF SODIUM BY FLAME PHOTOMETER.

Sample	Photometer Readings.	Concentration of Na, ppm.	Average Na,Concn.
Kerosene	5+1+2+0 6+1+1+1 4+2+1+1	1 1 1	1
Diesel B	10+5+3+2 12+2+2+1 15+3+1+1	1 ppm 1 1 ppm	1 ppm
Kerosene + 5ppm Na.	50+25+20+1 45+20+10+1 45+25+15+3	5 ppm 4 ppm 4.5 ppm	4.5 ppm
Kerosene + 10ppm Na (diluted to 5)	55+25+10+5 50+20+5+5 55+20+10+10	4.5 x 2 4 x 2 5 x 2	9
Kerosene + 20ppm Na (diluted to 5)	45+20+20+5 60+75+15+5 55+25+10+10	4.5 x 4 5 x 4 5 x 4	19
Kerosene + 30ppm NA (diluted to 5)	45+25+10+5 55+25+10+5 50+25+10+5	4.5 x 6 5 x 6 4.5 x 6	28
Kerosene + 40ppm Na (diluted to 5)	45+25+5+5 45+20+10+10 50+15+10+10	4.5 x 8 4.5 x 8 4.5 x 8	38
Kerosene + 50ppm Na (diluted to 5)	50+20+10+7 55+20+10+5 60+15+10+10	4.5 x 10 4.5 x 10 5 x 10	47
Kerosene + 60ppm Na (diluted to 5)	45+20+20+5 55+22+11+7 50+20+15+5	4.5 x 12 5.0 x 12 4.5 x 12	57

TABLE 6(4) COMBUSTION GAS ANALYSIS.

(Fuel : Kerosene + 5% sulphur)

Manometer pressure diff. inch.	Secondary Air rate, litres/min	Average O_2 , %	Average CO_2 , %	Average CO , %	Average SO_3 , ppm.
2	33.0	-	-	-	-
4	34.5	1.0	13.8	0.00	13
6	36.0	-	-	-	-
8	38.5	3.4	11.9	0.01	43
10	40.0	-	-	-	-
12	43.5	4.4	11.2	0.02	49
14	44.0	-	-	-	-
16	45.0	5.5	10.0	0.02	45
18	46.5	-	-	-	-
20	49.0	6.8	9.6	0.00	28

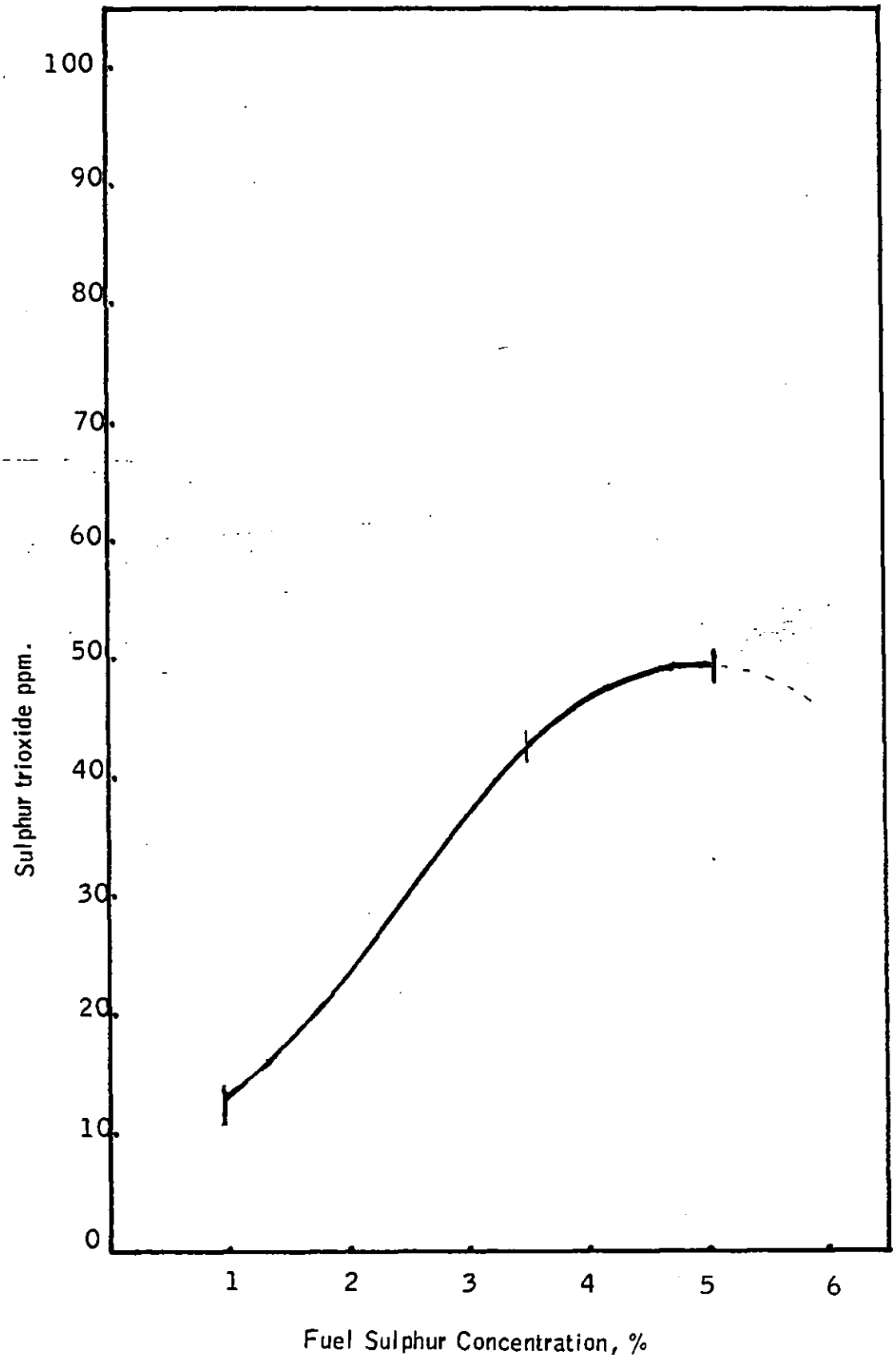

Figure 6 (1) Relation of formation of sulphur trioxide to fuel sulphur concentration.

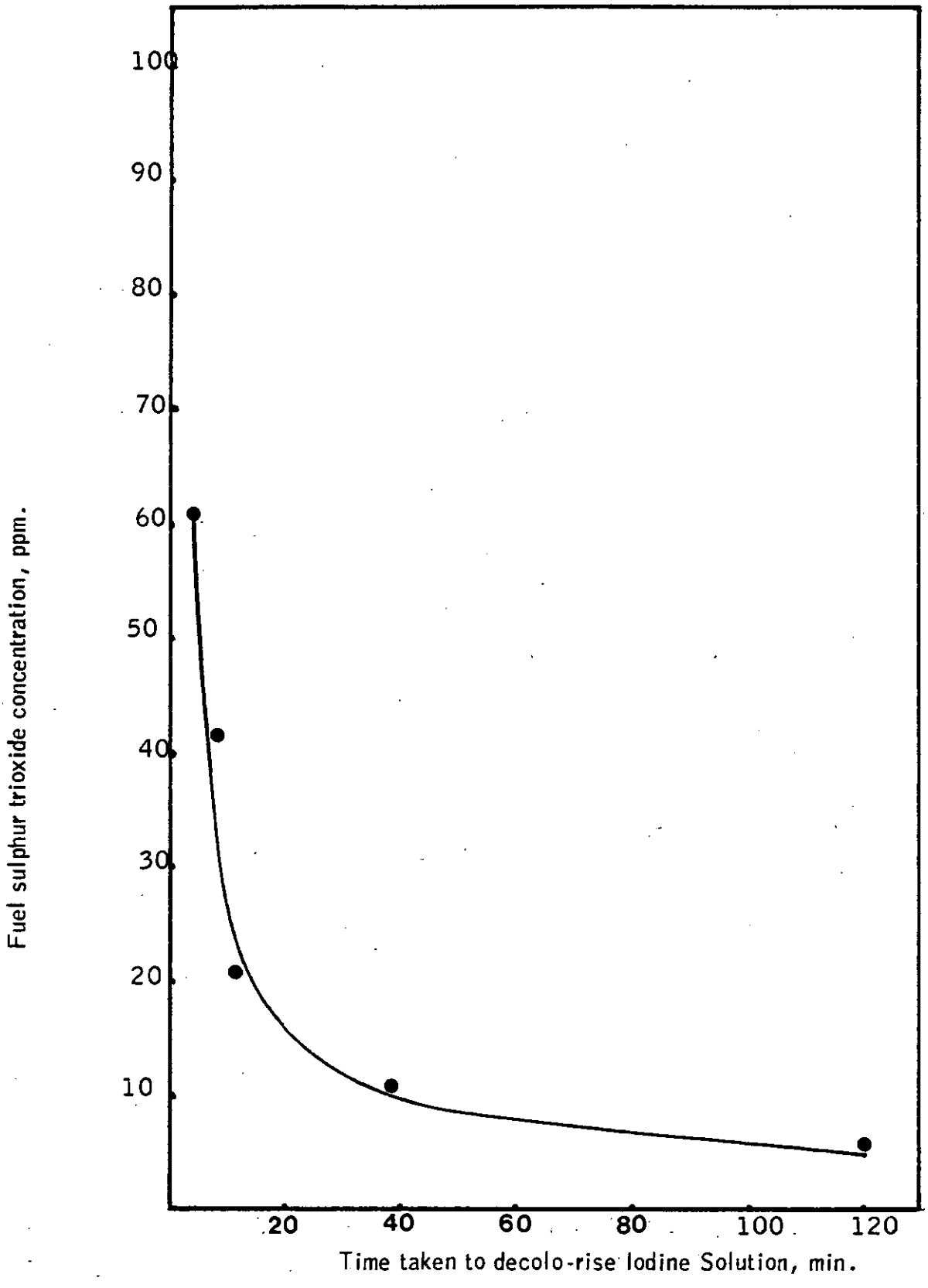

Figure 6 (2). Relation of concentration of sulphur trioxide to time to decolo-rise iodine solution.

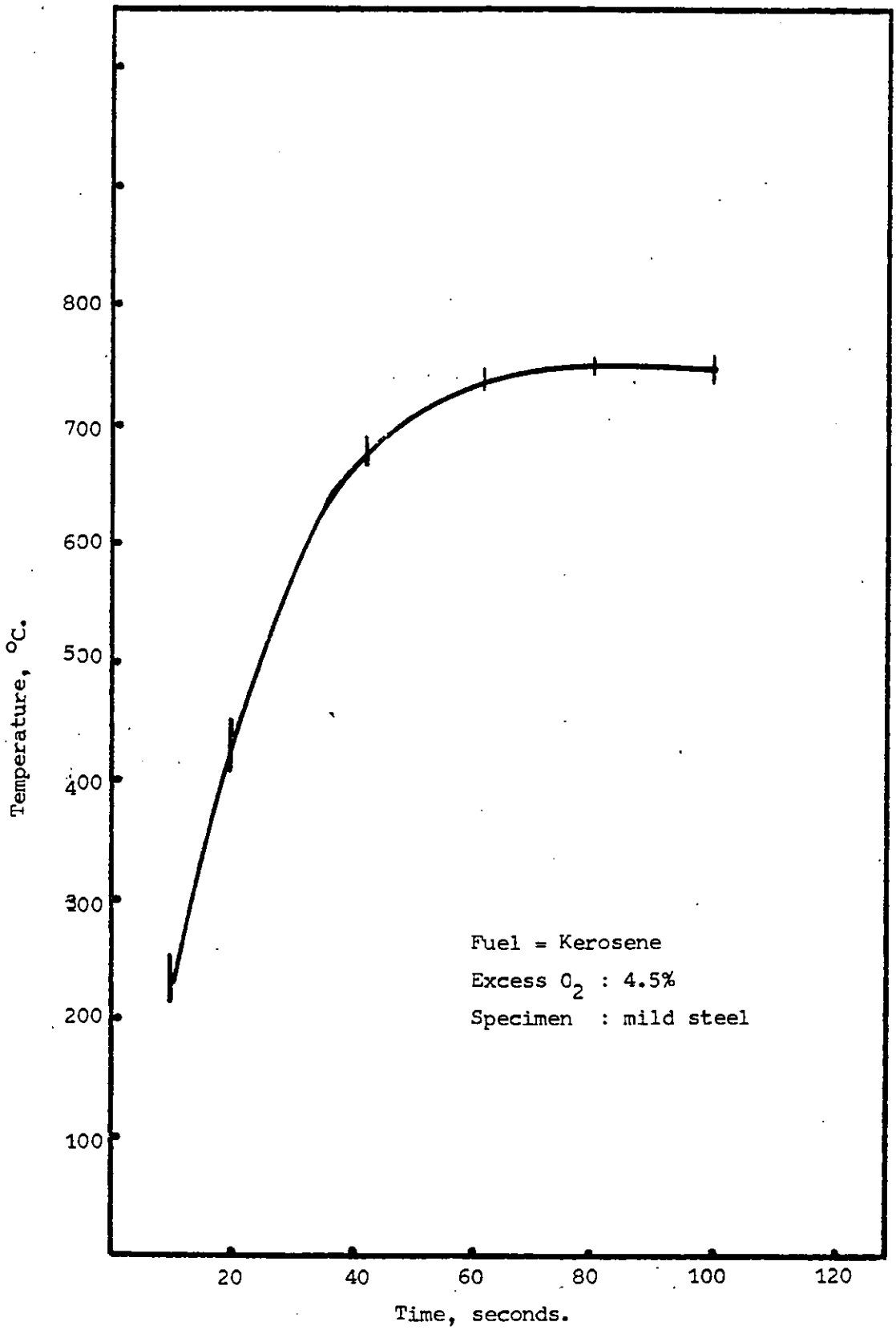

Figure 6 (3) The rate of temperature rise of the metal specimens on introducing into hot combustion gas at 730° C.

metal | s | Plastic

(a) after one hour

M | Scale | Plastic

(b) after three hours.

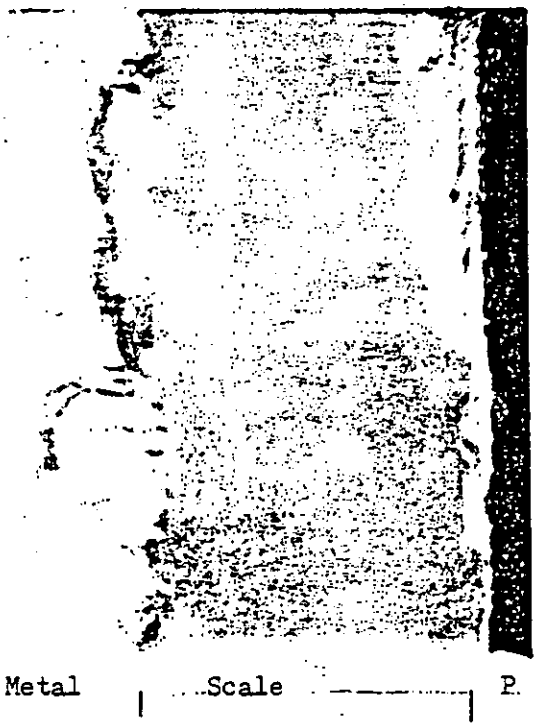

Metal | Scale | P.

(c) after six hours

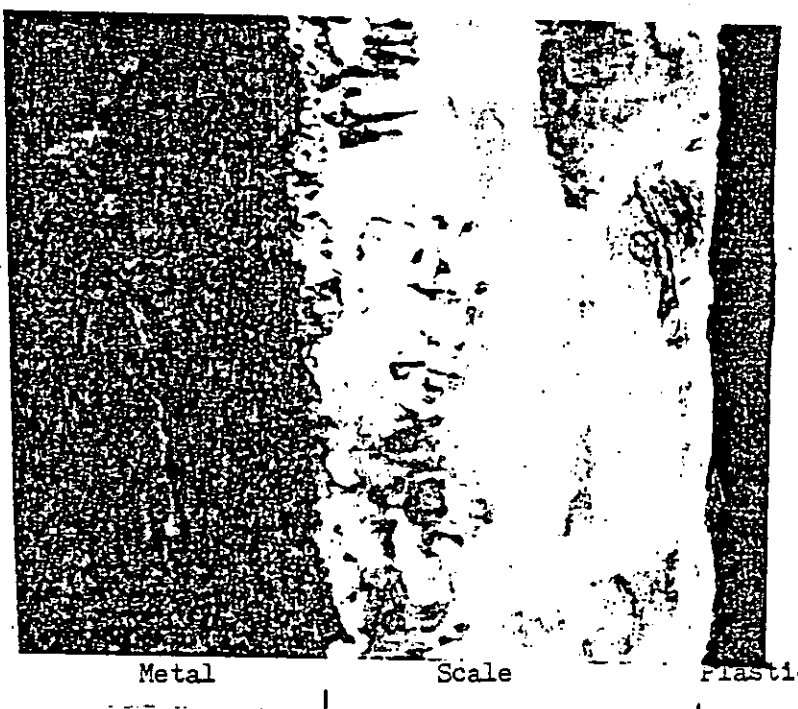

Metal | Scale | Plastic

(d) after twenty hours.

Fig 6(4). Metallographic section through metal/ scale interface of mild steel at 730°C (unetched x 400)

TABLE 6 (5) PERSONAL ACCURACY OF WEIGHING IN CHEMICAL BALANCE.

SAMPLE	INITIAL WEIGHTS	FINAL WEIGHTS	DIFFERENCE
MILD STEEL	7.7010	7.7013	.0003
	7.7015	7.7011	.0004
STAINLESS STEEL TYPE 347	8.2110	8.2105	.0005
	8.2103	8.2100	.0003
N90	9.6355	9.6350	.0005
	9.6450	9.6454	.0004
N105	10.5830	10.5836	.0006
	10.5755	10.5760	.0005
IN657	12.8775	12.8770	.0005
	12.7811	12.7808	.0003

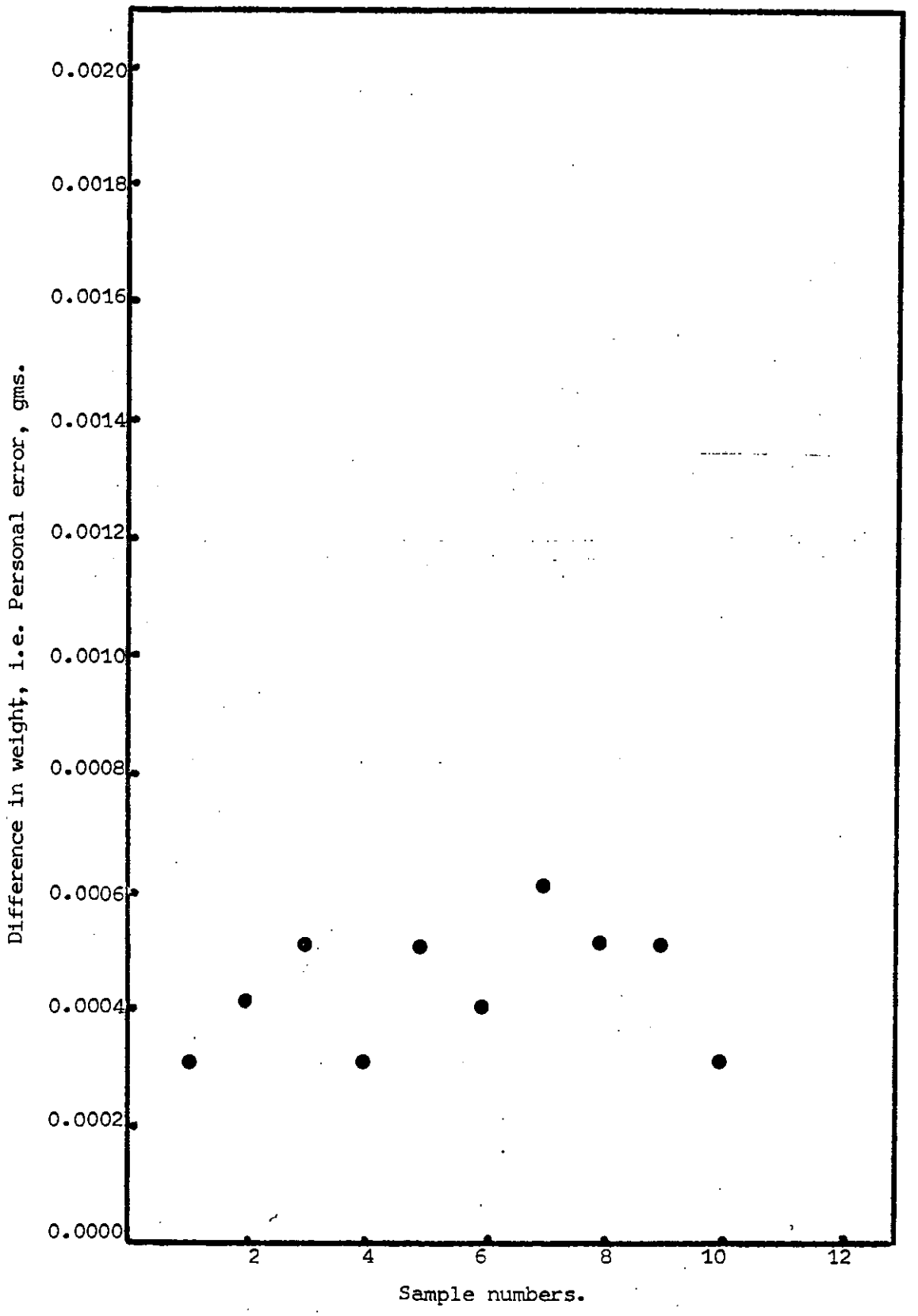

Figure 6 (**5**) Personal Accuracy of Weighing Samples on a chemical Balance.

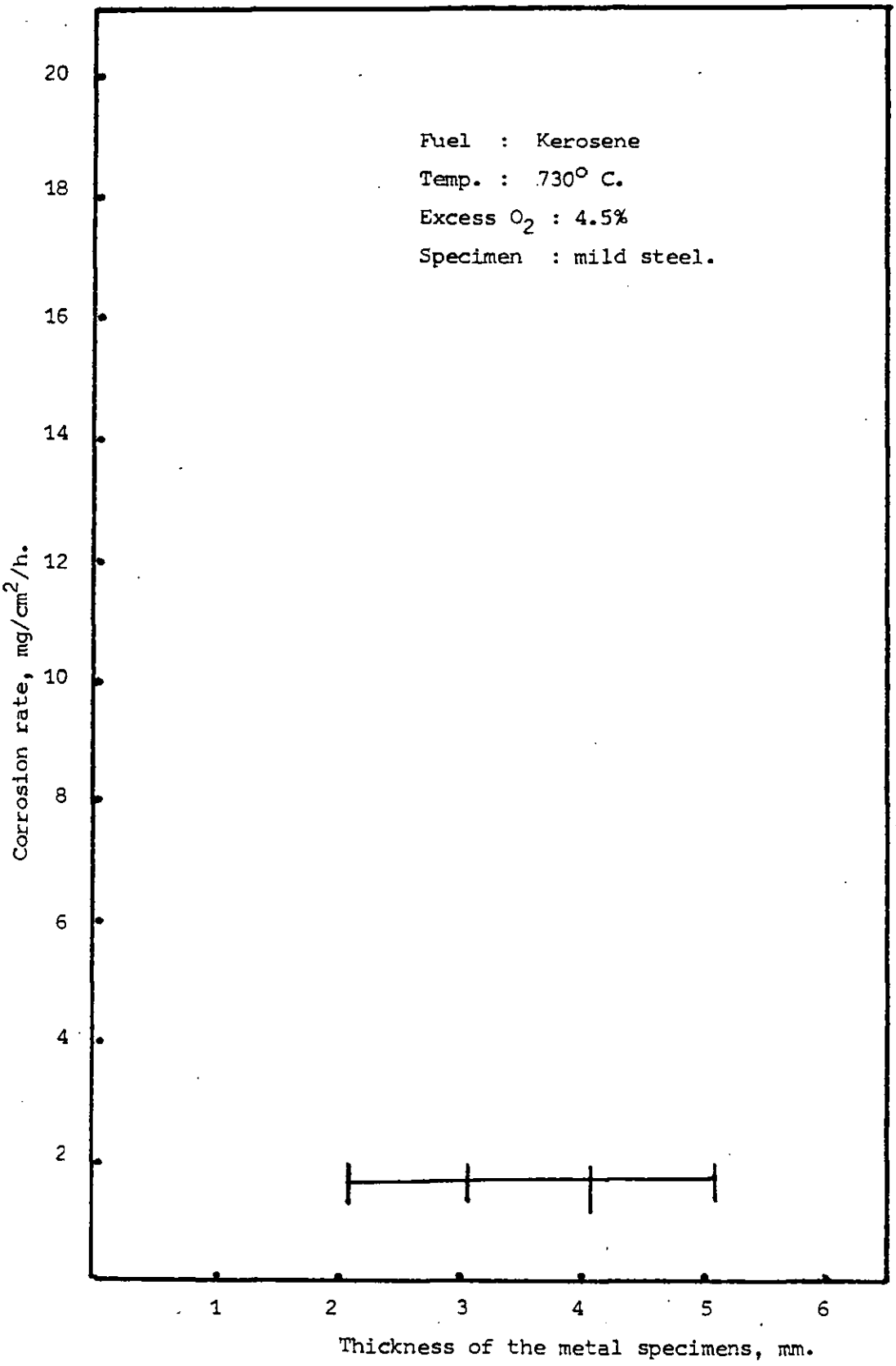

Figure 6 (**6**) Relation of Corrosion rate to the thickness of the metal specimens.

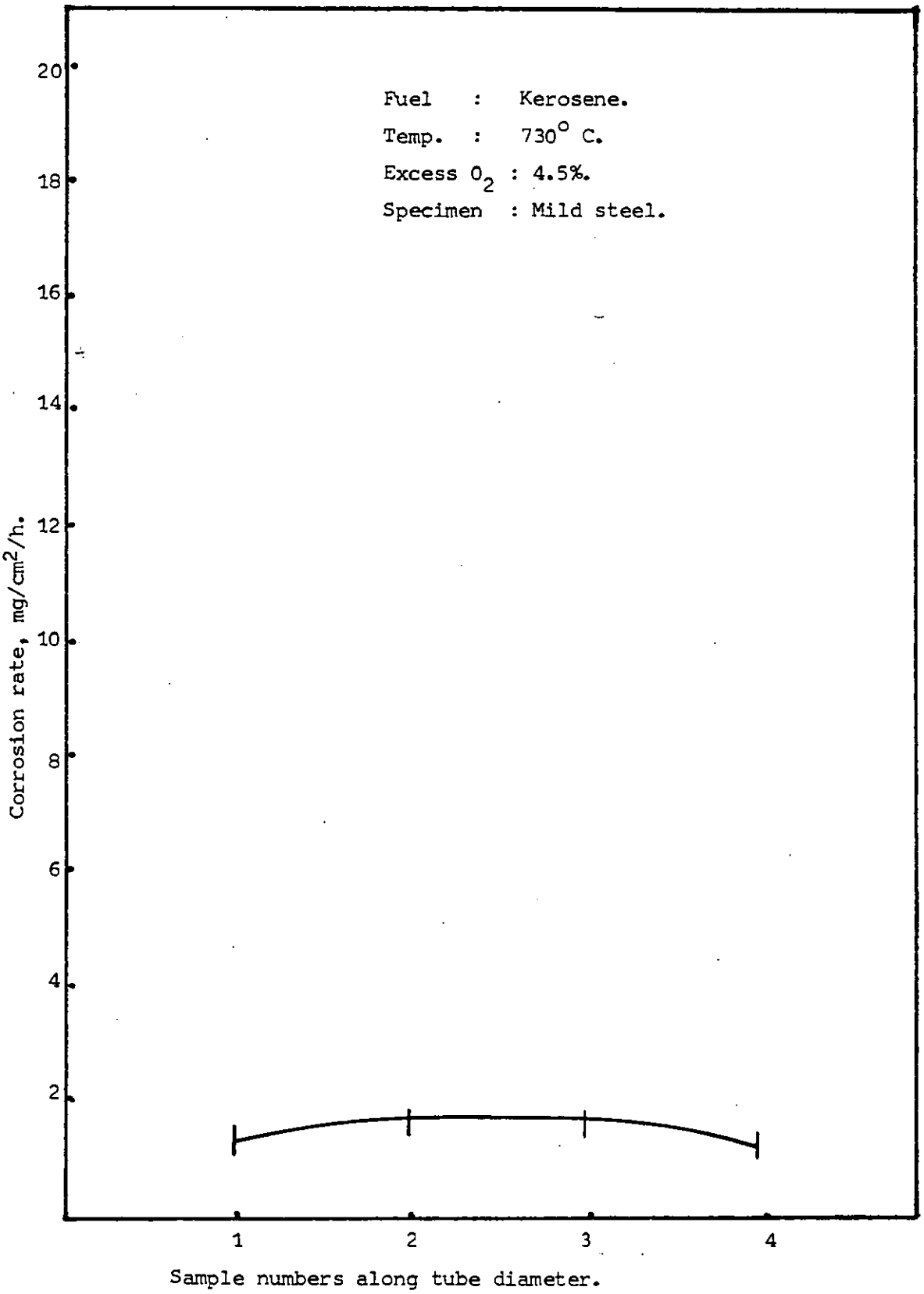

Figure 6 (7) Relation of corrosion rate to sample position along tube diameter.

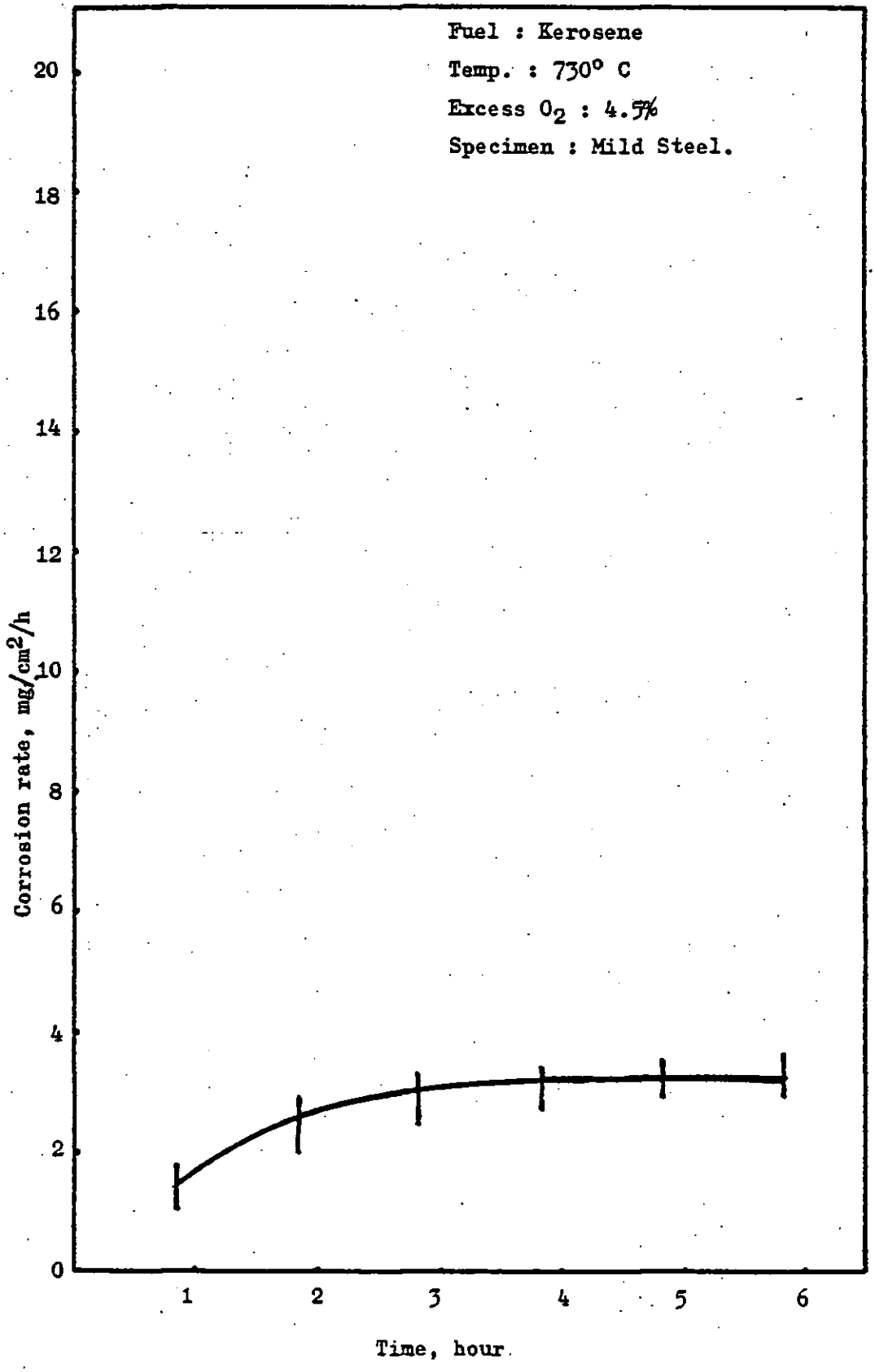

Figure 6 (8) Relation of corrosion rate to time of exposure.

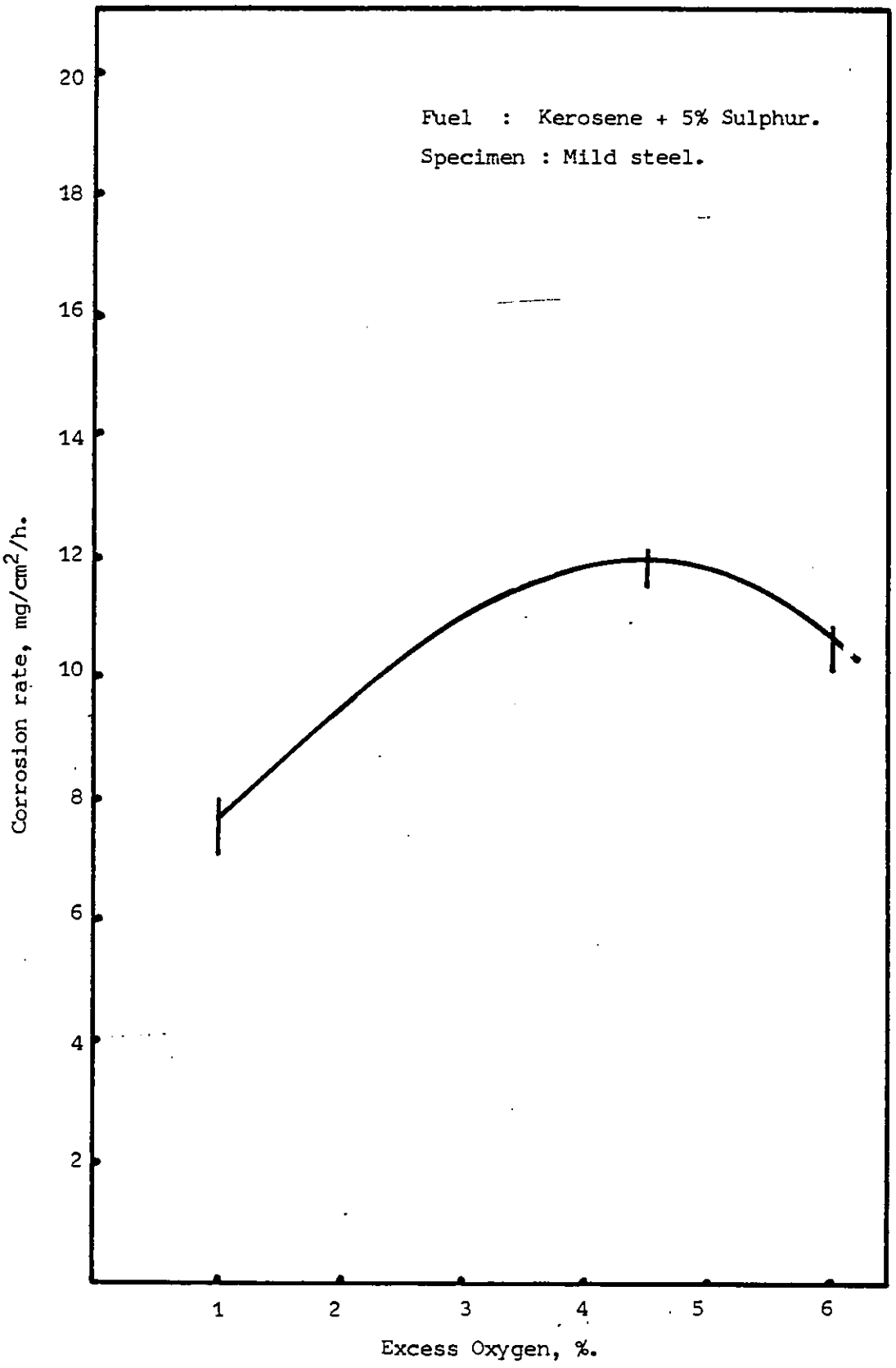

Figure 6 (9) Relation of corrosion rate to excess oxygen. Concentration of combustion gases.

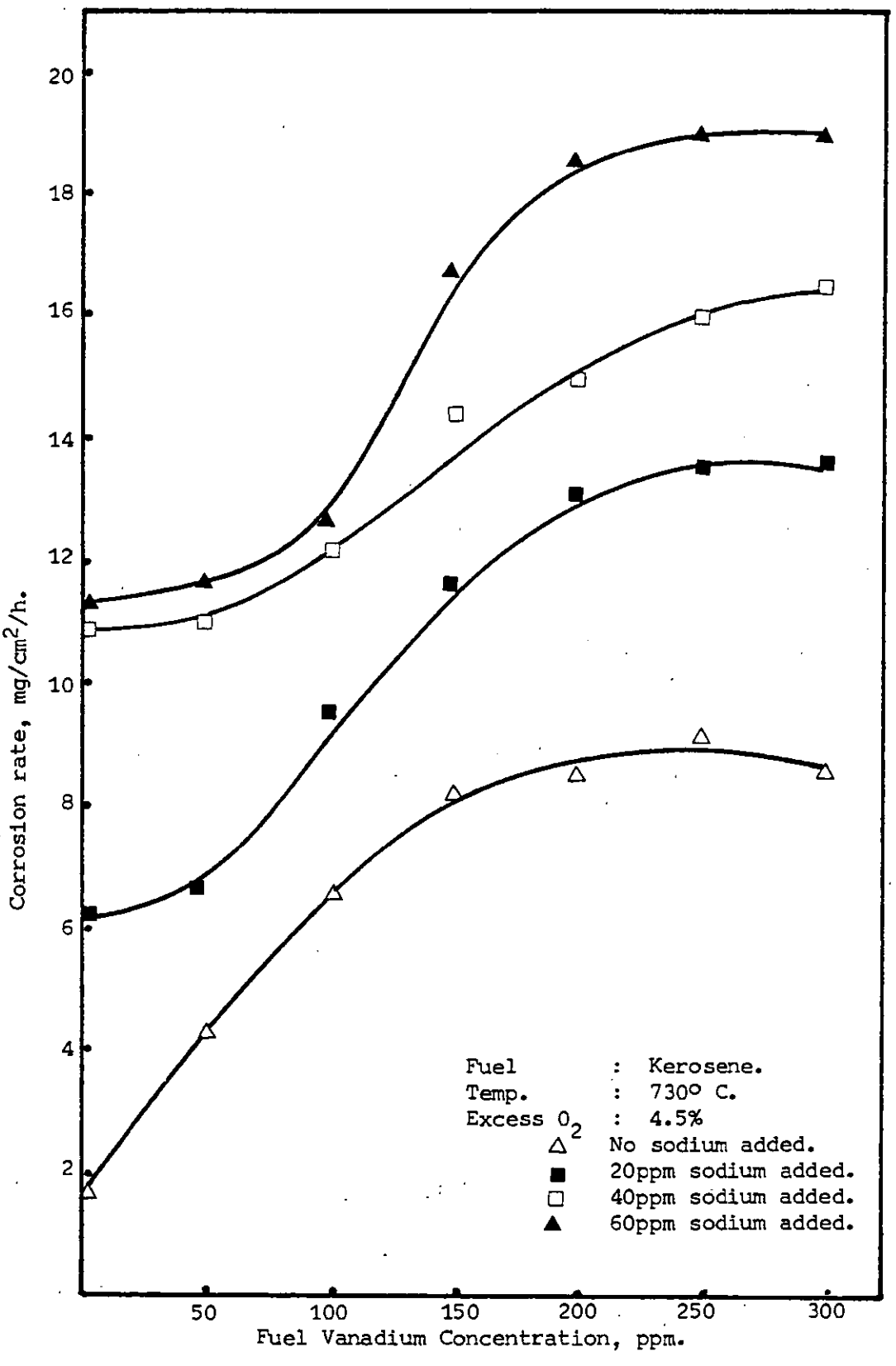

Figure 6 (10)Relation of Corrosion rate of mild steel to fuel vanadium concentration at different concentrations of sodium with no sulphur added.

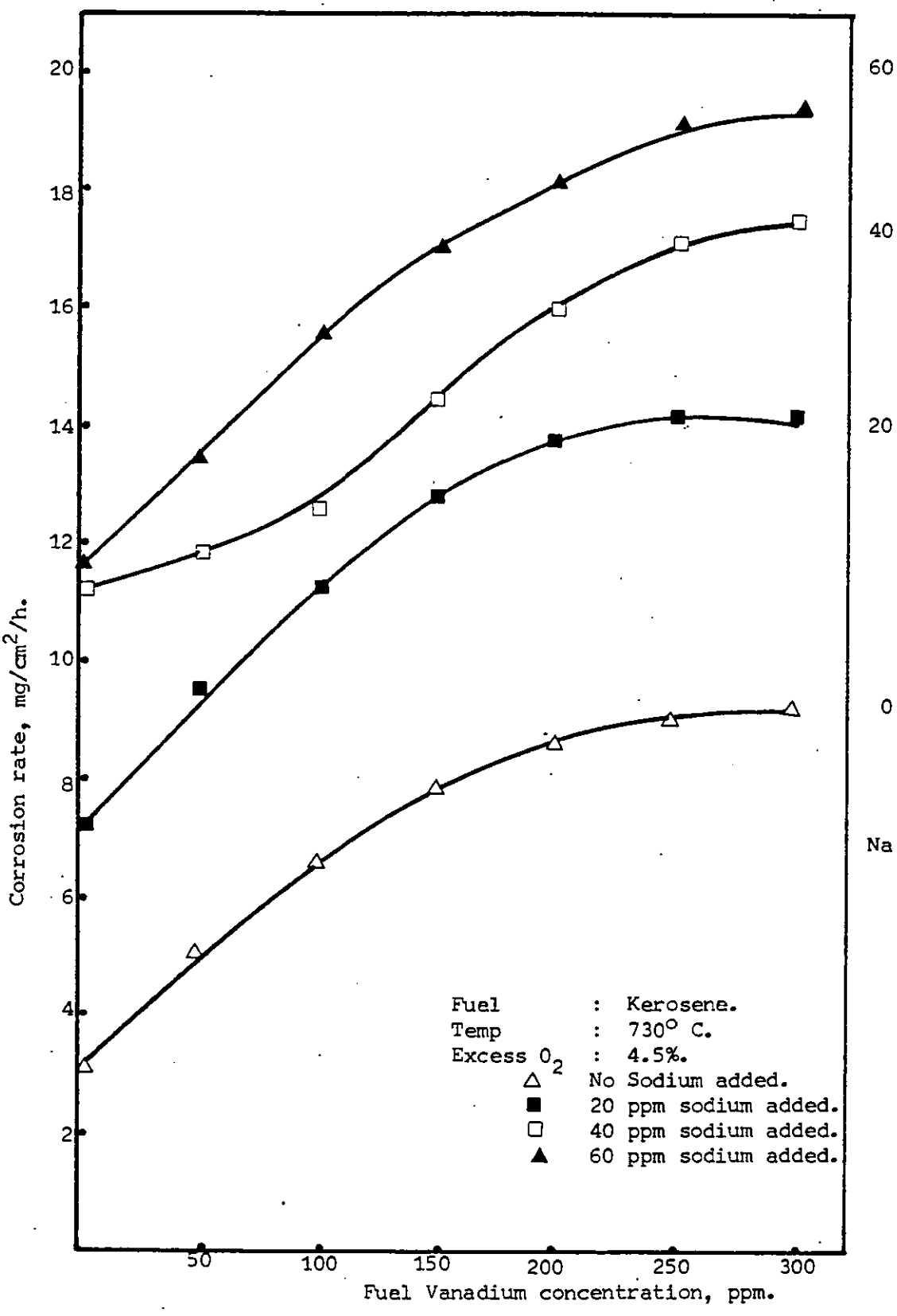

Figure 6 (11) Relation of corrosion rate of mild steel to fuel vanadium concentration at different concentrations of sodium with 1% sulphur added.

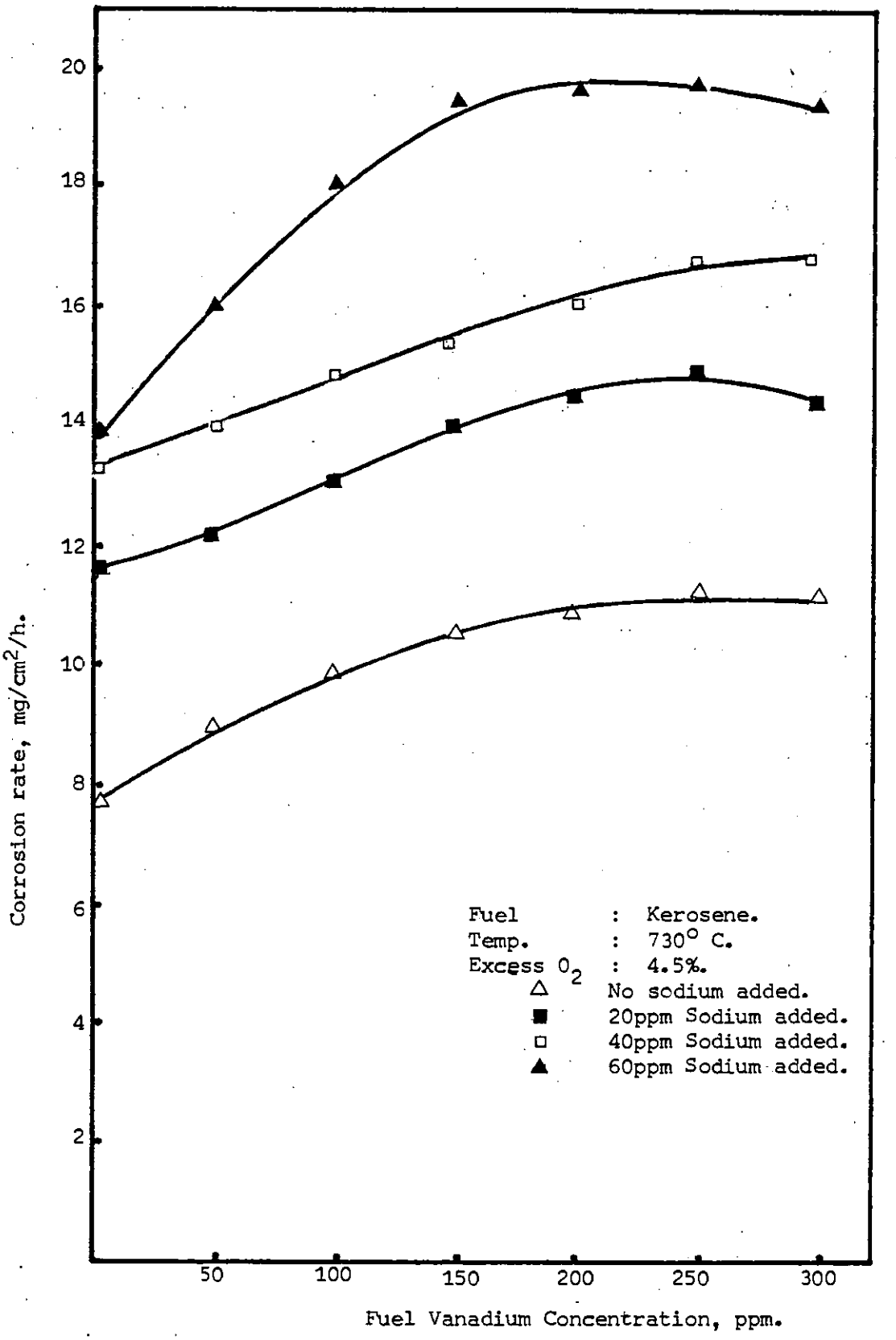

Figure 6 (12) Relation of Corrosion rate of mild steel to fuel vanadium concentration at different concentrations of sodium with 2% sulphur added.

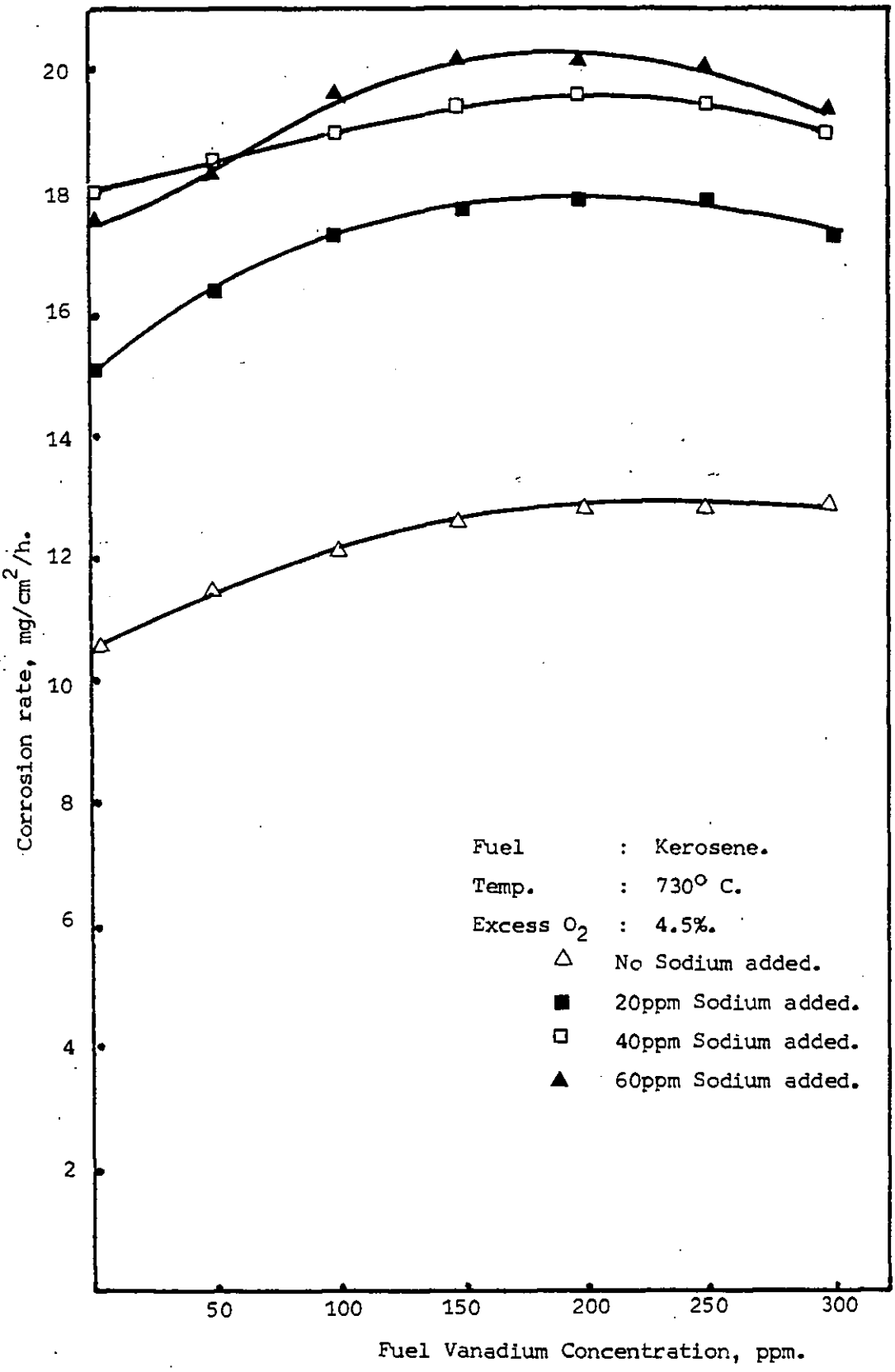

Figure 6 (13) Relation of corrosion rate of mild steel to fuel vanadium Concentration at different concentrations of sodium with 3% sulphur added.

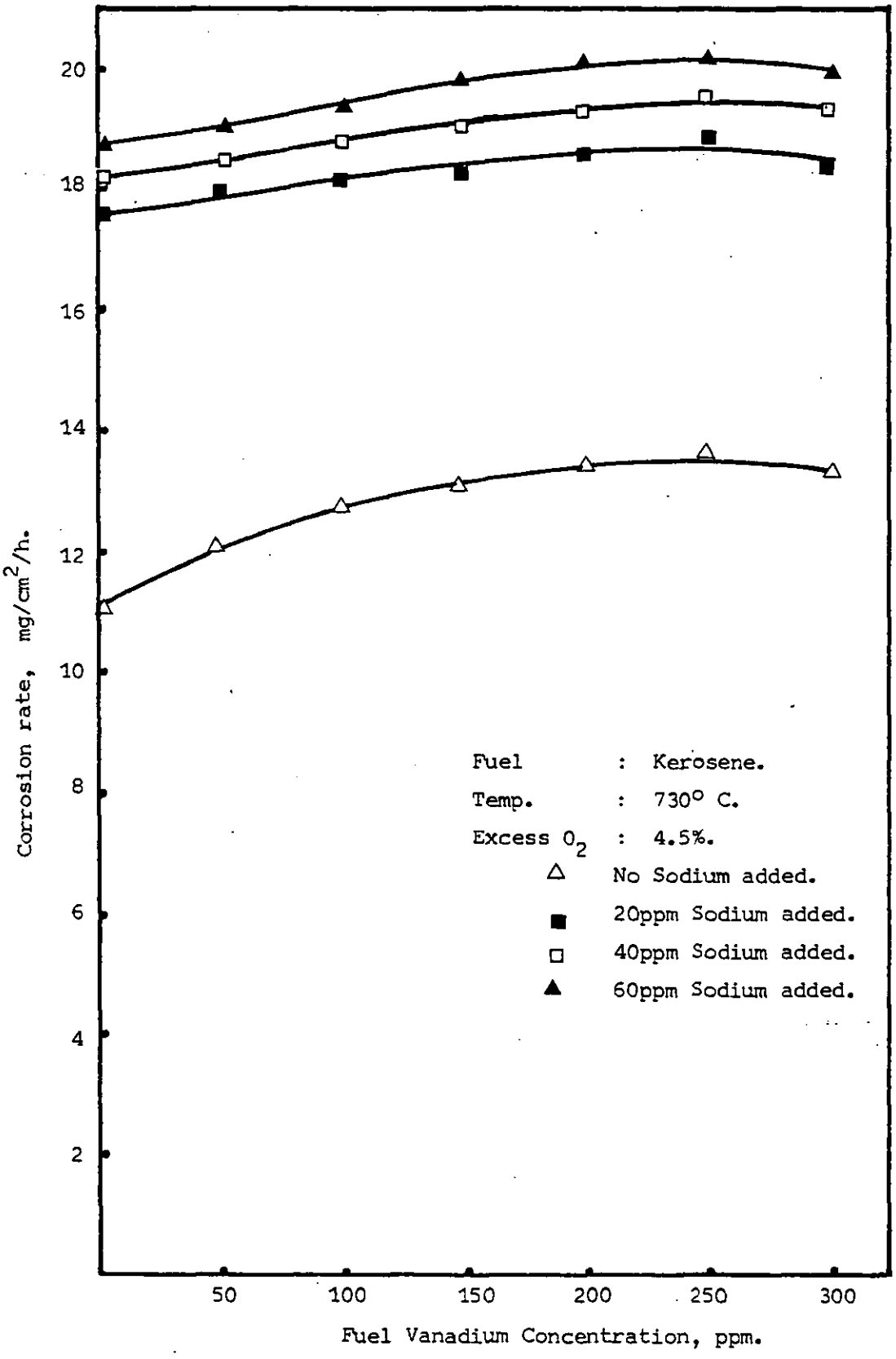

Figure 6 (14) Relation of Corrosion rate of mild steel to fuel vanadium concentration at different concentrations of sodium with 4% sulphur added.

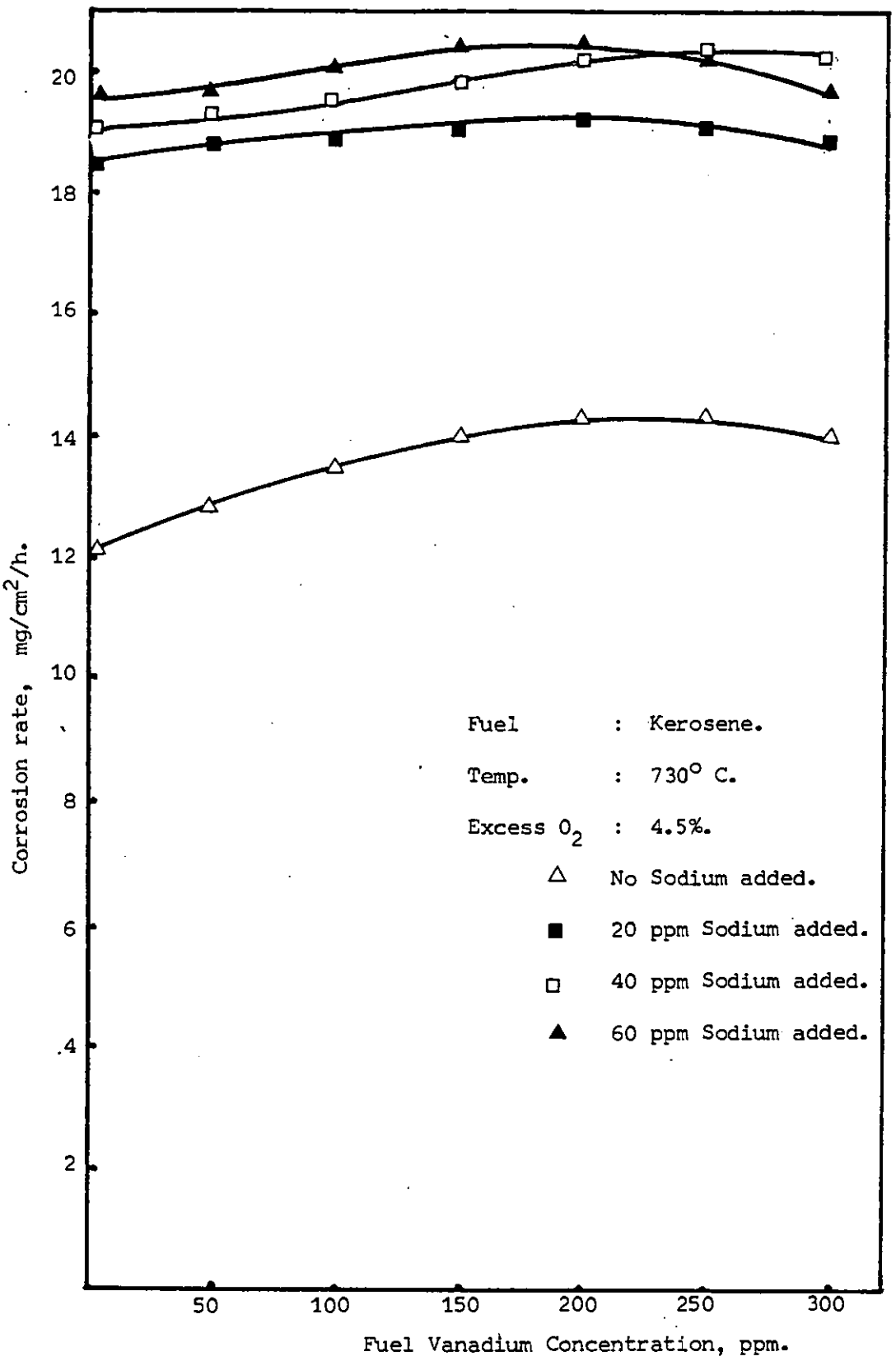

Figure 6 (15) Relation of corrosion rate of mild steel to fuel vanadium concentration at different concentrations of sodium with 5% sulphur added.

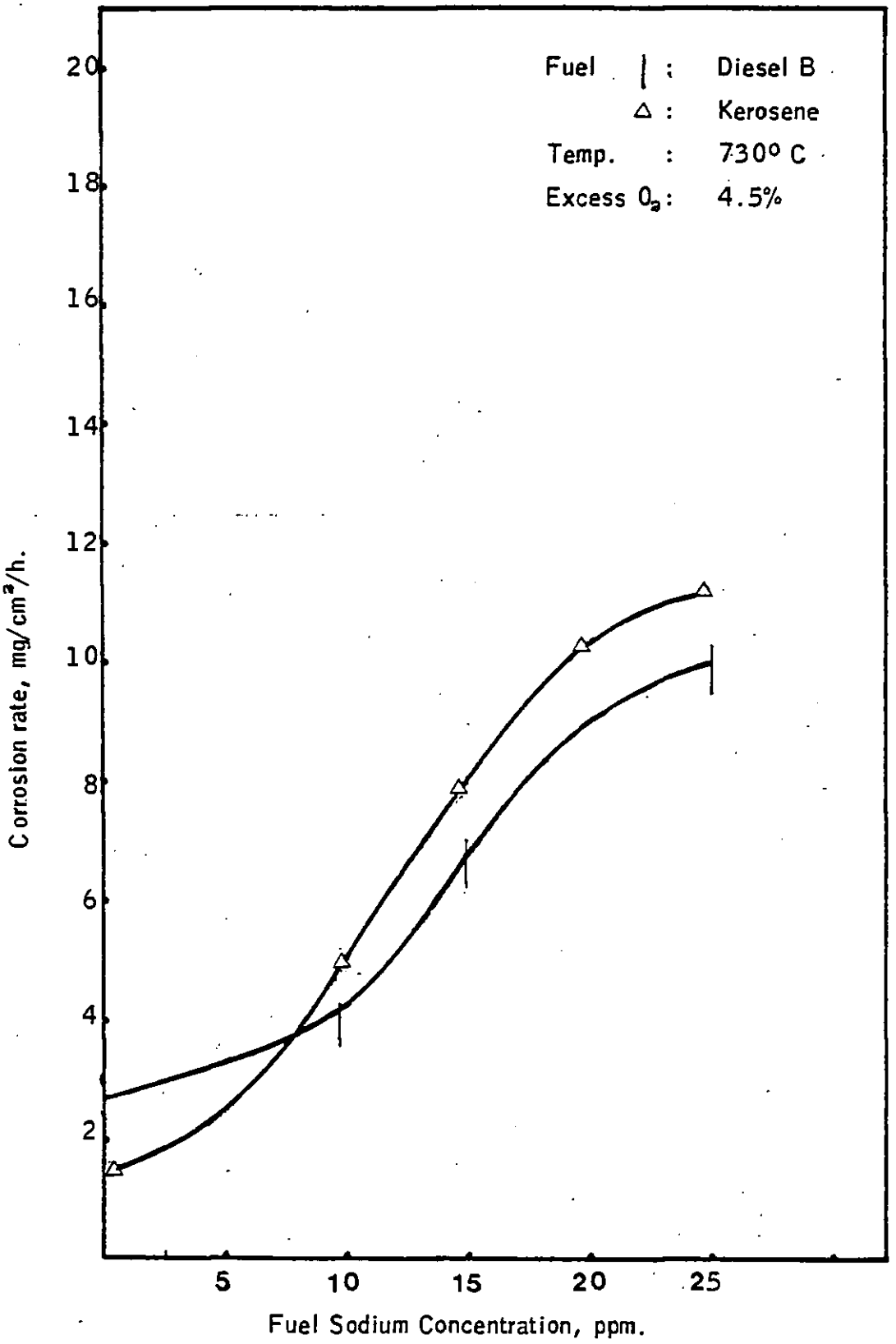

Fig. 6[16] Relation of corrosion rate of mild steel to fuel sodium concentration.

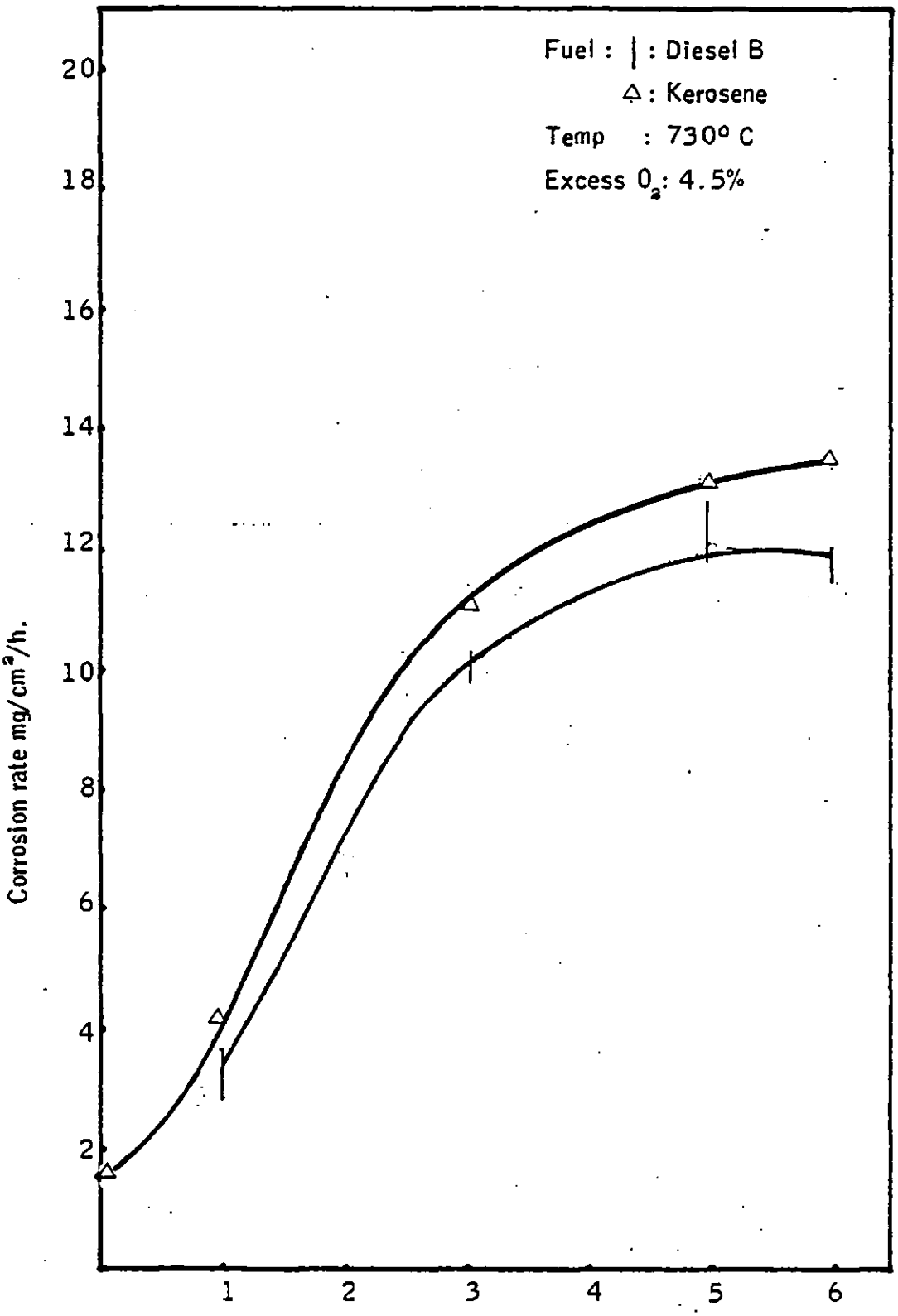

Fig. 6(17). Relation of corrosion rate of mild steel to fuel sulphur concentration.

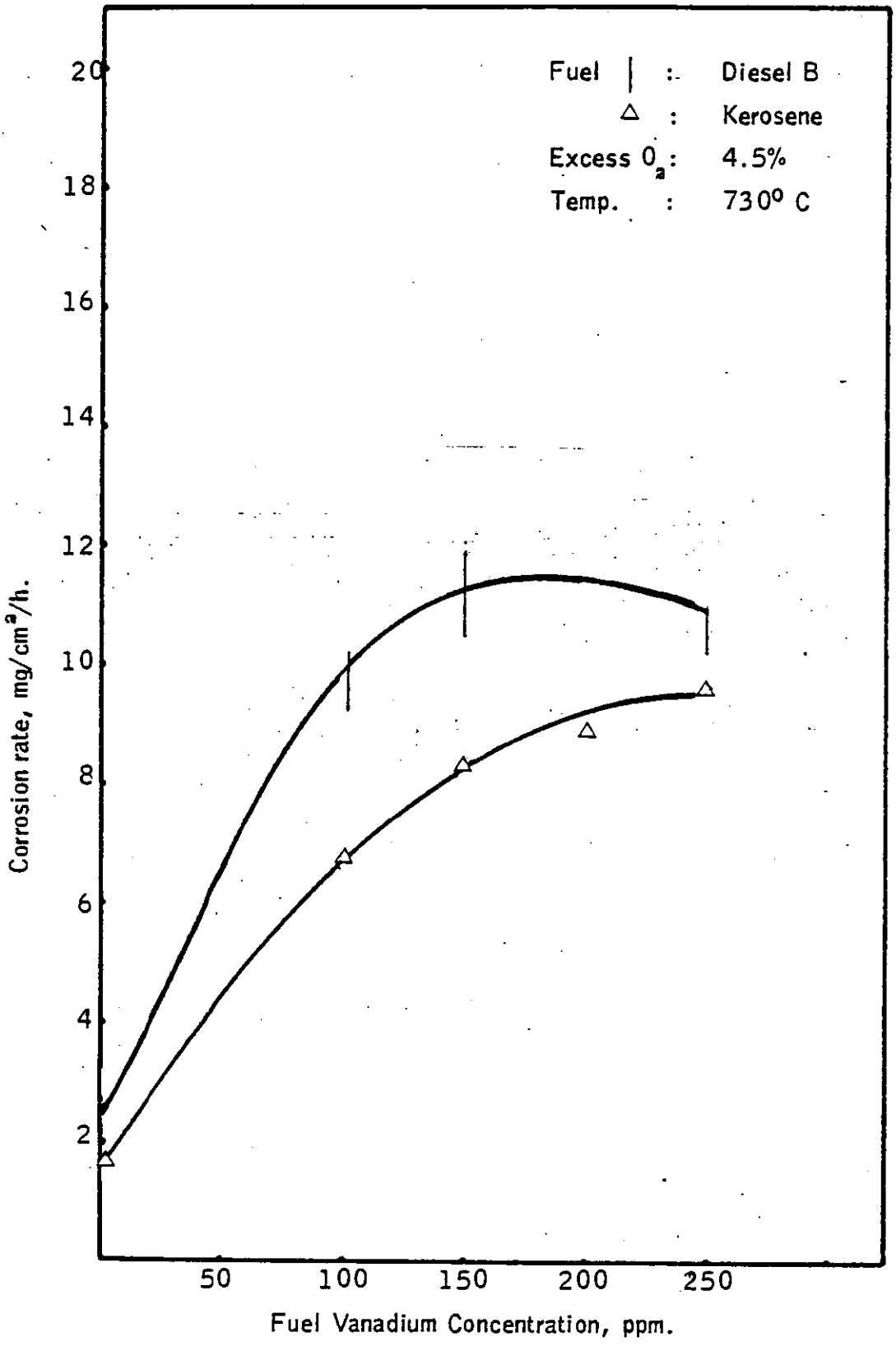

Fig. 6(18). Relation of corrosion rate of mild steel to fuel vanadium concentration .

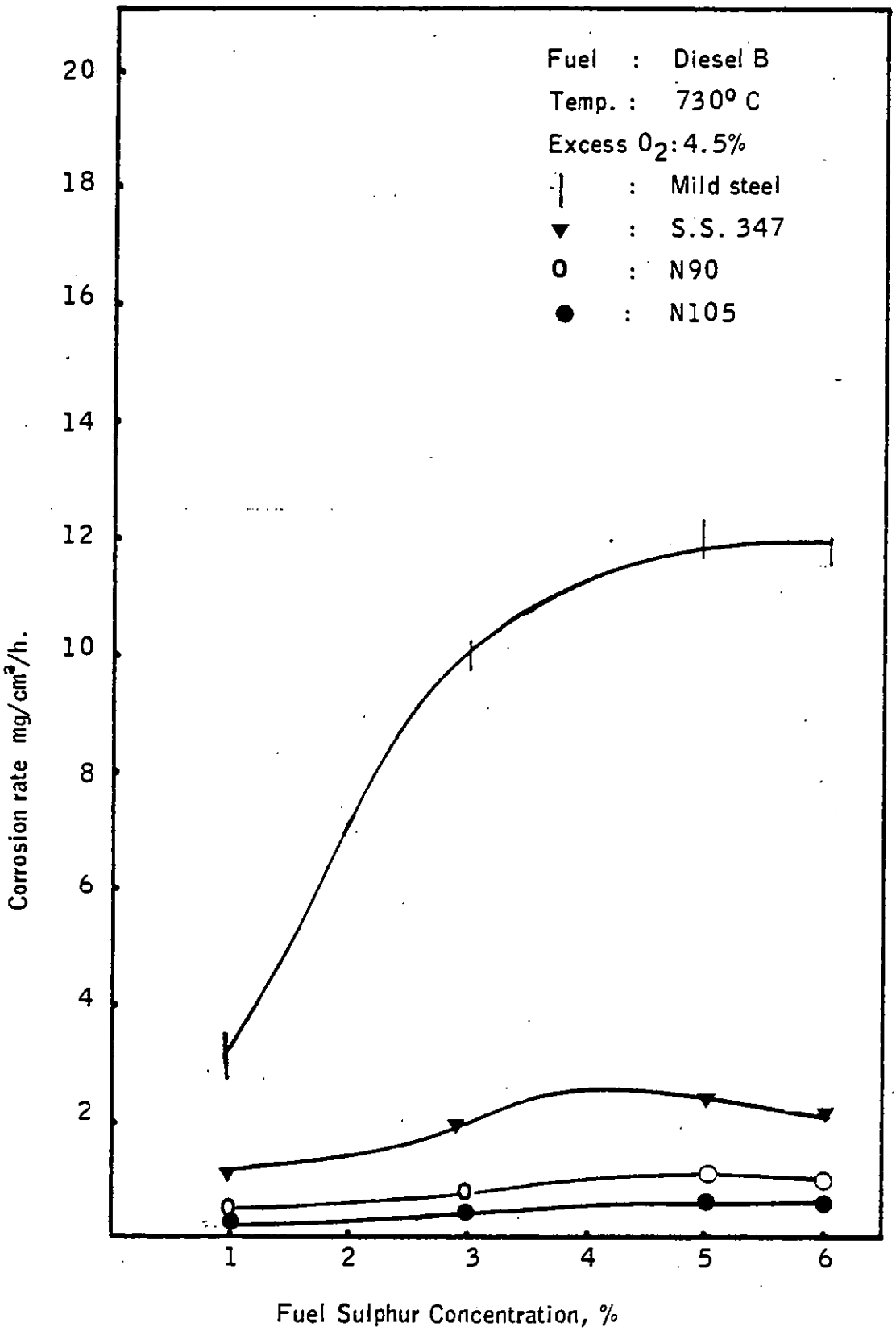

Fig. 6(20). Relation of Corrosion rate of various metals to fuel Sulphur Concentration.

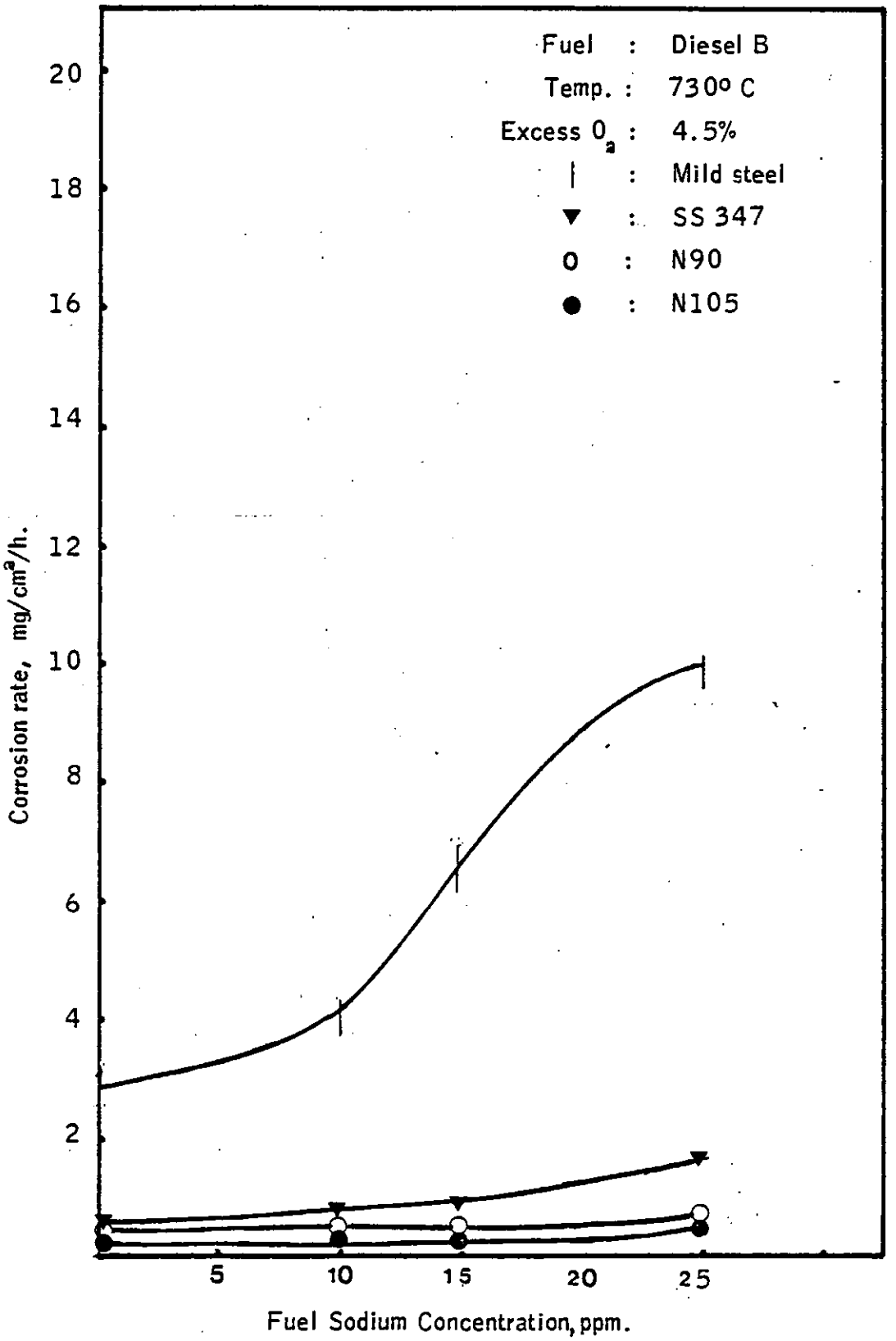

Fig. 6-(19). Relation of Corrosion rate of various metal to fuel sodium concentration.

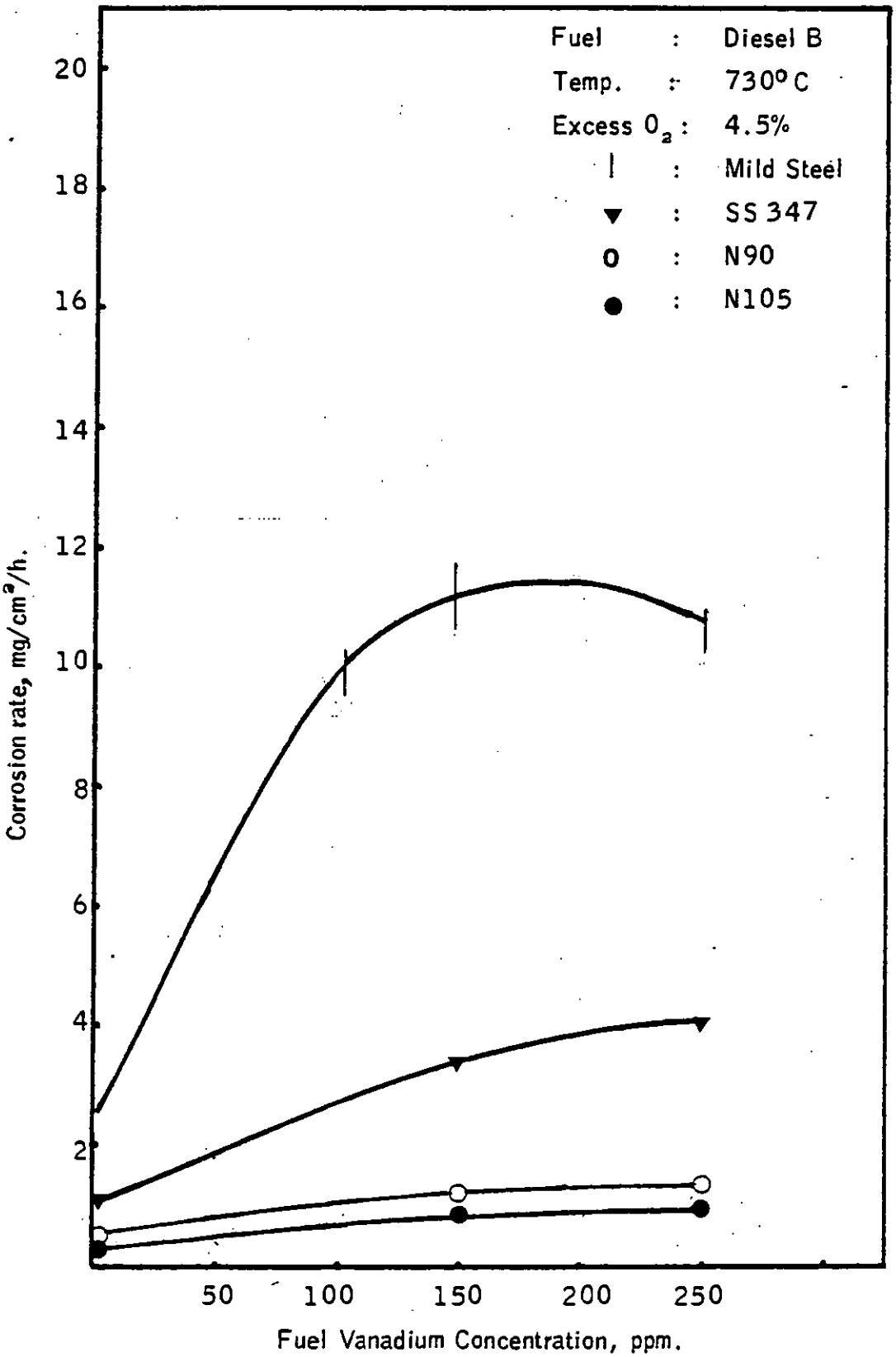

Fig. 6[21]. Relation of Corrosion rate of various metals to fuel vanadium Concentration.

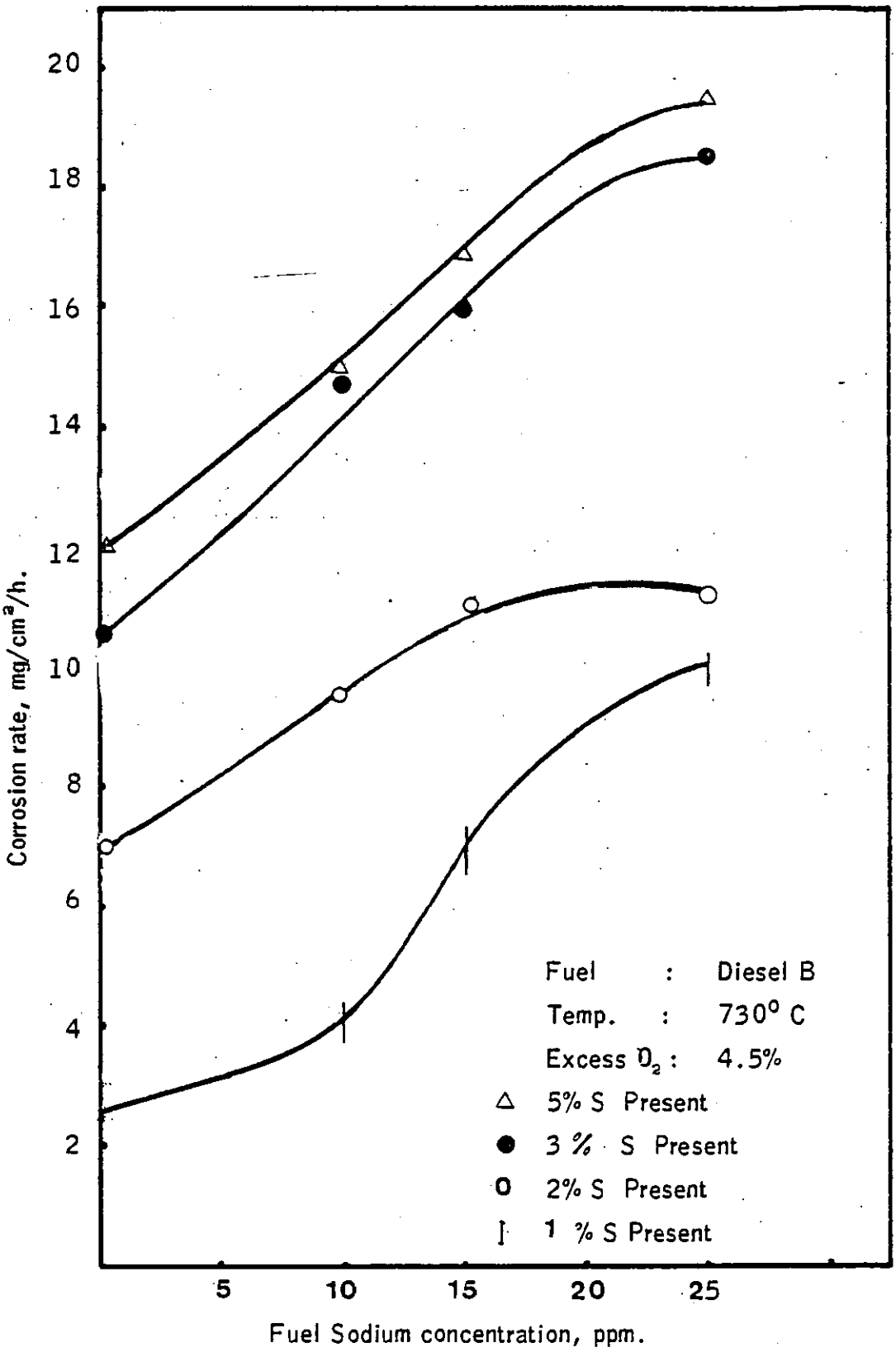

Fig. 6 (2 2). Relation of corrosion rate of mild steel to fuel sodium concentration at different concentration of sulphur present.

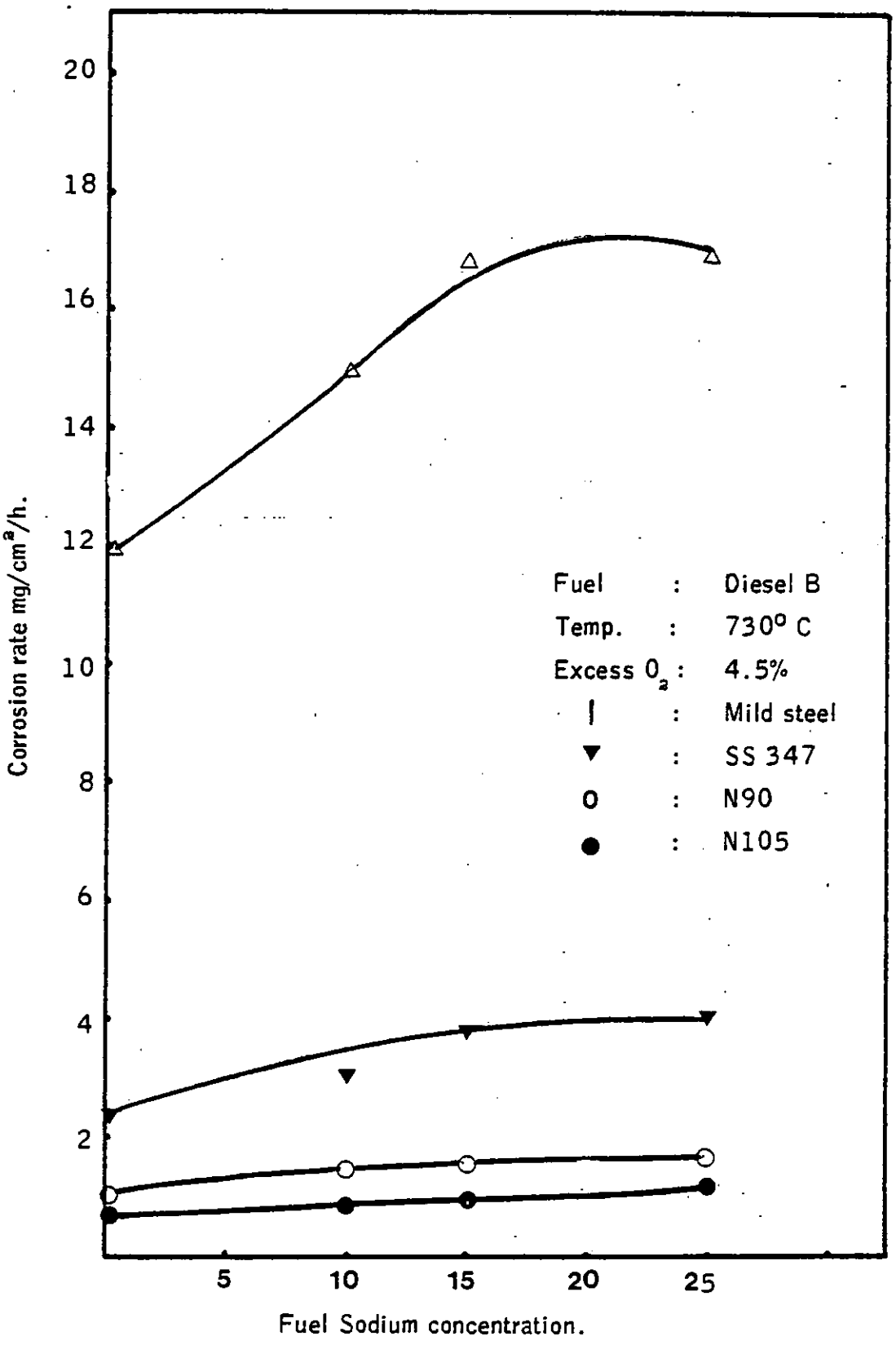

Fig. 6(23) Relation of Corrosion rate of different metal to fuel sodium concentration in presence of 5% sulphur.

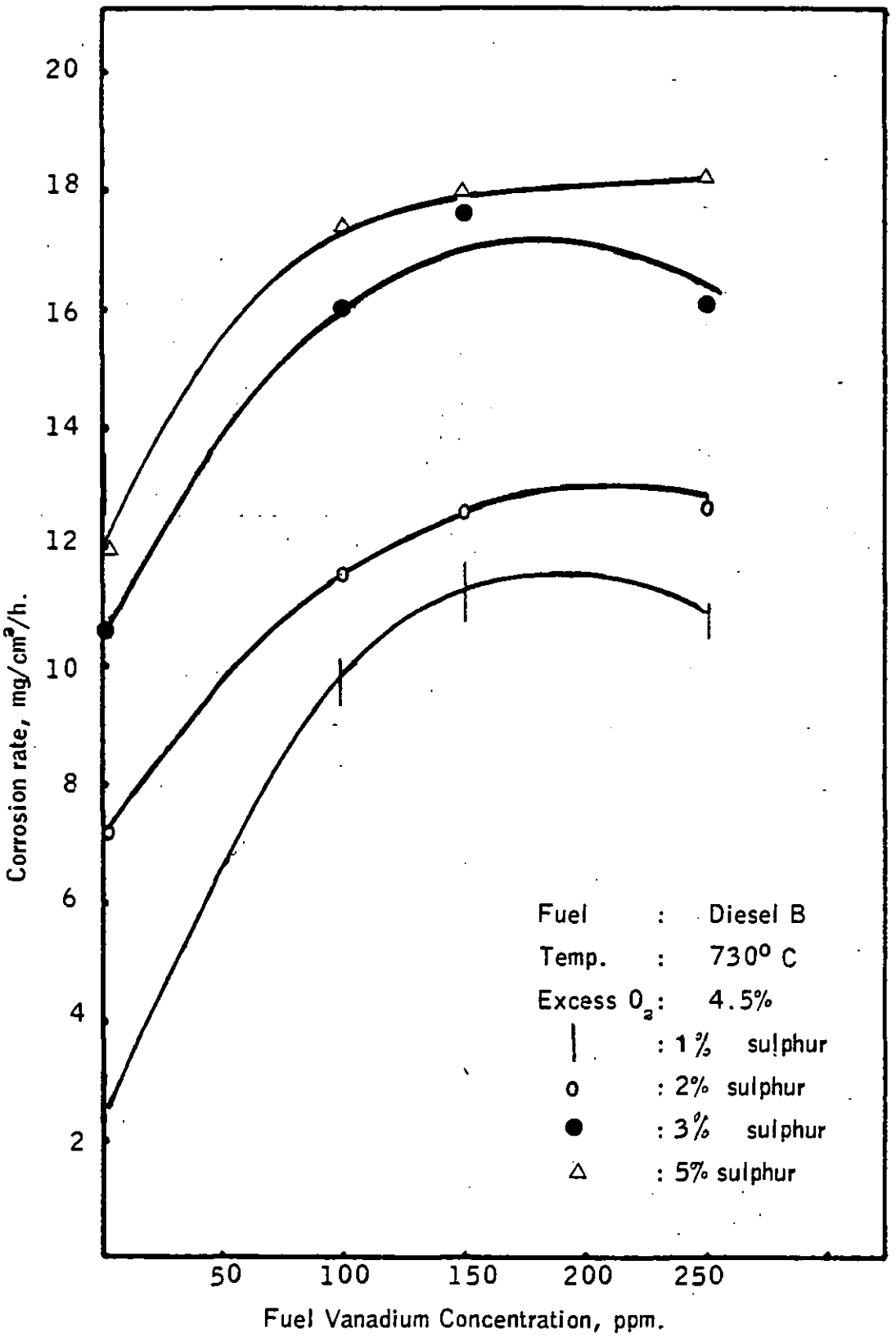

Fig. 6 (24) Relation of Corrosion rate of mild steel to fuel Vanadium Concentration in presence of sulphur.

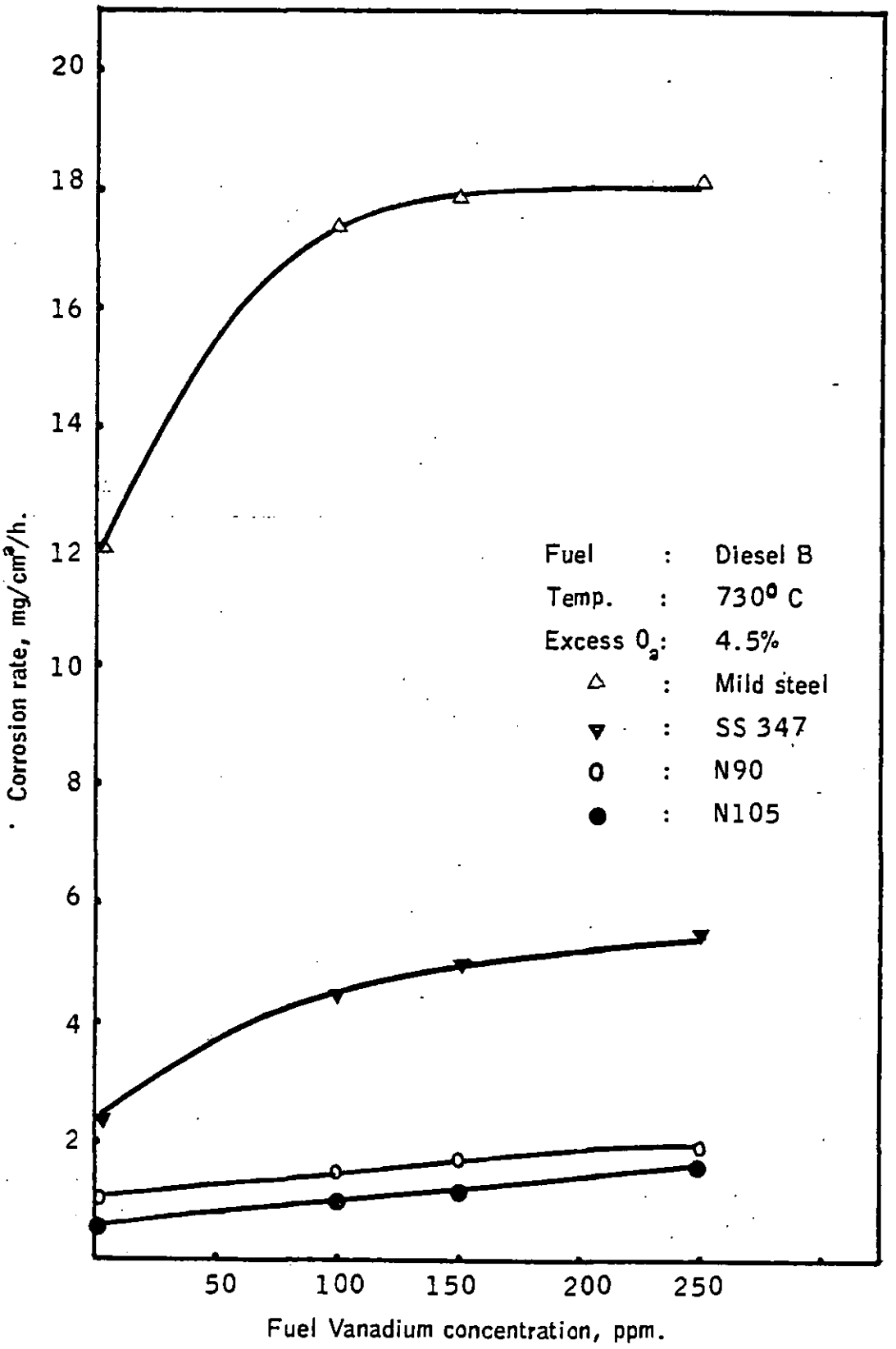

Fig. 6 (25) Relation of corrosion rate of different metal to fuel vanadium Concentration in presence of 5% sulphur.

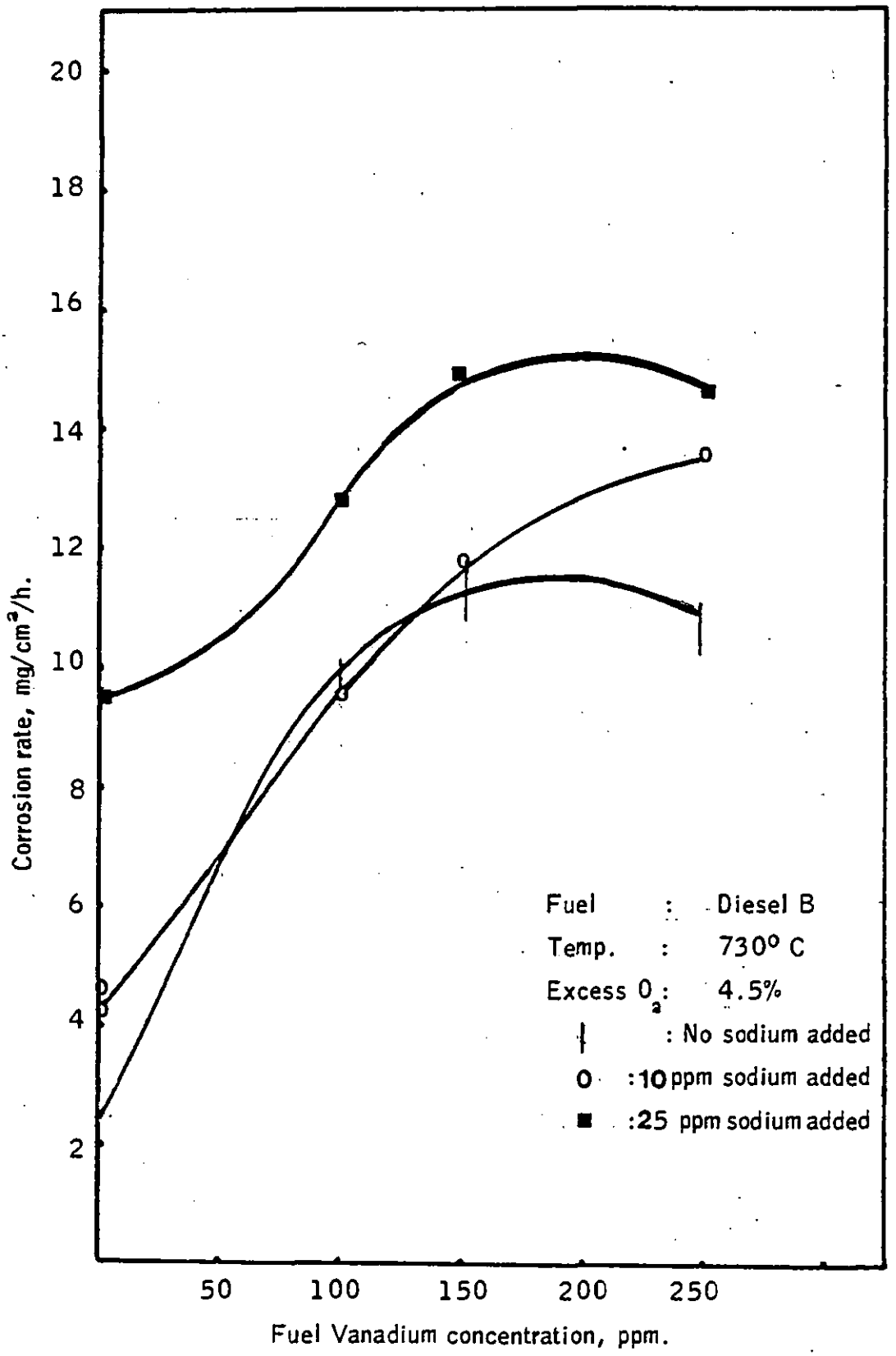

Fig. 6 (26) Relation of Corrosion rate of mild steel to fuel vanadium concentration in Presence of sodium.

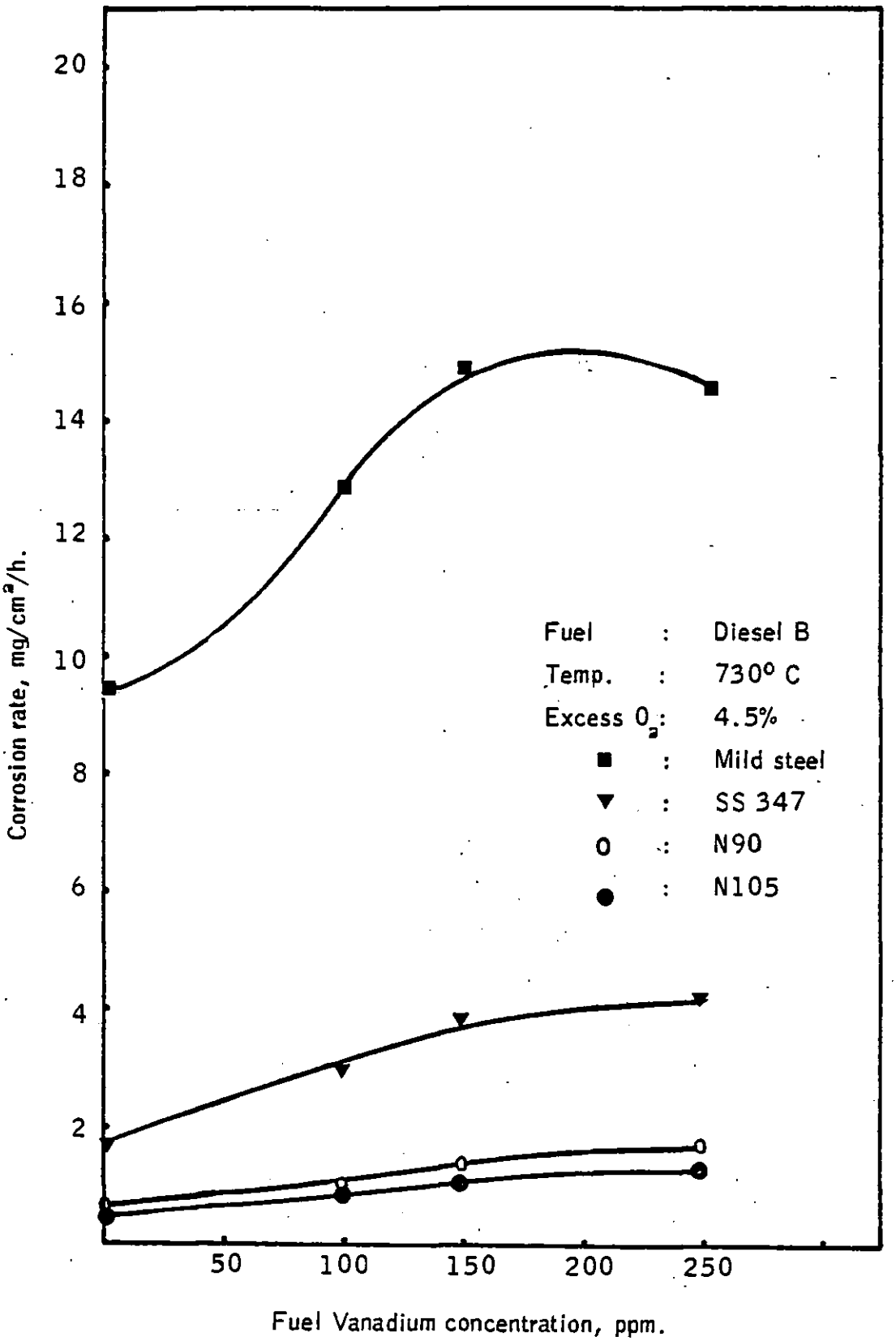

Fig.6(27) Relation of Corrosion rate of different metal to fuel vanadium Concentration in presence of 25 ppm sodium.

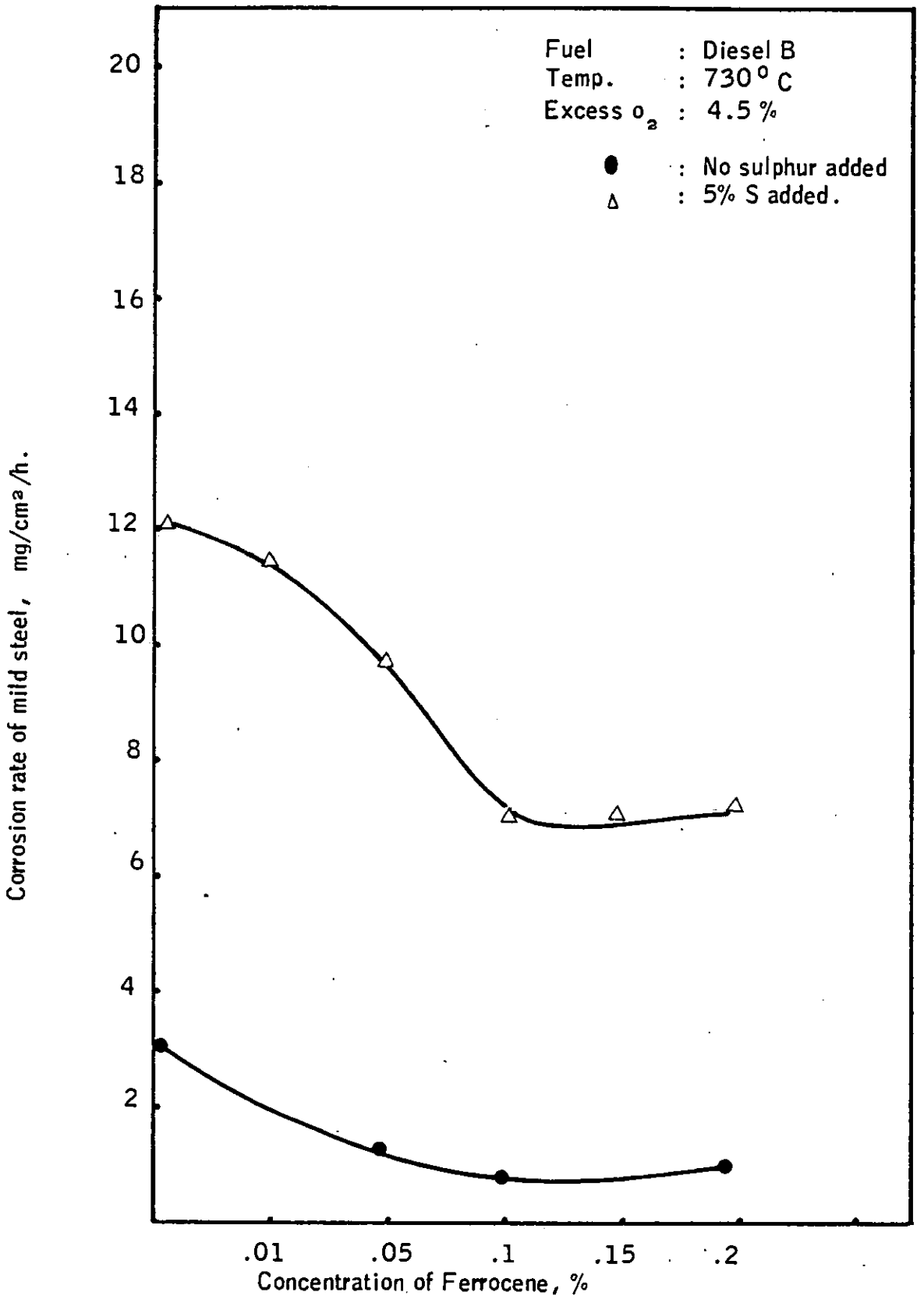

Figure 6 (28). Relation of Corrosion rate of mild steel to fuel additive concentration.

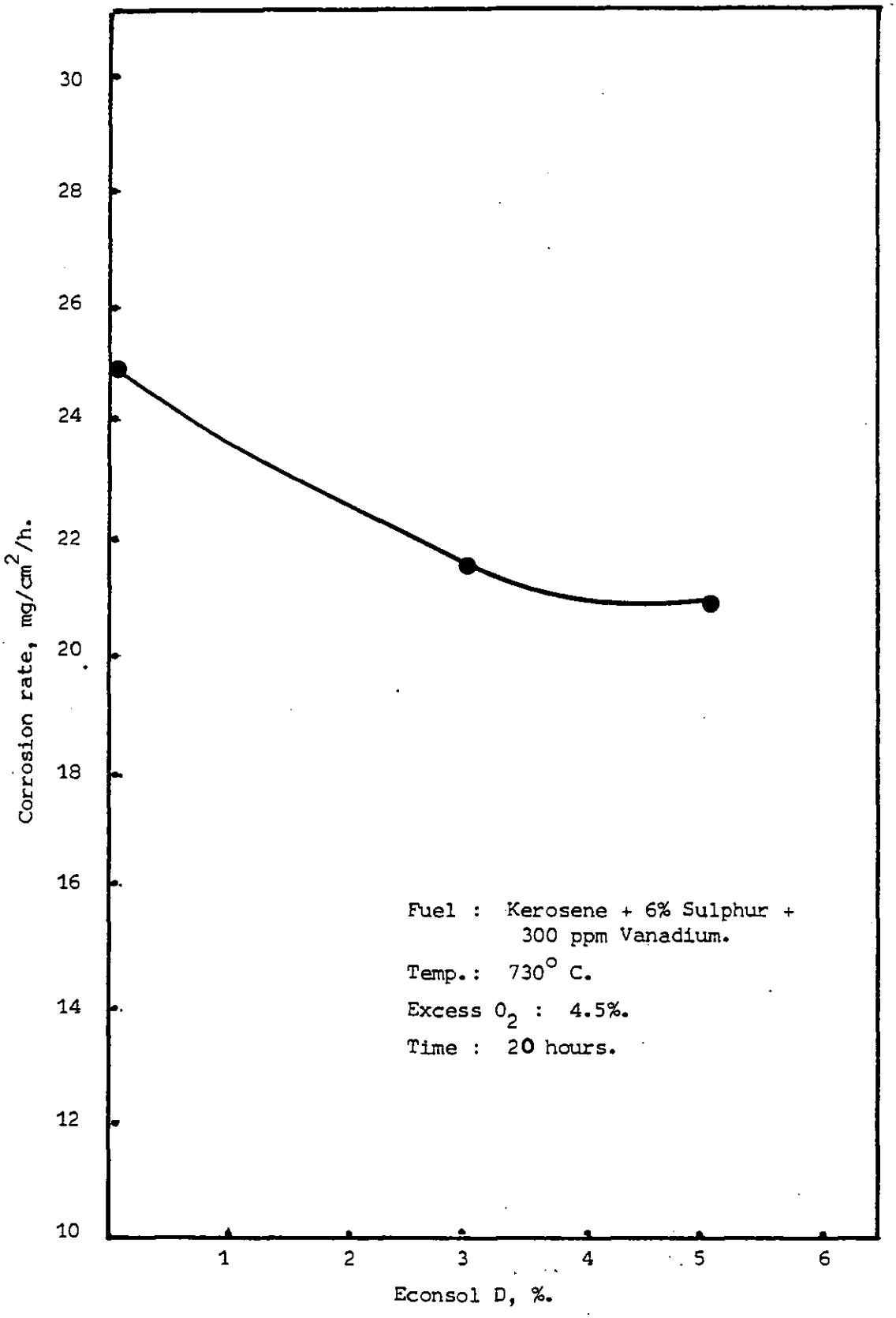

Figure 6 (29) Relation of corrosion rate of mild steel to fuel additive (Econsol D) concentration.

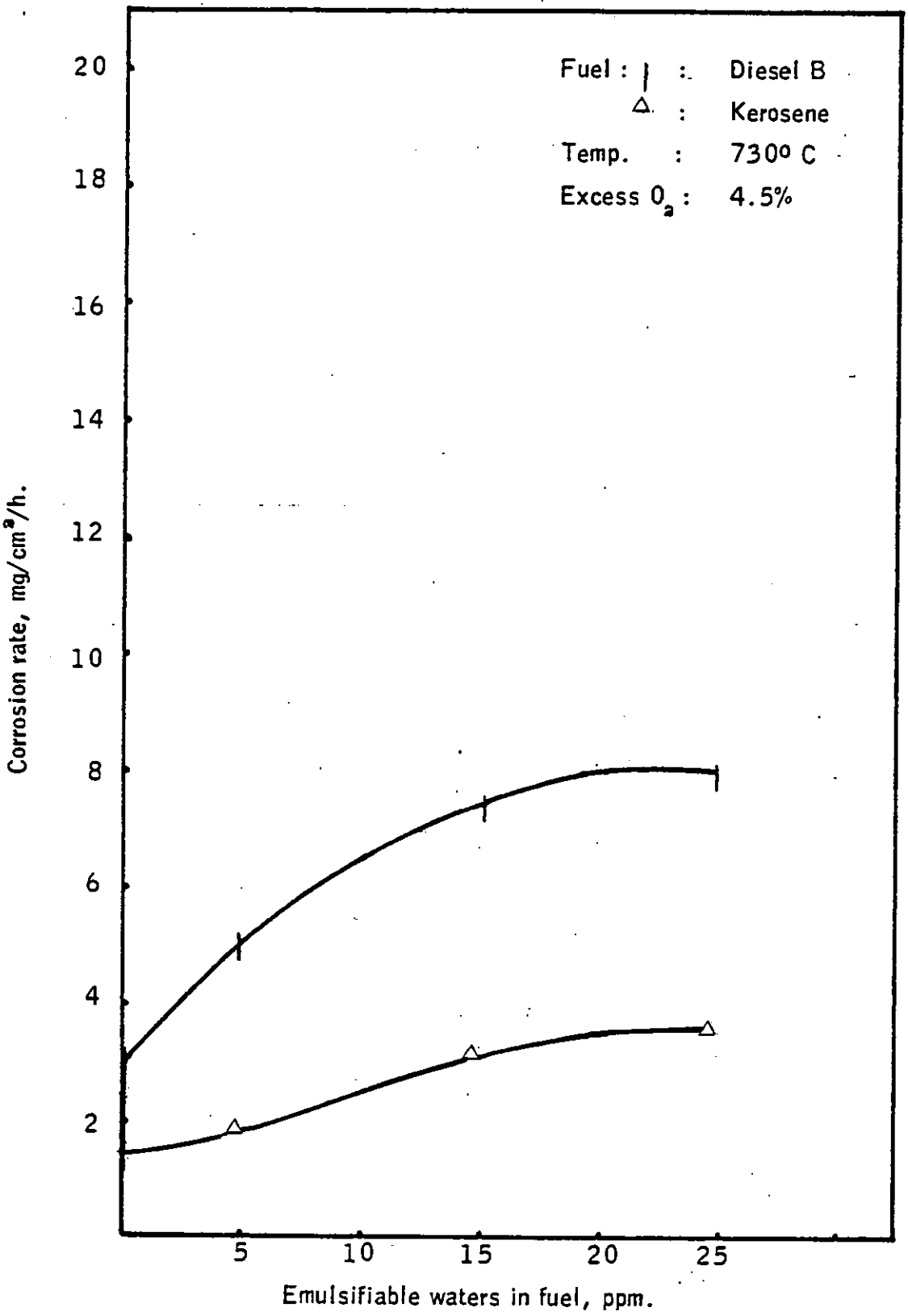

Fig. 6(30) Relation of Corrosion rate of mild steel to emulsification of oil.

TABLE 6(6) CORROSION RATE OF DIFFERENT ALLOYS AFTER EXPOSING IN COMBUSTION GASES FOR 20 HOURS USING KEROSENE.

Explanatory diagram of selection of concentrations.

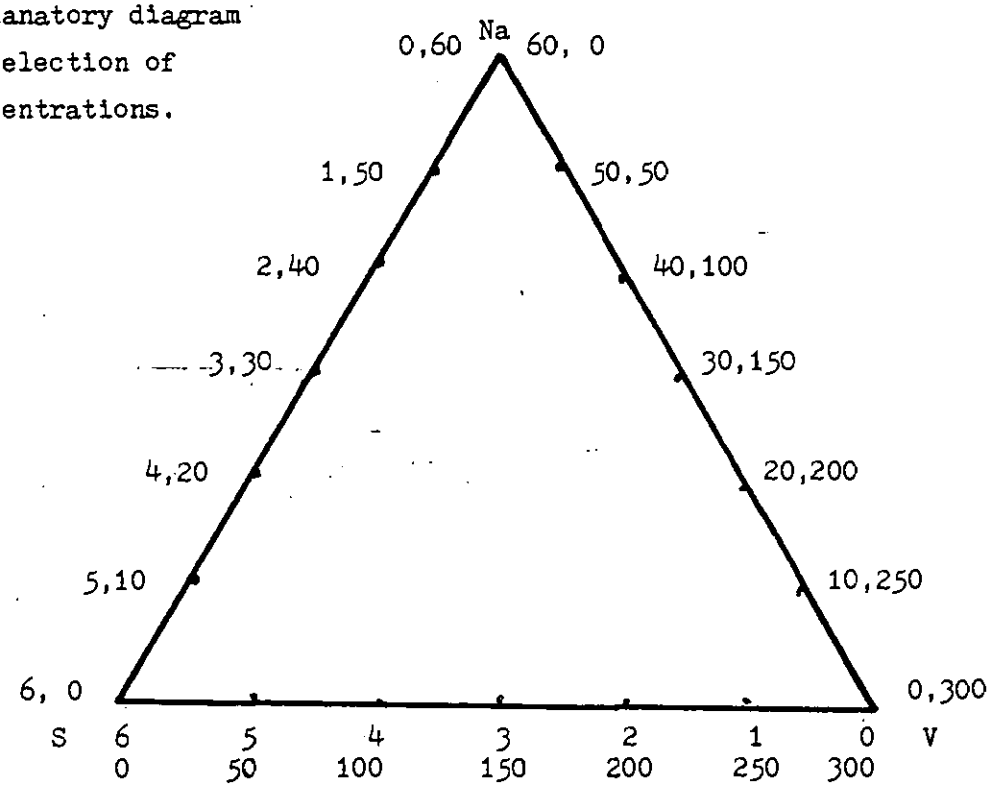

Impurities added, ppm			Corrosion rate, mg/cm^2/h			
Na	S	V	Mild Steel	SS 347	N105	IN657
0	0	0	4.5	1.5	0.8	1.1
60	0	0	11.0	1.8	0.9	2.5
0	6	0	13.0	2.0	0.9	2.8
0	0	300	11.0	2.1	0.9	2.9
60	6	0	18.5	2.5	1.2	3.0
0	6	300	20.5	2.5	1.1	3.5
60	0	300	15.5	2.4	1.2	2.6
60	6	300	24.0	3.0	1.5	4.0

TABLE 6(7) COMPOSITION OF ALLOYS TESTED.

	Mild Steel.	S.S. 347.	Nimonic 90	Nimonic 105	IN657
C	0.065	0.045	0.085	0.13	0.10
Si	0.012	0.57	0.05	0.21	0.50
Mn	0.318	1.60	0.08	0.06	0.30
Cr	0.044	17.68	19.40	14.90	48.00
Ni	0.032	9.15	59.32	52.29	Bal.
Mo	0.017	-	-	5.0	-
S	0.044	0.003	0.003	0.004	-
P	0.008	0.032	-	-	-
Ti	0.013	-	2.40	1.30	-
Nb	0.018	0.77	-	-	4.10
Cu	0.092	-	0.05	0.06	
Fe	Bal.	70.15	0.93	0.58	1.00
Al	0.039	-	1.43	4.63	-
Co	-	-	16.00	19.8	-
Zr	0.005	-	0.055	0.095	-
Pb ppm	-	-	1.9	0.8	-
Mg	-	-	-	-	-
B ppm	-	-	40	51	-
Bi ppm	-	-	0.1	.1	-
Ag ppm	-	-	0.2	0.1	-
V	0.005	-	-	-	-
Sn	0.007	-	-	-	-
Tungsten	0.025	-	-	-	-
Nitrogen.	-	-	-	-	0.16

TABLE 6 (8) MEASUREMENT OF VHN (Vickers Hardness Numbers) OF MATERIALS USED BEFORE AND AFTER EXPOSURE IN HOT COMBUSTION GASES (By Vickers Pyramid Hardness testing machine load 20 Kilos.).

MATERIALS	VHN Before Exposure	VHN After 5 hours Exposure
Mild Steel	220, 208 210, 218 211, 214 } **213**	121, 119 118, 127 122, 126 } **122**
Stainless Steel Type 347.	187, 201 199, 182 191, 189 } **191**	200, 207 204, 202 205, 203 } **203**
N90	355, 360 351, 358 355, 359 } **356**	361, 359 366, 365 363, 366 } **363**
N105	362, 358 360, 365 359, 366 } **361**	367, 370 368, 366 369, 367 } **368**
IN657	234, 232 228, 239 235, 230 } **233**	194, 211 208, 195 210, 199 } **203**

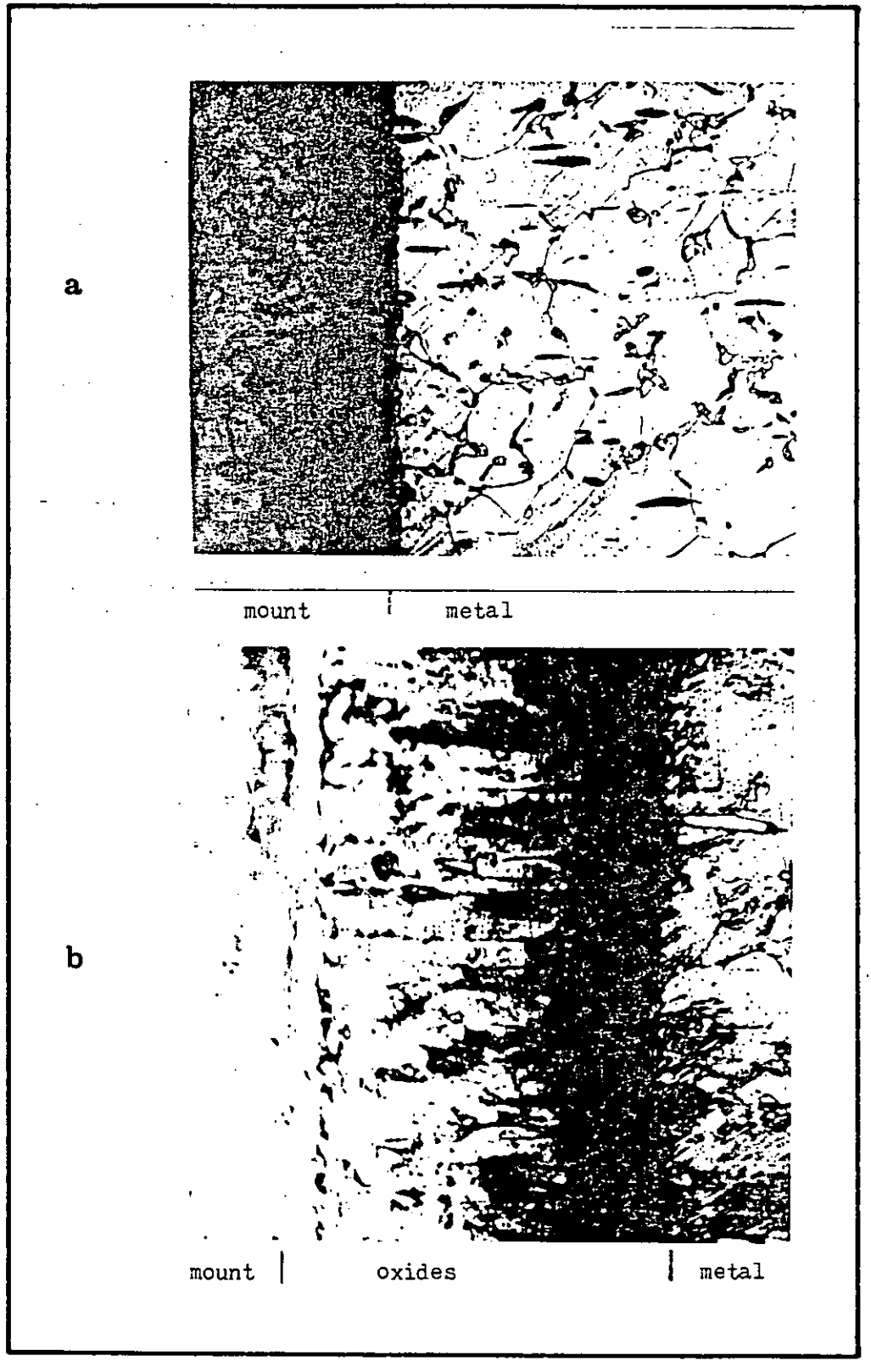

Figure 6(31). Micrograph of mild steel (x 400, etched)

a) before exposure in hot gas

b) after exposure in hot gas for five hours.

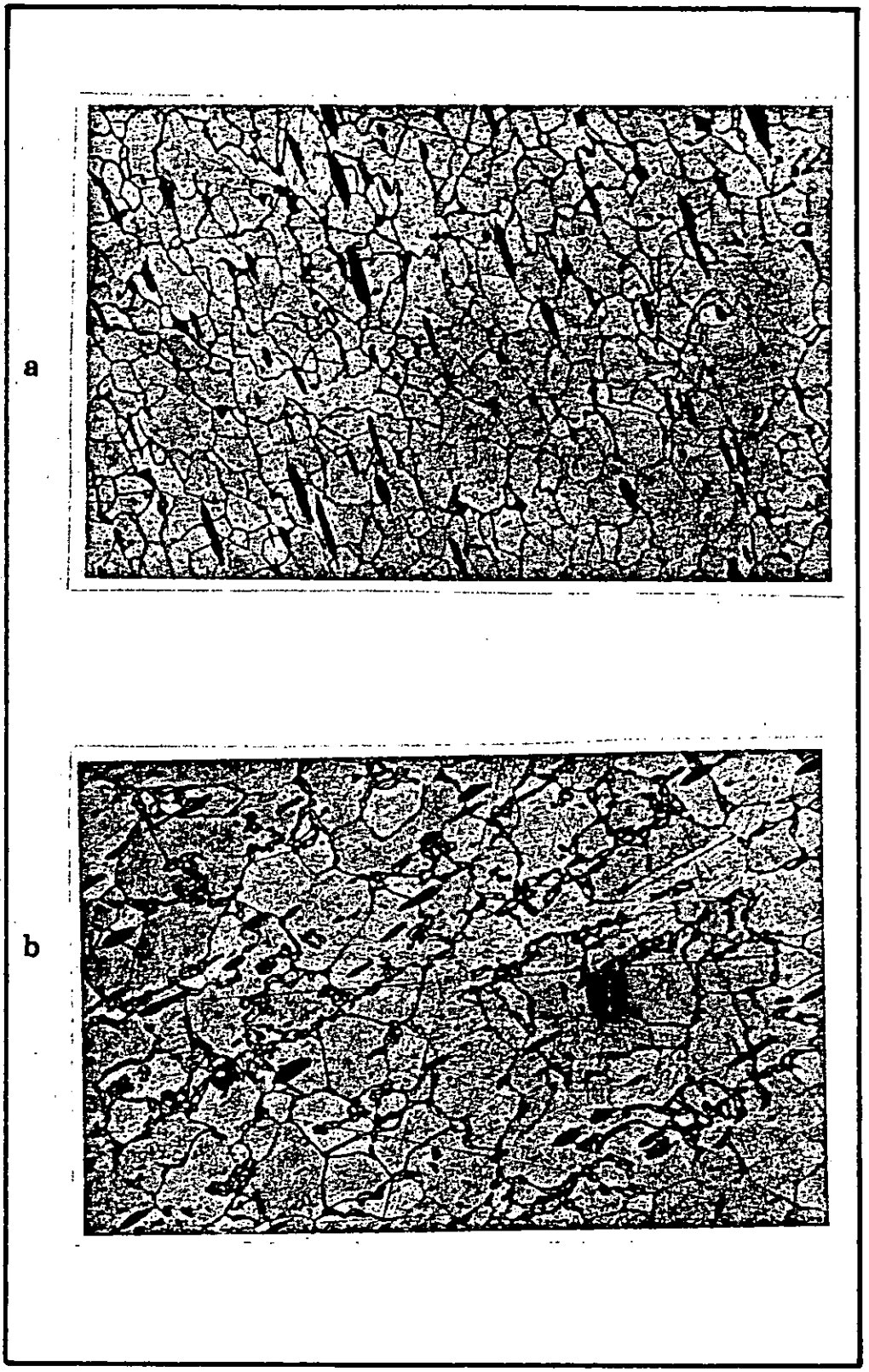

Figure 6(32). Micrograph of mild steel (x 400, etched)

a) structure before exposure in hot gas

b) structure after five hours exposure in hot gas.

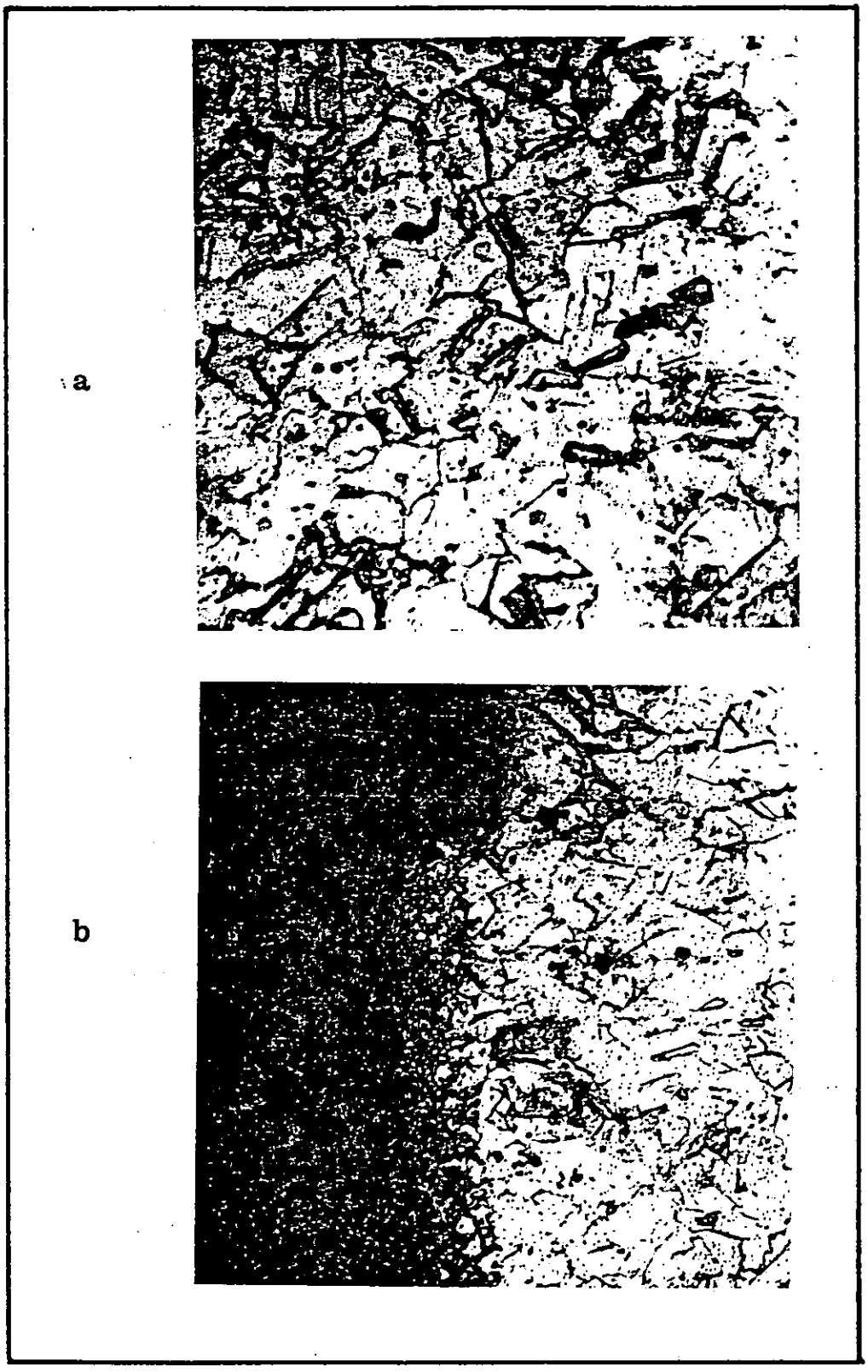

Figure 6(33). Micrograph of stainless steel type 347 (x 400 etched)
a) before exposure
b) after five hours exposure.

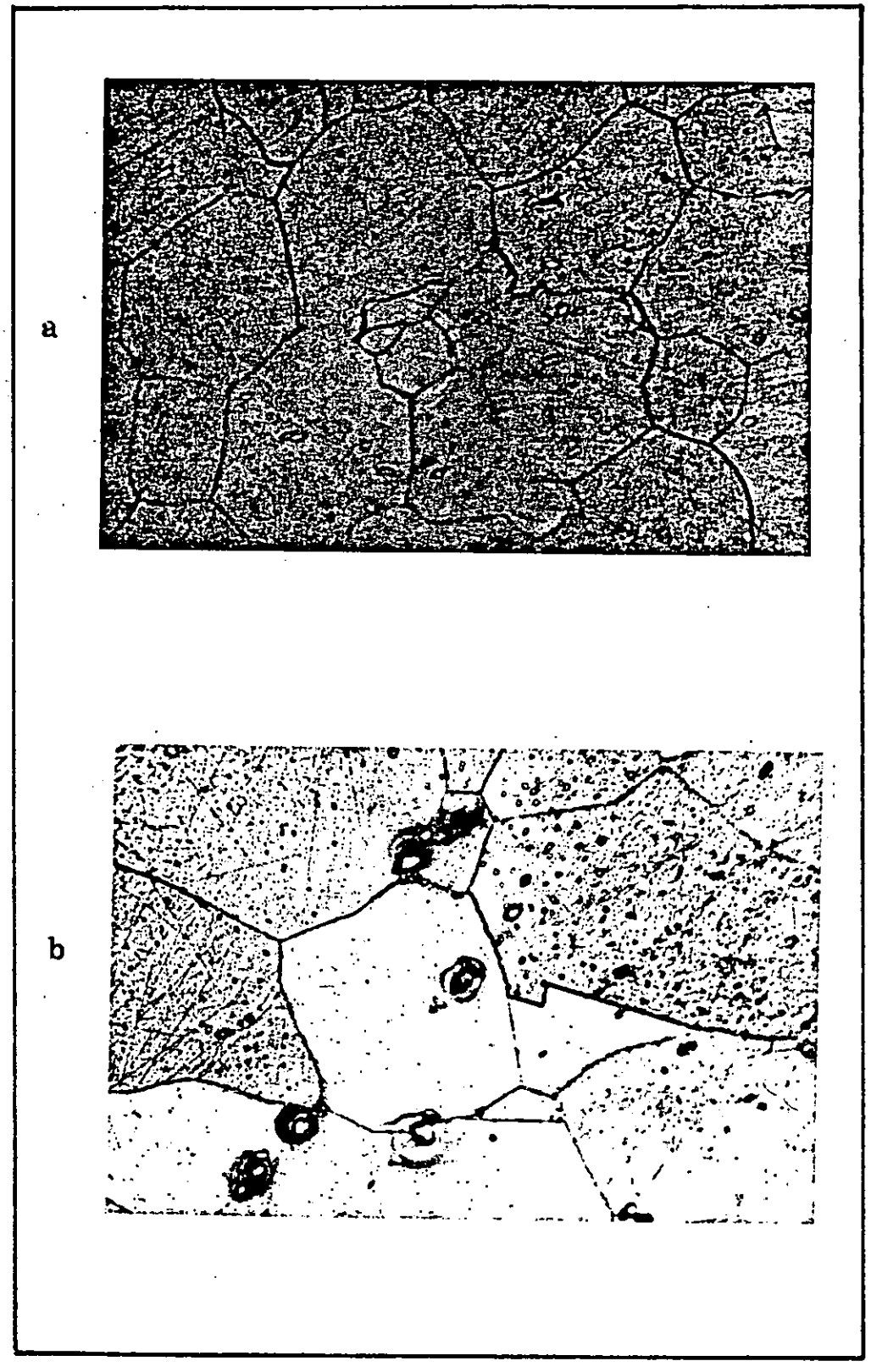

Figure 6(34). Micrograph of Nimonic N90 (x 400 etched)

a) before exposure

b) after five hours exposure

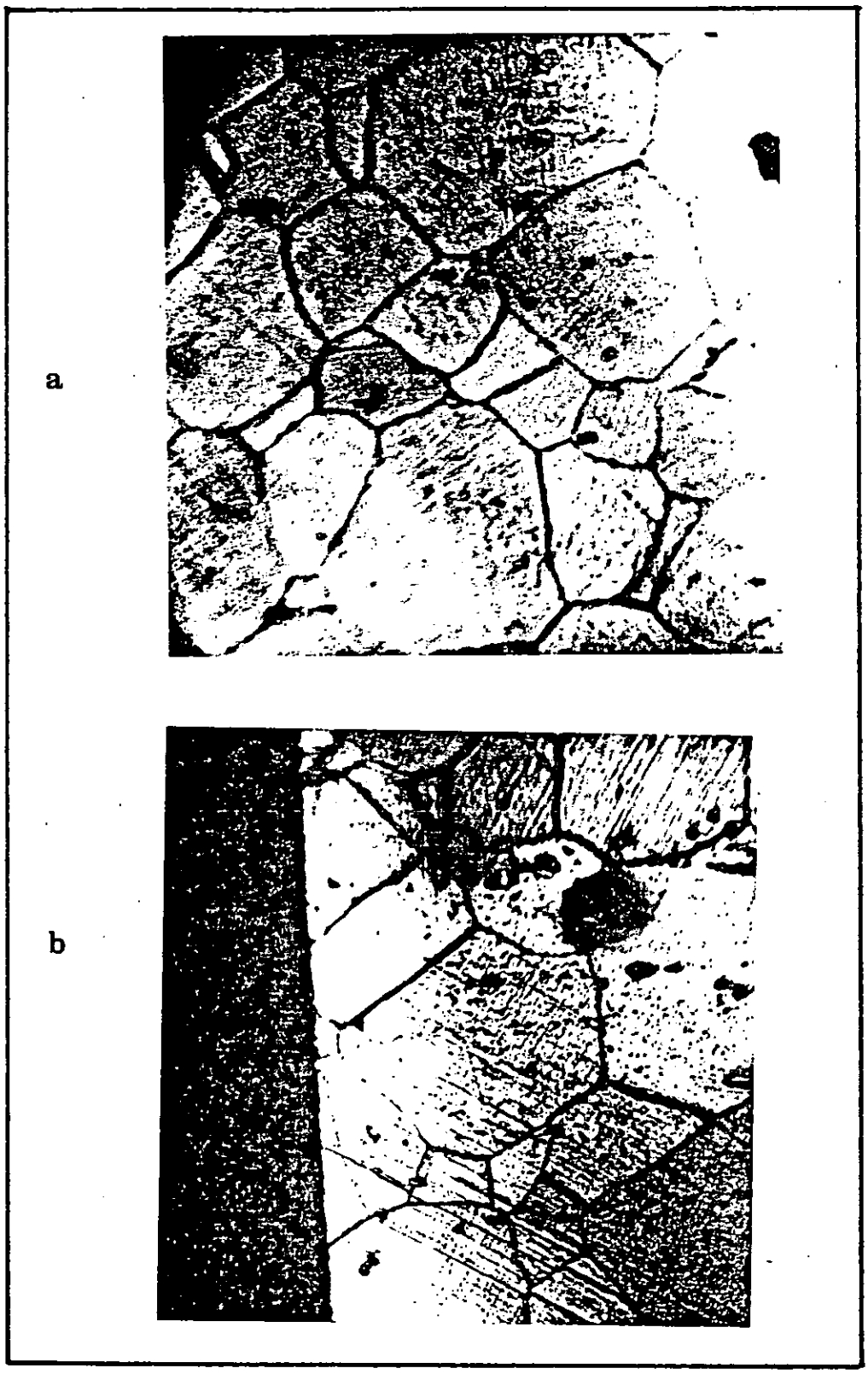

Figure 6(35). Micrograph of Nimonic N105 (x 400 etched)

a) before exposure

b) after five hours exposure.

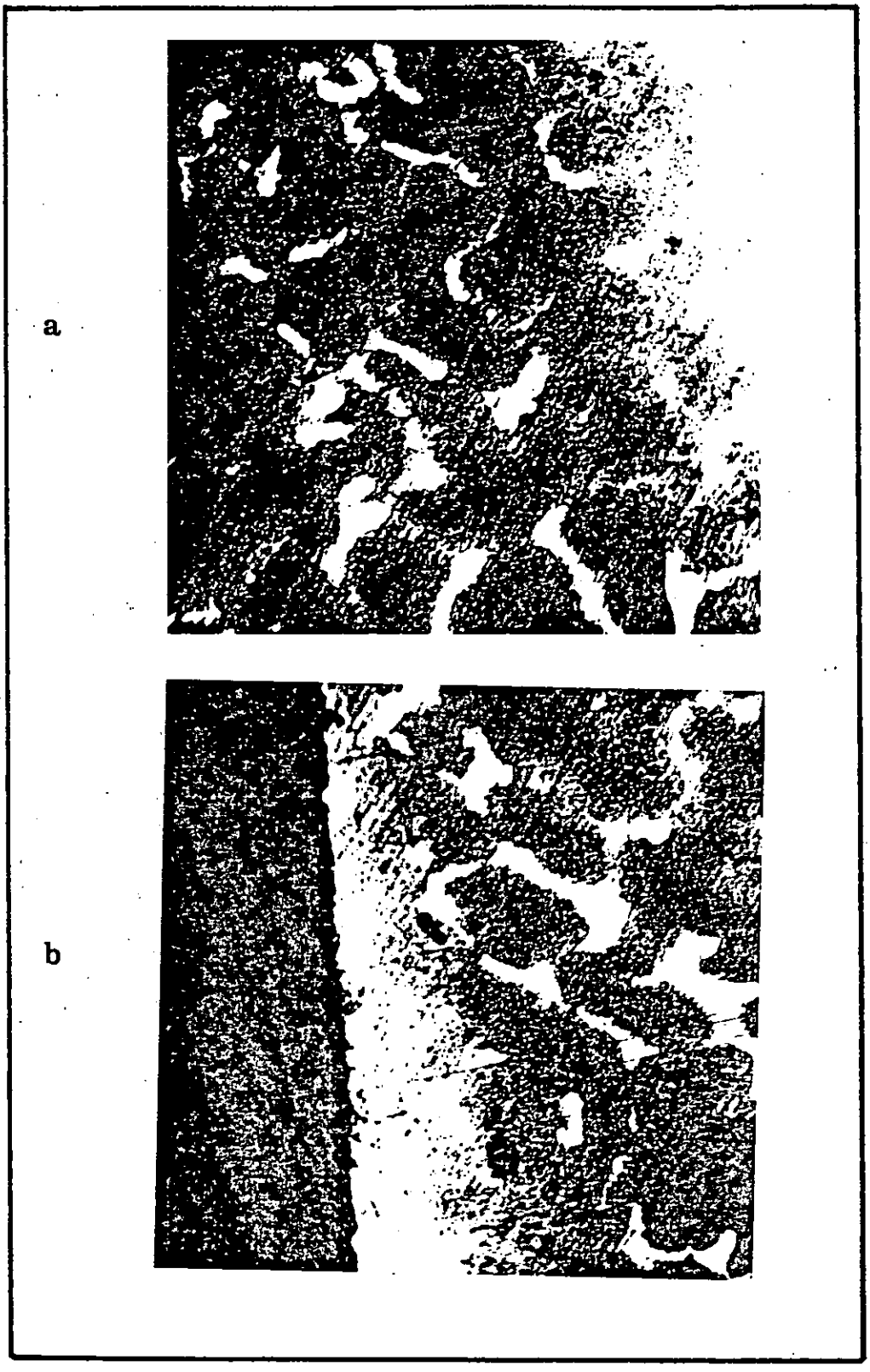

Figure 6(36). Micrograph of IN657 (x 400 etched in acid ferric chloride for ten minutes)

a) before exposure

b) after five hours exposure.

TABLE 6(9) IDENTIFICATION OF OXIDE LAYERS BY X-RAY DIFFRACTION.

Time of exposure : 3 hours.
Temperature : 730° C.
Material : Mild steel.
P : Powder photograph.
D : Diffractometer trace.
O : Outside layer.
I : Inside i.e. second layer.
A : Additive (Ferrocene)

Sample No.	Expt. No.	X-Ray Method	Oxide layer	Fuel	Oxides * + identified
1/1	K1Ø	P	0	Kerosene (no sulphur)	Fe_3O_4, trace FeO
1/2	D1Ø	P	0	Diesel B(DB) (1% S).	FeO, little Fe_3O_4
1/3	D1D	P	0	DB + 5% S	Fe_3O_4, FeO
1/4	D2E	P	0	DB + 25 ppmNa	Fe_3O_4, FeO
1/5	D3E	P	0	DB +250ppm V	Fe_3O_4, FeO
1/5	D3E	D	I	DB +250ppm V	Fe,FeO,Fe_3O_4
1/6	D9E	P	0	DB+5%S+25ppmNa	FeO
1/7	D13E	P	0	DB+5%S+250ppmV	FeO
1/7	D13E	D	I	DB+5%S+250ppmV	Fe, FeO
1/8	D18E	P	0	DB+25ppm Na + 250ppm V	Fe_3O_4
1/8	D18E	D	I	DB+25ppm Na + 250ppm V	Fe_3O_4, Fe
1/9	D14OE	P	0	DB+25Na + 250V + 5%S	Fe_3O_4, FeO
1/9	D14OE	D	I	DB+25Na + 250V + 5%S	FeO, Fe, tr.Fe_3O_4
1/10	D1Ø/A	P	0	DB + A	Fe_3O_4, FeO
1/11	D1D/A	P	0	DB + 5%S + A	Fe_3O_4, tr.FeO

* No order of occurrence can be implied from a single entry.

\+ any oxide present at 2% could not be identified.

TABLE 6(10) - IDENTIFICATION OF OXIDE LAYERS BY X-RAY DIFFRACTION.

Sample No.	Expt. No.	Fuel.	Material	Time of exposure h.	Temp. °C.	X-Ray method	Oxides Identified.
2/1	K101	Kerosene	MS	20	730	P	Fe_3O_4, tr.FeO
2/2	K101	Kerosene	SS347	20	730	D	Fe_2O_3
2/3	K101	Kerosene	N105	20	730	D	.Fe_2O_3, tr.Ni.oxide
2/4	K101	Kerosene	IN657	20	730	D	.Fe_2O_3, tr.Cr.oxide
2/5	K108	K+6%S+300V	MS	20	730	P	FeO, Fe_3O_4
2/6	K108	K+6%S+300V	SS347	20	730	D	.Fe_2O_3, FeO
2/7	K108	K+6%S+300V	N105	20	730	D	Fe_2O_3, tr.NiO
2/8	K108	K+6%S+300V	IN657	20	730	D	.Fe_2O_3 (may contain Cr_2O_3)
2/9	K108	K+6%S+300V	IN657	20	200	P	Fe_2O_3, tr.$VOSO_4$
2/10	K114	K+60Na+6S+300V	MS	20	730	P	FeO, tr.Na_2SO_4,tr.Fe_3O_4
2/11	K114	K+60Na+6S+300V	SS347	20	730	D	.Fe_2O_3, FeO, tr.Na_2SO_4
2/12	K114	K+60Na+6S+300V	N105	20	730	D	Fe_2O_3, tr.Na_2SO_4
2/13	K114	K+60Na+6S+300V	IN657	20	730	D	Fe_2O_3, tr.Na_2VO_3,tr.Na_2SO_4
2/14	K114	K+60Na+6S+300V	IN657	20	200	P	$(Mg_{0.59}Al_{0.3})(Fe^{3+}_{3.56}Al_{0.44})(SO_4)_6(OH)_2.7H_2O$,tr.$Na_2VO_3$
2/15	K122	K + S + V + AX *	IN657	20	200	P	$Na_2V(SO_4)_2$ $4H_2O$, tr.Fe_2O_3
2/16	Mixed	Mixed.	IN657	60	730	D	Fe_2O_3, FeO

* AX = additive (Econsol D)

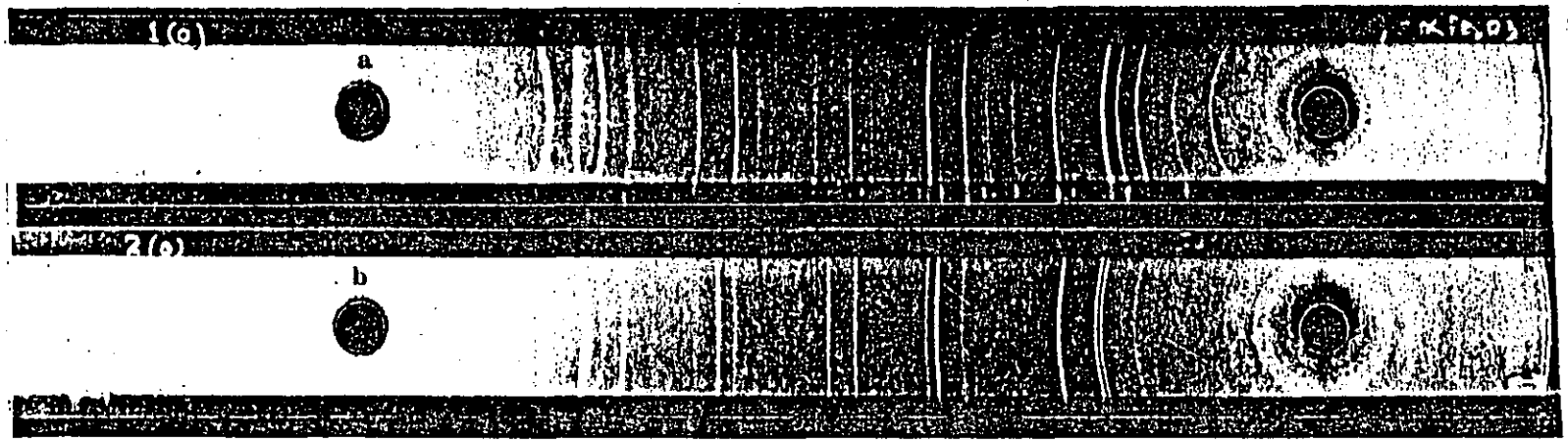

Figure 6 (37) X-Ray Powder Photograph (19 cm camera, Co Kα radiation) of outer oxide layer formed on mild steel after exposing for 3 hours at 730 C in combustion gases, when using - (a) Kerosene, (b) Diesel B.

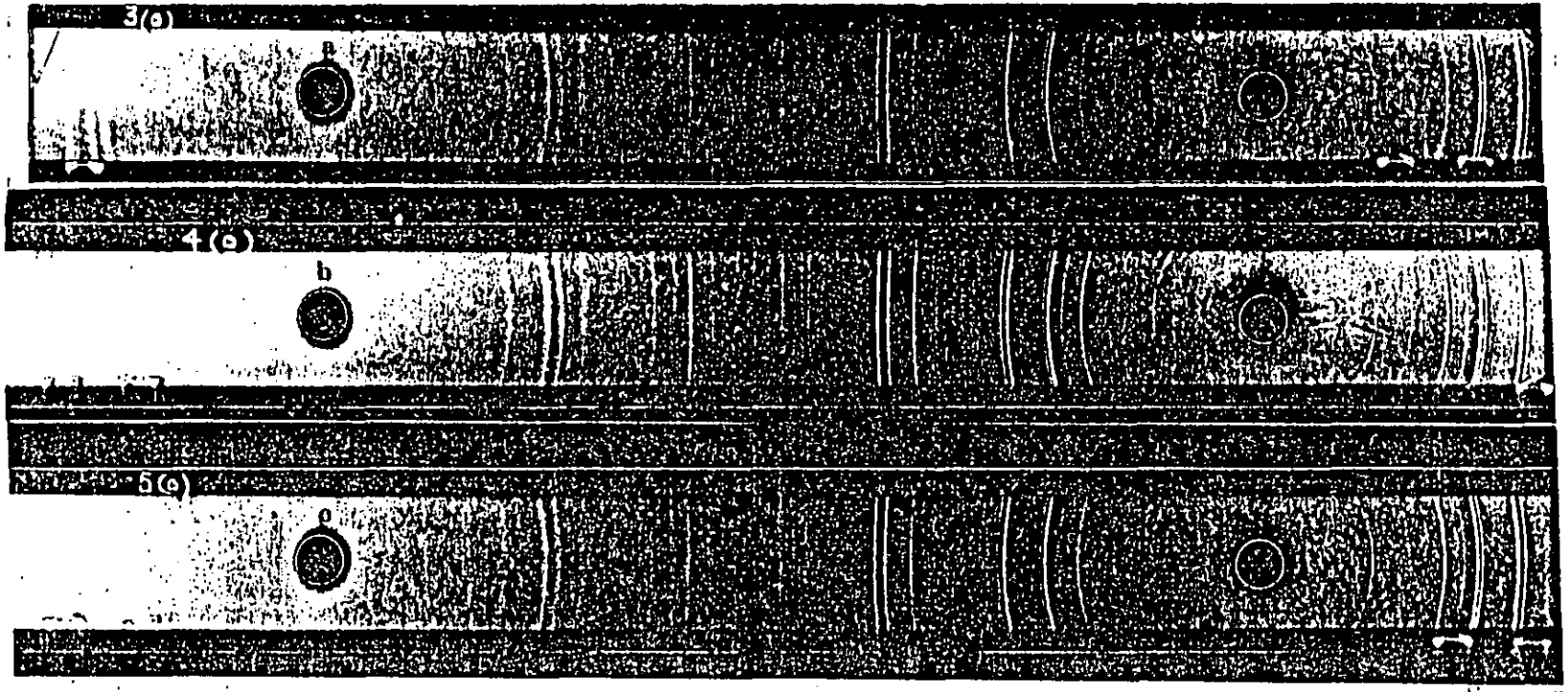

Figure 6 (38) X-Ray Powder Photograph (19 cm camera, Co Kα radiation) of outer oxide layer formed on mild steel after exposing for 3 hours at 730° C in combustion gases, when using, (a) Diesel B with 5% sulphur, (b) Diesel B with 25 ppm sodium, (c) Diesel B with 250 ppm vanadium.

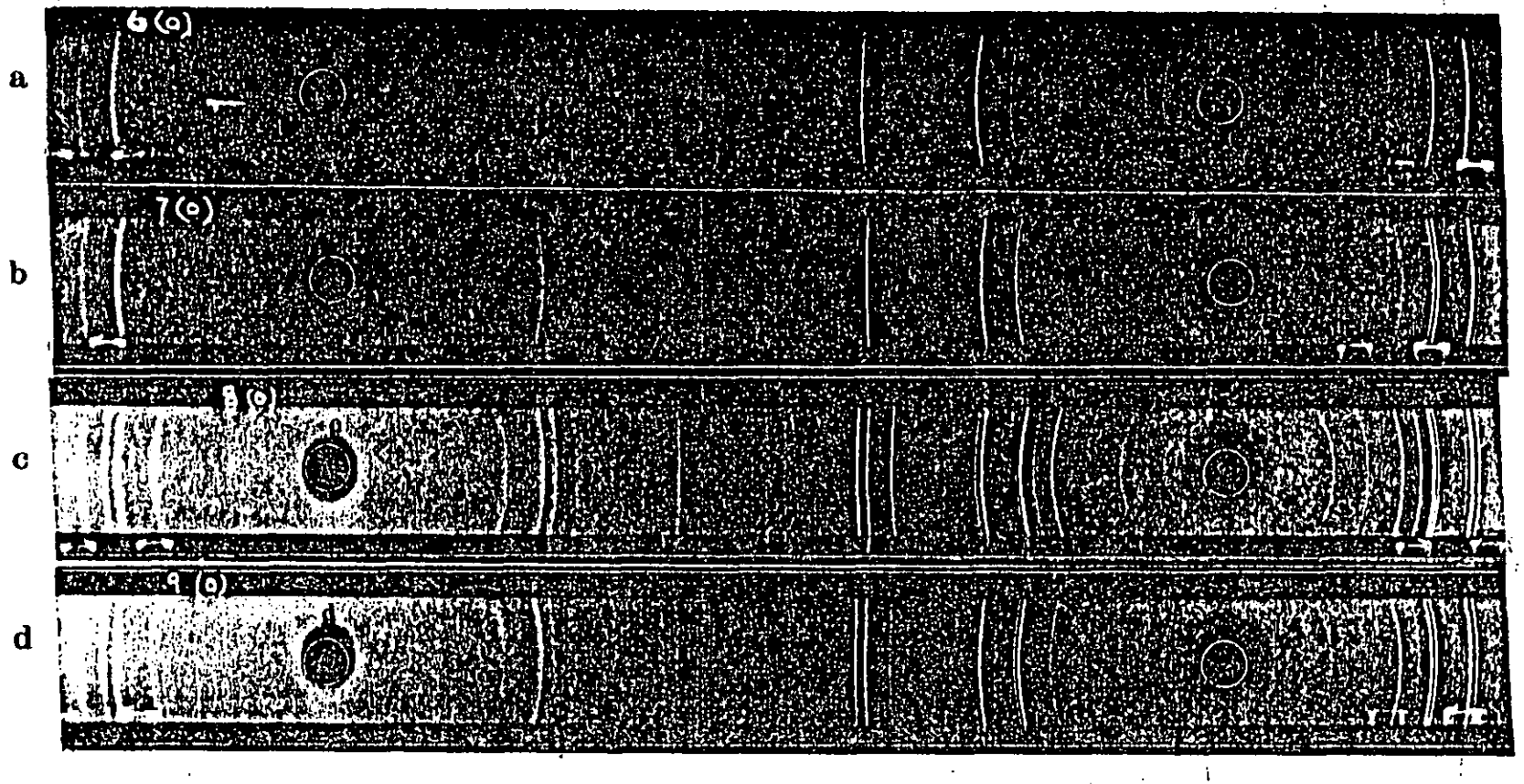

Figure 6 (39) X-Ray Powder Photograph (19 cm camera, Co Kα radiation) of outer oxide layer formed on mild steel after exposing for 3 hours at 730° C in combustion gases,
- when using (a) Diesel B with 25 ppm sodium and 5% sulphur. (b) Diesel B with 5% sulphur and 250 ppm vanadium. (c) Diesel B with 25 ppm sodium and 250 ppm vanadium. (d) Diesel B with 25 ppm sodium, 5% sulphur and 250 ppm vanadium.

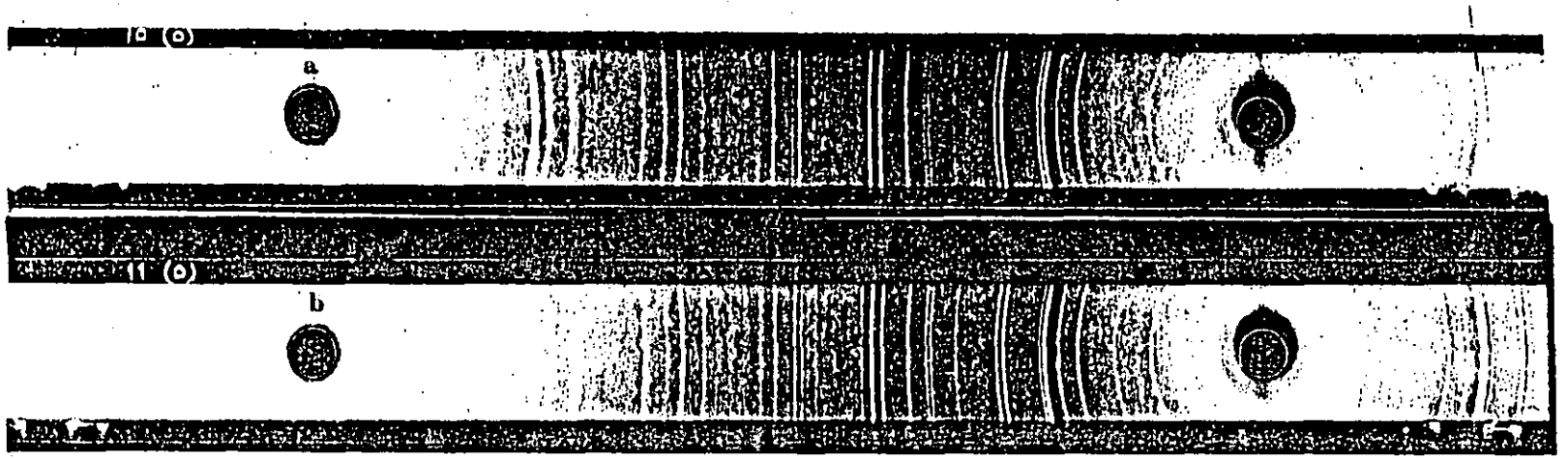

Figure 6 (40) X-Ray Powder Photograph (19 cm camera, Co Kα radiation) of outer oxide layer formed on mild steel after exposing for 3 hours in combustion gases, - when using (a) Diesel B with 0.1% Ferrocene. (b) Diesel B with 5% sulphur and 0.1% Ferrocene.

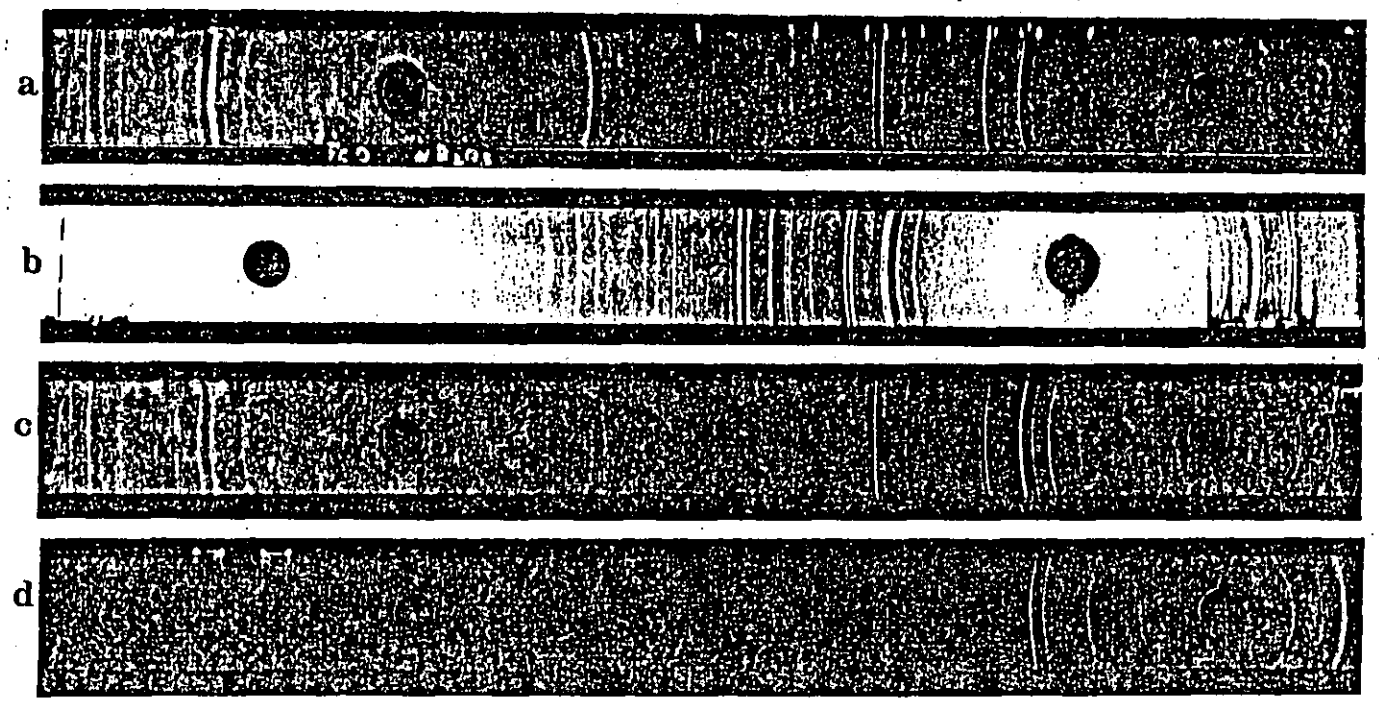

Figure 6 (41) X-Ray Powder Photograph (19 cm camera, Co Kα radiation) of outer oxide layer formed on mild steel after exposing for 20 hours at 730° C in combustion gases, - when using, (a) Kerosene, (b) Kerosene with 6% sulphur and 300 ppm vanadium, (c) Kerosene with 60 ppm sodium, 6% sulphur and 300 ppm vanadium, (d) Mixed slag deposits.

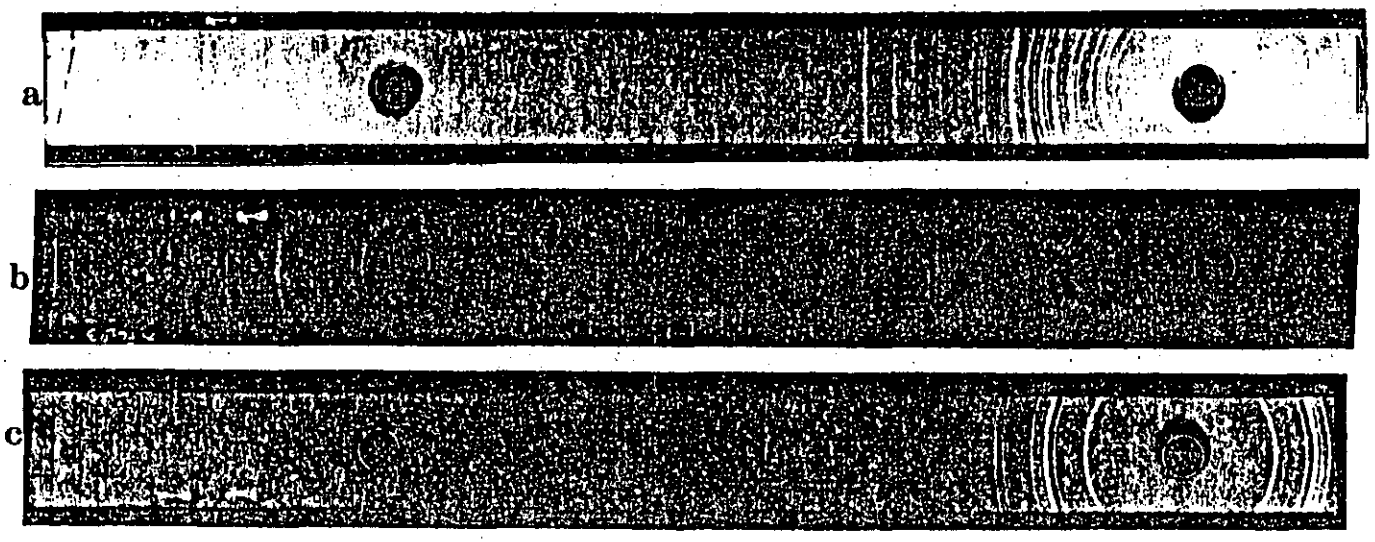

Figure 6 (42) X-Ray Powder Photograph (19 cm Camera, Co Kα radiation) of oxide layer formed on IN657 after exposing for 20 hours at 200° C in combustion gases, - when using (a) Kerosene with 6% and 300 ppm vanadium, (b) Kerosene with 60 ppm sodium, 6% sulphur and 300 ppm vanadium, (c) Kerosene with 6% sulphur, 300 ppm vanadium and 5% Econsol D.

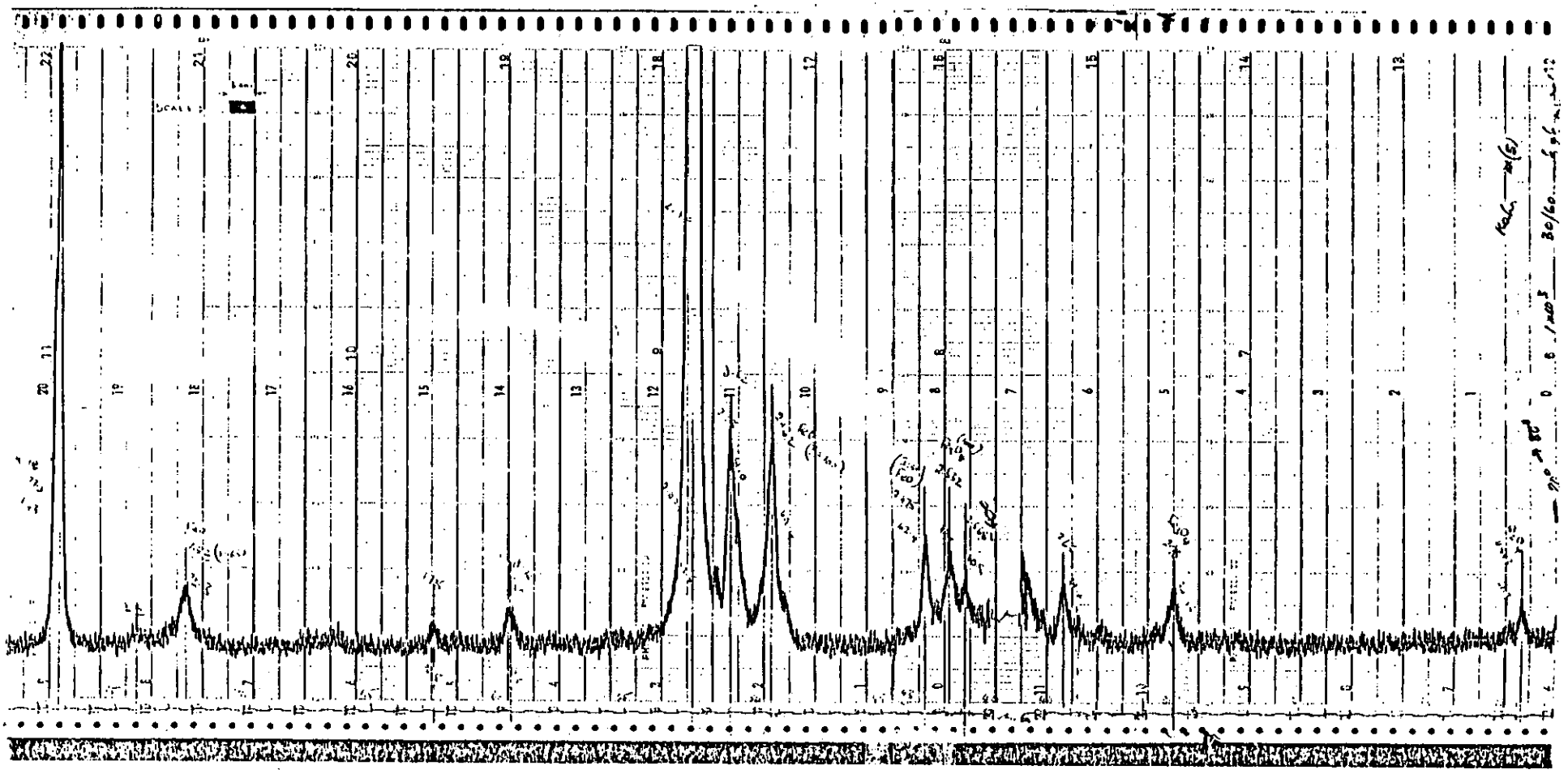

Figure 6 (43) X-Ray Diffractometer trace of the second oxide layer formed on mild steel after exposing for 3 hours at 730° C in combustion gases, - when using Diesel B with 250 ppm vanadium.

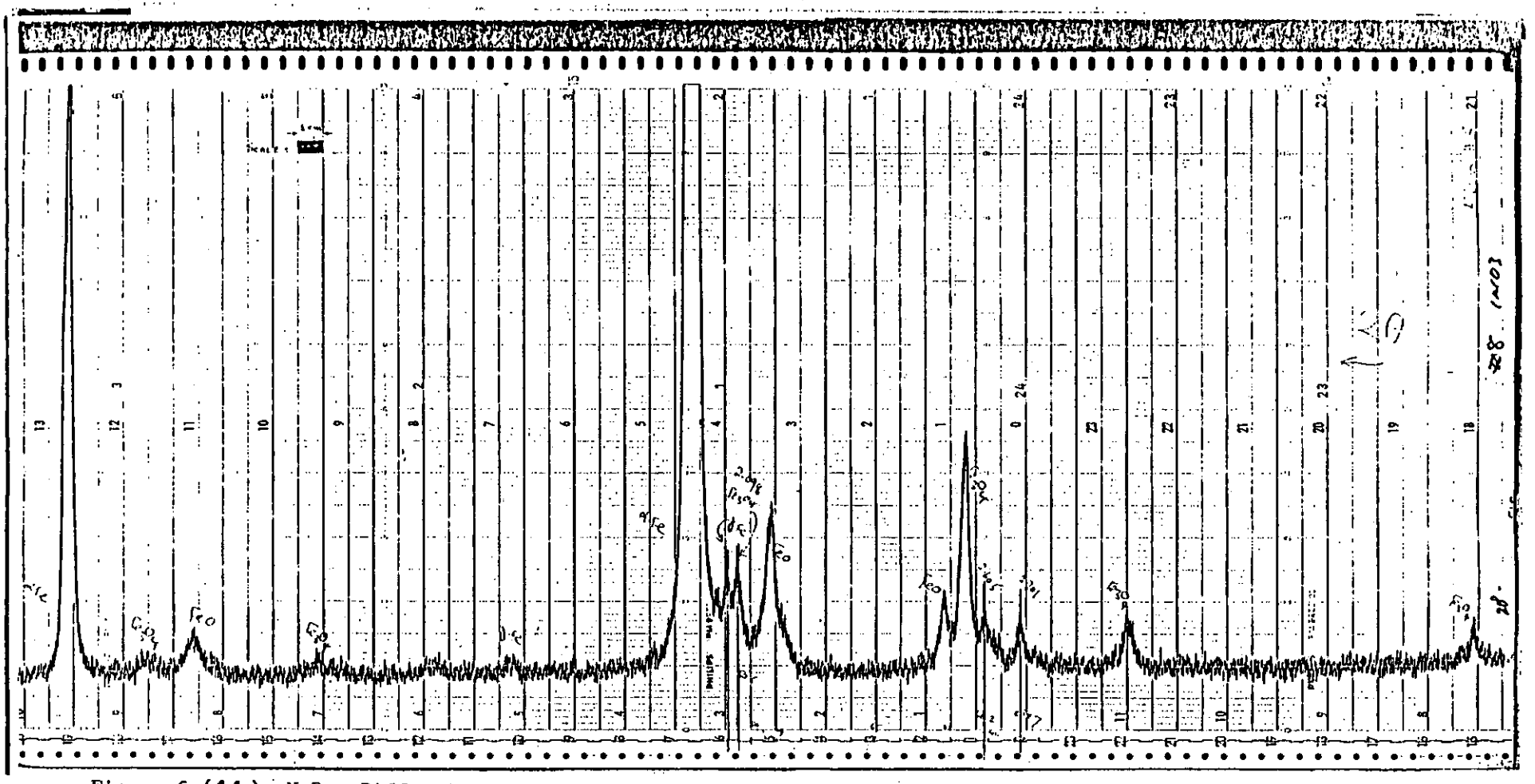

Figure 6 (44) X-Ray Diffractometer trace of the second oxide layer formed on mild steel after exposing for 3 hours at 730° C in combustion gases, - when using Diesel B with 25 ppm sodium and 250 ppm vanadium.

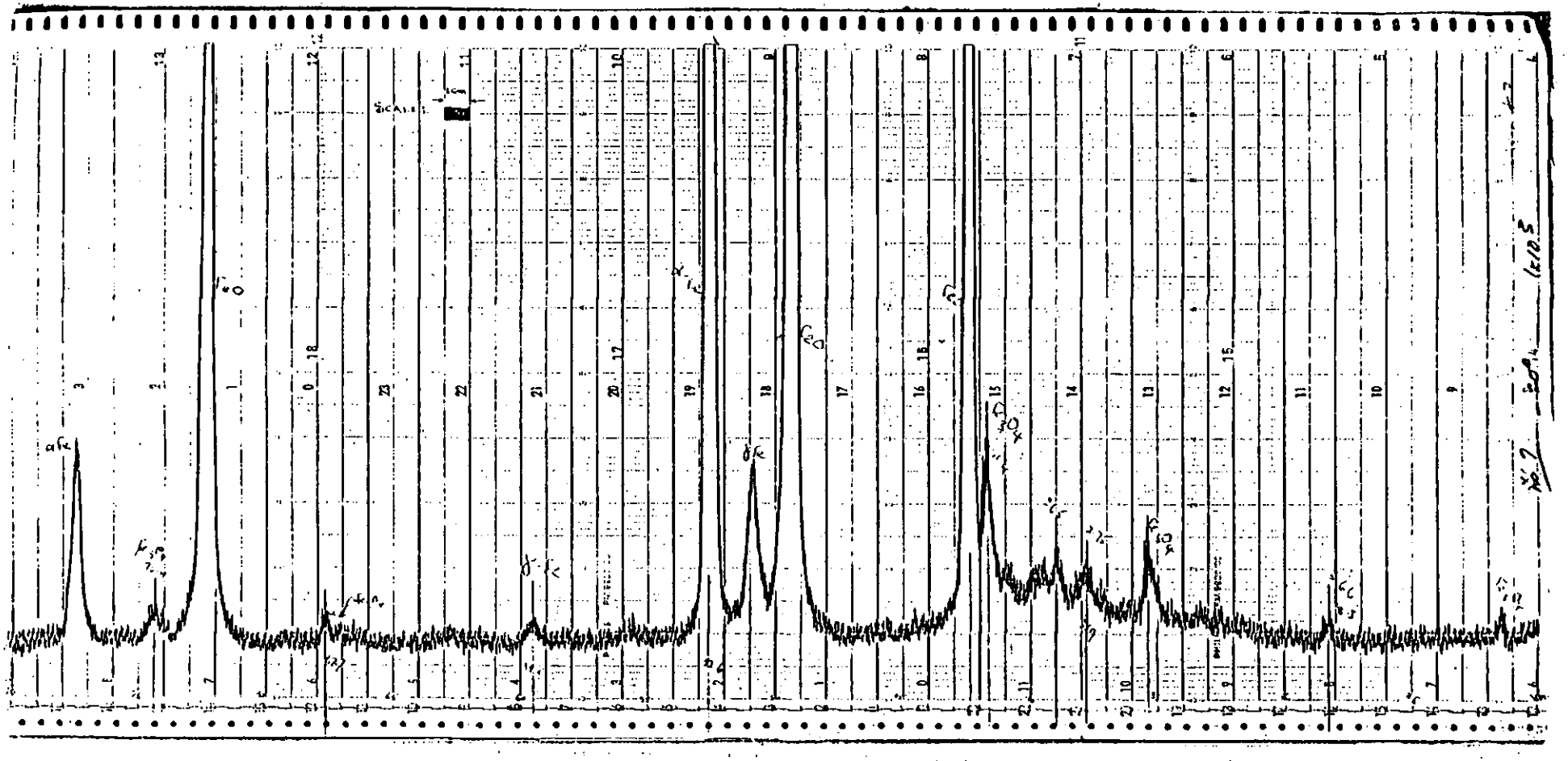

Figure 6 (45) X-Ray Diffractometer trace of the second oxide layer formed on mild steel after exposing for 3 hours at 730° C in combustion gases, - when using Diesel B with 5% sulphur and 250 ppm vanadium.

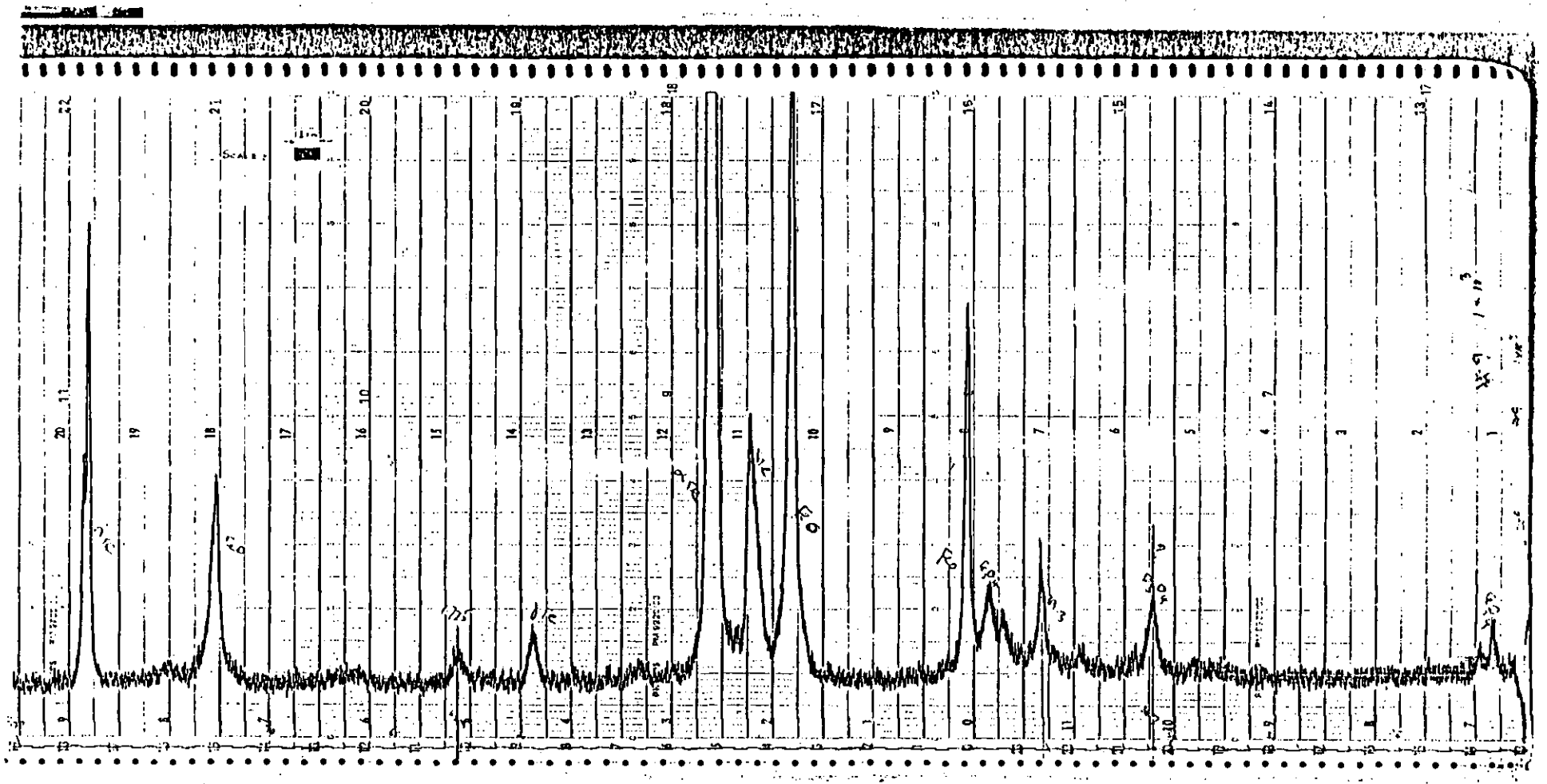

Figure 6(46) X-Ray Diffractometer trace of the second oxide layer formed on mild steel after exposing for 3 hours at 730° C in combustion gases, - when using Diesel B with 25 ppm sodium 5% sulphur and 250 ppm vanadium.

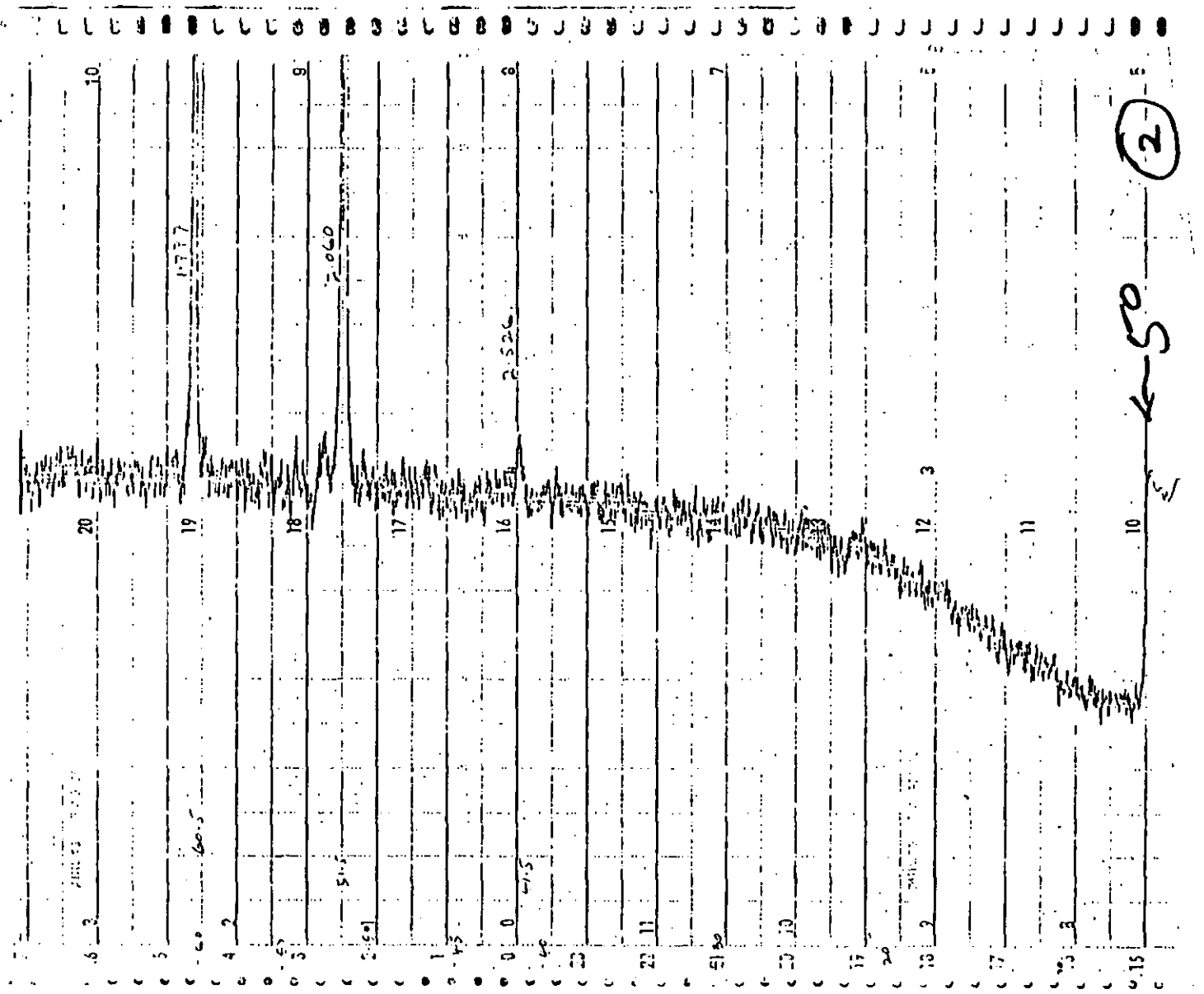

Figure 6 (47) X-Ray Diffractometer trace of the oxide layer formed on Stainless Steel type 347 after exposing for 20 hours at 730° C in combustion gases, – when using Kerosene.

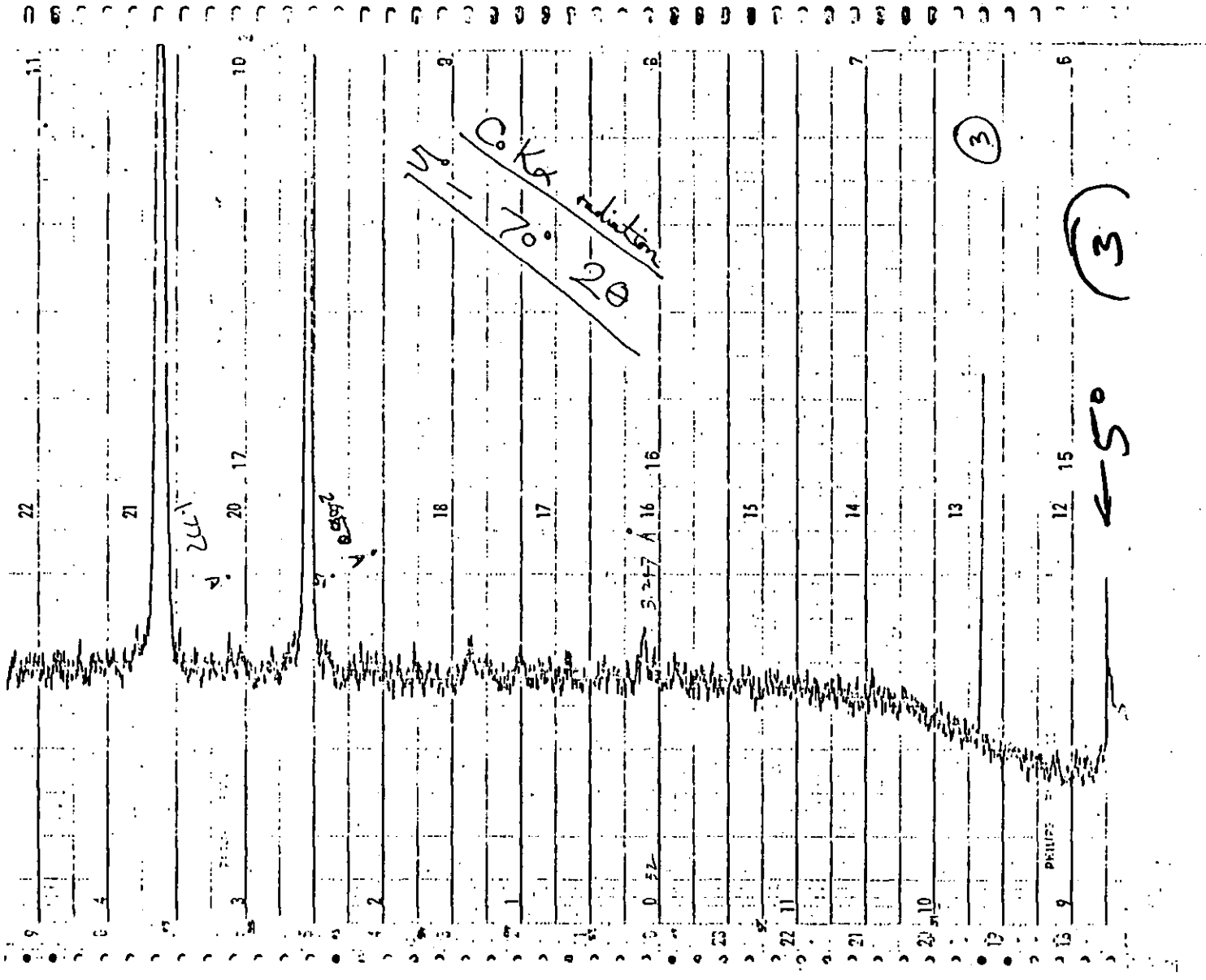

Figure 6 (48) X-Ray Diffractometer trace of the oxide layer formed on N105 after exposing for 20 hours at 730° C in Combustion gases, - when using Kerosene.

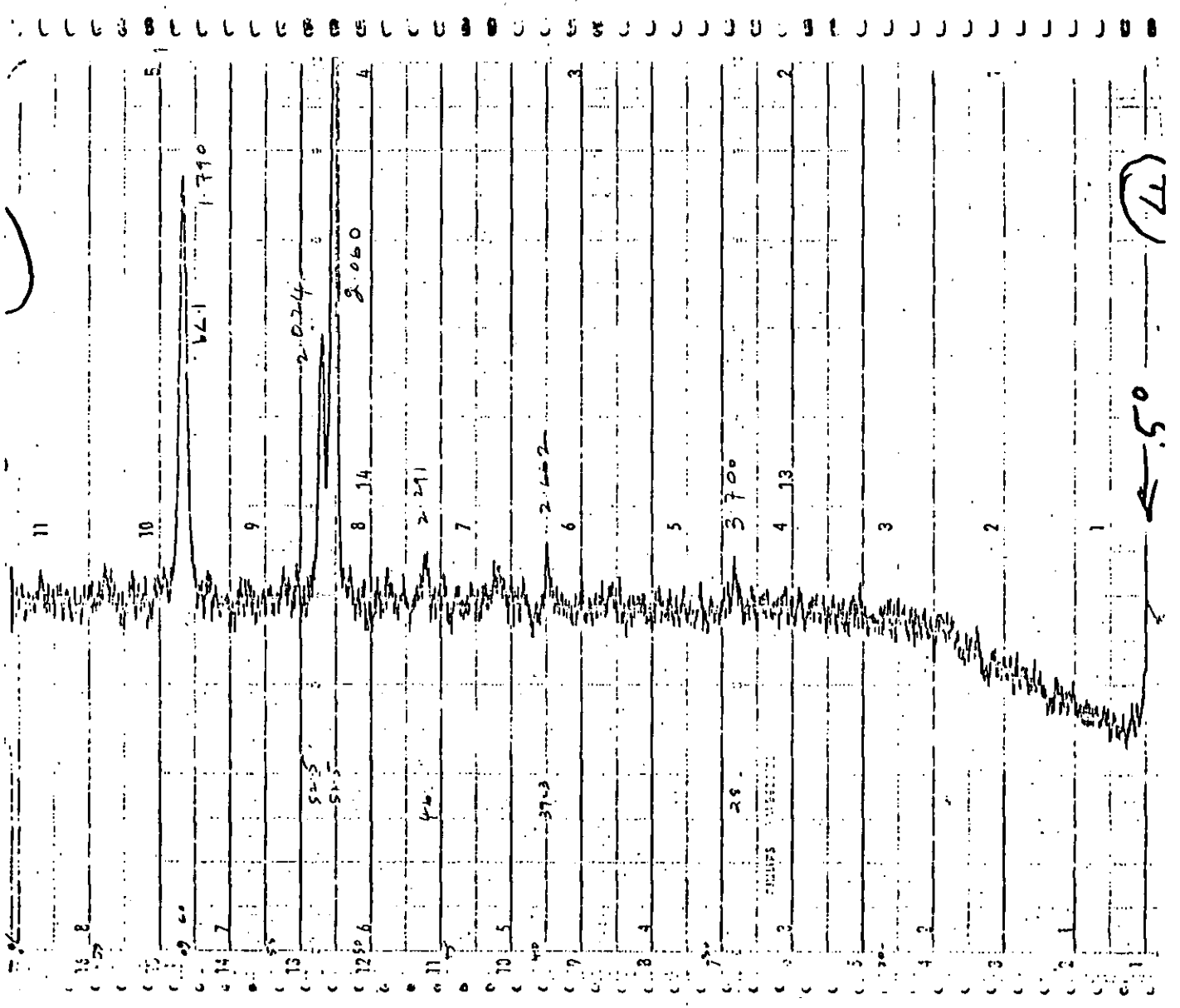

Figure 6 (49) X-Ray Diffractometer trace of the oxide layer formed on IN657 after exposing for 20 hours at 730° C in combustion gases, - when using Kerosene.

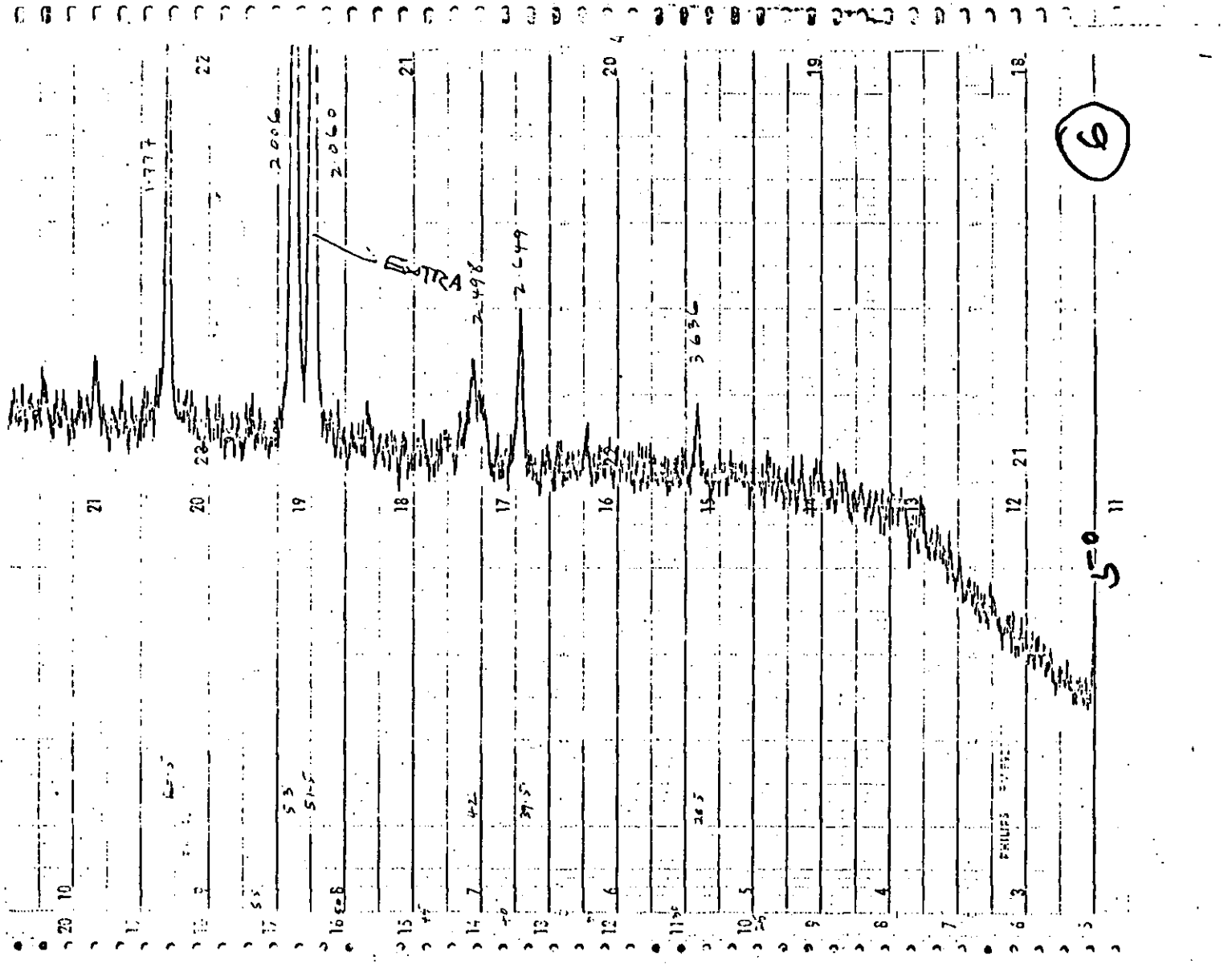

Figure 6 (50) X-Ray Diffractometer trace of the oxide layer formed on stainless steel type 347, after exposing for 20 hours at 730° C in combustion gases, - when using Kerosene with 5% sulphur and 300 ppm vanadium.

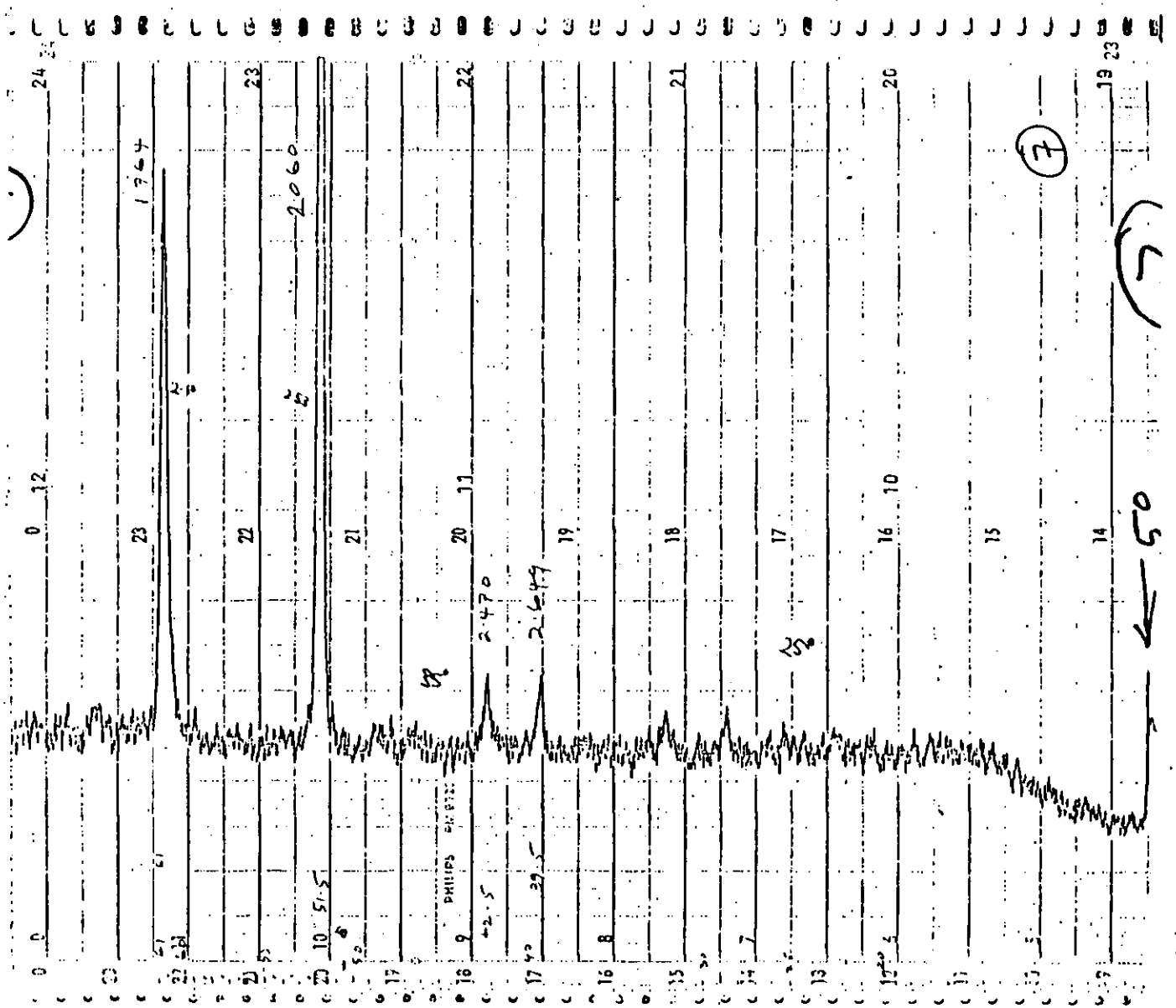

Figure 6 (51) X-Ray Diffractometer trace of the oxide layer formed on N105 after exposing for 20 hours at 730° C in combustion gases, when using Kerosene with 6% sulphur and 300 ppm yanadium.

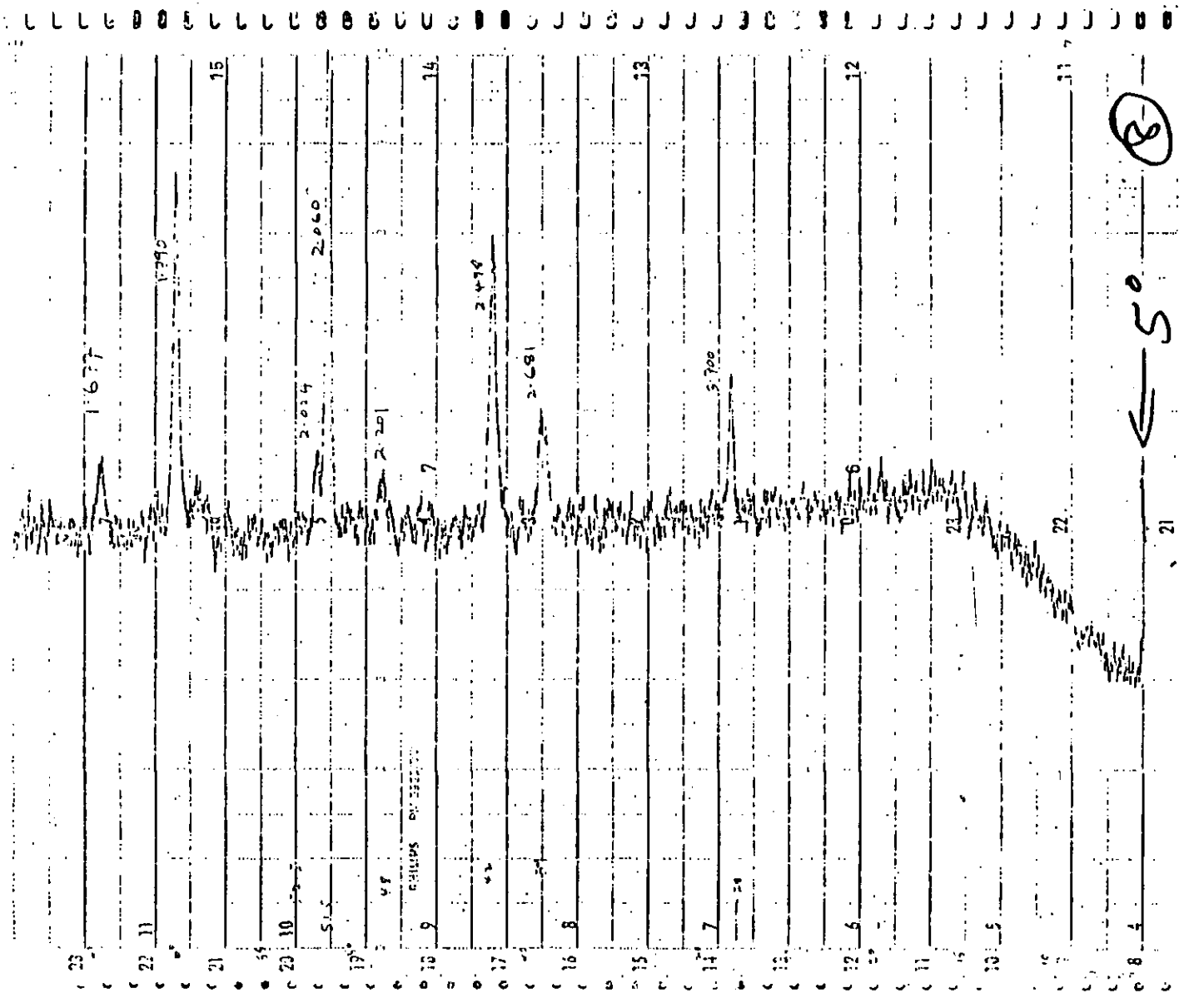

Figure 6 (52) X-Ray Diffractometer trace of the oxide layer formed on IN657 after exposing for 20 hours at 730° C in combustion gases, - when using Kerosene with 6% sulphur and 300 ppm vanadium.

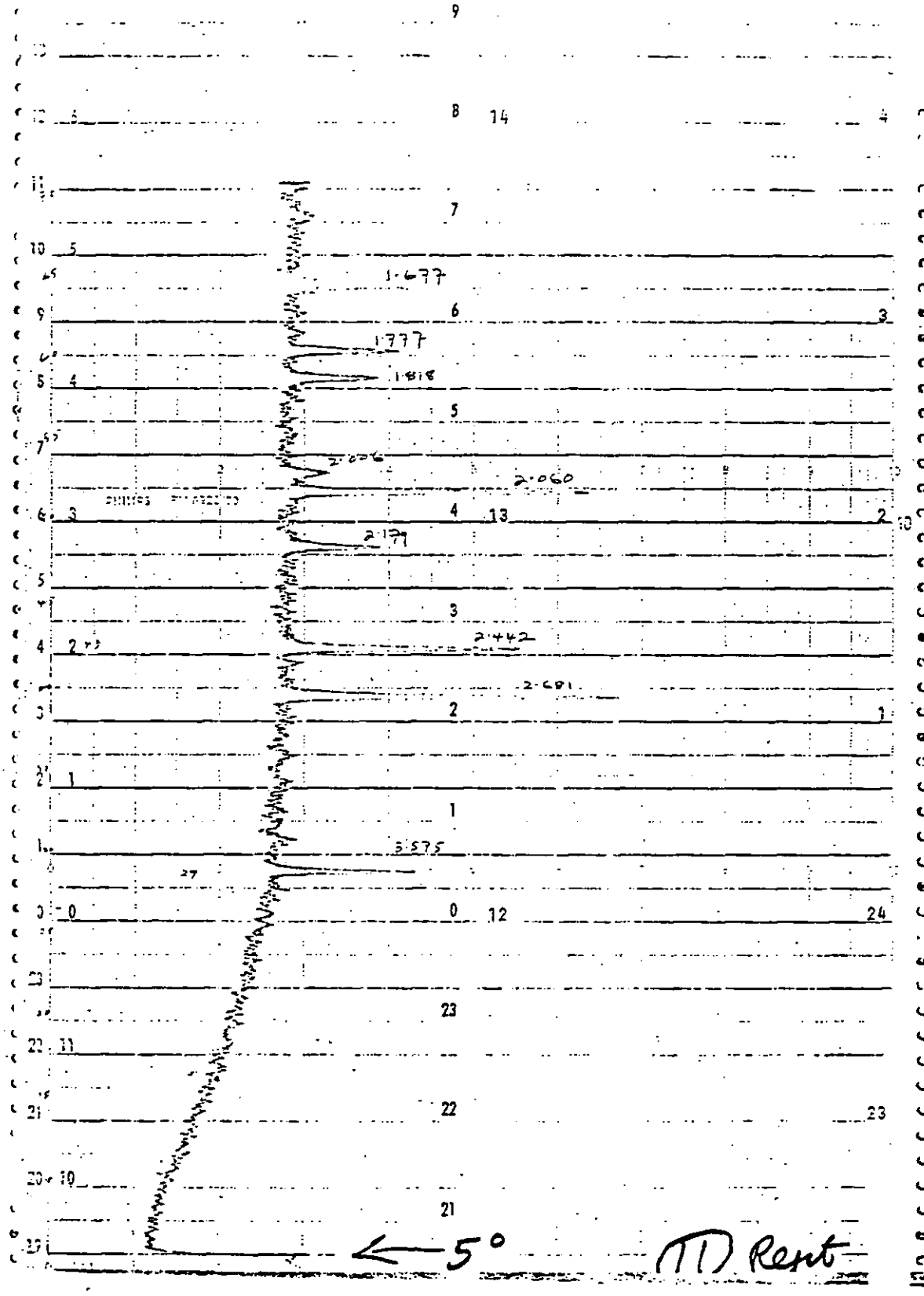

Figure 6 (53) X-Ray Diffractometer trace of the oxide layer formed on stainless steel type 347 after exposing for 20 hours at 730° C in combustion gases, - when using Kerosene with 60 ppm sodium, 5% sulphur and 300 ppm vanadium.

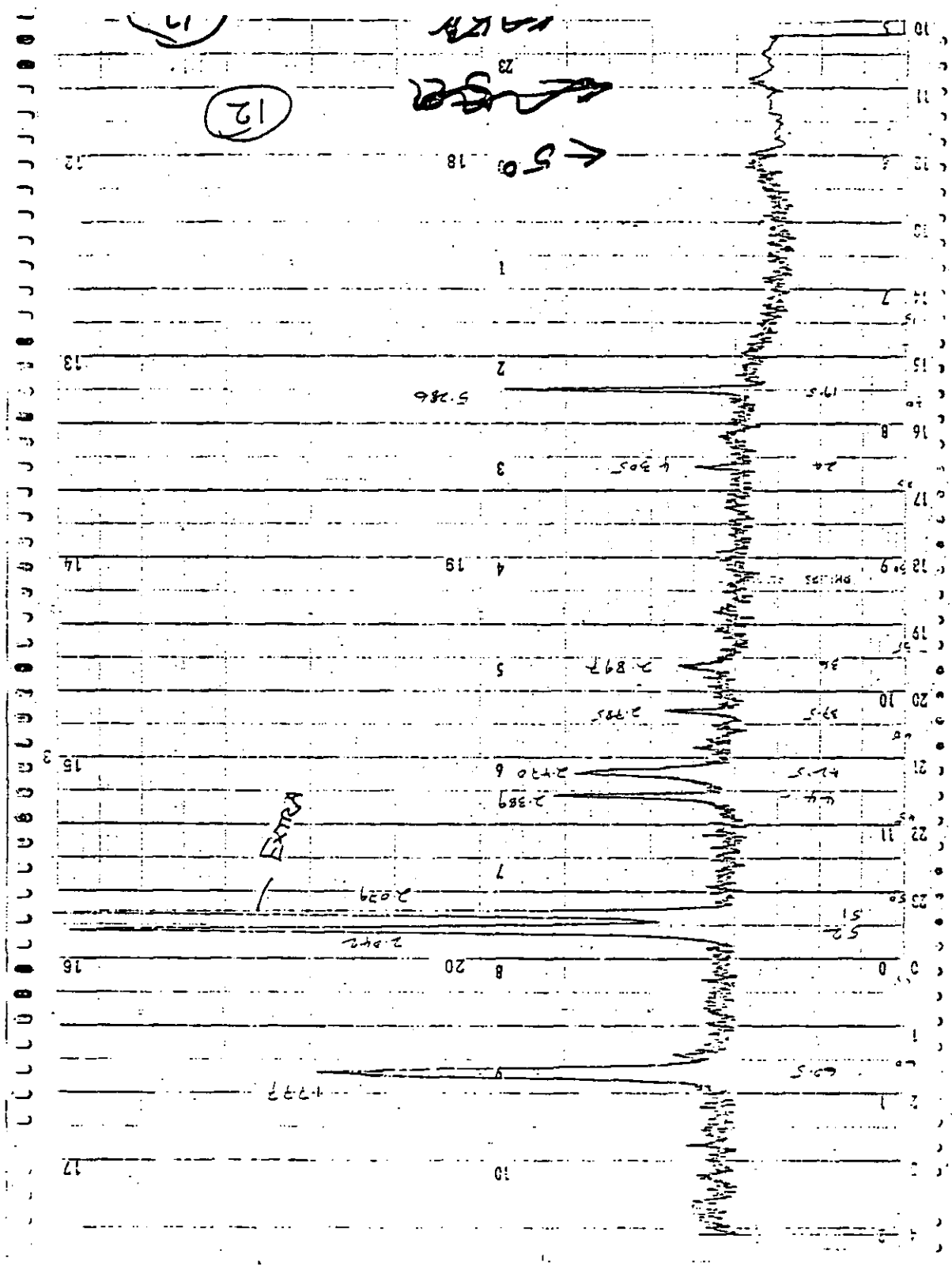

Figure 6 (54) X-Ray Diffractometer trace of the oxide layer formed on N105 after exposing for 20 hours at 730° C in combustion gases, - when using Kerosene with 60 ppm sodium, 6% sulphur and 300 ppm vanadium.

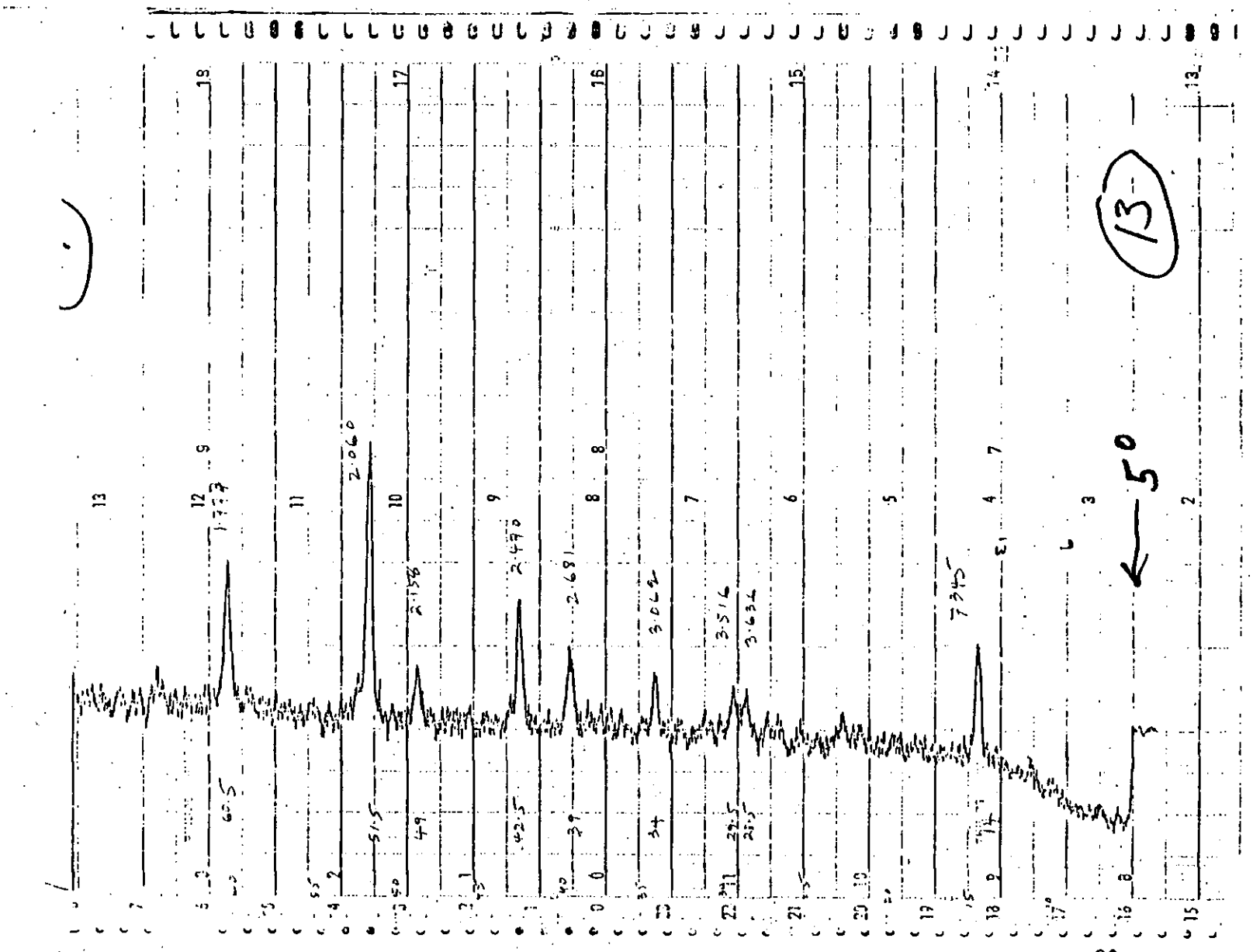

Figure 6 (55) X-Ray Diffractometer trace of the oxide layer formed on IN657 after exposing for 20 hours at 730° C in combustion gases, - when using Kerosene with 60 ppm sodium, 6% sulphur and 300 ppm vanadium.

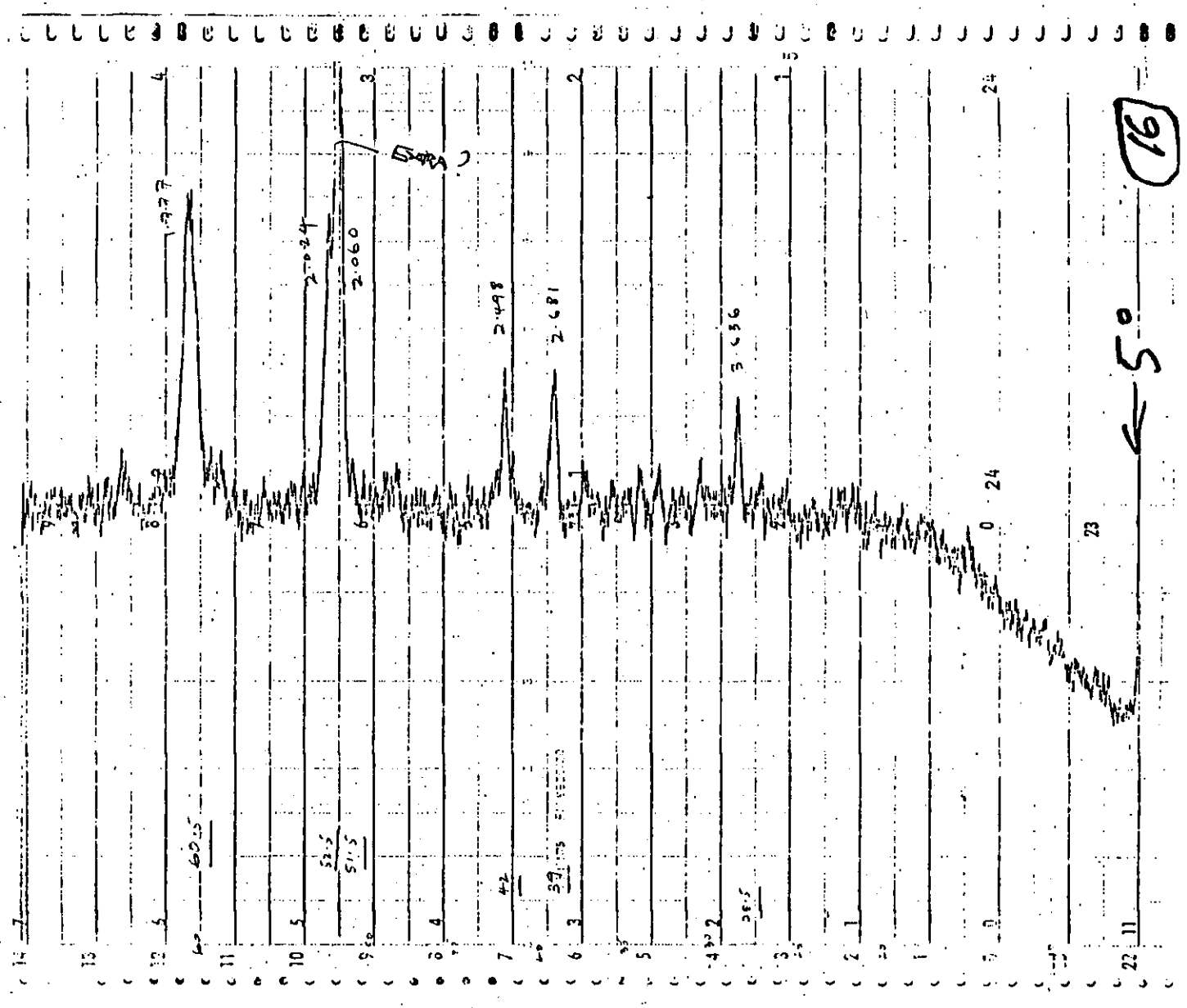

Figure 6 (56) X-Ray Diffractometer trace of the oxide layer formed on IN657 after exposing for over 60 hours at 730° C in combustion gases, - when using mixed fuels.

TABLE 6(11) - IGNITION DELAY TIME OF KEROSENE WITH ADDITIVES

Temp. °C.	Ignition Delay time, Seconds.									
	Kerosene	Kerosene + 5% sulphur	Kerosene + 15% sulphur	Kerosene + 60 ppm Na.	Kerosene + 30 ppm Na.	Kerosene + 100ppm V.	Kerosene + 300ppm V.	Kerosene + 0.1% Ferrocene	Kerosene + 1% Ferrocene	
300	2.70									
320	1.50	1.35								
340	1.20	1.26								
360	1.10	1.10			1.08					
380	0.90	1.00		0.98	0.96					
400	0.80	0.85	0.97	0.93	0.90	0.90	0.94			
420	0.76	0.80	0.90	0.87	0.82	0.84	0.88			
440	0.70	0.72	0.81	0.81	0.75	0.78	0.82			
460	0.65	0.70	0.74	0.75	0.70	0.72	0.76			
480	0.63	0.68	0.72	0.69	0.66	0.68	0.70			
500	0.55	0.56	0.66	0.66	0.58	0.63	0.66	1.22		
510	0.50	0.52	0.62	0.65	0.58	0.60	0.65	1.17		
520	0.54	0.52	0.60	0.62	0.57	0.58	0.61	1.11		
530	0.50	0.48	0.59	0.61	0.54	0.57	0.60	1.04		
540	0.45	0.47	0.58	0.57	0.54	0.54	0.57	0.98		
550	0.47	0.47	0.55	0.55	0.52	0.53	0.56	0.93		
560	0.46	0.45	0.51	0.54	0.48	0.50	0.52	0.87	1.18	
570	0.45	0.44	0.51	0.51	0.48	0.48	0.52	0.82	1.12	
580	0.42	0.44	0.50	0.50	0.45	0.47	0.48	0.77	1.07	
590	0.42	0.43	0.50	0.50	0.44	0.45	0.46	0.75	1.05	
600	0.40	0.41	0.48	0.47	0.42	0.43	0.45	0.68	0.95	
610	0.39	0.41	0.45	0.43	0.40	0.42	0.43	0.62	0.85	
620	0.35	0.40	0.42	0.44	0.40	0.41	0.41	0.59	0.80	
630	0.38	0.40	0.40	0.41	0.39	0.40	0.41	0.53	0.77	
640	0.35	0.35	0.39	0.40	0.38	0.38	0.38	0.50	0.70	
650	0.35	0.34	0.39	0.37	0.36	0.37	0.40	0.47	0.63	
660	0.34	0.34	0.38			0.36	0.36	0.43	0.57	
670	0.33	0.34	0.35			0.34	0.35	0.39	0.51	
680	0.34	0.33	0.34			0.33	0.33	0.35	0.44	
690	0.30	0.33	0.33			0.33	0.33	0.33	0.39	
700	0.30	0.32	0.33			0.32	0.33	0.32	0.34	
710	0.30	0.30								
720	0.29	0.30								
730	0.28	0.30								
740	0.28	0.29								
750	0.28	0.28								

TABLE 6(12) - IGNITION DELAY TIME OF DIFFERENT FUEL.

Temp. °C.	Ignition Delay time, Seconds.							
	Cyclohexane	n - Hexane	n - Pentane	Benzene	Kerosene + 20% Cyclohexane	Kerosene + 20% n - Hexane	Kerosene + 20% n - Pentane	Kerosene + 20% Benzene.
300								
320								
340								
360								
380						1.22		
400					1.06	1.12	1.30	
420					0.97	1.04	1.10	
440					0.90	0.97	0.99	0.99
460					0.82	0.91	0.91	0.89
480					0.73	0.78	0.85	0.85
500	1.12	1.35	1.23		0.63	0.71	0.78	0.80
510	1.00	1.24	1.15		0.64	0.63	0.76	0.71
520	0.91	1.15	1.10		0.60	0.61	0.68	0.79
530	0.82	1.05	1.03		0.57	0.60	0.64	0.77
540	0.76	1.00	0.95		0.54	0.60	0.63	0.73
550	0.70	0.93	0.88		0.50	0.53	0.60	0.69
560	0.65	0.81	0.80		0.48	0.55	0.60	0.65
570	0.56	0.78	0.76		0.47	0.52	0.56	0.59
580	0.50	0.75	0.70		0.44	0.50	0.55	0.56
590	0.48	0.70	0.65		0.43	0.45	0.50	0.54
600	0.45	0.65	0.62		0.40	0.45	0.46	0.53
610	0.42	0.53	0.59		0.38	0.42	0.44	0.48
620	0.39	0.51	0.55		0.36	0.38	0.43	0.46
630	0.37	0.45	0.54		0.34	0.36	0.41	0.43
640	0.34	0.42	0.50		0.34	0.35	0.40	0.39
650	0.32	0.42	0.46		0.33	0.34	0.38	0.37
660	0.30	0.38	0.42		0.30	0.32	0.36	0.34
670	0.28	0.32	0.40		0.30	0.30	0.36	0.34
680	0.25	0.30	0.36	1.88	0.29	0.29	0.35	0.29
690	0.24	0.28	0.35	1.65	0.28	0.29	0.32	0.27
700	0.25	0.26	0.31	1.58	0.27	0.28	0.30	0.24
710	0.24	0.24	0.28	1.31	0.27	0.28	0.29	0.22
720	0.23	0.21	0.27	1.20	0.27	0.26	0.28	0.20
730	0.23	0.20	0.26	1.01	0.26	0.26	0.28	0.19
740	0.22	0.19	0.25	0.81	0.26	0.25	0.27	0.17
750	0.20	0.18	0.24	0.55	0.26	0.24	0.27	0.17

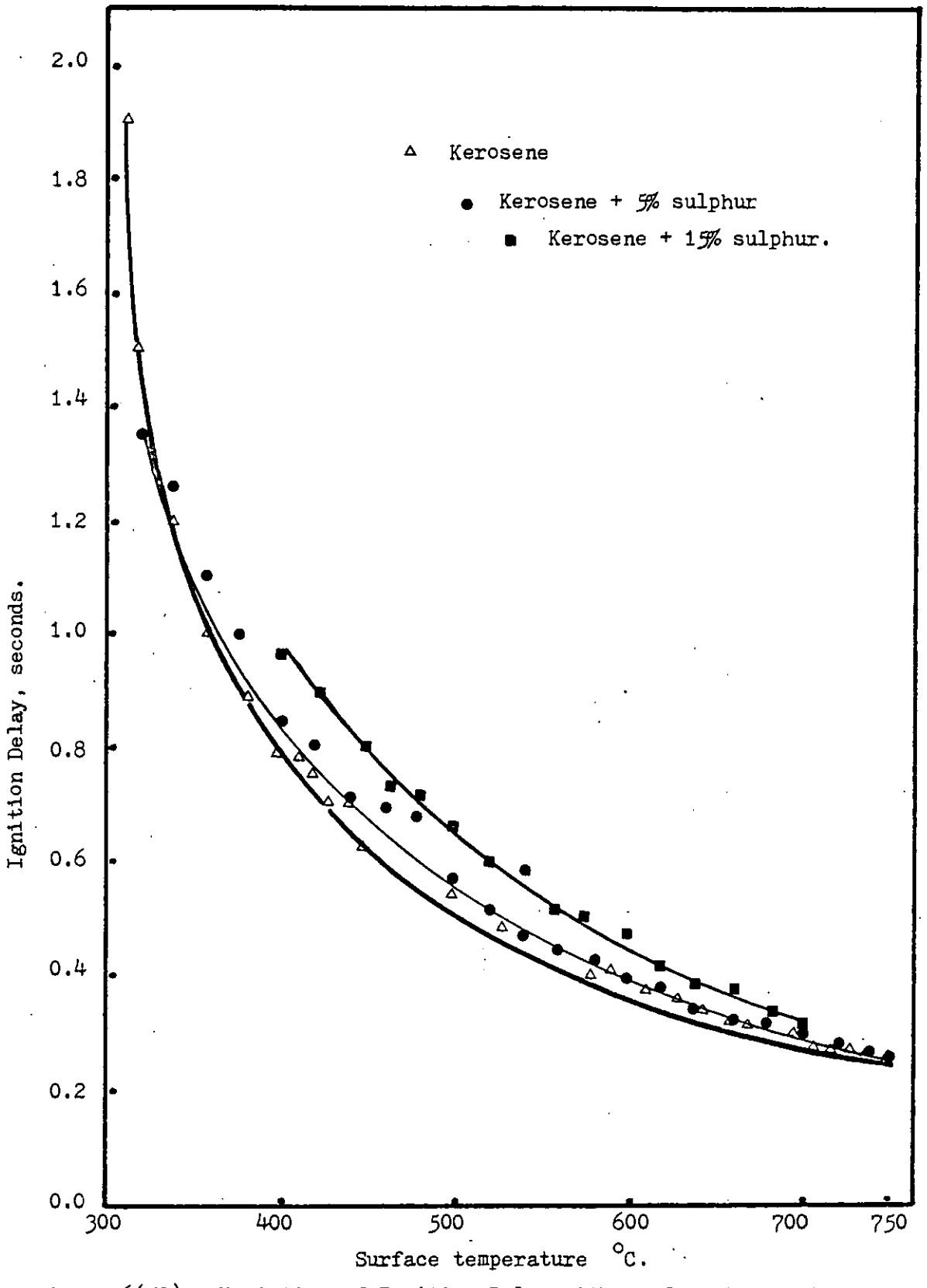

Figure 6(57). Variation of Ignition Delay with surface temperature using Kerosene with different concentration of sulphur.

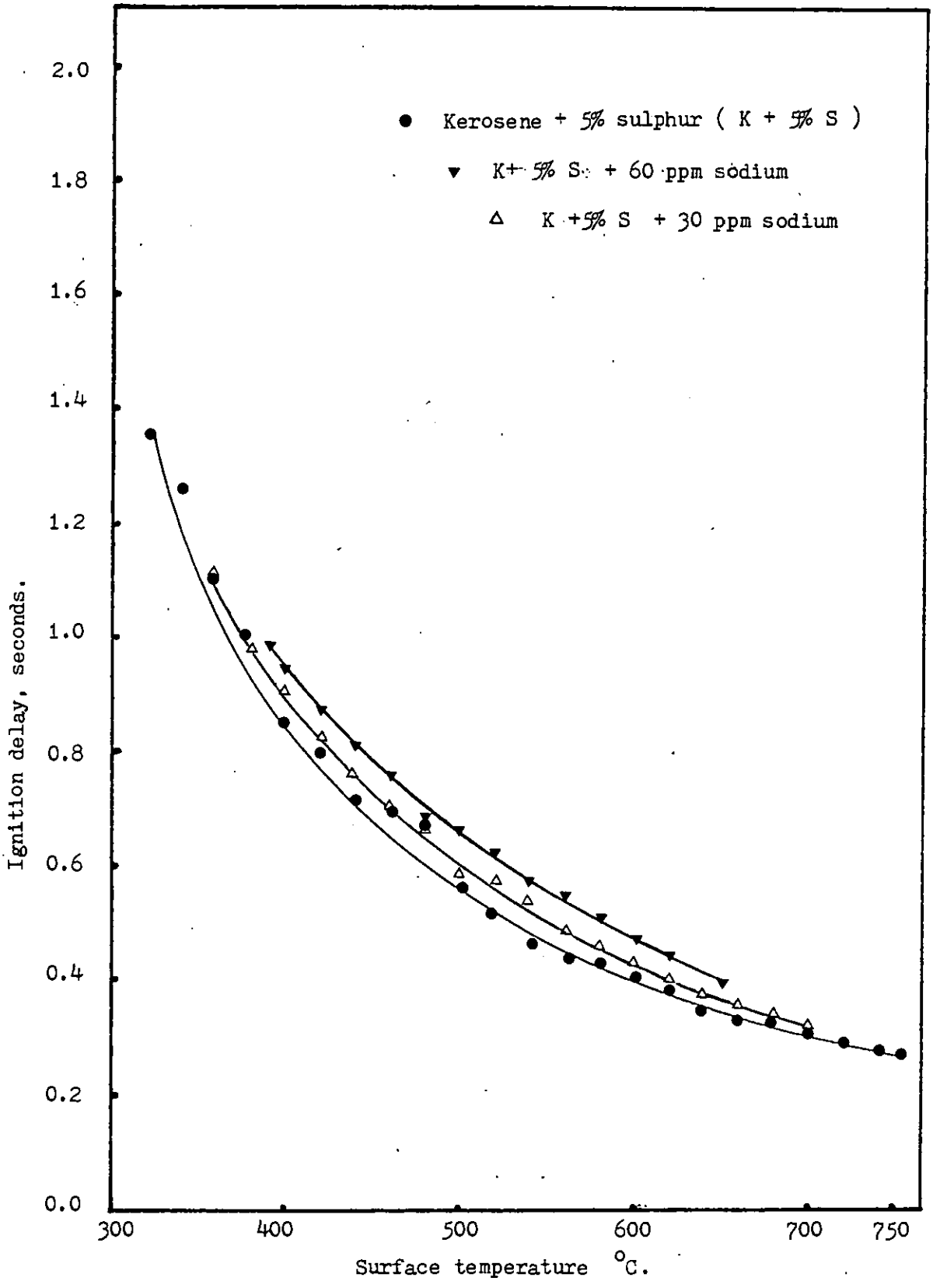

Figure 6(58). Variation of Ignition delay and surface temperature using Kerosene with different concentration of sodium.

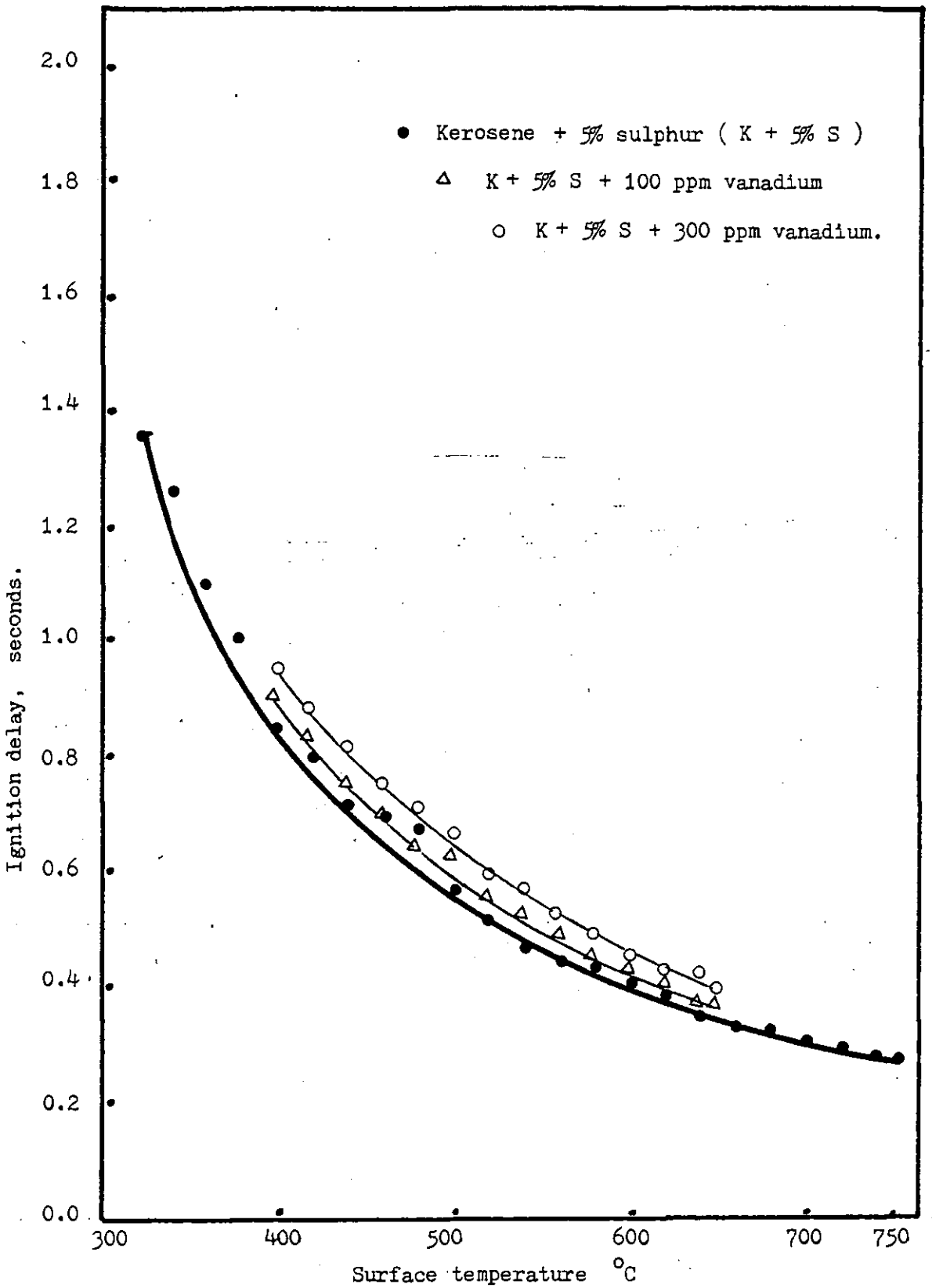

Figure 6(59) Variation of Ignition delay with surface temperature using Kerosene with different concentration of vanadium.

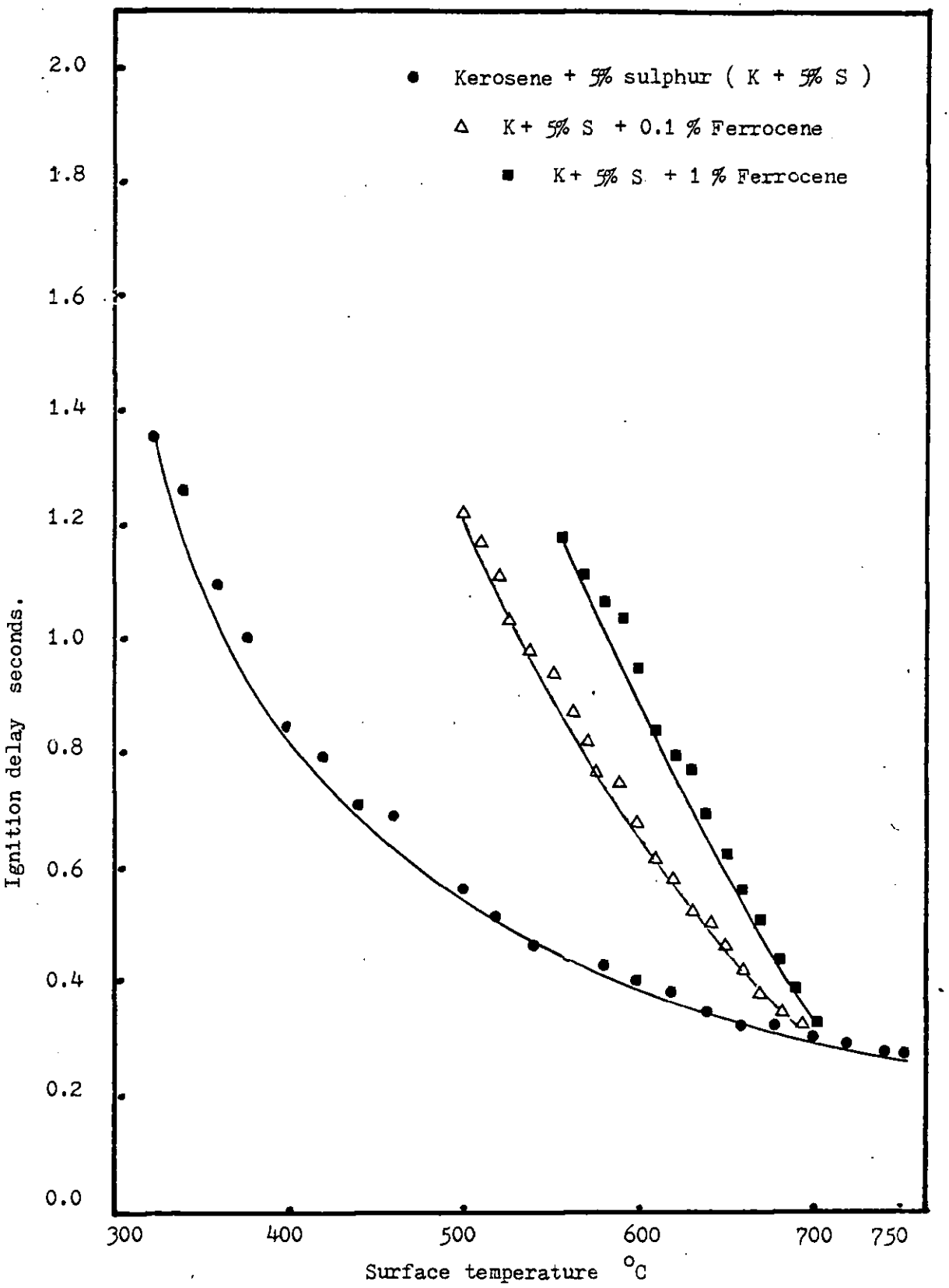

Figure 6(60). Variation of Ignition delay with surface temperature using Kerosene with different concentration of Ferrocene.

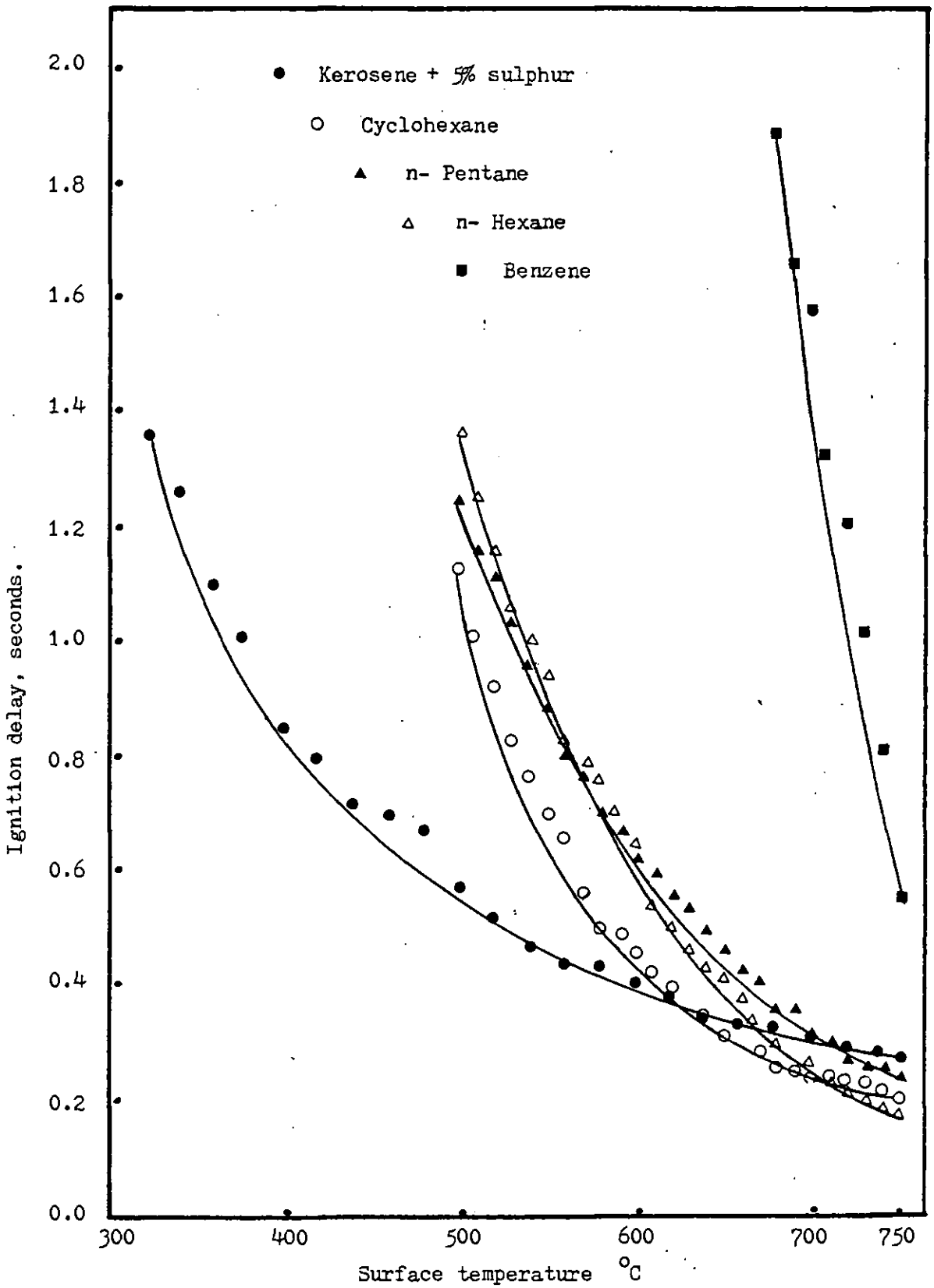

Figure 6(61) Variation of surface temperature with Ignition delay of Kerosene, Cyclohexane, n-Pentane, n-Hexane and Benzene.

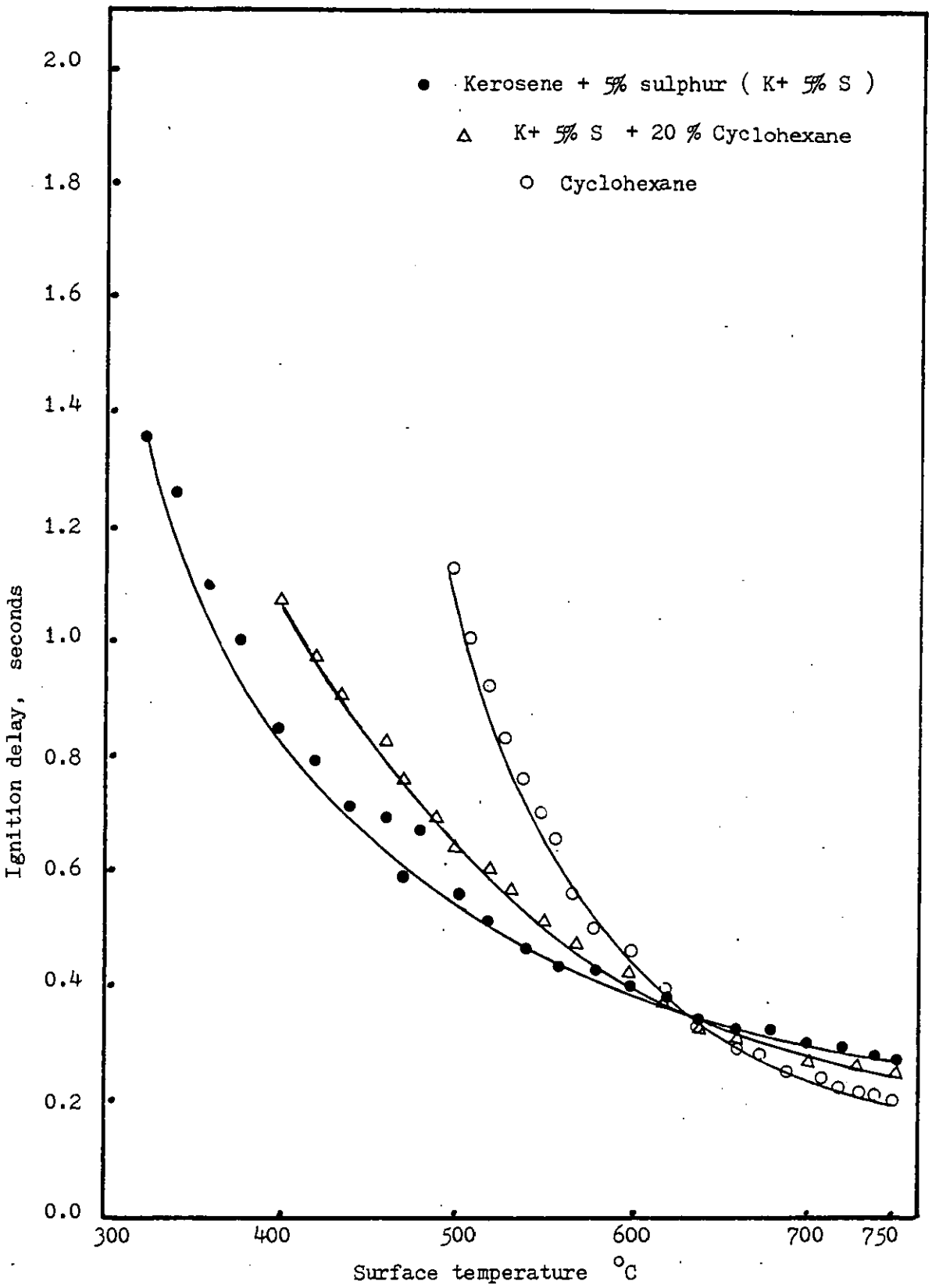

Figure 6(62). Variation of Ignition delay with surface temperature using Kerosene with Cyclohexane.

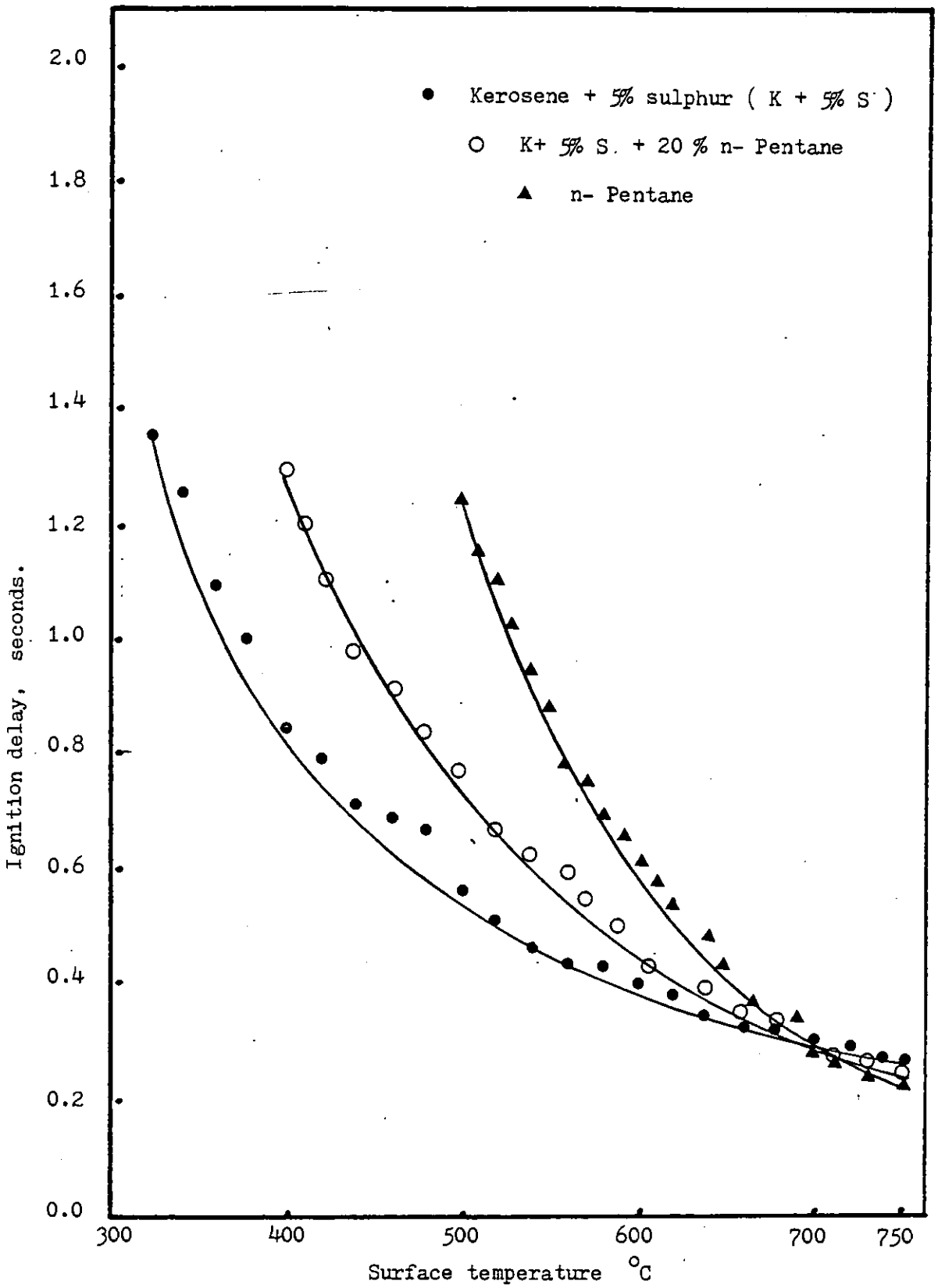

Figure 6(63) Variation of Ignition delay with surface temperature using Kerosene with n- Pentane.

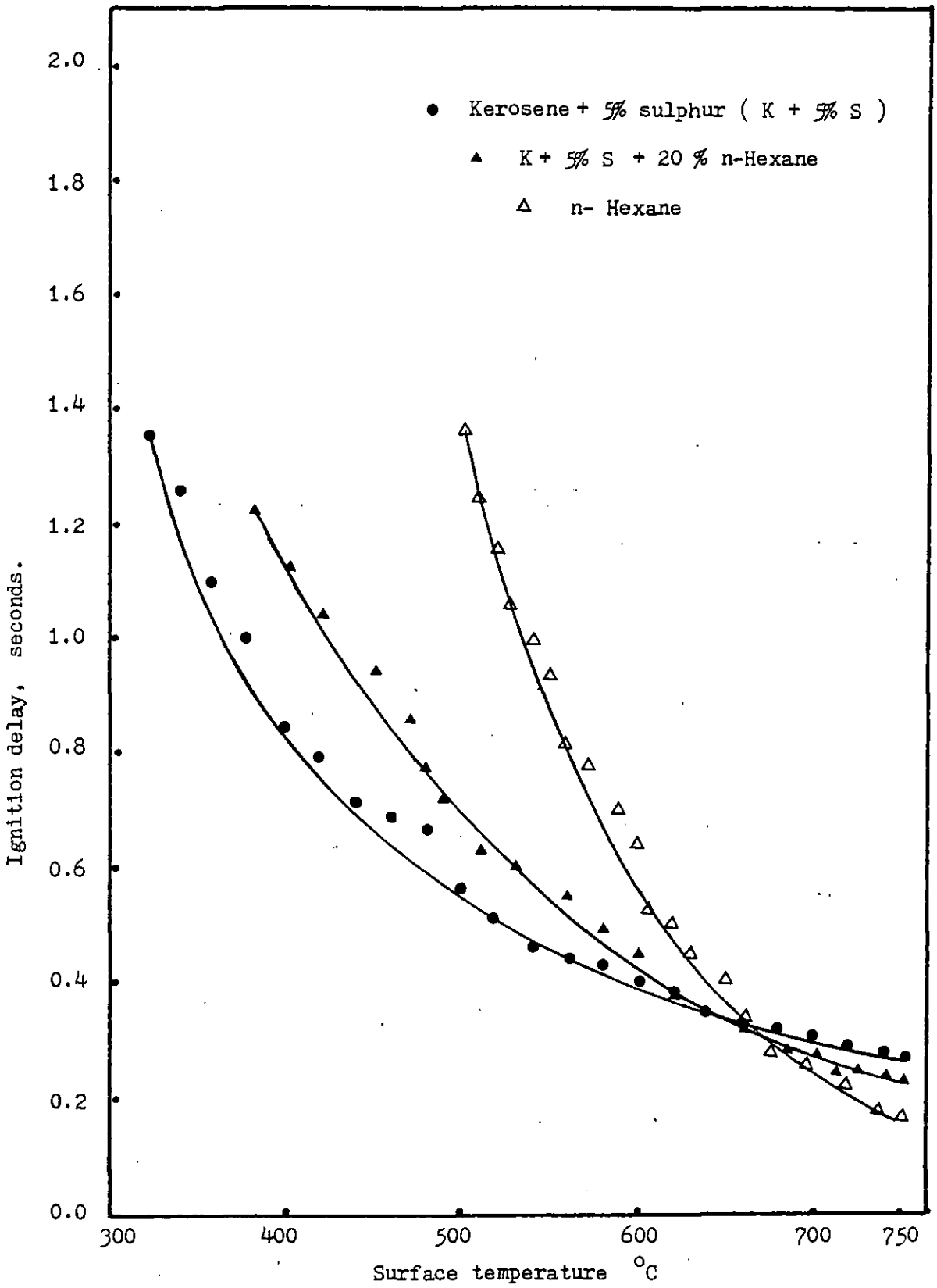

Figure 6(64) Variation of Ignition delay with surface temperature using Kerosene with n- Hexane.

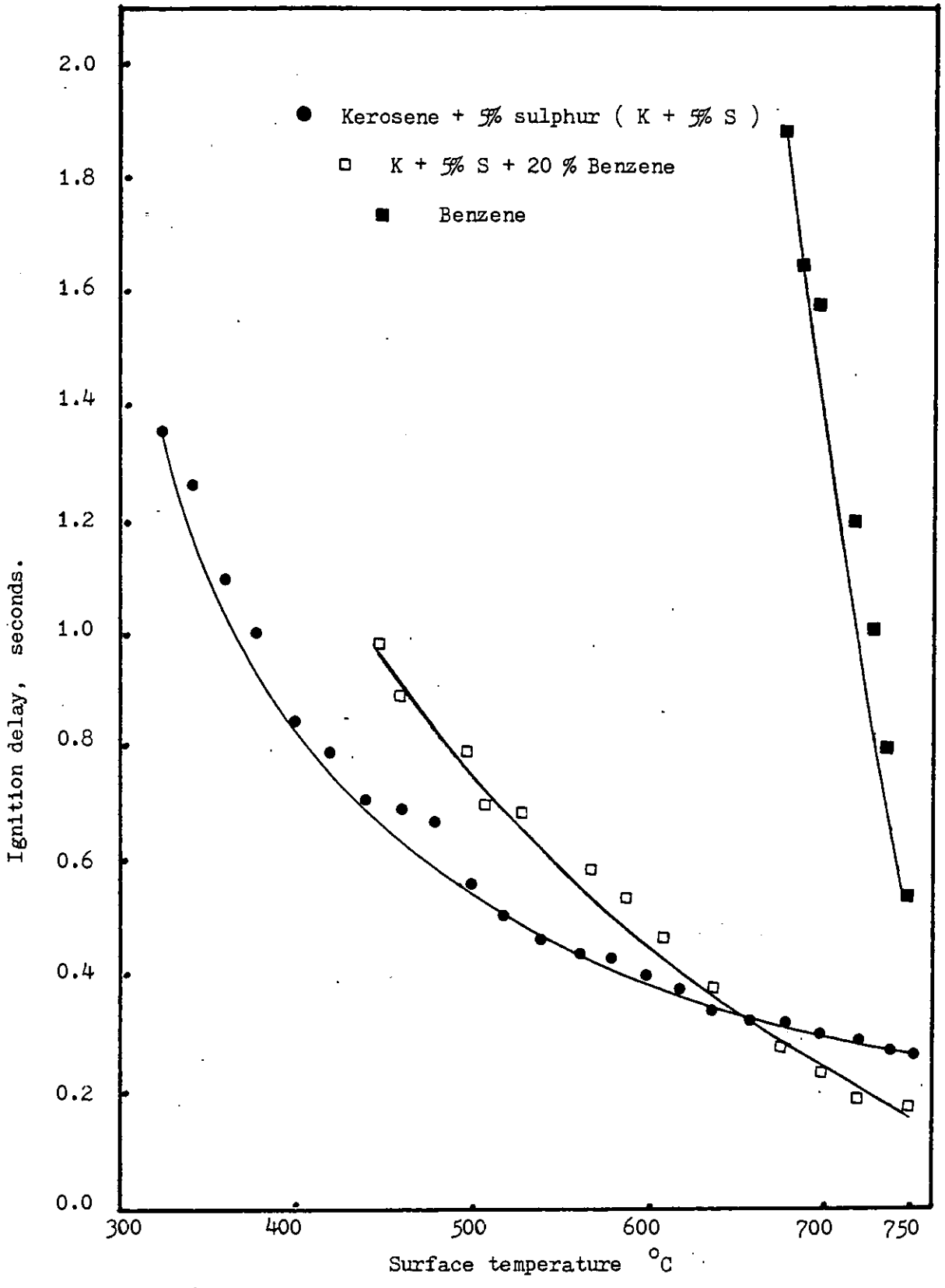

Figure 6(65) Variation of Ignition delay with surface temperature using Kerosene and Benzene.

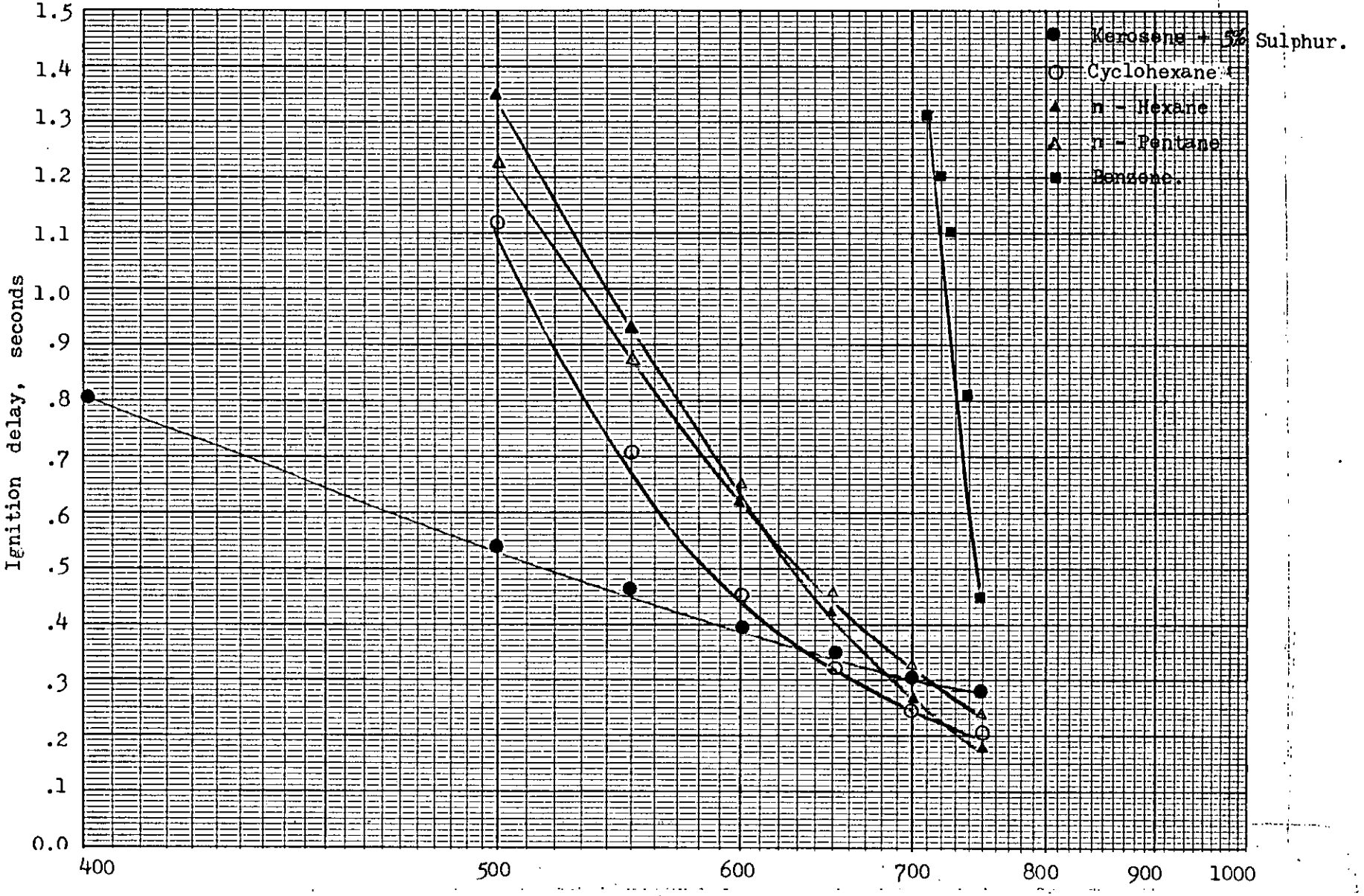

Figure 6(66) Variation of Ignition delay with ln. of surface temperature of different fuels.

TABLE 6(13) PROPERTIES OF FUELS USED FOR IGNITION DELAY EXPERIMENTS.

Fuels	Formula	Molecular Mass	Specific gravity @ 15°C	Boiling range °C
Kerosene	-	-	0.79	160-290
Cyclohexane	$CH_2(CH_2)_4CH_2$	86.14	0.776	80- 82
n- Hexane	$CH_3(CH_2)_4CH_3$	86.18	0.670	67- 70
n- Pentane	$CH_3(CH_2)_3CH_3$	72.15	0.625	35- 37
Benzene	C_6H_6	78.12	0.87	80- 82

TABLE 6(14) SULPHUR TRIOXIDE CONCENTRATIONS IN COMBUSTION GASES PRODUCED BY BURNING DIFFERENT FUELS.

Fuels	Sulphur trioxide concn., ppm.					
Kerosene	1,	2,	1,	1,	2	~ 1
Kerosene + 1% sulphur (K + 1% S)	7,	12,	9,	8,	9	~ 9
Kerosene + 3% sulphur (K + 3% S)	35,	31,	38,	36,	36	~ 35
Kerosene + 5% sulphur (K + 5% S)	54,	49,	51,	48,	47	~ 51
K + 3% S + 2% cyclohexane	28,	33,	27,	35,	33	~ 31
K + 3% S + 5% cyclohexane	13,	17,	18,	19,	17	~ 17
K + 3% S + 20% cyclohexane	10,	13,	11,	13,	14	~ 12
K + 5% S + 20% cyclohexane	29,	37,	31,	35,	34	~ 33
K + 3% S + 2% n-hexane	22,	21,	22,	20,	24	~ 22
K + 3% S + 5% n-hexane	12,	15,	19,	18,	14	~ 16
K + 3% S + 20% n-hexane	7,	9,	9,	11,	8	~ 9
K + 5% S + 20% n-hexane	23,	25,	28,	25,	24	~ 25
K + 3% S + 2% n-pentane	17,	25,	22,	22,	27	~ 23
K + 3% S + 5% n-pentane	20,	22,	17,	16,	19	~ 19
K + 3% S + 20% n-pentane	11,	9,	14,	13,	16	~ 13
K + 5% S + 20% n-pentane	25,	28,	27,	29,	27	~ 27
K + 5% S + 20% Benzene	36,	43,	46,	40,	48	~ 43

CHAPTER SEVEN

DISCUSSIONS AND INTERPRETATION OF RESULTS.

The experimental results discussed in this chapter follow the order in which they are presented in the previous chapter.

7.1 Test fuel analysis.

Test fuels were analysed for their sulphur and sodium concentrations before and after the addition of these elements taking into consideration the amounts already present in the fuels. See table 6(1). Sulphur was added in the form of carbon disulphide, and sodium as Nuosyn sodium, an oil soluble compound containing 5% sodium as metal (received from Durham Chemicals Ltd.). The theoretical sulphur and sodium concentrations agreed reasonably well (within 6%) with the experimental results shown in tables 6(2) and 6(3). Vanadium was added as Nuodex Vanadium, a vanadium soap of naphthenic acid dissolved in white spirit, with a metal content of 3%. The vanadium concentrations in the test fuels were not measured experimentally. Additional materials present in the compounds other than sulphur, sodium and vanadium were not taken into consideration in the final corrosion measurements. These additional materials are taken to be constant.

7.2 Combustion gas composition.

The combustion flue gas composition was measured initially for different air flow rates as shown in table 6(4). For corrosion rates measurements, the air flow and fuel flow rates were kept constant to reduce the possibility of error due to variation in flue gas composition.

7.3 Effect of temperature and thermal cycling.

The combustion conditions were adjusted to keep the temperature at the sampling point at 730 $\pm$ 10^{o} C. Temperatures were

measured by thermocouples calibrated by a suction pyrometer, using a comparative measurement method, thus reducing the possibility of error. The rate of temperature rise of a mild steel specimen is shown in figure 6(3). The specimens reached the final temperature in about 60 seconds.

From figure 6(4) it can be seen that the thickness of the oxide layers increases over a period of three hours exposure time. After three hours the oxide layers break and, due to the blast of hot combustion gases, the oxides flake away. A fresh oxide starts forming. Although the oxide layers gradually continue to increase in thickness, over 20 hours, the flaking-off process leaves some gaps containing softer carbonaceous materials between the harder oxides. Unfortunately, it was not possible during this programme to examine the different parts of the oxide layers by scanning electron microscopy.

7.4 Corrosion rate measurement.

Coupon testing, used in this experimental programme, is the traditional method for the study of general corrosion problems. Its advantages have already mentioned in chapter 2.8. All possible precautions were taken to minimise errors in obtaining results by weight-loss method. The similar treatment given to the materials for corrosion rate measurement justifies the results of the weight-loss method.

7.5 Personal accurecy in weighing.

The maximum error due to personal accuracy in weighing is 0.6 mg as shown in figure 6(5). In the case of mild steel specimens the error in the weights of the oxides were well within 5% but in the case of Nimonic alloys the maximum error was within 15% for three hours exposure. On increasing the time of exposure to 20 hours the maximum error in the weight of oxides was brought down to less than 10%.

7.6 Effect of thickness of Specimen.

Small changes in the thickness of the specimens did not have any significant difference in corrosion rate as shown in figure 6(6).

7.7 Effect of position of the coupons.

The effect of corrosion on the position of the coupons along the tube diameter is shown in figure 6(7). It can be seen that the corrosion rate of specimens placed in the centre slots were slightly higher than those in the slots nearer to the pipe wall. This was possibly because of the slightly higher temperature at the centre of the pipe. The error in the corrosion rate due to the position was minimised by always putting samples of some materials in the same slots.

7.8 Time of exposure.

The effect of time of exposure on corrosion rate is shown in figure 6(8). It can be seen that after about two and a half hours the rate of increase in corrosion begins to decrease. Rasborough (90, 185) pointed out that corrosion rates are significantly higher within the first hour, after which the deposition rate becomes steady. The experimental results seem to confirm this statement. Marson and Cobb (165) also exposed mild steel specimens for three hours at 650^{o} C for their laboratory experiments. Accordingly mild steel was exposed for three hours. For steels and alloys some tests were carried out for 20 hours exposure time. As expected, the deposits increased significantly, but still longer exposure time is necessary to obtain results comparative with boiler and gas turbine conditions.

7.9 Effect of excess oxygen.

Rosborough (185) and Ahmed (2,3,4) suggested that corrosion rate is highest at about 4.5% excess oxygen conditions in the combustion gases. Some tests were done using different excess air, and

the results are shown in figure 6(9). As expected the corrosion rate is highest at about 4.5% excess oxygen conditions. Accordingly all the experiments were carried out at 4.5% excess oxygen conditions in order to maximise corrosion.

7.10 Computer Programme.

The computer programme was written on the basis of the experimental results shown in figures 6(10), 6(11), 6(12), 6(13), 6(14) and 6(15), obtained by using Kerosene fuel under the specified conditions. This was done to show the usefulness of the programme as a prediction method. The programme can be used for other criteria by calibrating and changing the appropriate data to suit particular conditions. The small differences in the predicted and experimental results shown on page 94 can be due to the fact that light fuel oils are more complex than Kerosene.

7.11 Three hours exposure time.

Comparing the corrosion rates of mild steel using Kerosene and Diesel B of figures 6(16), 6(17) and 6(18), it can be seen that without the addition of sodium, sulphur and vanadium, corrosion rates are slightly higher using Diesel B (2.5 $mg/cm^2/h$) than when using Kerosene (1.5 $mg/cm^2/h$). On addition of sodium or sulphur the corrosion curve alters, and corrosion is slightly higher with Kerosene than with Diesel B, but the addition of vanadium makes Diesel B more corrossive than Kerosene. The differences are small but the reason is not clear. Corrosion rate increases rapidly on addition of upto 4% sulphur, 150 ppm vanadium, and 25 ppm sodium. After these concentrations, the rate of increase tends to stabilise. Comparing corrosion rates of mild steel, SS347, N90 and N105 it can be seen that the corrosion rate of mild steel is much higher than the other materials. The corrosion rate of SS347 is slightly higher, and that of N90 is slightly lower than that of N90 alloy. See figures 6(19), 6(20), 6(21), 6(23), 6(25), and 6(27). Figures 6(22) and 6(24) shows that on increasing sulphur concentration in presence of sodium

and vanadium respectively, corrosion rate increases. Figure 6(26) shows that on increasing sodium concentration in presence of vanadium, corrosion rate also increases up to a certain concentration of vanadium, after which the rate of increase levels off.

7.12 Twenty hours exposure time.

Lengthening the exposure time to 20 hours the corrosion rate of all the materials increased but the increase was not very high when compared with the results of three hours exposure time. See table 6(6). This would be expected if one takes into account the formation of protective oxide layers. The corrosion rate of IN657 steel type 347, after 20 hours exposure.

7.13 Effect of additives.

The addition of Ferrocene which is a compounded form of two cyclopentadienyl anions and one ferrous ion, reduces corrosion rate. Looking at figure 6(28) it can be seen that at a concentration of 0.1% Ferrocene, the corrosion rate reduces to a minimum, after which the reduction rate remains steady. It is possible that ferrous ions become attached to the metal, forming a more protective oxide layer. Visual inspection also showed an orange coloured solid material on the surface of the test coupons. Furthermore X-ray analysis of the oxides showed that the addition of Ferrocene helped to reduce the formation FeO as shown in table 6(9).

The addition of up to 3% Econsol D reduced corrosion rate, as shown in figure 6(29).

Emulsification of the test fuel with small amount of atomised water slightly increased the corrosion rate, as shown in figure 6(30). This confirms the experimental findings of research workers in Sweden, as discussed by Rosborough (185).

7.14 Metallurgical.

The composition of steels and alloys tested are shown in table 6(7). The materials used for corrosion investigation have been regarded as a single feed stock considered from the engineering point of view, and detailed metallurgical investigations into, for example, grain sizes, heat treatment, etc., are outside the scope of this programme. It was considered that as the materials were operating at high temperatures attaining these temperatures in a short time (figures 6(3)), any metallurgical differences would be neutralised by the methods of corrosion testing used in this programme.

A simple index such as Vickers Hardness Number (VHN) can tell a physical metallurgist much about the conditions of the metals. The hardness range before and after the exposure in hot combustion gases are shown in table 6(8). These results confirmed the expectations of the Senior Lecturer in Material Science, Mr. M. Evans. Mild Steel, for example, softened after exposure to hot gas, whereas stainless steel and Nimonic alloys slightly hardened. IN657 softened slightly possibly because of the high niobium content in the alloy. Measurement of hardness after exposure could provide an index of tendency to corrosion-erosion. Grits or particles in the combustion gases would be expected to do more damage to the softer materials.

Michrographs of different materials taken before and after the exposure in hot combustion gases are shown in figures 6(31), 6(33), 6(34), 6(35), and 6(36). The structures did not (nor were they expected to) change significantly. As mentioned in the preface, it was not possible to analyse the oxide layers by scanning Electron microscopy.

7.15 Identification of oxides by X-ray diffraction.

Examination of the X-ray diffraction results shown in tables 6(9) and 6(10) raises the following comments:

In table 6(9), comparison of the powder photographs (P) with diffractometer results (D) of samples 1/5, 1/7, 1/8, and 1/9, shows no significant differences. After the outside layer had been scraped off, one would expect the inner layer to include metallic iron together with any oxides which might be present, and this is in fact the case.

The most significant aspect of table 6(9) is the relationship between the presence of sulphur and the type of oxide. Sample 1/1 suggests that in the absence of sulphur (Kerosene has no sulphur) the dominant oxide is magnetite (Fe_3O_4) with only a trace of wiistite (FeO). When the sulphur content is 1% or more (Diesel B contains 1% sulphur) wiistite becomes a significant component. With 1% sulphur but no sodium or vanadium present wiistite is infact the dominant phase and there is only a little magnetite (sample 1/2). In sample 1/3 (5% sulphur), 1/4 (25 ppm sodium), and 1/5 (250 ppm vanadium) wiistite, is present together with magnetite. Therefore. increasing sulphur, sodium and vanadium individually helps the formation of magnetite. In sample 1/6, both 5% sulphur and 25 ppm sodium were added, and wiistite was again the main oxide present, while the magnetite completely disappeared. A similar result was obtained after adding 5% sulphur and 250 ppm vanadium (sample 1/7). But on the addition of 250 ppm vanadium and 25 ppm sodium, magnetite became the only oxide phase, and wiistite disappeared (sample 1/8). The addition of all three impurities together in the above concentrations (the maximum amount of impurities used in these experiments), once again led to the appearance of wiistite (sample 1/9), so proving that sulphur assists in the formation of wiistite.

Ferrocene was added to Diesel B, whereupon magnetite became the prominent oxide formed (sample 1/10). In sample 1/11, both 5% sulphur and ferrocene was added to the fuel but magnetite was again prominent, whereas wiistite, which might have been expected because of the sulphur present, disappeared. Therefore, it is reasonable to believe that Ferrocene helps to suppress the formation of wiistite.

Comparison of corrosion rates of the above samples, shows that the maximum individual additions of sulphur, sodium and vanadium to Diesel B (samples 1/3, 1/4 and 1/5) have the corrosion rates of 12, 9 and 11 $mg/cm^2/h$ respectively (figures 6(19), 6(20) and 6(21)). Collective maximum additions of sulphur-sodium and sulphur-vanadium (samples 1/6 and 1/7), give the corrosion rates of 18 and 17.5 $mg/cm^2/h$ respectively (figures 6(22) and 6(24)). On the other hand, maximum addition of sodium and vanadium give lower corrosion rate of 14.5 $mg/cm^2/h$ (figure 6(26)).

Table 6(10) gives the X-ray results of steels and alloys after 20 hours exposure. Sample 2/1, which gave magnetite with only a trace of wiistite on mild steel after 20 hours exposure, confirms the similar result obtained after only 3 hours exposure, as seen in table 6(9). In sample 2/5, where maximum sulphur and vanadium were added, increasing the exposure time to 20 hours caused the formation of magnetite. In sample 2/10, where all the three impurities were present at maximum level, the oxide layer shows traces of sodium sulphate (Na_2So_4), leading one to expect a predominance of Wiistite, confirmed by the fact that magnetite is only found in trace quantities.

The exposure of stainless steel type 347 for 20 hours (sample 2/2) produced haematite (Fe_2O_3) almost exclusively. With the addition of sulphur and other impurities wiistite appears at a similar content level as haematite. When all impurities are present as maxima a trace of Na_2SO_4 appears as well (sample 2/11). With stainless steel, as in the case with mild steel, sulphur is linked with the appearance of wiistite in these longer exposures.

With nimonic N105 alloy (sample 2/3 and 2/7), without the addition of impurities in the fuel the resulting oxide is identified as haematite with a trace of nickel oxide. This pattern is unchanged with the maximum additions of sulphur and vanadium. When all three impurities are present as maxima the trace of nickel oxide is no longer detectable, but a trace of Na_2So_4 is found (sample 2/12). The corrosion rate of N105 is the least of

all those materials investigated. It is somewhat surprising, however, that for an alloy such as Nimonic 105 (Table 6.7), in which the iron content is as low as 0.58%, the resultant oxide should be almost entirely haematite (Fe_2O_3).

After exposure to 20 hours, without any additions (sample 2/4), the specimen of IN657 showed haematite with a trace of chromium oxide. With the maximum sulphur and vanadium additions the results are the same (sample 2/8). With all the three impurities at maximum concentrations the trace of chromium oxide disappears, and traces of Na_2VO_3 and Na_2SO_4 (sample 2/13) are found. At 200° C with sulphur and vanadium additions at maximum level haematite is the main oxide, there is no trace of chromium oxide but there is a trace of $VOSO_4$ (sample 2/9). When all three impurities are present at maximum level, and the sample at 200° C a specific complex compound was identified (hydrated basic sulphate of magnesium iron and aluminium) together with a trace of Na_2VO_3. Sample 2/15 was exposed in combustion gas with the addition of Econsol D at 200° C. This produced a hydrated sodium vanadium sulphate with a trace of haematite. A specimen of IN657 exposed to a variety of coditions for more than 60 hours at 730° C gave haematite and wiistite as the oxides identified. Although this alloy contains 1% iron, samples exposed to 730° C show a predominance of haematite in the oxide layer. At 200° C the complex hydrated sulphate is very interesting since neither magnesium nor aluminium is listed as being present in the composition of the alloy. These metals, present in the hydrated sulphate, may have come from the fuel, see table 2(3).

Finally the specimen exposed to varied conditions shows haematite and wiistite. The latter is not surprising since both oxidising and reducing conditions were prevailing, and over such a long exposure (60 hours) one has also to consider the possibility of contamination of iron oxides from the combustion chamber.

These results were discussed with Dr. F. Stott (226), of UMIST who commented that at high temperatures the formation of iron

oxides (FeO, Fe_2O_3, Fe_3O_4) is dependent on the partial pressure and activity of oxygen. At high sulphur concentrations, oxygen activity decreases and it is not expected to get higher oxides. These comments agreed with the results obtained by X-ray diffraction analysis.

7.16 Ignition delay.

The purpose of the first series of experiments was to determine whether Kerosene had comparable ignition delay properties after the addition of impurities such as sulphur, sodium, vanadium and oil soluble additives.

Figure 6(57) shows that the addition of sulphur in the form of carbon disulphide (CS_2) in Kerosene slightly shifted the ignition delay curves upwards, but not significantly. This small shift may have been caused by the addition of CS_2 liquid, rather than the sulphur content. It is therefore, reasonable to deduce that sulphur in itself had no significant effect on the ignition delay property. Similar comments can be made in the cases of sodium and vanadium, by observing the figures 6(58) and 6(59). Figure 6(60) shows the ignition delay time vs. temperature of Kerosene with Ferrocene as an additive. The addition of Ferrocene not only causes a sharp increase in the ignition delay curve, but also increase the temperature required for the initial ignition. Looking at figure 6(28) it can be seen that addition of 0.1% Ferrocene reduces corrosion rate from 12 to 7 $mg/cm^2/h$.

Careful study of the ignition delay curves of Kerosene and light hydrocarbons in figure 6(61) shows that after a temperature of about 550° C the rate of decrease of ignition delay is slower with Kerosene than with light hydrocarbons. At 750° C, Kerosene has an ignition delay of 0.28 seconds compared with the ignition delays of 0.20, 0.18, 0.24, 0.55 seconds for cyclohexane, n-hexane, n-pentane and benzene respectively. On referring to table 6(14), it can be seen that the sulphur trioxide concentration in the combustion gas using Kerosene is 51 ppm. Using fuels

containing 20% each of cyclohexane, n-hexane, n-pentane and benzene in Kerosene the sulphur trioxide concentration in reduced to 33, 25, 27 and 43 respectively at the operating temperature. The reason behind this phenomenon is very complex, and may be dependent on the physical properties, and rate of reactions of the physical properties and rate of reactions of the fuels at higher temperatures. Ignition delay characteristics are a good indicator of the behaviour of the fuel in the flame zone, and the rate of production of various oxides (4). Results described above show that ignition delay property could also be used as a measure of determining the usefulness of a fuel as an additive. The exact relationship of ignition delay to the reaction which leads to the formation of sulphur trioxide is complex. It is possible that a short ignition delay would mean early initiation of reaction in the flame zone. This allows greater time for carbon monoxide to mop up automatic oxygen in competition with, say, sulphur dioxide (carbon dioxide being more reactive than sulphur dioxide).

From the ignition delay curves of n-pentane and n-hexane in figure 6(66) it can be seen that the curves diverge at a temperature above 600° C approximately. These divergences were in accordance with the expectations of Dr. P. Beadle and his colleagues at the Fuel Division of B.P. Research Laboratories, Sunbury. They suggested that the diverging of the curves were not likely to be caused by chemical effect, but more likely to be due to physical causes. It is known for example, that the evaporation rate of n-pentate is least dependent upon temperature and therefore, it was to be expected that the ignition delay of n-pentane at hgiher temperatures should be different from n-hexane. A suggested further line of research would be the investigation of ignition delays of their isomers.

7.17 General discussion on the formation of SO_3 and ignition delay properties.

(a) formation of SO_3.

The mechanism of the formation of SO_3 in H_2S flames, proposed by Levy and Merryman (140) involved O atom chain operating in the following manner:

$$SO + O_2 \rightleftharpoons SO_2 + O \quad \ldots\ldots\ldots \quad 7.1$$

$$O + H_2S \rightleftharpoons OH + SH \quad \ldots\ldots\ldots \quad 7.2$$

$$OH + H_2S \rightleftharpoons H_2O + SH \quad \ldots\ldots\ldots \quad 7.3$$

$$SO_2 + O \rightleftharpoons SO_3 \quad \ldots\ldots\ldots\ldots \quad 7.4$$

Gaydon (77) agreed with the view (53) that the amount of SO_3 formed would depend as the composition of the flame gases as well as upon the concentration of atomic oxygen.

The most likely overall process of formation of SO_3 was proposed by Hedley (97). Oxygen atoms react with the most easily oxidisable substance available which happens to be SO_2. This results in the formation of excited sulphur trioxide which subsequently collides with a third body (e.g. H_2O) to give normal SO_3.

$$SO_2 + O \longrightarrow SO_3^* \quad \ldots\ldots\ldots \quad 7.5$$

$$SO_3^* \longrightarrow SO_3 + h \quad \ldots\ldots\ldots \quad 7.6$$

$$SO_3^* + M \longrightarrow SO_3 + M \quad \ldots\ldots\ldots \quad 7.7$$

This transient quantity of SO_3 is considerably in excess of the equilibrium concentration, and therefore begins to dissociate. The dissociation continues until the theoretical concentration is reached which will be governed by the gas temperature. It would appear that if the gases are kept at high temperature to allow longer time for the SO_3 to be dissociated, then the SO_3 will be low.

Ahmed (2,3,4) confirmed this hypothesis and showed that the theory can be represented as:

$$SO_2 + O \xrightarrow{k_1} SO_3 \xrightarrow{k_2} SO_2 + \tfrac{1}{2}O_2 \qquad \ldots\ldots 7.8$$

where k_1 and k_2 are two specific rate constants (units of $k = sec^{-1}$). On the assumption that the concentrations of atomic oxygen and sulphur trioxide are small compared with sulphur dioxide, it was proposed that the Kinetics of the primary process producing SO_3 as these of first order reaction. On similar grounds, the dissociation of SO_3 was also taken as first order reaction. Thus two consecutive first order reactions were obtained with the rates dependent solely on (O) and (SO_3) respectively. From the experimental results it was also shown (2) that the rate of formation of SO_3 was approximately eight times the rate of its dissociation.

(b) ignition properties.

Processes involved in the oxidation of even the simplest hydrocarbon, i.e. methane has not been fully understood (79). In the pre-mixed, high temperature (flame) combustion of hydrocarbons, from that responsible for low temperature slow oxidation, the majority of enthalpy of reaction is released rapidly in a narrow reaction zone leading to the production of high temperatures. It is evident that the problem of finding exact mechanism of combustion of hydrocarbon is extremely difficult. It is possible that hydrocarbons which tend to imitate early reactions bring forward the recombination region of the flame and thus allow greater time for CO to compete with SO_2 for reacting with available atomic oxygen. It is also known that standard free energy change for the carbon monoxide oxidation is much greater than that for sulphur dioxide oxidation. Therefore it would be expected that former reaction would take preference over the latter, and under the circumstances oxidation of SO_2 will be reduced.

Ahmed (2,3) proposed that the ignition properties of hydrocarbons have an effect on the formation of SO_3. He measured ignition delay of four hydrocarbons upto 650° C. The experimental result presented in this programme confirms the extrapolated results upto 750° C. The measurement of ignition delay at higher temperatures was not possible due to the difficulty in minimising response time, and other technique are under consideration for future research. The results show that the ignition delay is critically dependent on the temperature of the heated surface. It decreases initially, reaching a minimum at a temperature near maximum boiling rate point. The ignition delay then increases with rise in temperature of the heated surface reaching a maximum, and then decreases with the rise in temperature of the heated surface. This pattern was possible to achieve only with Kerosene droplets (2,3). The ignition delay curves of hydrocarbons cyclohexane, n-hexane, n-pentane, benzene, and Kerosene-hydrocarbon mixtures exhibit no such definite characteristics. Some of these had been earlier predicted (189) and the results appear to be in complete agreement.

The purpose of the exercise was to determine whether fuels producing less SO_3 compared to Kerosene have shorter ignition delays. It was also intended to confirm if the hydrocarbons with shorter ignition delays than Kerosene, could be used as an additive to reduce the formation of SO_3. It can be seen that fuels, viz. cyclohexane, n-hexane, n-pentane and benzene, those that produced less SO_3 have steeper slope of their ignition delay curves compared with Kerosene. The general shape of the curves of different fuels can give an indication of the likely values of ignition delays at higher temperatures. Thus fuels having steeper slope of ignition delay curve compared with Kerosene will be expected to have less SO_3 formation on combustion than Kerosene.

CHAPTER EIGHT

CONCLUSIONS AND RECOMMENDATIONS.

8.1 Conclusions.

On the basis of the experimental results the following broad conclusions can be made:

(1) The individual presence of sulphur, sodium, or vanadium as an impurity in the fuel increases corrosion rate. The rate of corrosion increases with the amount of impurity present up to a certain concentration, after which there is a fall in the rate of increase in the corrosion.

(2) When there is more than one impurity present, the rate of corrosion is increased in the presence of sulphur as in S-Na, S-V, and S-Na-V. When sodium and vanadium are present together, the corrosion rate also increases but the rate of increase levels off after a certain concentration.

(3) The addition of oil soluble additives such as Ferrocene, and Econsol D to the fuel reduces corrosion.

(4) The computer programme in Appendix 6.1 predicts corrosion rate of mild steel for fuel containing known concentrations of impurities.

(5) Analysis of the oxide layer by X-ray diffraction showed that -

a) the FeO content in the surface oxide layers increases with the sulphur content of the fuel.

b) Ferrocene inteferes with the reactions involving sulphur and the oxide system of iron, suppressing the formation of FeO.

(6) The elemental impurities used in these experiments had no effect on the ignition delay of Kerosene, but the addition of Ferrocene made a significant change in the ignition delay.

(7) There appears to be a connection between the ignition delay curve and the formation of sulphur trioxide at the operating temperature.

8.2 Recommendations.

The following recommendations are suggested for further research.

(1) The computer programme could be expanded to cover a wide spectrum of conditions by the addition of criteria based on further experimental results.

(2) In-situ electrochemical studies would be a valuable complement to the X-ray differection analysis already carried out, and produce Kinetic results more directly.

(3) Electron microscopic examination of the samples after testing and/or the use of other modern techniques like Auger, LEED, would reveal more about the mechanism of corrosion and elemental distribution of impurities in the oxide layers.

(4) The differences in ignition delay of fuels already investigated, could be studied further by using their isomers, change of droplet size and effect of surface tension for example.

CHAPTER NINE

REFERENCES.

001. Amgwerd, P., Schlapfer, P. and Preis, J.H.;
Schweiz. Arch. Angew. Wiss 15, No.10. (1949).

002. Ahmed, S.H. and Zaczek, B.J.;
A Kinetic Study of factors influencing SO_3 formation in a Pre-mixed laminar flame. J.Inst. Fuel, 50, 107-110, June (1977).

003. Ahmed, S.H.;
Corrosive effects of Combustion gases produced from liquid fuels.
Enfield College of Technology, Research Bulletin, No.1., 19-37 (1971).

004. Ahmed, S.H.;
Formation of SO_3 in an oil-fired laboratory Combustor.
Unpublished work.

005. Annamalai, K.; Kuppu, V. and Sreenath, A.V.;
Nomograms for the estimation of maximum possible levels of Carbon monoxide in the Combustion Products of hydrocarbon fuels.
J.Inst.F., 45, 48-50, January (1972).

006. Alexander, P.A., Fielder, R.S., Jackson, P.J., Raask, E. and Williams, T.B.; Acid deposition in oil-fired boilers: Comparative trials of additives and testing techniques.
J. Inst. Fuel. 34, 53, (1961).

007. Alexander, P.A. and Marsden, R.A.;
Corrosion of Superheater Materials by residual oil ash. Mechanism of Corrosion by fuel impurities.
Edited by Johnson and Litler, Butterworths, (1963).

008. Alexander, P.A.;
Laboratory Studies of the effects of sulphates and Chlorides on the oxidation of superheater alloys.
Mechanism of Corrosion by fuel Impurities.
Edited by Johnson and Litler, Butterworths (1963).

009. Archer, J.S. and Eisenklam, P.;
Multistage combustion of residual Fuel oil;
Part 1: The effect of using air or steam for the atomisation of residual fuel oil in a high intensity first stage gasifier.
J.Inst. Fuel, 43, 397-404, October, (1970).

010. Archer, J.S., Grout, P., and Eisenklam, P,;
Multistage combustion of residual fuel oil,
Part 2:The characteristics of a second stage combustion chamber and a two stage combustion system.
J.Inst.Fuel, 43, (1970).

011. Barrett, R.E.;
High temperature corrosion studies in an oil-fired Laboratory Combustor.
J. Engineering for Power, Transactions, ASME, Vol.85, Series A, 288-296, (1967).

012. Barrett, R.E.; Hummel, J.D.; and Reid, W.T.;
Formation of SO_3 in a Non-Catalytic Combustor.
J. Engineering for Power, Tranaactions, ASME, Vol.88, Series A. 165-172, (1966).

013. Beltzer, M.; Campion, R.J. and Peterson, W.L.;
Measurement of vehicle particulate emissions.
Soc. Automotive Engineers:Automative Engineering Congress, Detroit, Michigan, Feb.25-Mar.1. (1974).

014. Burrows, B.W. and Hills, G.J.;
Electrochemistry of deposits of inorganic Constituents of fuels at high temperature (with discussion).
J.Inst.Fuel, 39, 168-180, April (1966).

015. Burnside, W.; Marskell, W.G. and Miller, J.M.;
The influence of superheater metal temperature on Acid Dew point of flue gases.
J.Inst.Fuel, 29, No.185, June (1956).

016. Buckland, B.O.;
The effect of treated High Vanadium Fuel on Gas Turbine, Load, efficiency and Life.
ASME, Paper No.58, G.T.P.-17, March, (1958).

017. Buckland, B.O.;
Corrosion and Deposits in Gas Turbines.
Induatrial and Engineering Chemistry, 2163- (1954).

018. Buckland, B.O.; Gardiner, C.M, and Sanders, D.G.;
Residual Fuel oil Ash Corrosion.
ASME Paper No. A52-161, November (1952).

019. Bowden, A.T.; Draper, P. and Rowling, H.;
The Problem of fuel oil ash deposition in open-cycle Gas Turbines.
J.Inst. Mech. E., 167, 291- (1953).

020. Bellan, J. and Summerfield, M.;
Theoretical Examination of assumptions commonly used for the Gas phase surrounding a Burning Droplet.
Combustion and Flame, 33, 107-122 (1978).

021. Bertrand, D.;
Survey of Contemporary Knowledge of Biochemistry.
Part 2. The Biogeochemistry of Vanadium.
Bull. Amer. Mus. Nat. Hist.; N.Y., 94, Art.7 (1950).

022. Babcock and Willcox Staff. Writers.
"Steam its generation and use".
The Babcock and Willcox Company, N.Y.
Ch.22, P-35 (1955).

023. Boreskov, G.K.;
Mechanism of oxidation of sulphur dioxide gas on oxide catalysts.
J.Phys. Chem. (USSR), 14, 1337, (1940).

024. Baker, D.W.C. et.al.
The Control of high-temperature fire-side Corrosion.
CEGB, London, 1977.

025. Blewden, H.S.; Hart, A.B.; Laxton, J.W. and Stevens, C.G.;
The effect of gas temperature on fire-side corrosion in residual-oil-fired boilers.
CEGB report:RD/L/R1838. (1973).

026. Bishop, R.J. and Samms, J.A.C.;
Pilot Scale investigations of the formation of bonded deposits.
Mechanism of Corrosion by fuel Improperties, edited by Johnson and Littler, Butterworth, London (1963).

027. Broadbent, D.S.;
The control of Sulphur and other Gaseous Emissions.
A three day International Symposium of IChemE and University of Salford.
The Chemical Engineer, 485,487, July (1979).

028. Bradbury, E.S.; Hancock, P. and Lewis, H.;
The Corrosion of Nickel Base Metals in Gas Turbine and Boiler Atmospheres.
Metallurgia, pp 3-14, January (1963).

029. Cooke, M.J.; Cutler, A.J.B. and Raask, E.;
Oxygen measurements in flue gases with a Solid electrolyte probe.
J.Inst.Fuel, 45, 153-156, March, (1972).

030. Crimmin, W.R.C. and Tittle, K.;
High temperature corrosion and fouling:
Thermogravimetric Studies of some sulphatic compounds.
C.E.G.B. North West Region Research Note 9 (1965).

031. Csaba, J.;
A method for the determination of adiabatic temperature and gas composition resulting from combustion of sulphur containing fuels.
J.Inst. Fuel. 47, 262-267, December (1974).

032. Coats, A.W.;
The chemistry of deposits in oil-fired boilers:
The $Na_2SO_4 - V_2O_5 - SO_3$ system.
J.Inst. Fuel, 42, 75, Feb., (1969).

033. Corey, R.C.; Cross, B.J. and Reid, T.W.;
External Corrosion of furnace-wall tubes.
II. Significance of sulfate deposits and sulphur trioxide in corrosion mechanism.
Transactions, A.S.M.E., 67, 289-302 (1945).

034. Cutler, A.J.B.;
Key Note Statement, Session 2, Inst. Fuel Conference on High Temperature Corrosion and deposits.
January (1971).

035. Cutler, A.J.B.; Halstead, W.D.; Laxton, J.W. and Stevens, C.G.;
The role of Chloride in the Corrosion Caused by flue gases and their deposits.
ASME, Paper No.70-WA/CD-1, December, (1970).

036. Chaikivsky, M. and Siegmund, C.W.;
Low excess air combustion of heavy fuel: high temperature deposits and corrosion.
ASME Paper No.64 WA/CD-2.

037. Crumley, P.H. and Fletcher, A.W.;
The formation of sulphur trioxide in Flue Gases.
J.Inst. Fuel, 29, No.187, 322-327, August (1956).

038. Chojnowski, B.;
A multipoint solid and gas sampling probe.
J.Inst. Fuel, 37, 79, February (1964).

039. Crossley, H.E.;
Prevention of Corrosion and Deposits.
Paper 16. C.E.G.B. Second liquid fuel Conference.

040. Crossley, H.E.;
External fouling and corrosion of boiler plant: a commentary.
J.Inst. of Fuel, 40, 342-347, Aug. (1967).

041. Cutler, A.J.B.; Flatley, T. and Hay, K.A.;
Fire-Side Corrosion in Power Station boilers.
C.E.G.B. Research Note No.8, October (1978).

042. Crossley, H.E.;
The advancement of Boiler Operating Conditions.
A.S.M.E. Paper No. 64-WA/CD-3 (1964).

043. Cortier, J.;
Corrosion of Superheater Spacer in a boiler burning fuel oil Low in Sodium and Vanadium.
Mechanism of Corrosion by Fuel Impurities, edited by Johnson and Littler, Butterworths, London (1963).

044. Condé, J.F.C.; Wareham, B.A.; Hancock, P. and Hurst, R.C.;
Inhibition of Hot Corrosion.
U.S./U.K. Navy Conference on Gas Turbine Materials in marine environment - Bath (1976).

045. Cullity, B.D.;
Elements of X-ray diffraction.
Addison-Wesley Publishing Company, Inc.

046. Collins, J.O. and Herbst, W.A.;
How Ash of Residual Fuel Oil affects High Temperature Boiler Operation.
Power, 98, 100 November, (1954).

047. Corbett, P.F.;
A phototurbidimatric Method for the Estimation of SO_3 in the Presence of SO_2.
J.Soc. Chem. Ind., 67, 227 (1948).

048. Davies, I. and Polfreman, P.W.;
Corrosion of gas turbines by sodium in distillate fuel oil.
J.Inst. Fuel. 48, 16-20, March, (1975).

049. Daebeler, O.F. and Smerke, J.J.;
The use of magnesium additives in oil-fired boilers.
ASME, Paper No. 63-WA-352.

050. Darling, R.F.;
Liquid fuel and the gas turbine: A ten year review.
Paper-18, Second liquid Conference, D-24-D33.

051. Davidson, D.C.;
Features on Fuel additives : 1. Assessing fuel additives.
The Steam and Heating Engineers, 36, 19-21 (1967).

052. Davidson, D.C.,
Fuel additives : 2. Corrosion in oil fired boilers.
The Steam and Heating Engineers, 36, 21-25, (1967).

053. Dooley, A. and Whittingham, G.;
"The oxideation of Sulphur Dioxide in gas flames".
Transactions of the Faraday Society, Vol.32, 354-362, (1946).

054. Dear, D.J.A.;
Water Washing of Heavy residual fuel oils.
Mechanism of Corrosion by fuel impurities, edited by Johnson and Litler, Butterworths, (1963).

055. Drake, P.F. and Harnett, C.G.;
Effects of gas-borne carbon, excess oxygen and sodium content on fuel oil ash corrosion of superheaters.
J.Inst.Fuel, 42, 339-343, September, (1969).

056. Davies, E.B. and Alexander, B.J.;
The use of Hetero-cyclic Testiary Amines for the control of corrosion caused by Flue gases.
J.Inst. Fuel, 33, 163-173, April (1960).

057. Dombrowski, N. and Johns, W.R.;
Thermal properties of combustion gases from a residual fuel-oil fired high intensity combustion chamber.
J.Inst. Fuel, 42, 194-199, May (1969).

058. Dunderdale, J.; Durie, R.A.; Mulcahy, M.F.R. and Schafer, H.N.S.;
Studies relating to the behaviour of sodium during the combustion of solid fuels.
Mechanism of Corrosion by fuel impurities, edited by Johnson and Littler, Butterworths, London (1963).

059. Demerdarche, A. and Sugden, T.M.;
Some reactions of sulphur compounds in flames.
Mechanism of Corrosion by fuel impurities, edited by Johnson and Littler, Butterworths, London (1963).

060. Elliot, P.; Ross, T.K. and Seltz, G.C.;
The mechanism of Vanadium Slag attack of Fe 23cr in air in the range 540° C to 820° C.
J.Inst. Fuel, 46, 73-87, February (1973).

061. Enyakin, Yu.P. and Dvorestskii, A.I.;
Combustion of high sulphur content oil with low excess air factors in furnaces with opposed firing burners.
Thermal Engineering, 15, 78-84, February (1968).

062. Exley, L.M.;
Practical review of residual oil firing problems and solutions in naval boilers.
Combustion, 41, 16-23, March (1970).

063. Engel, B.;
On the erosion and corrosion damage caused by the use of Heavy fuel oils in Engines, Boilers and Gas Turbines.
Erdöl and Kohle, 3, No.7, 321-27, (1950).

064. Evans, V.R.;
The Corrosion and Oxidation of Metals,
London, Arnold, (1960).

065. Edwards, C.J.A.;
Literature survey. Fire side Deposits and Corrosion in oil fired Navel steem raising Installations. Compiled for Panel A Admiralty Fuels and Lubricants Advisory Committee. B.P. Publicn., September, (1964).

066. Eisenklam, P.;
Discussion in mechanism of corrosion by Fuel Impurities, 278, Butterworths, London, (1963).

067. Francis, W.;
Boiler House and Power Station Chemistry.
Pergamon Press, (1965).

068. Fenimore, C.P. and Jones, G.W.;
Determination of oxygen atoms in lean, flat, pre-mixed flames by reaction with nitrous oxide.
J. Physical Chemistry, Vol.62, 178-183 (1958).

069. Finfer, E.Z.;
Fuel oil additives for controlling air contaminant emissions.
J. Air Pollution Control Association, 17, 43 (1967).

070. Frederick, S.H. and Eden, T.F.;
Corrosion aspects of the Vanadium problems in the Gas turbines.
Proc. I.Mech.E., 168, No.3, 125- , (1954).

071. Flint, D. and Lindsay, A.W.;
Catalytic Oxidation of Sulphur dioxide on Heated Quartz Surfaces.
Fuel, Vol.30, No.12, 288, (1951).

072. Fielder, R.S.; Jackson, P.J. and Raask, E.;
Determination of sulphur trioxide and sulphur dioxide in Flue gases.
J.Inst. Fuel, 33, No.229, 85. (1960).

073. Futler, T.S.;
"Solving Problems in Materials".
ASTM Bulletin, No. 185, 60, October (1952).

074. Gills, B.G.;
Production and emission of Solid SO_x and NO_x from liquid fuel flames.
J.Inst. Fuel, 46, 71-76, February, (1973).

075. Gunn, D.C.;
Combustion in Shell boilers.
Talk at the Institute of Fuel, members day, 16 July, (1974).

076. Gunn, D.C.;
Deposits and Corrosion in Boilers fired with domestic refuse.
J.Inst. Fuel, 47, 225-229, December (1974).

077. Gaydon, A.G.;
Continuous Spectra in flames:the role of Atomic oxygen in Combustion.
Proc. Royal Soc. of London, 183, 111-124, (1944).

078. Garner, F.H.; Green, S.J.; Hooper, F.D. and Pegg. R.E.;
The metallic elements in residual fuel oils.
J. Inst. Pet., 39, 278, (1953).

079. Gøksoyr, H. and Ross, T.K.;
The determination of Sulphur Trioxide in flue gases.
J.Inst. Fuel, 35, No.255, 177-179, April (1962).

080. Geib, K.H. and Hartek, P.;
The addition reactions of Hydrogen and Oxygen Atoms at low temperatures.
Transactions of the Farraday Soc., 30, 131-134, (1934).

081. Greatorex, R.;
Some aspects of impurities in fuel oils.
Mechanism of Corrosion by fuel impurities edited by Johnson and Litler, Butterworths, London (1963).

082. Gavin, S.A., Billingham, J., Chubb, J.P., and Hancock, P.;
Effect of trace impurities on hot ductility of as-cast cupronickel alloys.
Metals Technology, 397-401, November, (1978).

083. Glaubitz, F.;
The prevention of corrosion in Oil Fired Boilers by Combustion of Oil with extremely low Excess Air Ratio.
Paper to European meeting 'Corrosion of Hot gases and combustion products', organised by D.A.C.H.E.M.A., Frankfurt, April (1965).

084. Gulbransen, E.A. and Jansson, S.A.;
Symposium on High Temperature Metallic Corrosion by Sulphur and its Compounds.
Corrosion Division, Electrochemical Soc., Detroit, Michigan, (1969).

085. Goldberg, H.J. and Kittle, P.A.;
The impact of elevated temperatures on the reactivity of alkaline additives used to control 'cold end' boiler corrosion.
J.Inst. of Energy, 52, pp.27, March (1979).

086. Green, R.K., Nourshargh, M. and Pitta, C.;
Reducation of Lead Pollution in engines by means of Water injection.
Paper presented at the Heat transfer and thermodynamics symposium, Leicester Polytechnic, 13-14 Nov. (1979).

087. Golden, J. and Mayne, J.E.O.;
Inhibition of the corrosion of Mild Steel by Zinc Potassium Chromate.
Br. Corros. Journal, 13, No.1. (1978).
and Private communication.

088. Hancock, P.;
Corrosion of alloys at high temperatures in atmospheres consisting of fuel combustion products and associated impurities.
H.M.S.O. London (1968).

089. Hansen, W.;
A successful additive against high temperature corrosion by residual fuel oil ash.
J.Inst. Fuel, 40, 348-351, August, (1967).

090. Holland, N.H.; O'Dwer, D.F.; Rosborough, D.F. and Wright, P.J.;
High temperature corrosion investigations in an oil-fired boiler at Marchwood Power Station.
J.Inst. Fuel, 41, 206-218, May (1968).

091. Holland, N.H.; Lamb, L.;Lees, B. and Laxton, J.W.;
Discussion on High temperature Corrosion Investigations on an oil-fired boiler at Marchwood Power Station.
J. Inst. Fuel, 43, 97-103, March, (1970).

092. Holland, N.H. and Rosborough, D.F.;
High temperature Corrosion trials at Marchwood Power Station:- Effect of Low excess air and magnesium hydroxide.
J.Inst. Fuel, 44, 300-308, June (1971).

093. Horn, G. and Street, P.J.;
Experiments with a pilot plant designed to superheat steam to 760° C. Part 1: Development and Instrumentation for Corrosion Studies.
J.Inst. Fuel, 41, 152-157, April, (1968).

094. Horn G. and Street, P.J.;
Experiments with a pilot plant designed to superheat steam to 760° C. Part 2:Flame and deposition studies.
J.Inst. Fuel, 41, 219-232, May (1968).

095. Helliwell, P.R.;
Incineration of Refuge Sludge.
Pollution Control Suplement, March, (1972).

096. Hedley, A.B.; Brown, T.D. and Shuttleworth, A.;
Vanadium Pentoxide Deposition from Combustion Gases.
J. Engg.for Power, pp.173, April (1966).

097. Hedley, A.B.;
Factors affecting formation of Sulphur trioxide in flame gases.
J.Inst. Fuel, 40, 142-151, (1967).

098. Hedley, A.B.; Nuruzzaman, A.S.M. and Martin, G.F.;
Progress Review No.62: Combustion of Single droplets and Simplified Spray Systems.
J. Inst. Fuel, 44, 38-53, January, (1971).

099. Halstead, W.D.;
Progress Review No.60 : Some Chemical aspects of fireside Corrosion in oil fired boilers.
J. Inst. Fuel, 43, 234-239, July (1970).

100. Harlow, W.F.;
Cause of High dew point temperature in Boiler Fuel Gases.
Proceedings of the Inst. Mech.E., London, Vol.151, 293-298, (1944).

101. Harlow, W.F.;
Cause of Flue gas Deposits and Corrosion in Modern Boiler Plants.
Proceedings of the Inst. Mech.E., London, Vol.160, 359-379, (1949).

102. Harris, G.T.; Child, H.C. and Kerr, J.A.;
Effect of the Composition of Gas-Turbine Alloys on resistance to Scaling and to Vanadium Pentoxide attack.
J. Iron and Steel Inst., 179, 241, (1955).

103. Halstead, W.D.;
The nature of H_2SO_4 in deposits of acid contaminated combustion grits.
J.Inst. Fuel, 51, 149-153, September (1978).

104. How, M.E.; Kear, R.W., and Whittingham, G.;
The formation and behaviour of SO_3 in a small scale pulverized-fuel-fired furnace.
J. Inst. Fuel, 31, 71-79, February, (1958).

105. Hart, A.B. and Lawn, C.J.;
Combustion of Coal and Oil in Power Station boilers.
C.E.G.B. Research Note No.5, August (1977).

106. Halstead, W.D.;
The acid dew point in Power Station flue gases - A review and assessment of available data.
C.E.G.B. report : RD/L/N91/74, (1974).

107. Honing, R.E.;
"Surface and thin film analysis of semi conductor materials".
Characterisation of Epitaxial semiconductor films : edited by Henry Kressel, Vol.2 of Methods and phenomena : Their application in Science and Technology.
Elsevier Scientific Publishing Company, (1976).

108. Harker, J.H. and Allen, D.A.;
The Calculation of the temperature and Composition of Flame gases.
J. Inst. Fuel, 42, 183-187, May, (1969).

109. Hosegood, E.A.;
Reactions of Sodium Compounds with the surface of aluminium Silicate particles during the combustion of pulverised fuel.
Mechanism of Corrosion by Fuel Impurities, edited by Johnson and Litler, Butterworths, London (1963).

110. Hedley, A.B.;
A Kinetic Study of Sulphur trioxide formation in a pilot scale furnace.
Mechanism of Corrosion by Fuel Impurities, edited by Johnson and Littler, Butterworths, London (1963).

111. Hills, G.F.;
Corrosion of metals by molten salts.
Mechanism of Corrosion by fuel impurities, edited by Johnson and Littler, Butterworths, London (1963).

112. Halstead, W.D.;
The Behaviour of sulphur and chlorine compounds in pulverised-coal fired boilers.
J. Inst. Fuel, 42 , 344-349, September, (1969).

113. Hancock, P. and Clifton, T.E.;
On line High Temperature Corrosion and fouling monitor.
Private communication.

114. Hancock, P.;
Influence of Vacancies produced by oxidation on the mechanical properties of nickel and nickel-chromium alloys.
Proceedings of the Conference by Metal Society at Royal Fort, University of Bristol, 13-16 September, (1976).

115. Hancock, P.; Hurst, R.C, and Wysiekierski, A.G.;
The influence of thermal cycling and surface degradation on Hot Corrosion.
The third conference on gas turbine materials in a marine environment. September (1976).

116. Holmes, D.R. and Rahmel, A.;
Edited Materials and Coatings to Resist High Temperature Corrosion. Applied Science Publishers Ltd., London (1978).

117. Hauffe, K.;
Oxidation von metallen and Metallegierungen.
Berlin, Springer (1956).

118. Hancock, P. and Fletcher, R.;
Oxidation of Nickel in the Temperature Range 700-1100° C.
Presented to Journees Internationales d'Etude Sur l'oxidation des Metaux, S.E.R.A.I, Brussels, October, (1965).

119. Hatt, B.A.;
X-ray diffraction, Private communication and Fulmer Newsletter No.40, November, (1979).

120. Jenkinson, J.R. and Zaczek, B.J.;
New lights in additives in oil fired boilers. Conference of the European Federation of Corrosion, Frankfurt am Main, 31 March to 2 April (1965).

121. Jenkinson, J.R. and Zaczek, B.J.;
Anti-Corrosion additives in oil-fired boilers.
Private communication.

122. Jenkinson, J.R.
Additives and Combustion.
The Steam and Heating Engineers, 25-29 June, (1967).

123. Jackson, P.J. and Raask, E.;
A Probe for Studying the deposition of Solid material from flue gas at high temperatures.
J. Inst. Fuel, 34, 275, Juley (1961).

124. Johnstone, H.F.;
The Corrosion of Power Plant Equipment by Flue Gases.
Univ. of Illinois, Engr. Exp. Station, Bulletin, 228, 122 (1931).

125. Johnstone, H.F.;
An electrical method for the determination of the Dew point of Flue Gases.
Univ. of Illinois, Engr. Exp. Station, Circular 20, (1929).

126. Jackson, P.S.,
Researches in the C.E.G.B. into fire side fouling and corrosion of boiler plant.
J. Inst. Fuel, 40, 335-341, August, (1967).

127. Jenkinson, J.R.;
Sulphur Oxide reactions.
Mechanism of Corrosion by Fuel Impurities, edited by Johnson and Littler, Butterworths, London (1963).

128. Johnson, J.B.; Nicholls, J.R.; Hurst R.C. and Hancock, P.;
The mechanical properties of surface oxides on Nickel-Base Superalloys - I. Oxidation.
Corrosion Science, Vol. 18, pp 527-541, (1978).

129. Johnson, J.B.; Nicholls, J.R.; Hurst, R.C. and Hancock, P.;
The mechanical Properties of surface scales on Nickel-Base superalloys - II. Contaminant Corrosion.
Corrosion Science, Vol.18, pp 543-553, (1978).

130. Karim, G.A. and Khan, M.O.;
The determination of Gross Kinetic data for the combustion of common fuels uaing a motored piston engine.
J. Inat. Fuel, 42, 190-193, May (1969).

131. Krause, H.H.; Levy, A. and Reid, W.T.;
Sulphur oxide reactions: Radio active sulphur and microprobe studies of Corrosion and deposits.
J. Engg. for Power, Transactions ASME, 90, 33-41, (1968).

132. Kiekenberg, I.H.;
Analyais of Vanadium in the presence of Iron oxide and Iron Salts.
Translation from Private communication.

133. Kiss, L.T.; Lloyd, B. and Raask, E.;
The use of copper oxychloride to alleviate boiler slagging.
J. Inst. Fuel, 45, 213, April (1972).

134. Kakabadse, G.J.; Manohin, B. and Vassiliou, E.;
High temperature reactiona involving vanadium oxides and certain salts.
Mechanism of Corroaion by Fuel Impurities, edited by Johnson and Littler, Butterworths, London (1963).

135. Kirsch, H.;
Corrosion in Combustion chambers caused by Slag attack and flue gases of varying composition.
Mechanism of Corrosion by fuel impurities, edited by Johnson and Littler, Butterworths, London, (1963).

136. Kubashewski, O. and Hopkins, B.E.;
"Oxidation of Metals and Alloys".
London, Butterworths, (1962).

137. Laxton, J.W.;
The influence of excess of oxygen and metallic additives on the formation and deposition of sulphur oxides in Flue Gases.
Mechanism of Corrosion by Fuel Impurities, edited by Johnson and Littler, Butterworths, London (1963).

138. Laxton, J.W. and Jackson, P.J.;
Automatic monitor for recording sulphur trioxide in flue gases.
J. Inst. Fuel, 37, 12, January, (1964).

139. Lees, B. and Mustoe, D.H.;
Effects of magnesium based additives on high temperature corrosion in an oil fired boiler.
J. Inst. Fuel, 45, 397-405, July (1972).

140. Levy, A. and Meryman, E.L.;
SO_3 formation in H_2S flames.
J. Engg. for Power, Transaction ASME, 87, 374-378 (1965).

141. Levy, A. and Merryman, E.L.;
Sulphur Chemistry and its role in Corrosion and Deposits.
J. Engg. for Power, Trans. ASME, A. 85, 229-234, (1963).

142. Levy, A. and Merryman, E.L.;
"A Progress report - Fundamentals of thermochemical corrosion reactions."
J. Engg. for Power, Trans. ASME, 87, 116-122, (1965).

143. Levy, A. and Merryman, E.L.;
The microstructure of H_2S flames.
Western State Section/Combination Institute, Paper 64-32, Fall meeting, (1964).

144. Levy, A. and Merryman, E.L.;
Interactions in Sulphur Oxide - Iron Oxide Systems.
J. Engg. for Power, Trans. ASME, 89, 297-303, (1967).

145. Lee, G.K., Friedrich, F.D. and Michell, E.R.;
Control of SO_3 in low-pressure heating boilers by an additive.
J. Inst. Fuel. 42, 67- (1969).

146. Land, T.;
The theory of acid deposition and its application to the dew-point meter.
J. Inst. Fuel, 50, 68-75, June (1977).

147. Lockwood, F.C. and Naguib, A.S.;
Aspects of combustion modelling in engineering turbulent diffusion flames.
J. Inst. Fuel, 49, 218-223, December (1976).

148. Littlejohn, R.F. and Watt, J.D.;
The distribution of mineral matter in pulverised fuel.
Mechanism of Corrosion by fuel impurities, edited by Johnson and Litler, Butterworths, London (1963).

149. Ladner, W.R. and Pankhurst, K.S.;
The formation of sulphur trioxide : the application of infra-red spectrometry to fundamental studies.
Mechanism of corrosion by fuel impurities, edited by Johnson and Littler, Butterworths, London (1963).

150. Lewis, H.;
The Kinetics of the oxidation process in Nickel-Chromium Base Alloys.
Presented to Journee Internationales d'Etude Sur l'oxydation des Metaux S.E.R.A.I., Brussels, October, (1965).

151. Leslie, W.C. and Fontana, M.G.;
Mechanism of rapid oxidation at High Temperature, High Strength Alloys containing molybdenum.
Trans. Amer. Soc. Metals, 41, 1213-1243, (1949).

152. La Nauze, R.D., Minchener, A.J., Rogers, E.A. and Stringer, J.;
High Temperature Corrosion in fluidised bed combustors.
J. Inst. of Energy, 52, 79, June (1979).

153. Meubus, P.;
High temperature reaction kinetics of Tungsten with Sulphur dioxide.
J. of the Electrochemical Society, Volume 125, No.10, 1636-1641, October, (1978).

154. Monroe, E.S.;
Equations for determining excess air from oxygen analysis of Combustion gases.
J. Inst. Fuel, 45, 167-169, March (1972).

155. Macfarlane, J.J.;
The formation of SO_3 in the Combustion products by Petroleum fuels.
Mechanism of Corrosion by fuel impurities, edited by Johnson and Litler, Butterworths, London, (1963).

156. Macfarlane, J.J.;
The relationship between combustion conditions and the corrosion of metal surfaces by fuel oil ash deposits.
N.G.T.E. report R255 July 1963 and Mechanism of Corrosion by fuel impurities, edited by Johnson and Litler, Butterworths, London, (1963).

157. Moore, M.J. and Crane, R.I.;
Conference on deposition and Corrosion in gas turbines.
London (1972).

158. McCullough, J. and Horsley, M.E.;
A preliminary thermochemical evaluation of additives for controlling low-temperature corrosion and acid Smut emission.
J. Inst. Fuel, 50, 46-49, March, (1977).

159. McEwan, M.W.;
Hot and Cold Studies on an oil-fired burner with swirler fitted in a refinery oil heater.
J. Inst. Fuel, 45, 107-112, February (1972).

160. Moreland, P.J. and Rowland, J.C.;
Technique and Instrumentation for Polarisation resistance measurements.
British Corrosion Journal, 12, No.2, 72-79, (1977).

161. Mah, A.D.;
Thermodynamic properties of Vanadium and its Compounds.
U.S. Bureau of Mines, Report 6727, (1966).

162. Morgan, E.S. and Roughton, J.E.;
Temperature of Solid Particles in the furnaces of Pulverised fuel fired boilers.
Mechanism of Corrosion by Fuel impurities, edited by Johnson and Littler, Butterworths, London, (1963).

163. Marson, C.W. and Cobb, J.W.;
Scaling by Air, Water Vapour and Carbon dioxide.
J. Soc. Chem. Ind., 46, 61T (1927).

164. Nelson, H.W.;
A review of available information on Corrosion and deposits in Coal and oil fired boilers and gas turbines.
ASME, Pergamon Press, London, (1959).

165. Nelson, H.W. and Caine, C.;
Corrosion of Superheaters and re-heaters in p.f. fired boilers.
Transactions, ASME, Series A. 82, July (1960).

166. Nelson, W., and Lisle, E.S.;
A laboratory evaluation of catalyst poisons for reducing High-Temperature Gas-Side corrosion and ash bonding in Coal fired boilers.
J. Inst. Fuel, 37, No.284, 378-385, (1964).

167. Niles, W.D. and Sanders, H.R.;
Relations of magnesium with inorganic constituents of heavy fuel oil characteristics and of compounds burned.
ASME Paper No. 60 - WA.278.

168. Niles, W.D. and Siegmund, C.W.;
Reaction between fuel ash components and additive combinations.
Mechanism of Corrosion by fuel impurities edited by Johnson and Litler, Butterworths, London (1963).

169. Needham, A.M. and Ounsted, D.;
Investigations into the origins and properties of acid smuts from oil-fired Power-Stations.
Mechanism of Corrosion by fuel impurities edited by Johnson and Litler, Butterworths, London (1963).

170. Ohno, Hideo, and Kazuo Furukawa;
Structural Analysis of some Molten Materials by X-ray Diffraction.
J. Chem. Soc. Faraday I. 74, 795-803, (1978).

171. Polfreman, P.W.;
The removal of sodium salts from gas turbine distillated fuel oil.
J. Inst. Fuel, 51, 139- (1978).

172. Parker, J.C.; Rosborough, D.F. and Virr, M.J.;
High-temperature Corrosion trials at Marchwood Power Station:- 1000 hour Corrosion probe trials.
J. Inst. Fuel, 45, 94-104, February (1972).

173. Parry, P.J.; Buchan, J., James, N.A. and Taylor, B.;
Wrought Nickel 50% Chromium alloy for use in high temperature corrosion gases.
J. Inst. Fuel, 47, 117-123, June (1974).

174. Peck, W.J., and Zaczek, B.J.;
Sulphur in Flue Gases.
Engineering, 184, 697, (1957).

175. Postnikov, V.D., Kirillow, I.P. and Kunin, T.L.;
The oxidation of gas high in So_2 and oxygen in the presence of a Vanadium Catalyst.
Zhurnal Prikladnoi Khini, 7, 869-74 (1934).

178. Pfefferkorn, G. and Vahl, J.;
Investigation of Corrosion Layers on steel using electron microscopy and electron defraction.
Mechanism of corrosion by fuel impurities, edited by Johnson and Littler, Butterworths, London (1963).

179. Penfoeld, D.;
The effect of V_2O_5 on the system K_2So_4-So_3.
J. Inst. Fuel, 151-154, May (1979).

180. Rylands, J.R. and Jenkinson, J.R.;
The Acid Dew Point.
J. Inst. Fuel, 27, 299-318, (1954).

181. Rahmel, A.;
Influence of Calcium and magnesium sulphates on the High temperature oxidation of Austrintic Chrome-Nickel Steels - in the presence of Alkali sulphates and sulphur trioxide.
Proc. Marchwood Conference, Mechanism of Corrosion by fuel Impurities, edited by Johnson and Littler, Butterworths, London, (1963).

182. Reese, J.R., Jonakin, J, and Carasristi, V.Z.;
Prevention of residual oil combustion problems by use of low excess air and magnesium additive.
Combustion, 36, No.5, 29-37, November, (1964).

183. Rendle, L.K. and Wilsdon, R.D.;
The prevention of Acid condensation in oil-fired boilers.
J. Inst. Fuel, 29, 372-80, (1956).

184. Richards, D.J.W., Jones, W.S. and Laxton, J.W.;
Monitoring and Control of flue gases.
C.E.G.B. Research Note. No.5, August, (1977).

185. Rosborough, D.F.;
Private Communication.

186. Salooja, K.C.;
Burner fuel additives.
J. Inst. Fuel, 45, 37-42, January, (1972).

187. Salooja, K.C.;
Improved Control of Smoke, Combustion efficiency and flame stability.
J. Inst. Fuel, 47, 203, September, (1974).

188. Samms, J.A.C. and Smith, W.D.;
High temperature gas side corrosion in water tube boilers.
BCURA, Review 209, monthly Bulletin 25, (1961).

189. Satcunathan, S. and Zaczek, B.J.;
The Spontaneous Ignition delay of liquid fuel droplets impinging on a hot surface.
Thermodynamic and Fluid Mechanics Convension, Bristol, 27-29th March, (1968).

190. Squires, R.T.;
Sulphur trioxide concentrations in an oil fired boilers:- Calculations using CHEMDEC.
CEGB Report - R/M/N943, Research Division, Marchwood Engineering Laboratories, May, (1977).

191. Sherburn, F.A. and Poole, A.G.;
Determination of Sodium in gas turbine fuel oil.
J. Inst. Fuel, 48, 21- , (1975).

192. Sampson, R. et .al.
A simple Model of Fuel Spray Burning.
1:Random Sprays.
Combustion and Flame, 31, 215-30, (1978).

193. Shreir, L.L.;
Corrosion, Vol. I and II.
Newnes-Butterworths, (1976).

194. Shirley, H.T.;
Effect of Sulphate-Chloride mixtures in Fuel-ash Corrosion of steels and High-Nickel Alloys.
The Journal of Iron and Steel Institute, Vol.182, pp 144-153, , (1956).

195. Salooja, K.C.;
Combustion with high efficiency and low Pollutant emission.
Energy World, 6-13, December, (1978).

196. Salooja, K.C.;
Some serious errors in So_3 determination in flue gases.
Energy World, 10-11th March, (1974).

197. Swithenbank, J., Brown, D.J. and Saunders, R.J.;
Some implications of the use of Pulsating Combustion for Power generation using gas turbines.
J. Inst. Fuel, 47, 181-189, September, (1974).

198. Snowdon, P.N. and Ryan, M.A.;
Sulphuric Acid Condensation from flue gases containing sulphur oxides.
J. Institute of Fuel, 42, 188-189, May, (1969).

199. Small. N.J.H.; Strawson, H. and Lewis, A.;
Recent advances in the Chemistry of Fuel Oil ash.
Mechanism of Corrosion by Fuel Impurities, edited by Johnson and Littler, Butterworths, London (1963).

200. Steel, J.S. and Brandes, E.A.;
Growth and adhesion of oxides in furnace deposits and their influence on subsequent deposition of ash Particles as Combustion Products.
Mechanism of Corrosion by Fuel Impurities, edited by Johnson and Littler, Butterworths, London, (1963).

201. Shirley, H.T.;
Sulphate-Chloride attack on high alloy steels and nickel-base alloys.
Mechanism of Corrosion by fuel Impurities, edited by Johnson and Littler, Buttersworths, London (1963).

202. Sulzer, P.T. and Bowen, I.G.;
Combustion of Residual Fuels in Gas Turbines.
Proc. Joint International Conference on Combustion.
Am. Soc. Mech. Eng./Inst. Mech. Eng. (1955).

/203. Tipler, W.;
Practical Experience with the use of Residual Fuel oils in Gas Turbines and use of Additives against Fuel oil Ash deposition and Corrosion.
International Congress of Combustion Engineers, Conference, Zurich, (1957).

204. Tolley, G.;
Catalytic oxidation of Sulphur dioxide on metal surfaces.
J. Soc. Chem. Ind., 57, 369-373 and 401-414, (1948).

205. Taylor, H.D.;
The Condensation of Sulphuric Acid on Cooled Surfaces Exposed to Hot Gases Containing So_3.
Trans. Faraday Soc., 47, 1114, (1951).

206. Thring, M.W.;
A World Energy Policy.
J. Inst. Fuel, 50, 179-184, December, (1977).

207. Toft, L.H. and Marsden, R.A.;
Metallurgical aspect of fireside corrosion of superheated tube materials.
Mechanism of Corrosion by fuel Impurities, edited by Johnson and Littler, Butterworths, London (1963).

208. Voorhies, A. et.al.
Improvement in fuel oil quality: 1. Demetallization of residual fuels, 2. Desulpharisation of residual fuels.
Mechanism of Corrosion by fuel Impurities, edited by Johnson and Littler, Butterworths, London (1963).

209. Volka, V.L. and Fostiev, A.A.;
Characteristic features of the reaction of $V_{2}0_{5}$ with $CaCo_3$ in Vaccum.
J. Inorg. Chem., U.S.S.R., 14, 184, (1969).

210. Wiedersum, G.C.;
Corrosion and deposits from Combustion gases: a review.
Mechanical Engineering, August, (1968).

211. Wright, W.;
CEGB/Boiler makers:- Fuel Technology Committee report on Symposium on HT Corrosion in oil-fired boilers. Item 65, Wolverhampton, November, (1967).

212. Wickert, K.;
Fouling and Corrosion in Coal-fired boilers.
Energie, 14, 4, 130-136, April, (1962).

213. Walker, V.;
Distribution of insoluble additive particles in a fuel spray.
Fuel, 35, 153, (1956).

214. Wyatt, L.M. and Evans, G.J.;
Operational and Experimental observations in the fire side corrosion of superheater and reheater tubes. Mechanism of Corrosion by fuel impurities edited by Johnson and Littler, Butterworths, London (1963).

215. Willeykeck, J.;
Operating Experience with Chemical-Slurry Spray process in Retarding Fire-Side Deposits and Corrosion. ASME Paper No. 62-WA-99.

216. Wong, E.L. and Potter, A.E.;
Reaction rates of hydrogen, ammonia and methane with mixtures of Atomic and Molecular oxygen. Journal of Chemical physics, 39, 2211-2217, (1963).

217. Whittingham, G.;
One day meeting:High temperature Corrosion and deposits by fuel impurities. J. Inst. Fuel, 44, 316-318, June (1971).

218. Williams, F.A. and Cawley, C.M.;
Impurities in coal and petroleum. Mechanism of corrosion by fuel impurities, edited by Johnson and Littler, Butterworths, London (1963).

219. Wagner, C.;
Reactions of Metals and Alloys with Oxygen, Sulphur and Halogens at High Temperatures. Corrosion and material Protection, 5, 9 (1948).

220. Whittingham, G.;
Third Symposium on Combustion and Flame explosion phenomenon, pp.453-459, Madison, Wis. (1948).

221. Young, W.E. and Hershey, A.E.;
A thermochemical Study of some additives to reduce Residual Fuel Ash Corrosion. Corrosion, Vol.13, 725t-732t, Nov. (1957).

222. Zaezek, B.J. and Grindley, R.;
Fuel additives in the fight against Corrosion. Paper presented at the Corrosion Convention, October, (1957).

223. Highton, N.H. and Webb, M.G.;

Sulphur dioxide from electricity generation: Policy options for pollution control.
Energy Policy, Vol.8, Number 1, 61, March (1980).

224. Mortimer, D.;

High Temperature Corrosion problems in power stations and materials selection procedures.
Bulletin No.80, The Institution of Corrosion Science and Technology, 13-16, May (1980).
and Private Communication.

225. Woods, G.C.;

"General aspects of High Temperature Corrosive attack : Influence of Alloy composition".
Meeting Point Pattern, course on High Temperature Corrosion, Commision of European Commodities, 7-26 (1978).

226. Stotts, F.H. and Smith, S.;

High Temperature Corrosion of an Fe-Ni-Cr alloy in gases of high sulphur and low oxygen potential.
Proc. Int. Conf. on Behaviour of High Temperature Alloys in Aggressive Environments.
Petten, Holland, (1979).,
and Private Communication.

CHAPTER TEN

APPENDICES.

2.1 Conversion of corrosion rates.

The corrosion rates of metal in terms of rate of penetration (mpy) can be calculated from Faraday's law if the current density is known. Conversely the corrosion current density can be evaluated from the rate of penetration. The following symbols and units have been adopted in deriving these relationships in which it is assumed that the corrosion is uniform and the rate is linear:

m	=	mass of metal corroded (g)
M	=	molecular mass ($g\ mol^{-1}$)
z	=	number of electrons involved in one act of reaction.
F	=	Faraday's constant, 96, 487 C ($1A = 1C_s^{-1}$)
I	=	current (A)
i	=	current density (Acm^{-2}) and i = I/S
t	=	time (s)
p	=	density of metal ($g\ cm^{-3}$)
S	=	area of metal involved (cm^2)
d	=	thickness of metal removed (cm)

From Faraday's law the weight loss per unit area is

$$\frac{m}{S} = \frac{Mit}{zF} \quad (g\ cm^{-2}) \quad \ldots \quad \ldots \qquad 8(1)$$

since m = pSd, then from equation 8(1)

$$pSd = \frac{MiSt}{zF} \quad \text{or} \quad pd = \frac{Mit}{zF} \quad \ldots \qquad 8(2)$$

and from equation 8(2) the rate of penetration d/t when i is in Acm^{-2} is given by:

$$\frac{d}{t} = \frac{Mi}{pzF} \quad (cm\ s^{-1}) \quad \ldots \quad \ldots \qquad 8(3)$$

If current density i' is in $mA\ cm^{-2}$, d in mm and t in years, then

$$\frac{d}{t} = \frac{10^{-1}}{365 \times 24 \times 60 \times 60} = \frac{Mi'}{pzF} \times 10^{-3} \quad (mpy)$$

$$\frac{d}{t} = 3.2706 \times \frac{Mi'}{zp} \quad (mpy)$$

5.1 : Determination of Sulphur Oxides.

5.1.1. Determination of Sulphur dioxide.

The major part of sulphur dioxide is abosrbed in the standard iodine solution. As just sufficient flue gas is passed to decolorise the iodine the sulphur dioxide concentration in the known volume of gas can be calculated directly.

To this must be added the relatively small quantity of sulphur dioxide retained in the isopropanol solution set aside for analysis. This is determined by analysing an aliquot of this solution in the following manner.

Measure the total quantity of the isopropanol solution reserved for analysis. Transfer exactly 20 ml of the measured solution to a 250 ml conical flask, and add 100 ml of distilled water and 1 ml of starch solution. Titrate with standard iodine solution (0.005 M) to the first permanent appearance of a blue colour.

The total sulphur dioxide concentration may be calculated from the equation:

$$Y = \frac{22.4\ (m + n)}{64.1\ (rt - d)} \times 10^3$$

Where Y is the concentration of sulphur dioxide in the flue gas (p.p.m. v/v).

m is the mass of sulphur dioxide equivalent to the amount of standard iodine solution placed in the iodine absorber wash bottle (mg).

n is the mass of sulphur dioxide in the total volume of the isopropanol solution reserved for analysis (mg). This is calculated from the titration.

r is the rate of flow of flue gas (litres/min at s.t.p.).

t is the time from starting the absorption to decolorisation of the iodine solution (min).

d is the dead-space of the apparatus for sulphur dioxide (litres).

The calculation can be simplified provided 20 ml of 0.05M iodine solution are always used in the wash bottle and 20 ml are always taken for iodometric titration from the isopropanol solution reserved for analysis.

In this case the equation reduces to:

$$\text{Sulphur dioxide (p.p.m. v/v)} = \frac{224 + 0.056aV}{(rt - d)} \times 102$$

where a is the <u>total</u> volume of the isopropanol solution reserved for the analysis (ml).

V is the volume of 0.005M iodine solution used in titration.

5.1.2. <u>Determination of Sulphur trioxide</u>.

Sulphur trioxide is determined also on the isopropanol solution reserved for analysis.

Measure the total volume of solution reserved for analysis. Transfer 20 ml of the test solution and add 5 drops of thoron indicator and titrate with standard barium perchlorate solution (0.0025M) until the solution retains a pink colour.

Sulphur trioxide may be calculated from the equation:

$$X = \frac{22.4.ap}{80.1\ b\ (rt-d)}$$

Where X is the concentration of sulphur trioxide (p.p.m v/v).

a is the total volume of isopropanol test solution reserved for analysis (ml).

h is the volume of the aliquot of the test solution selected for titration (ml).

p is the mass of SO_3 in the aliquot of volume b (ug). This is calculated from the titration.

r is the rate of flow of flue gas (litres/min at s.t.p.).

t is the time from starting the absorption to decolorisation of the iodine solution (min).

d is the dead space of the apparatus for sulphur trioxide (litres).

This equation can be simplified provided a 20ml aliquot is always taken from the isopranol solution reserved for analysis.

In this case the above equation reduces to:

$$\text{sulphur trioxide (p.p.m v/v)} = \frac{0.014\ ap}{(rt - d)}$$

5.2 : Analysis of X-ray Diffraction Powder Photography.

Specimen : Grind it as finely as possible with the morter and pestle, and use a fine wire to pack it tightly into a Lindemann glass tube. Fine grinding and tight packing prevent "spottiness" of the lines on the film. Seal the tube with a lighted match, to produce a specimen 1-2 cm. long, which can be mounted in the camera with a little plasticene.

Camera : The specimen mount can be centred by means of the larger of the two knobs on the camera. The mount is moved down when this knob is screwed in. There is no effect when the knob is unscrewed.

The smaller knob moves one of the two short pins seen inside the camera at the top. The film is placed in the camera with its ends against these pins, so that movement of the sliding pins presses it firmly in position against the inside wall of the camera.

Two collimators are provided, an entrance collimator with a slit to admit a fine beam of X-rays and an exit collimator with a yellowish fluorescent screen (being lead glass for safety) to show when the beam is on. These collimators are not interchangeable.

Centring the Specimen : (i) Remove the exit collimator, mount the specimen in its holder with a little plasticene, and place the eyepiece over the entrance collimator. Leave the camera lid off. (ii) place the camera on the centring stand and switch on the illumination. The specimen should appear as a dark horizontal line across the circular field of view. Rotate the specimen holder slowly, and adjust the specimen by hand until it does not wobble as it rotates, although it may still move bodily up and down in the field of view. (iii) Rotate the specimen until it is at its highest point in the field of view, and screw in the adjusting knob until the dark line appears central. Unscrew the knob and rotate the

specimen again. Repeat if necessary, until there is no movement of the dark line as the specimen rotates.

Loading the Camera : (i) Remove the entrance collimator and take the camera, lid, and both collimators into the darkroom. Lay these out, together with the box of film and the film punch, so that they can be found easily in the dark.

(ii) In total darkness, take a film from the box, punch collimator holes, and cut it to length. Taking great care not to knock the specimen, place the film in the camera with its ends against the clamping pins. Slide the movable pin to the right and lock it in position. Replace the camera lid and screw in the two collimators.

X-ray tube and supplies : The X-ray tube has a water cooled cobalt target. The water is circulated by a separate pump with a pressure switch to prevent application of H.T. to the tube if the water flow is inadequate. The tube has four windows, to allow the use of four x-ray beams simultaneously, if required. Over each window there is a rotatable metal disc carrying several different absorbers. The absorber to be used (as a filter, to produce monochromatic x-rays) depends on the target material.

Tube voltage and current can be varied independently by the two large knobs on the control panel.

Making an Exposure : (i) Lift the safety shield and place the camera in position, making sure that it is close enough to operate the microswitch mounted on the arm. (ii) Use the second camera to close the microswitch on the other arm. (iii) Select the filter. (iv) Mount the small motor (for rotating the specimen) on the camera, making sure that the pin engages properly in the slot.
(v) Switch on the pump, and the key switch on the illuminated sign above the machine. (vi) Check that the voltage and current controls are at zero, and press the "on" switch (marked ~) on the control panel. Set tube

voltage to 40 kV and current 30 mA. (vii) There should be a small, rather faint, greenish fluorescent spot on the screen of the exit collimator when the X-ray beam is on.

Exposure time may be 1 to 4 hours depending on the specimen.

Theory : For any type of X-ray diffraction, Bragg's equation applies:-

$$X = 2d \sin\theta \quad \ldots\ldots\ldots\ldots (1)$$

For cubic structures, it can be shown that

$$a = d(h^2 + k^2 + l^2)^{\frac{1}{2}} \quad \ldots\ldots (2)$$

Where a = length of the unit cell

d = separation of the sat of crystal planes of which h, k and l are the Miller Indices.

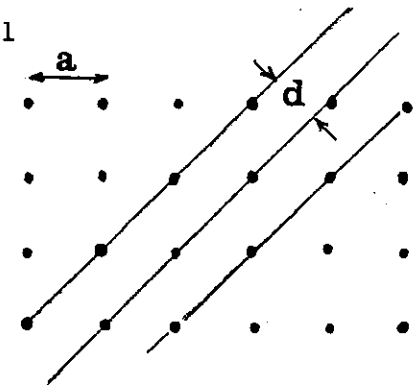

From (1) and (2)

$$\sin^2\theta = \frac{\lambda^2}{4a^2}(h^2 + k^2 + l^2)$$

or $$\sin^2\theta = \frac{\lambda^2}{4a^2}(h^2 + k^2 + l^2)$$

or $$\sin^2\theta = \frac{\lambda^2}{4a^2} \cdot N \quad \text{where N is an integer}$$

i.e. $$\sin^2\theta = C.N \quad \text{since } \frac{\lambda^2}{4a^2} \text{ is constant.}$$

Thus 20 rings on the film will give 20 integers, each integer being equal to $h^2 + k^2 + l^2$ for a particular set of crystal planes. The integers are therefore characteristics of the type of crystal structure, according to the following rules:-

(1) For a face-centred cubic structure h, k and l must be either all even or all odd.

(2) For a body centred cubic structure (h + k + l) must be an even number.

Interpretation of the photograph :

(1) Place the film on the Vernier measuring scale and measure the diameters "S" of all the rings around the exit hole (the dark ring). The rings are not true circles but from the diagram.

$s = r.4\theta$

where

r = camera radius

θ = Bragg angle

The camera radius is 57.3 mm so that s in mm = 4θ in angle.

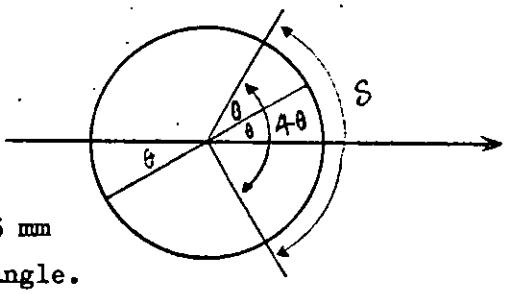

(2) Measure the diameters s' of the rings around the entrance hole (faint lines).

From the diagram

$s' = 4\theta$

$4\theta = 360 - 4\theta'$

Therefore, Bragg angle $\theta = (90 - \theta')$

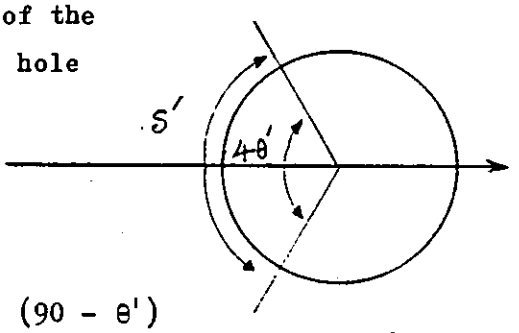

(3) Tabulate all values of θ and $\sin^2\theta$

By trial and error, find a constant C which when divided into each of the values of $\sin^2\theta$, always gives an integer.

since $C = \frac{\lambda^2}{4a^2}$, "a", the length of the unit can be found.

(4) Find from tables, the type of crystal structure corresponding to the values of N obtained.

6.1 Computer Programme to predict corrosion rates.

```
LIST

CORRSN        10:04        15-DEC-80


5       REM   PROGRAM TO FIND CORROSION RATE AT A GIVEN CONCENTRATION OF
10      REM   SODIUM, SULPHUR AND VANADIUM.
15      REM   COMBUSTION CONDITIONS ARE CONSTANT
20      REM   ATOMISING AIR FLOW 6 KG/SQ.CM.
25      REM   SECONDARY AIR FLOW 43 LITRES / MINUTE
30      REM   PIPE DIAMETER 76CM.
35      REM   FLUE GAS TEMPERATURE AT SAMPLE POINT: 720-740 DEG C
40      REM
45      REM   EXCESS OXYGEN 4.5 PER CENT.
50      REM
55      REM
60      REM
100      DIM A(24,7)
200      MAT READ A
300      PRINT "TO END PROGRAM TYPE -1,-1,-1"
400      PRINT "CONCENTRATION OF SULPHUR, SODIUM, VANADIUM ARE" ;
500      INPUT S, N, V
600      IF S <> -1 THEN 1000
700      IF N <> -1 THEN 1000
800      IF V <> -1 THEN 1000
900      STOP
1000     IF S < 0 THEN 1400
1100     FOR I = 0 TO 5
1200     IF S <= I THEN 1600
1300     NEXT I
1400     PRINT "SULPHUR CONCENTRATION IS NOT VALID"
1500     GO TO 400
1600     IF N < 0 THEN 2000
1700     FOR J = 0 TO 60 STEP 20
1800     IF N <= J THEN 2200
1900     NEXT J
2000     PRINT "SODIUM CONCENTRATION IS NOT VALID"
2100     GO TO 400
2200     IF V < 0 THEN 2600
2300     FOR K = 0 TO 300 STEP 50
2400     IF V <= K THEN 2800
2500     NEXT K
```

```
2600    PRINT "VANADIUM CONCENTRATION IS NOT VALID"
2700    GO TO 400
2800    LET P = 1 + 4 * I + J/20
2900    LET Q = 1 + K/50
3000    LET R = A(P,Q)
3100    IF V = K THEN 3400
3200    LET R1 = A(P,Q-1)
3300    LET R = (R-R1)/50 * (V-K+50) +R1
3400    IF N = J THEN 4000
3500    LET R1 = A(P-1,Q)
3600    IF V = K THEN 3900
3700    LET R2 = A(P-1,Q-1)
3800    LET R1 = (R1-R2)/50 * (V-K+50) + R2
3900    LET R =(R-R1)/20 *(N-J+20) +R1
4000    IF S = I THEN 5200
4100    LET R1 = A(P-5,Q)
4200    IF V = K THEN 4500
4300    LET R2 = A(P-5,Q-1)
4400    LET R1 = (R1-R2)/50 * (V-K+50) + R2
4500    IF N = J THEN 5100
4600    LET R2 = A(P-6,Q)
4700    IF V = K THEN 5000
4800    LET R3 = A(P-6,Q-1)
4900    LET R2 = (R2-R3)/50 * (V-K+50) + R3
5000    LET R1 = (R1-R2)/20 * (N-J+20) + R2
5100    LET R = (R-R1) * (S-I+1) + R1
5200    PRINT "CORROSION RATE AT GIVEN CONDITION IS",R
5300    GO TO 400
5400    DATA 1.5,4.2,6.5,8.1,8.5,9.0,8.8
5500    DATA 6,6.5,9.5,11.5,13,13.5,13.5
5600    DATA 11,11,12,14.5,15,16,16.5
5700    DATA 11.2,11.5,12.5,16.5,18.5,19,19
5800    DATA 3,5,6.6,7.9,8.6,9.1,9.3
5900    DATA 7.1,9.5,11.2,12.7,13.6,14.1,14.2
6000    DATA 11.2,11.7,12.6,14.5,16.0,17.1,17.5
6100    DATA 11.5,13.5,15.6,17,18.2,19.3,19.8
6200    DATA 7.5,9,9.9,10.5,10.8,11.1,11.1
6300    DATA 11.5,12.2,13.0,14,14.5,14.8,14.5
6400    DATA 13.1,14.1,14.9,15.5,16.1,16.7,17
6500    DATA 13.5,15.9,18.1,19.4,19.8,19.4,19.5
6600    DATA 10.5,11.5,12,12.5,12.8,12.8,12.8
6700    DATA 15,16.5,17.4,17.7,17.8,17.8,17.5
6800    DATA 18,18.6,18.8,19.4,19.5,19.5,18.8
6900    DATA 17.5,18.3,19.6,20.4,20.3,20.1,19.5
7000    DATA 11,12,12.6,13,13.3,13.5,13.3
7100    DATA 17.5,17.9,18.1,18.3,18.5,18.5,18.4
7200    DATA 18,18.5,18.7,18.9,19.3,19.5,18.2
7300    DATA 18.5,18.9,19.4,19.7,20,20.1,19.9
7400    DATA 12.1,12.8,13.5,13.9,14.2,14.2,14.1
7500    DATA 18.5,18.6,18.9,19.1,19.2,19.2,18.5
7600    DATA 19,19.2,19.5,19.8,20.3,20.5,20.5
7700    DATA 19.5,19.7,20.3,20.5,20.5,20.2,19.5
7800    END
```

```
READY
RUN

CORRSN      10:06          15-DEC-80


TO END PROGRAM TYPE -1,-1,-1
CONCENTRATION OF SULPHUR, SODIUM, VANADIUM ARE ?0,0,0
CORROSION RATE AT GIVEN CONDITION IS       1.5
CONCENTRATION OF SULPHUR, SODIUM, VANADIUM ARE ?1,2,3
CORROSION RATE AT GIVEN CONDITION IS       3.5324
CONCENTRATION OF SULPHUR, SODIUM, VANADIUM ARE ?5,60,300
CORROSION RATE AT GIVEN CONDITION IS       19.5
CONCENTRATION OF SULPHUR, SODIUM, VANADIUM ARE ?-1,60,300
SULPHUR CONCENTRATION IS NOT VALID
CONCENTRATION OF SULPHUR, SODIUM, VANADIUM ARE ?0,-1,0
SODIUM CONCENTRATION IS NOT VALID
CONCENTRATION OF SULPHUR, SODIUM, VANADIUM ARE ?0,0,-300
VANADIUM CONCENTRATION IS NOT VALID
CONCENTRATION OF SULPHUR, SODIUM, VANADIUM ARE ?7,60,400
SULPHUR CONCENTRATION IS NOT VALID
CONCENTRATION OF SULPHUR, SODIUM, VANADIUM ARE ?3,20,100
CORROSION RATE AT GIVEN CONDITION IS       17.4
CONCENTRATION OF SULPHUR, SODIUM, VANADIUM ARE ?3.2,10.5,100
CORROSION RATE AT GIVEN CONDITION IS       15.0155
CONCENTRATION OF SULPHUR, SODIUM, VANADIUM ARE ?4.2,20,5,200
CORROSION RATE AT GIVEN CONDITION IS       12.582
CONCENTRATION OF SULPHUR, SODIUM, VANADIUM ARE ?4,400,200
SODIUM CONCENTRATION IS NOT VALID
CONCENTRATION OF SULPHUR, SODIUM, VANADIUM ARE ?5,50,200
CORROSION RATE AT GIVEN CONDITION IS       20.4
CONCENTRATION OF SULPHUR, SODIUM, VANADIUM ARE ?-1,-1,-1


TIME:  0.37 SECS.

READY
BYE
Job 30  User KHAN FR    EN [130620,23]
Logged-off TTY106  at 10:11:11  on 15-Dec-80
Runtime: 0:00:01, KCS:16, Connect time: 0:12:12
Disk Reads:161, Writes:9, Blocks saved:36
```

ACKNOWLEDGEMENTS.

I wish to express my respect to the late Dr. B.J. Zaczek for helping me in initiating this programme of investigation.

I am grateful to Dr. S.H. Ahmed, Director of Studies for his supervision, helpful advice and guidance given throughout the duration of the investigation.

My sincere thanks to Dr. John Golden for his interest and advice during the experimental programme and for his invaluable assistance in the discussion of the draft thesis.

I have great pleasure in thanking Mr. D.F. Rosborough, Research Associate, Esso Research Limited, Abingdon, who is also President, Institute of Energy for his discerning advice and help throughout the duration of the research programme and for supplying light fuel oil for experimental work.

My sincere thanks particularly to the following, who have not only contributed very willingly from their store of memory but also offered practical assistance: Mr. A.J. Spackman, Mr. M. Evans, Mr. N. Mahmood, Mr. A. White, Mr. M. Smutkochorn, Mr. J. Webster, Mr. P. Lister, Mr. J. Mattick, Mr. T. Sandell, Mr. D. Bartlett, Mr. W. Blatchford, Mr. C. Freshwater, Mr. C. Willgress, Mr. G. Savage, Mr. D. Walters, Mr. R. Singh, Dr. David Puxley (L.R.S. of British Gas Corporation), Mr. T. Harbottle (Durham Chemicals Ltd.), Dr. P. Beadle (B.P. Research Laboratories), Prof. P. Hancock (Cranfield Institute of Technology), Mr. D. Ward, (INCO Europe Ltd.), Dr. C. Booker, (City of London Polytechnic), Dr. F. Stott (UMIST) and Mrs. Karen Scales for typing this thesis.

Finally,I must acknowledge an immense debt of gratitude to my brother, Mr. D.U. Khan; my brother-in-law, Mr. S. Ahsan and Mr. R. Leurs a friend of the family, without whose continual encouragement and financial support this work could never have been undertaken.